UNIVERSITE PARIS-SUD

École Doctorale de Cancérologie

Discipline: Immunologie

THESE DE DOCTORAT

Intitulée:

Differential effects of the cytokine Thymic Stromal Lymphopoietin on human dendritic cell subsets

Soutenue par

Carolina MARTINEZ CINGOLANI

Le 29 novembre 2013

Directeur de Thèse :   Vassili SOUMELIS

Composition du jury :

Président du jury :	Annelise BENNACEUR
Rapporteur :	Selim ARACTINGI
Rapporteur :	Christophe CAUX
Examinateur:	Annelise BENNACEUR
Examinateur:	Matthew COLLIN

Table of Contents

PREAMBLE

The human body is in permanent contact with millions of microbes that live around it, on it or within it. The immune system, in all its complexity ensures the maintenance of our internal homeostasis. Numerous cellular and molecular actors participate in time and space in the orchestration of the immune response. These actors have been classified as part of the innate or adaptive immune systems. The innate system is characterized by an immediate antigen non-specific response. It is constituted by cells at the barrier surfaces and several types of immune cells such as macrophages, granulocytes, mast cells, eosinophils and natural killer cells. The adaptive immune system is characterized by a response that is specific to the pathogen. This specific response is provided by B and T lymphocytes and generates a long-term immunological memory.

At the interface between these two systems we find dendritic cells (DCs). These cells detect when the tissue microenvironment equilibrium is perturbed, and they sense, capture and process foreign antigens. First, activated DCs help in the recruitment of innate actors to the tissue. Then they migrate to the lymph nodes where they activate naïve T cells in an antigen-dependent manner, activating the adaptive immune response. To link a specific T cell response to the type of inflammation, DCs integrate multiple signals provided by the inflammatory milieu. As a first level of complexity, the type of T cell antigen-specific response depends on the type of antigen and molecules that activated the DCs. A second level of complexity is added by the fact that DCs constitute a heterogeneous and dynamic population and different DC subsets are associated with specific T cell outcomes.

In the context of allergic inflammation, DCs are activated by tissue factors that instruct them to induce an excessive immune response to certain non-pathogenic antigens called allergens. One of these factors is Thymic Stromal Lymphopoietin (TSLP), a cytokine produced by the skin keratinocytes that activates DCs. TSLP-activated DCs mediate the recruitment and activation of innate cells such as basophils and eosinophils and induce the differentiation of naïve T cells into effector cells with a pro-allergic phenotype, called inflammatory Th2.

To induce a Th2 polarization, TSLP-activated DCs need to get in contact with the naïve T cells in the lymph nodes, yet the mechanism by which TSLP-treated DCs migrate is unknown. Although TSLP has been shown to stimulate several immune cells in the murine system, interestingly in humans, TSLP preferentially targets primary DCs. The DC subsets activated by TSLP may have differential implications in TSLP-linked allergic disorders. Nevertheless, human DC diversity and the potential differential effects of TSLP on human DC subsets remain unexplored. In this context, I dedicated my PhD work to the study of TSLP effects on human DC subsets. I assessed the differential response of human DC subsets to TSLP and studied the effects of TSLP s on DC migration.

As a framework of my study, I will introduce DCs, their ontogeny, function and classification into subsets. Then, I will introduce our current knowledge on human TSLP biology and the role of TSLP-activated DCs in the human immune response.

My results will be presented in three chapters. First, I will present a submitted article showing that TSLP and TGF-β synergize to induce Langerhans cell differentiation from BDCA1^{+} but not BDCA3^{+} blood DCs. Then I will present our published results showing that TSLP induces DC migration. Finally I will present a manuscript in preparation assessing the molecular mechanisms implicated in TSLP-induced DC migration.

In the discussion section at the end of this manuscript I will put my results in perspective to published studies in related topics.

In the appendix, I will show ongoing work on the study of TSLP effects on DC subsets and other projects in which I collaborated during my PhD thesis.

LIST OF ABBREVIATIONS

DCs:	Dendritic Cells
CBA:	Cytometric bead Array
CDPs:	Common Dendritic cell Precursors
CLA:	Cutaneous Lymphocyte Associated protein
CLPs:	Common Lymphoid Precursors
CMPs:	Common Myeloid Precursors
Flt3L:	Fms-like tyrosine kinase 3 Ligand
Flu:	Influenza virus
GATA2:	GATA-binding factor 2
Giα:	Small G inhibitory protein α
GM-CSF:	Granulocyte-Macrophage Colony-Stimulating Factor
GMPs:	Granulocyte-Macrophage Precursors
GPCR:	G-Protein-Coupled Receptor
HSCs:	Hematopoietic Stem Cells
IFN:	Interferon
IL:	Interleukin
LCs:	Langerhans Cells
LCH:	Langerhans Cell Histiocytosis
LPS:	Lipopolysaccharide
M-CSF:	Macrophage Colony-Stimulating Factor
M-CSFR:	Macrophage Colony-Stimulating Factor Receptor
MDPs:	Macrophage/Dendritic cell Progenitors
MHC:	Major Histocompatibility Complex
MLPs:	Multi-Lymphoid Progenitors
MMPs:	Matrix Metalloproteases
MTOC:	Microtubule-Organizing Center
PAMPs:	Pathogen-Associated Molecular Patterns
PBMCs:	Peripheral Blood Mononuclear Cells
PDCs:	Plasmacytoid Dendritic Cells
Pre-DCs:	Precursors for Dendritic Cells
PRRs:	Pattern Recognition Receptors
PTX:	Pertussis Toxin
TGF:	Transforming Growth Factor
TLRs:	Toll-like receptors
TNF:	Tumor Necrosis Factor
TSLP-DCs:	Thymic Stromal Lymphopoietin-Primed Dendritic Cells
TSLP-PDCs:	Thymic Stromal Lymphopoietin Primed Plasmacytoid Dendritic Cells
TSLPR:	Thymic Stromal Lymphopoietin Receptor

INTRODUCTION

1.1 DENDRITIC CELLS: HISTORY OF A MAJOR DISCOVERY

The first evidence of the existence of DCs was made by a medical student called Paul Langerhans in 1868 [1, 2]. He had discovered in epidermal tissue sections, what he thought was a new cell type of the nervous system that was named then Langerhans cells (LCs) (Figure 1-1). The origin of LCs and their link to immunology was not known. The major discovery in the history of DCs was made in 1973 when Ralph Steinman and Zanvil Cohn identified a new cell type in the spleens of mice [3]. They found that these cells were different from macrophages and other leukocytes and because they had tree-like cytoplasmic extensions they decided to name them dendritic cells (Figure 1-1). Within few years they enriched this spleen population and did functional studies revealing the potent T cell-activating capacity of DCs [4]. In the meanwhile, LCs were ontogenically linked to melanocytes [5] and to keratinocytes [6]. They were also linked to histiocytes when they were found within the bone and lung lesions of patients suffering from a disease called first "histiocytosis X" (later on called LC histiocytosis) [7]. The demonstration that LCs were bone marrow-derived leukocytes, and several studies showing their immunological role [8, 9], led to the final recognition of LCs as DCs in 1985 by Gerold Schuler and Ralph Steinman [10]. This last study showed that LCs, after several days in culture, acquired a mature DC phenotype and induced a strong response in naïve T cells.

The three major criteria defining DCs were proposed by Steinman in 1991 [11]: (1) dendritic morphology, (2) constitutive expression of high levels of major histocompatibility complex (MHC) class two molecules and (3) capacity to induce proliferation of naïve CD4 T cells in a mixed leukocyte reaction.

In the last 30 years, the studies of DC biology have multiplied and have rapidly shed new light on their origin and function. Today, DCs are still considered to be the most powerful stimulators of naïve T cells and the key cells initiating and shaping the immune cell response.
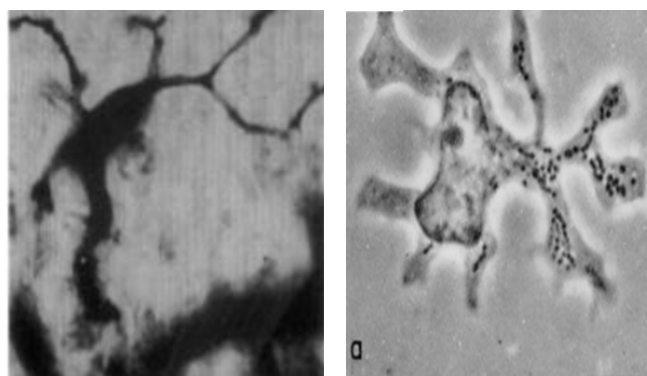
Figure 1-1: Stellar morphology of dendritic cells.

Left, a Langerhans cell seen by Paul Langerhans in 1686, adapted from Jolles, S., 2002. Right, a dendritic cell seen by Ralph Steinman in 1973, Steinman, R. 1973.

1.2 ORIGIN OF HUMAN DENDRITIC CELLS

The DC pool needs to be continuously maintained in the organism. Different factors and cells participate in this process. DC requirements and sources differ in steady-state and inflammatory conditions. The purpose of this chapter is to review our current knowledge on the origins of human DCs and the missing links in DC generation during inflammation. Due to their particular development, a separated paragraph will be dedicated to LC ontogeny. Finally a brief description of the transcription factors that are involved in DC development will be given.

1.2.1 FROM MICE TO HUMANS

Human DCs are generated on a regular basis from hematopoietic stem cells (HSCs) located in the bone marrow. Several experiments in mice, of isolation and further transplantation of bone marrow precursor cells, have helped to clarify the ontogeny of DC and monocyte-macrophage lineages [12, 13].

The current models propose that bone marrow HSCs, characterized by the expression of the surface molecule CD34, give rise to non-self renewing multipotent progenitors which give rise to proliferating progenitors that gradually become lineage-restricted. Two early committed progenitors have been identified in mice and human, the common lymphoid precursors (CLPs) and the common myeloid precursors (CMPs) [14]. For a long time it was believed that the CLPs gave rise to the lymphoid lineages and plasmacytoid dendritic cells (PDCs) whereas the CMPs gave rise to monocytes, macrophages and DCs. Today, we know that both precursors maintain the capacity to generate DCs and PDCs [15, 16] depending mainly on the expression of Fms-like tyrosine kinase 3 ligand (Flt3L) [17-19]. Indeed, Flt3L injection, in humans leads to massive expansion of blood PDCs and DCs [20].

A scheme showing all the intermediate precursor populations that give rise to DCs in mice and humans is depicted in Figure 1-2.

In mice it has been proposed that in addition to CMPs there are also granulocyte-macrophage precursors (GMPs) and macrophage/DC progenitors (MDPs) (Figure 1-2A). The MDPs give rise to monocytes and to common DC precursors (CDPs). The CDPs further develop into PDCs and precursors for DCs (pre-DCs) that do not have anymore the potential to give rise to monocytes. At a steady state, pre-DCs are found in the bone marrow, the blood and the spleen. They acquire further surface phenotype and morphology of DCs and enter the peripheral tissues, including the lymphatic tissues [13, 21].

The equivalents of MDPs and CDPs have not yet been described in humans. Yet, it has been shown that there are progenitors with combined myeloid and lymphoid potentials [22]. GMPs and the multi-lymphoid progenitors (MLPs) appear to have DC potential. The circulating human blood precursors of DCs (equivalents of mice pre-DCs) must exist. However, a clear

phenotype, distinct from those of the terminally differentiated DCs has not been identified (Figure 1-2B). I will detail the precursor capacity of human blood DC subsets, and the hypothesis that these cells may be the equivalents of the murine pre-DCs, in the "General discussion and perspectives" chapter of this manuscript.

During inflammatory conditions, other cellular precursors of DCs have been found. In vitro experiments with human cells have shown that exposure to cytokines such as granulocyte-macrophage colony-stimulating factor (GM-CSF) and Interleukin (IL)-4, induces the differentiation of human monocytes into immature DCs [23]. An addition of proinflammatory cytokines such as Tumor Necrosis Factor (TNF)-α [24], microbial products such as lipopolysaccharide (LPS) or T cell-derived CD40L further activates them into mature DCs whereas exposure to macrophage colony-stimulating factor (M-CSF) induces monocytes to differentiate into macrophages. This confirms mice studies showing that under inflammatory conditions, blood monocytes give rise to macrophages and DCs [21]. DCs can also be generated in vitro from CD34^{+} HSCs isolated from human peripheral blood or cord blood. This differentiation is dependent on Flt3L and further GM-CSF and TNF-α stimuli [25, 26]. This suggests that under inflammatory conditions, the CD34^{+} HSC circulating in human blood could be a new source of DCs besides monocytes. Finally, the possibility that inflammatory tissue signals activate the potential precursor role of blood DCs remains elusive and will be discussed later in this manuscript.
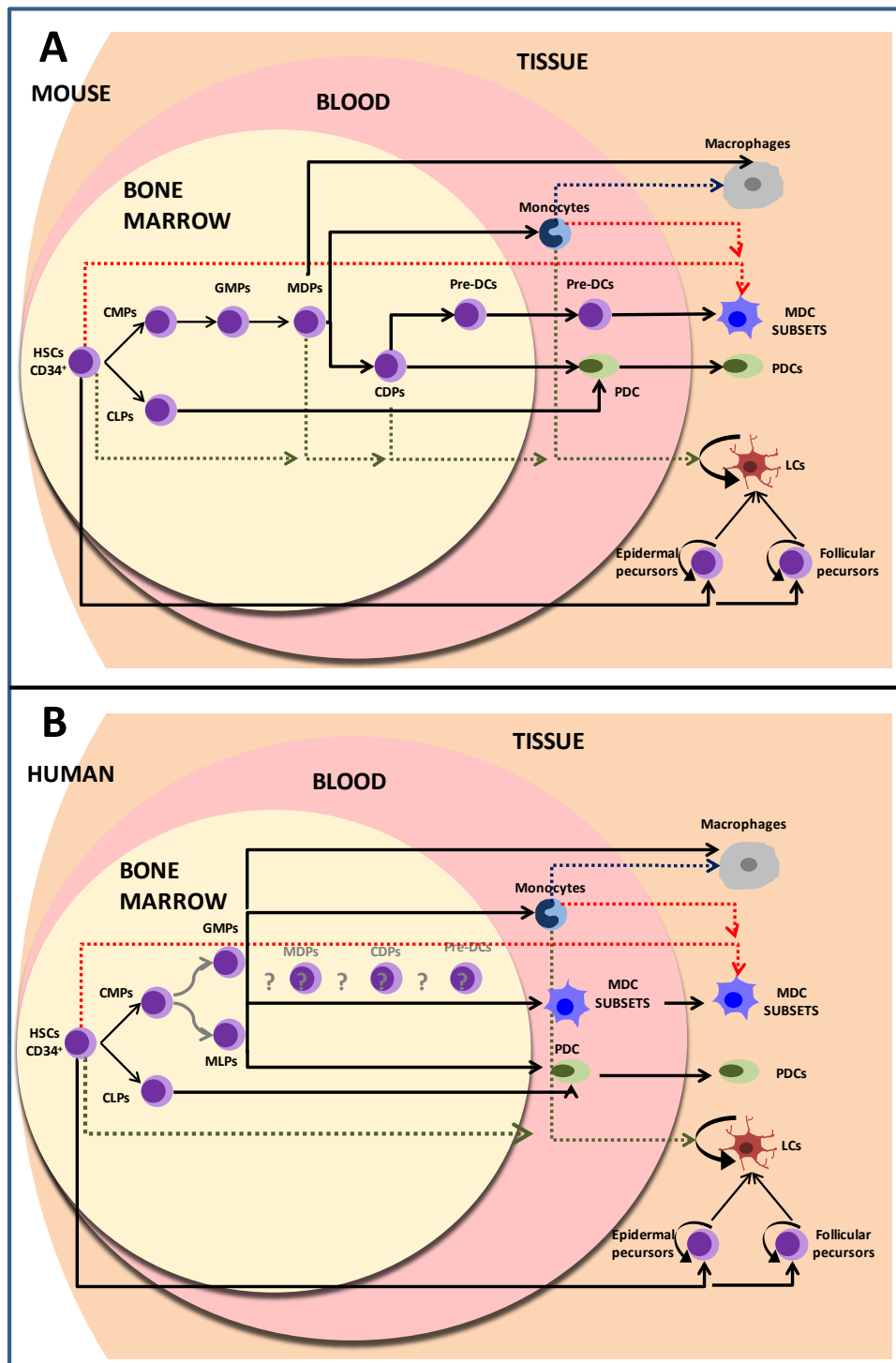
Figure 1-2 : Dendritic cell ontogeny.

A. Dendritic cell development in mice. **B.** Dendritic cell development in human. Grey arrows show undetermined relationships. Pointed arrows show the precursor-cell relationships under inflammatory conditions. (HSCs, hematopoietic stem cells; CMPs, common myeloid precursors; CLPs, common lymphoid precursors, GMPs, granulocyte-macrophage precursors; MDPs, macrophage/DC progenitors; CDPs, common dendritic cell precursors; pre-DCs, precursors for dendritic cells; MDCs myeloid dendritic cells, PDCs, plasmacytoid dendritic cells; MLPs, multi-Lymphoid progenitors, LCs Langerhans cells).

1.2.2   LANGERHANS CELL ORIGINS

LCs have been shown to have a particular ontogeny. Recent experiments in mice showed that in contrast to other DCs, LCs develop from an embryonic precursor that colonizes the epidermis before birth. Then, in the adult mouse, LCs self-renew from unknown local precursors in the epidermis [27] (Figure 1-2).

In human, these findings are confirmed by the fact that LCs proliferate in situ [28-30] and donor LCs were shown to persist in human skin that was transplanted into immunodeficient mice [31]. Moreover, human limb transplants showed that donor LCs persist for years [32, 33]. Finally, several reports have shown that there are proliferating cells in the bulge region of the hair follicle that could contribute to LC generation [34].

The fact that mice lacking the transforming growth factor (TGF)-β1 do not have LCs [35] shows that this factor is essential for LC development. Studies in humans confirmed this finding; TGF-β1 is required for the in vitro generation of LCs from human $CD34^+$ precursors [36, 37] or $CD14^+$ monocytes [38] (Figure 1-2). In addition it was recently shown that the macrophage colony-stimulating factor receptor (M-CSFR) is required for the development of LCs in mice. The high affinity ligand of this receptor, IL-34, might be essential for the development of LCs precursors, LCs differentiation, survival or proliferation [28]. Further experiments on IL-34 and human LC development are needed to translate this finding into human biology.

The in vitro generation of LCs from $CD34^+$ precursors and $CD14^+$ monocytes confirmed that in humans, just as in the mouse model, blood precursors are recruited to renew LCs in inflammatory conditions [39]. Blood $CD34^+$ cells stimulated with a combination of Fl3L, GM-CSF, TNF-α and TGF-β, as well as $CD14^+$ monocytes stimulated with GM-CSF, IL-4 and TGF-β differentiate into *bona fide* LCs [23, 37, 38]. This shows that as opposed to steady state conditions, in inflammatory contexts tissue –derived cytokines can trigger the differentiation of circulating precursors into LCs.

Whether blood DCs can differentiate into LCs under inflammatory conditions remains controversial. Ito, T et al. showed that a fraction of human blood $CD1a^+$ DCs stimulated with GM-CSF, IL-4, and TGF-β can give rise to LCs in vitro [40]. However in my experience and also as published by other groups [41], human blood DCs do not express CD1a at the cell surface or at the gene transcriptional level [42]. This discrepancy might be due to the use of different cell isolation methods. To obtain the $CD1a^+$ DCs, Ito, T. et al. enriched the DC fraction of peripheral mononuclear cells, by magnetically depleting $CD3^+$ (Lymphocytes) and $CD14^+$ (monocytes) cells. This depletion was followed by a positive selection of $CD4^+$ cells (DCs) and further sorting of lineage (CD3, CD7, CD14, CD16, CD19) –negative and $CD1a^+$ cells. Monocytes can express CD4 marker [43]. And $CD14^+$ monocytes that may have escaped the depletion can have been selected. Activated monocytes can further down-regulate CD14 and up-regulate CD1a. Whether CD4 positive selection may have activated the monocytes is not clear.

To my knowledge, Ito, T. et al study is the only published work that assesses human DCs capacity to differentiate into LCs. The possibility that inflammatory cytokines from the tissues can instruct human blood CD1a⁻ DCs to differentiate into LCs remained unknown. The data presented in the first section of the "Results" chapter reveal the capacity of blood DCs to differentiate into LCs.

1.2.3   TRANSCRIPTION FACTORS INVOLVED IN DENDRITIC CELL DEVELOPMENT

Recent descriptions of human DC deficiency have been helpful to identify several transcription factors implicated in DC development [44-46].

By analogy to mice, it seems that Ikaros, PU.1, Gfi1 and Id2 are involved in DC development in humans. These transcription factors regulate genes that encode proteins of the early hematopoiesis (such as *Flt3, Il7r, and Stat3*); therefore their mutations lead to severe defects in global hematopoiesis [45].

More specific transcription factors are linked to DC ontogeny. This is for example the case of E2-2; indeed, human deficiency on E2-2 leads to a PDC impaired function [47].

Moreover, mutation of GATA-binding factor 2 (GATA2) is the cause of a DC deficiency called DC, monocyte, B and natural killer lymphoid deficiency [48]. The loss of GATA2 is characterized also by the absence of MLPs and diminished GMPs numbers. The transcription factor IRF8 was found to compromise DC and monocyte development as well. But in contrast to the GATA2 mutation, the IRF8 mutation is associated to an expansion of all the progenitor compartments [49].

A transcription factor mutation affecting exclusively DC development has not yet been identified and could have important implications in our comprehension of DC generation under inflammatory conditions. A common transcription factor to all human DC subtypes has been found: zbtb46 [50, 51], but its contribution to human DC development has not been clarified.

1.3 LYFE CYCLE OF HUMAN DENDRITIC CELLS

It is important to understand that a single DC may induce different T cell outcomes depending on the combination of signals that the DC receives. The purpose of this chapter is to highlight the special features that allow DCs to sense a wide range of signals from the tissue microenvironment and differentially induce particular T cell responses. In a separated paragraph, I will present the model of DC and DC precursor migration to the lymph nodes and the tissues. The particular effects of TSLP on human DC biology will be addressed later in the introduction.

1.3.1 DENDRITIC CELL CHARACTERISTICS AND FUNCTION

Fully differentiated, patrolling DCs are found in almost all the peripheral tissues at steady state. They get activated when they sense a particular threat.

Indeed, DCs express a broad set of receptors that allow them to recognize danger signals. Through different cytokine and chemokine receptors, they recognize microenvironment signals secreted by the neighboring cells in response to microbes. Through the pattern recognition receptors (PRRs) they recognize conserved molecules from microbes called pathogen-associated molecular patterns (PAMPs) [52]. These receptors include the Toll-like receptors (TLRs), C-lectins, NOD like receptors and RIG-I like receptors. These recognize different molecules from glycoproteins and polysaccharides to double or single stranded nucleic acids. Finally the Fc and complement receptors allow DCs to capture antigens from microbes and apoptotic cells.

Once they get activated, DCs change their morphology, and phenotype. They up-regulate major histocompatibility molecules, costimulatory molecules (CD80, CD83, CD86 and CD40) and chemokine receptors that trigger migration [53]. All these changes enable them to interact with T cells. Nevertheless they first secrete inflammatory mediators, cytokines and chemokines that induce the recruitment and activation of different actors of the innate immune response such as granulocytes, natural killer cells, and other DCs (Figure 1-3) [10, 48].

Next, they enter the afferent lymphatics and reach the draining lymph nodes were they present the captured antigens to T cells. The endogenous proteic antigens are loaded onto MHC molecules of class I to be presented to cytotoxic T cells expressing the surface marker CD8. This response leads to cell apoptosis. The exogenous proteic antigens are bound to MHC class II molecules and presented to T cells expressing the surface marker CD4 leading to a T helper cell response [54]. The exogenous molecules can also be presented in the context of MHC class I molecules to CD8 T cells, a process called cross-presentation. DCs indeed, cross-present exogenous antigens that can come from infected neighboring cells, or when they are infected themselves. The CD8 cytotoxic T cell response leads to the apoptosis of the infected

cell. This mechanism is also required for antitumoral responses even if the mechanisms are not well understood yet [55]. Finally the lipidic antigens are presented through the CD1 (a-d) molecules to T cells and natural killer T cells.

In conclusion, DCs interact directly and indirectly with all the cell types responsible for the regulation of the innate and adaptive immune systems. The way DCs induce particular immunological responses that are adapted to the requirements of the inflammatory milieu, will be presented in the next chapter.
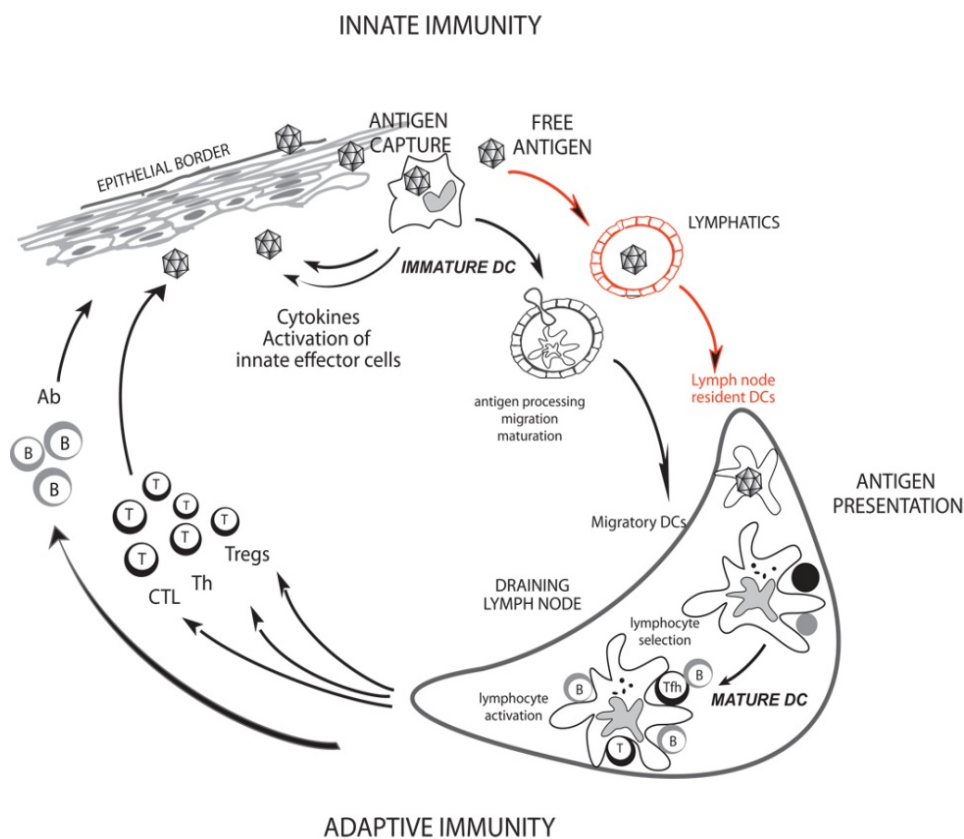
Figure 1-3: Dendritic cells at the interface between innate and immune systems. Adapted from Ueno H. et al., 2010.

Immature dendritic cells capture antigens at the periphery and become activated. They release inflammatory mediators in situ. They process the captured antigen and in parallel acquire a mature phenotype. They migrate through the afferent lymphatics to the lymph nodes to present the antigens to the CD4 T and CD8 T cells. T helper cells develop into follicular T helper cells that induce B cell activation to antibody secreting cells, T regulatory cells that mediate tolerance and T helper cells inducing Th1, Th2 and Th17 responses. T helper cells activate the cytotoxic CD8 T cells to induce clearance of infected cells. (DC, dendritic cells; Tfh, T follicular helper cells; B, B lymphocyte; Tregs, T regulatory cells; Th, T helper cells; CTL, cytotoxic T lymphocytes; Ab, antibody).

1.3.2 T CELL POLARIZATION BY DENDRITIC CELLS

The special feature of DCs in comparison with other antigen-presenting cells is their unique capacity to prime naïve CD4 T cells leading to the generation and proliferation of antigen-specific helper and memory T cells [54].

DCs and T cells interactions in the lymph nodes are complex and give rise to different types of T cell responses that depend on the priming of the DCs themselves. Therefore depending on the activating stimuli (tissue factors), DCs express one or another combination of what can be called DC factors, cytokines and surface molecules, which are sensed by naïve T cells. Then, the naïve T cells get differentiated into different types of T helper cells. The T helper cells secrete T cell factors that define the type of T cell response (Figure 1-3).

In summary, DCs activated by intracellular bacteria and viruses, can produce large amounts of IL-12, and induce T helper cells that secrete IFNγ and TNF-α. This T helper response is called Th1 (Figure 1-4).

DCs activated by extracellular microbes such as helminthes induce T cells that produce IL-4, IL-5, and IL-13. This immune response is called a Th2 response. It characterizes the allergic responses (Figure 1-4).

DCs secreting variables amounts of IL-1b, IL-23, IL-6 and TGF-β induce a Th17 response. The T helper cells induced are characterized by the secretion of IL-17A, IL-17F and IL-22 (Figure 1-4). They are responsible for immunity against extracellular microbes and fungi. They promote an important neutrophil response and are often linked to autoimmune diseases such as psoriasis.

The Th1, Th2 and Th17 are not the only T cells that result from the DC-T interaction. In fact, DCs can also induce regulatory T cells that have an important role in the immunological tolerance [56]. The priming of T regulatory cells seems to be achieved at the steady state, by the constant presentation of self antigens in the context of MHC class I, or when DCs stimulate T cells while expressing low amounts of costimulatory molecules. T regulatory cells regulate the immune response through the secretion of IL-10 and TGF-β and play an important role in the responses towards human microbiota (Figure 1-4).

Finally, concerning B cell activation, it is known that a group of T helper cells, present in the B follicular zones induce the B cell activation. It has been proposed that there are different T follicular helper cells depending on the DC-T cell priming (Figure 1-4). Moreover, the DCs also directly induce the activation of B cells and their differentiation to antibody-secreting cells [57] (Figure 1-3).
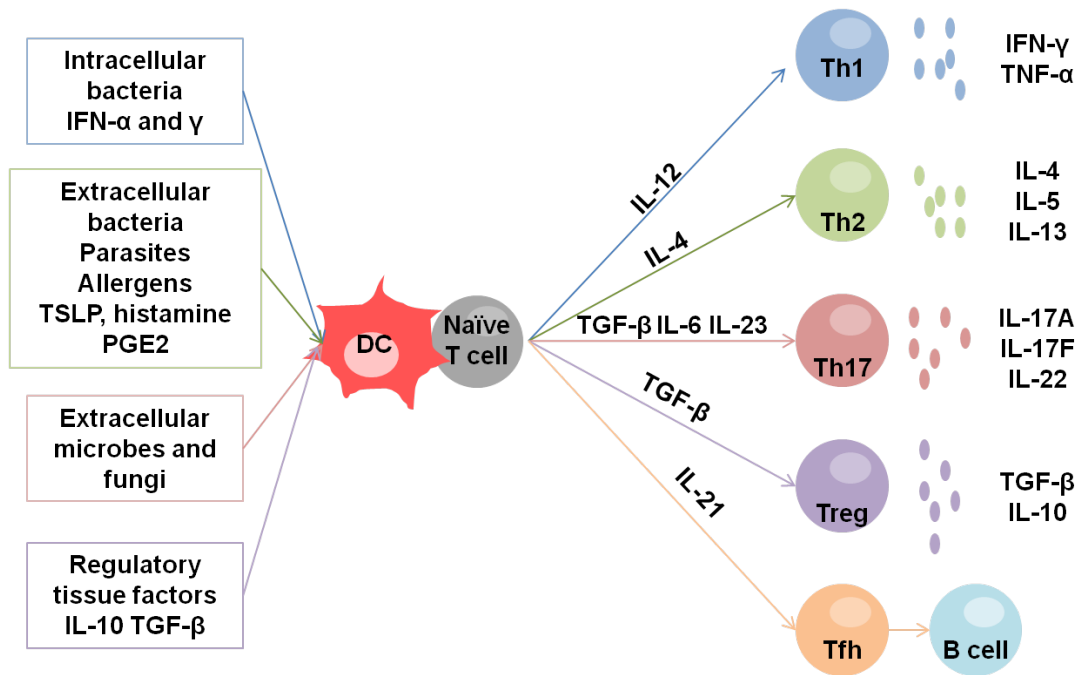
Figure 1-4: Dendritic cells induce different T cell responses.

Immature dendritic cells become activated by different microbes and tissue factors. Differentially activated DCs induce the polarization of naïve T cells into Th1, Th2, Th17 Tregs (regulatory T cells) and Tfh (T follicular helper cells). The different T cell profiles are defined by the cytokines secreted.

In order to prime naïve T cell differentiation, tissue-residing DCs must travel considerable distances, from the inflammation sites, to lymph nodes. Moreover, the peripheral pools must be replenished with new DCs. In the next chapter, the different molecules that are implicated in the process of DC migration will be reviewed.

1.3.3   HUMAN DENDRITIC CELL MIGRATION

Although free antigen can enter the afferent lymphatics and be presented by resident DCs in the lymph nodes [58] (Figure 1-3), DCs get activated in the periphery and migrate themselves to the lymph nodes to present the antigens. Again, most of our knowledge about DC trafficking comes from studies in mice mainly on LC migration.

LCs are retained in the epidermis through the expression of E-cadherin that mediates their binding to keratinocytes [59]. During inflammation, the DCs themselves and the surrounding cells secrete IL-1β and TNF-α that induce the down-regulation of E-cadherin and the up-regulation of the chemokine receptor CCR7 that mediates the lymph node homing [60-62]. Indeed, CCR7 has been shown to mediate migration of mouse skin DCs to lymph nodes under inflammatory and even steady state conditions [63]. Although in this last case, much less is known.

The two ligands of CCR7, CCL19 and CCL21 are expressed by the endothelial cells of the lymphatic vessels in the dermis. This means that first LCs need to migrate from the epidermis to the dermis. This seems to be mediated by the interaction between the chemokine receptor CXCR4 present in mature LCs and its ligand CXCL12 present in the dermis [53, 64-66] (Figure 1-5).

Once in the dermis, non-soluble CCL21 gradients guide the LCs into the lymphatic vessels [67, 68]. LCs squeeze through the gaps present in the basement membrane and are driven to the lymph nodes by a passive flow [69].

Finally, once in the lymph nodes, gradients of CCL19 and CCL21 will further guide the DCs to the T cell zone [70].

Besides chemokine – chemokine receptor interactions, there are other molecules implicated in the entrance of DCs to the lymphatics. Mature DCs also upregulate the receptor for sphingosine-1-phosphate, an inflammatory molecule implicated in leukocyte migration. Nevertheless its role in DC trafficking is still not defined [71].

Proteases such as the matrix metalloproteases (MMPs) are expressed by mature DCs. Activated LCs secrete MMP-2 and MMP-9 that help them to degrade the surrounding collagen matrix and trespass epidermal basal membrane [72]. The matrix metalloproteases can also act in DC migration via their action on chemokines, indeed they can mediate chemokine proteolysis into agonistic or antagonistic chemotactic fragments [73].

Finally during inflammation the lymphatic endothelial cells upregulate adhesion molecules such as E-selectin, ICAM-1 and Vcam-1 that interact with integrins expressed by mature DCs [74]. Nevertheless migration of DCs into the lymph nodes seems to be a process independent from integrins [75].

DC precursor migration from blood to the peripheral organs is less well understood. CCR6 is a skin-homing receptor that is mainly expressed on differentiated LCs. It binds to the CCL20 chemokine present in the epidermis. The LC precursors (monocytes and CD34$^+$ HSC) express low levels of CCR6; instead they highly express CCR2 that allows them to bind the CCL2 present in the dermis. Under inflammatory conditions, both CCL2 and CCL20 are secreted, and LC precursors can be recruited to the dermis through CCR2 and give rise to LCs that will be attracted to the epidermis through CCR6 [27, 76].

The model of LC migration is depicted in Figure 1-5. Excluding the dermis-epidermis passage, this model can be applied to DCs in general. Indeed monocytes and immature DCs express CCR1, CCR2, CCR3 and CCR5 that allow them to reach the inflamed tissues [53]. These chemokine receptors are down-regulated upon activation and replaced by high levels of CCR7 that allow them to reach the lymph node.

This model implies that the microenvironment inflammatory signals regulate the chemokine receptors on the surface of the DCs. However the tissue factors that regulate DC precursor homing to the inflamed tissues are less known. In particular the tissue factors that allow CCR6 up-regulation by DC precursors remain poorly defined.
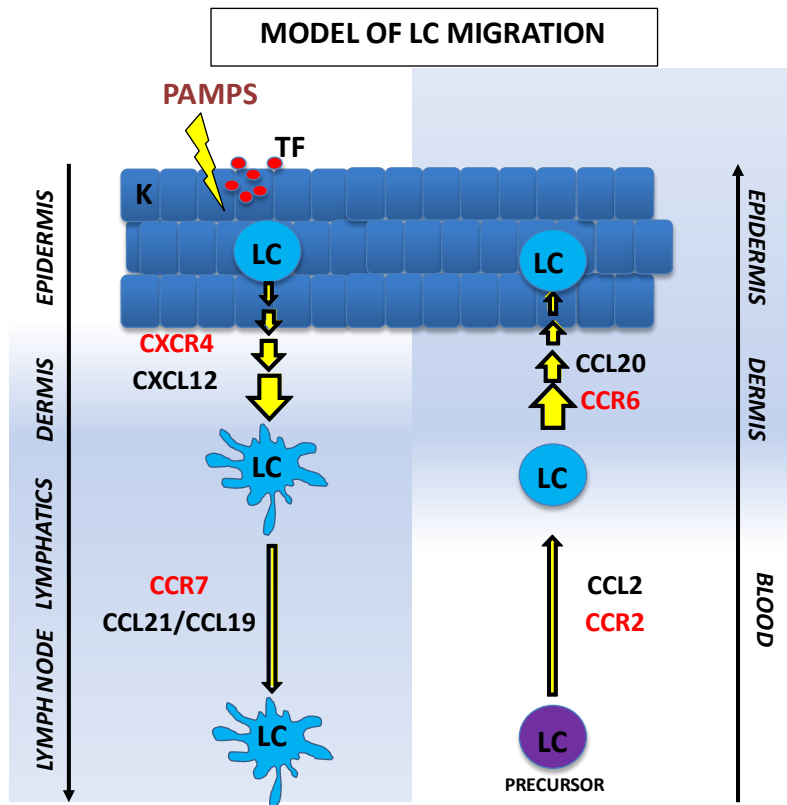
Figure 1-5 : Model of Langerhans cell migration.

First, Langerhans cells sense a threat in the epidermal layer, they get activated and upregulate the chemokine receptor CXCR4. This receptor allows LCs to sense a gradient (light blue background) of its ligand, CXCL12 that directs them to the dermis. Once in the dermis the expression of CCR7 receptor allows them to bind CCL19 and CCL21 expressed by the afferent lymphatic epithelial cells and in the lymph nodes. On the other hand, Langerhans cells precursors in the blood express CCR2 that mediates their homing to the dermis. There, the expression of CCR6 allows them to sense CCL20 gradients that will position them in the epidermis. (PAMPS, pathogen-associated molecular patterns; TF, tissue factors; K, keratinocytes; LC, Langerhans cells).

1.4 HUMAN DENDRITIC CELL SUBSETS

During my PhD thesis, in 2010, several publications appeared showing functional differences between human blood DC subsets. These functional differences represent a second level of complexity in the induction of T cell responses. I was studying TSLP effects on DC migration and my interest in the function of DC subsets led me to address the differential response of DC subsets to TSLP stimulation. The DC population is heterogeneous and the different subsets have overlapping phenotypes, therefore the purpose of this chapter is to present the DC diversity in human blood, lymphoid organs and tissues in a comprehensive way. After defining the nature and phenotype of the DC subsets, I will dedicate a paragraph to the studies that have assessed the functional differences between DC subsets.

Increasing evidence has highlighted the fact that the DC population is heterogeneous. Initially, LCs and PDCs were defined as different types of DCs [10, 77]. Then, the study of human blood, skin, lymph nodes, thymus and other tissues has confirmed the presence of several dynamic subsets of DCs in different maturation states [41]. Today, gene transcriptomic data on these different subsets are available. The comparison between the genes expressed in one or another sub-population has allowed defining their correspondent gene signatures. Statistical tools such as the hierarchical clustering and principal component analysis allow the unbiased and simultaneous analysis of all the genes (variables) from the different sub-populations and, preserving the variance of the data, provide a summary of the information were the similarities and differences between the datasets is easier to interpret. Furthermore the different signatures can be confronted to several public databases and translated as profiles enriched for different biological relevant gene sets (gene enrichment analysis). These types of analysis have further highlighted the different gene expression profiles of DC subsets and the relationships between them [42, 78-81].

In general the DC subsets can be defined according to the expression of different combinations of surface markers that allow their isolation from different human samples. Several studies attempted to correlate these different phenotypes to distinct functions in the immune response in steady-state and pathological conditions [25, 78, 82]. Nevertheless, no exclusive surface markers or functions can be attributed to the distinct subsets and their clearest classification may be the one linked to their location. Therefore I will present the different DC subsets according to their anatomical distribution based on the latest review of Collin et al on human DC subsets [83]. A summary of the different DC subsets and their phenotypes is shown in Figure 1-7 and Table 1-1.

1.4.1 BLOOD DENDRITIC CELLS

The blood DC subsets are very well characterized in humans and seem to be the ones that replenish the tissue and lymphoid organs pools. The first study in 1993, characterizing blood DC compartment, defined three initial subsets according to the surface markers CD33 and CD14 [84]. This study included a population of monocytes ($CD33^+CD14^{bright}$) and two populations of DCs, ($CD33^{dim}CD14^{dim}CD16^-$ or $CD33^{bright}CD14^{dim}CD16^-$).

Later on in 2000, Dzionek et al, described blood DC subsets as we know them today; they used the surface markers BDCA-2 and BDCA-4 to identify PDCs, BDCA-1, and BDCA-3 to identify two subsets of myeloid DCs [85].

By inmmunohistological techniques like the Giemsa/May Grunwald staining, PDCs have a smooth, round, plasma-cell morphology; they display an eccentric kidney-shaped nucleus and have a violet basophilic cytoplasm that contains a pale Golgi zone. Myeloid BDCA-1$^+$ and BDCA-3$^+$ DCs are less rounded cells, with numerous short processes and more hyperlobulated nuclei (Figure 1-6).

The three blood DC subsets express high levels of major histocompatibility complex class II molecules (HLA-DR) and lack typical lineage markers such as CD3 (T cells), CD19/CD20 (B cells) and CD56 (natural killer cells) [86].

<div align="center">

PDCs   **BDCA-1$^+$**   **BDCA-3$^+$**

</div>
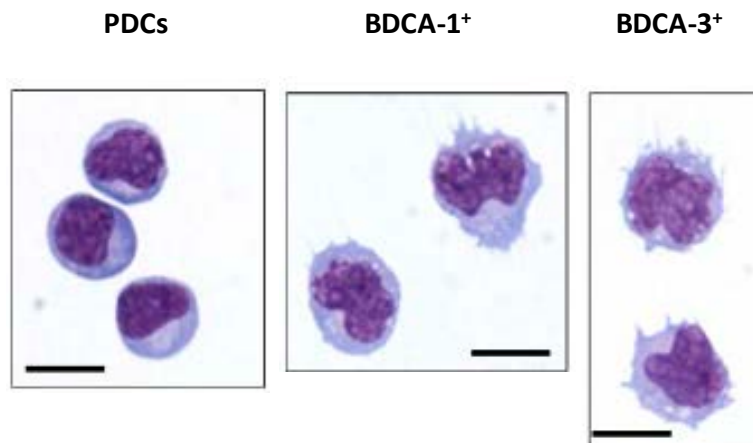
Figure 1-6: Blood and tonsillar dendritic cell morphology. Adapted from Segura et al., 2013.

These images correspond to Giemsa/May-Grunwald staining of sorted DC subsets from the tonsils. PDCs are round-shaped and have a lymphoid-like morphology. The myeloid BDCA-1+ and BDCA-3+ subsets present short cytoplasmic processes and lobulated nuclei. (Bar corresponds to 10 μm).

1.4.1.1 PLASMACYTOID DENDRITIC CELLS

PDCs constitute between 1 to 2 % of peripheral blood mononuclear cells (PBMCs). They are very different from DCs. They have round plasma-cell morphology and the capacity to secret large amounts of type-1 interferons after viral encounter [77, 87, 88].

In terms of surface markers, they are distinguished by the expression of CD123 (IL-3 receptor), BDCA-2 and BDCA-4 and the lack of myeloid surface markers (CD11c and CD11b). They express the endosomal nucleic acid–sensing TLR7 and TLR9 that allow them to recognize single-stranded RNA, and unmethylated CpG-containing DNA respectively [89]. The response to these stimuli is rapid IFN secretion, which helps the activation of natural killer and B cells, establishing PDCs as a key link between innate and adaptive immunity.

PDCs circulate in the blood and enter the T cell rich areas of lymphoid organs through the high endothelial venules. Under steady-state conditions they are hardly found in peripheral tissues.

1.4.1.2 MYELOID DENDRITIC CELLS

DCs are characterized by the expression of the myeloid surface markers CD11c, CD13, CD33 and CD11b. As PDCs, they also express CD4. They do not express at the steady state CD14 or CD16 which characterize human blood monocyte subsets.

They are separated into two subsets, the BDCA-1^{+} and the BDCA-3^{+} subset (also called CD1c and CD141, respectively). In the last two years, several studies including cross-species comparisons of transcriptomic profiles, have shown that these two subsets are the equivalent of the mice myeloid subsets CD8α[-] and CD8α[+] respectively [90-93]. Nevertheless these two subsets in mice show clear functional differences that are less evident in their human counterparts.

BDCA-1[+] DENDRITIC CELLS

BDCA-1[+] DCs are the major population of human DCs. They are approximately 1% of PBMCs. Besides the typical myeloid antigens, they also express CD172 (also named SIRPα).

The expression of the TLRs 1 to 8 allows them to recognize several pathogen associated molecules as LPS, flagellin and double stranded RNAs. They express dectins 1 (CLEC7a) and 2 (CLEC6A) that account for fungi recognition, DEC205 and macrophage mannose receptor (CD206) [42]. Once activated, they are very good stimulators of naïve CD4 T cells, and are also able to cross-present antigens to CD8 T cells [91, 94].

Depending on the antigen and TLR involved, they prime different types of T cell responses, owing to their capacity to secrete different combinations of the cytokines TNF-α, IL-8, IL-10, IL-12 and IL-23 [95].

BDCA-3[+] DENDRITIC CELLS

This is the minor subset in human blood; it corresponds to 0.1% of PBMCs. The expression of the lectin CLEC9A, the chemokine receptor XCR1, the cellular adhesion molecule Necl2, and high TLR3 have identified them as the human counterpart of the CD8α[+] mouse subset [90-93, 96, 97]. Via CLEC9A, these cells have a good capacity to take up necrotic material from dead cells, and via TLR3 and 8 they can sense viral nucleic acids. Mice CD8α^{+} cells have been functionally defined as "cross-presenting" cells in opposition to the CD8α^{-} cells. Human blood BDCA-3^{+} cells can indeed cross-present antigens to CD8 T cells, but as opposed to mice, they cannot be defined as the main cross-presenting subset as the BDCA-1^{+} has a similar capacity [55, 94]. They can secrete the cytokines TNF-α, CXCL10, and IFNλ and IL-12 [41, 92, 95].

Careful attention must be taken for their isolation, as BDCA-3 surface marker can be up-regulated upon maturation by other DC subset as well [85].

1.4.2   DENDRITIC CELL SUBSETS IN THE SECONDARY LYMPHOID ORGANS

The spleen and tonsils do not receive lymphatic flux. Therefore DC subsets in these organs are more likely resident cells coming from blood. In contrast, in the lymph nodes there are resident cells coming probably form blood and cells that have migrated from the peripheral organs.

1.4.2.1   *TONSILS*

In human tonsils, DCs are found mainly in the T cell zones and also in the germinal centers. The phenotype of DC populations was first described based on the expression of HLA-DR, CD11c, CD13 and CD123 by Summers et al. [98]. The initially identified HLA-DR[mod]CD11c^{-} CD123^{+}, HLA-DR [high]CD11c^{+} and HLA-DR[mod] CD11c^{+}CD13^{+} cells turned out to be the PDCs, and the DC subsets BDCA-1^{+} and BDCA3^{+} respectively [80]. These subsets are present at frequencies of 62.9%, 32.5% and 4.6% of lineage negative mononuclear cells respectively [80]. There is also a population of CD14^{+} cells that has been shown to have a macrophage-like morphology [99]. Tonsillar human subsets express higher amounts of TLR, C-lectin, cytokine and chemokine receptors than their blood counterparts, but they still present an unactivated phenotype at the steady-state [80, 94]. The immune-cytological

morphology of tonsillar DCs is equivalent to the one of blood DCs (Figure 1-6). In contrast to blood subsets, the tonsillar subsets do not cycle, confirming the fact that they are terminally differentiated cells [99].

1.4.2.2   SPLEEN

In the human spleen, DCs correspond to less than 1% of mononuclear cells. They are found in the periphery of the white pulp, the T cell zone and also the B cell zone [100]. Due to human tissue sample availability, tonsils are better characterized than spleen. Nevertheless we know that both organs contain the same subsets of DCs and that in general, in both cases DCs are found mainly in an unactivated state and do not express costimulatory molecules [94, 99, 100].

1.4.2.3   LYMPH NODES

Human lymph nodes contain PDCs and different DC subsets in the T cell zones. Angel C. et al showed in 2009 that in human lymph nodes there were $CD209^+$ cells expressing different combinations of CD206, CD14 and CD68, and cells expressing CD1a, CD207 and CD208. He suggested that the populations expressing CD209 were resident cells in the lymph nodes and the populations expressing CD1a, CD207 and CD208 came from the periphery [101]. Therefore, this suggested that we could find lymph nodes resident DCs and DC that had emigrated from distant sites. Van de Ven et al also studied the presence of DC subsets in human lymph nodes finding two subsets ($CD1a^{hi}$ and $CD1a^{int}$) that would come from the skin and one subset ($CD1a^-CD14^-$) of resident cells [82]. A fourth subset ($CD1a^-CD14^+$) would correspond to macrophages and not to DCs.

Finally a recent work from Segura et al, showed that human lymph nodes contain six different populations of DCs [99]. The largest population corresponds to PDCs (around 80% of lineage negative and $HLADR^+$ cells). Then the $CD11c^+CD14^-$ cells (30%) can be further divided into $BDCA-1^+$, $BDCA-3^+$ (or Clec9A), $CD1a^+$, $CD206^+$ and LCs (30%, 6%, 15%, 20% and 5% of $CD11c^+CD14^-$ cells respectively). They also found $CD14^+$ cells that correspond to macrophages.

This study showed that while PDCs, $BDCA-1^+$ and $BDCA-3^+$ DCs are also found in several lymph nodes, the $CD1a^+$, $CD206^+$ and LC populations are found only in the skin-draining lymph nodes, showing that the first three populations are resident cells, and the other three correspond to populations that have migrated from the skin. They also suggested that the $CD206^+$ population found in the lymph nodes corresponds to the $CD14^+$ population present in the dermis that would lose the CD14 marker before entering the lymph node.

The resident populations have an unactivated phenotype as in the spleen and tonsils. It has been shown that these populations can capture, process and present soluble free antigens that reach the lymph nodes through the afferent lymphatics [58]. The populations coming from the skin have a more activated phenotype, they express several costimulatory molecules and the lymph node homing chemokine receptor CCR7.

1.4.3 DENDRITIC CELLS IN THE THYMUS

Little is known today about the different DC subsets present in human thymus. In 2001, Bendriss-vermare et al and Vandenabeele et al showed that human thymus contains PDCs and two subsets of mature DCs, $CD11c^+CD11b^-CD45RO^{low}$ and $CD11c^+CD11b^+CD45RO^{high}$ DCs [102, 103]. The equivalent of these subsets to the ones found in other locations is not known. The thymic DCs derive from a thymic precursor, they are present in the cortex and the medulla of the thymus where they positively and negatively select the thymocytes [104]. Therefore they are more importantly involved in the presentation of self-antigens and the induction of central tolerance.

1.4.4 DENDRITIC CELL SUBSETS IN PERIPHERAL TISSUES

DCs are present in almost all the peripheral tissues except the brain [105]. Excluding LCs, all contain the same type of DC subsets [41]. Nevertheless the best characterized peripheral tissue in humans is still the skin.

For many years, LCs were considered as the only DCs present in the skin and mucosae, until 1993 when Nestle et al defined two additional DC subsets in the dermis, the $CD1a^+$ and the $CD14^+$ dermal DCs [106]. In mice there is a population of Langerin$^+$ dermal cells, but these have not been identified in humans [107]. In steady-state conditions no PDCs are found in the peripheral tissues.

Langerhans cells are found in the basal and supra-basal layers of the epidermis and in the respiratory, gastric and vaginal tracts mucosae. They are characterized by a high expression of CD1a, the expression of CD207 (langerin) and the absence of CD14 [108].

The hallmarks of LCs are the Birbeck granules. These rod-shaped compartments contain langerin and are part of the endosomal pathway [109] [110]. No essential specific function has been attributed to these granules. Indeed, a single individual reported to lack Birbeck granules, owing to a heterozygous point mutation in langerin gene, showed no particular functional phenotype [111, 112]. Moreover some reports claimed that pig's skin epidermal LCs do not have Birbeck granules at all [113].

LCs also express adhesion molecules like CLA (cutaneous lymphocyte associated protein), Epcam and E-cadherin that mediate their adhesion to keratinocytes. They express the chemokine skin-homing receptor CCR6 and upon activation they upregulate CCR7 to migrate to the lymph nodes [114].

Dermal DCs are divided in two HLADR$^+$ subsets. The dermal CD1a$^-$CD14$^+$ and the CD1a^{dim}CD14$^-$ referred as CD14$^+$ and CD1a$^+$ cells respectively [25]. The dermal CD1a$^+$ are more or less 40% of CD45$^+$ cells in digested skin, whereas, CD14$^+$ are less abundant (less than 10%)[115].

It has been difficult to relate these dermal subsets to the BDCA-1$^+$ and BDCA-3$^+$ subsets identified in blood and in the lymphoid organs. Haniffa et al have recently tried to find these equivalences, finally describing three dermal DC subpopulations [41]. Within the Lineage$^-$ and HLA-DR$^+$ populations of the skin, they defined first a CD14$^+$ subset. Then within the CD14$^-$ cells, a subset of CD11c$^+$BDCA-1$^+$CD1a$^+$ BDCA-3 $^{+and-}$ cells and a new subset of CD11c^{lo}BDCA-1$^+$CD1a^{lo}BDCA-3^{hi} cells. In this study they suggested that these two last subsets are related to the BDCA-1$^+$ and BDCA-3$^+$ blood subsets respectively, and that the new BDCA-3^{hi} was ignored until now due to the fact that the other subsets might upregulate BDCA-3 marker as well. They found that the CD14$^+$ subset is more similar to monocytes and therefore would probably arise from this blood population.

In general, DC subsets in the tissue seem to be more activated than their blood counterparts, nevertheless it is difficult to identify if this happens in vivo or whether it is related to the different isolation protocols used.

Finally, under inflammatory conditions, the blood monocytes have been implicated in the generation of infiltrating inflammatory DCs [116]. These cells express BDCA-1, CD1a, CD206, FcεR1, SIRPα and no CD209 or CD16. They stimulate TH17 cells. Inflammatory DCs were before identified as inflammatory epidermal and iNos producing DCs (IDECS and TiPs) in atopic dermatitis and psoriasis respectively [117, 118]. They prime completely different T cell responses and therefore prove that different inflammatory DCs rise out from monocytes in different pathological conditions [119].

In summary, the final global characterization of the different human subsets of DCs has highlighted the relationship between them. Today, more than a classification that depends on an activation state, different combinations of surface markers have been defined to identify different sub-populations of DCs that are repeatedly found in several tissues. We are now able to distinguish between populations that reside in the different sites from populations that are migrating. The existence of DC subsets opens up a new field of research concerning their functional differences and their differential implications under inflammatory conditions.
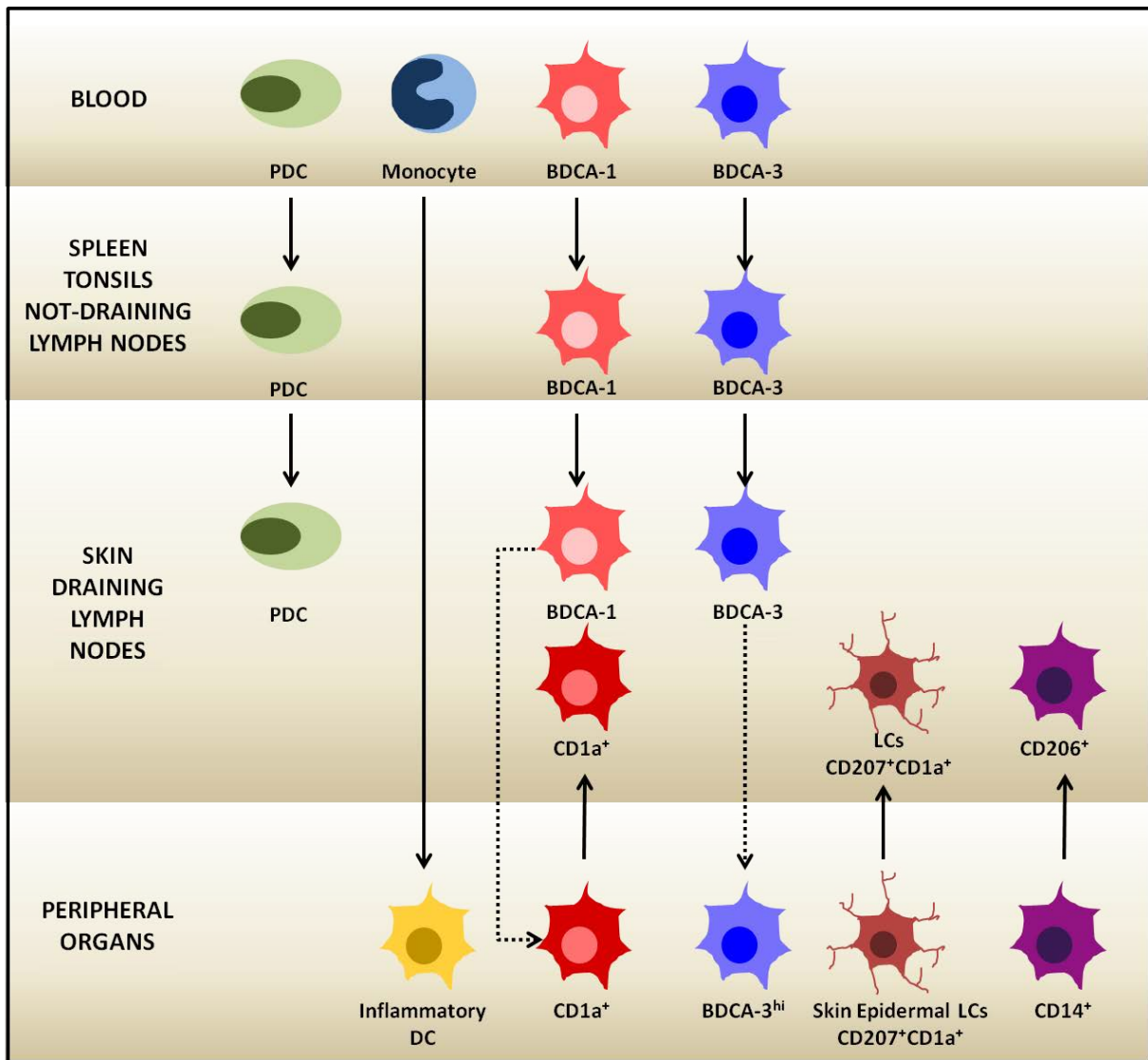
Figure 1-7: Human dendritic cell subset distribution in different anatomical sites.

Plain arrows represent direct relationships. Excepting inflammatory DCs, which have a developmental relationship with monocytes, all the other plain arrows represent relationships based on migration and homing to the different locations. Pointed arrows represent only suggested relationships.

	CD1	PRRs	ADHESION MOLECULES	CHEMOKINE RECEPTORS	FUNCTION	REFERENCES
BLOOD AND SLO BDCA-1 (CD1c)	CD1a$^-$	CLEC6a$^+$	CD11c^{hi}	CCR2$^+$	They secrete CCL3, TNFα, and IL-12 when stimulated through TLR7/8.	Mittag, D. 2011
	CD1c$^+$	CLEC7a$^+$	CD11b$^+$	CCR5$^+$	They efficiently induce Th1 and Th2 responses if they are in tonsils, but more efficiently Th1 than Th2 if they are in blood.	Segura, E. 2012
		DEC205$^+$	CD62L$^+$	CCR7$^+$ in SLO	They crosspresent if they come from tissue, the ones from blood crosspresent only if they are stimulated with TLR ligands.	Segura, E. 2012
		CD206$^+$	CLA$^+$	CXCR4$^+$ in SLO		
		TLR1$^+$		CX3CR1$^+$		
		TLR2$^+$				
		TLR3$^+$				
		TLR4$^+$				
		TLR5$^+$				
		TLR6$^+$				
		TLR7$^+$				
		TLR8$^+$				
		SIRP1a$^+$				
BLOOD AND SLO BDCA-3 (CD141)	CD1a$^-$	CLEC9a$^+$	CD11c^{lo}	CCR2$^+$ in SLO	They secrete low CCL3 and TNFα, and IL-12 when stimulated through TLR7/8	Mittag, D. 2011
	CD1c$^-$	DEC205$^+$	CD11b$^-$	CCR5$^+$	They secrete TNFα, CXCL10, IFNλ and little IL-12.	Haniffa, M. 2012; Lauterbach, H. 2010
		CD206$^+$ in SLO	MRC2$^+$	CCR7$^+$ in SLO	They efficiently induce Th1 and Th2 responses if they are in tonsils, but more efficiently Th1 than Th2 if they are in blood.	Segura, E. 2012
		TLR1$^+$	Necl2$^+$	CXCR4$^+$ in SLO	They crosspresent if they come from tissue, the ones from blood crosspresent only if they are stimulated with TLR ligands.	Segura, E. 2012
		TLR2$^+$	CD62L$^+$	CX3CR1$^+$ in SLO		
		TLR3$^+$	CLA$^+$	XCR1$^+$		
		TLR6$^+$				
		TLR8$^+$				
		MRC2$^+$				
SKIN LC	CD1a$^+$	CD207$^+$	CD11c^{lo}	CCR2$^-$	Upon CD40L stimulation, they produce IL-8 and IL-15.	Kletchevsy, E. 2008
	CD1c$^+$	DEC205$^+$	CD11b$^-$	CCR5$^-$	Efficient crosspresenting capacity.	Kletchevsy, E. 2008
		CD206$^-$	Epcam$^+$	CCR6$^+$	They stimulate effitiently naïve CD4 and CD8 T cells. They induce preferentially Th2 responses.	Kletchevsy, E. 2008
		CD208$^+$	E-cadherine$^+$	CCR7^{lo}	Possible role in tolerance. They induce proliferation of autologous memory Tregs.	Seneschal, J. 2012
		CD209$^-$		CXCR4$^+$	When stimulated with VitD3 they induce TGF-β -secreting Tregs.	van der Aar, A.M. 2011
		CLEC9a$^-$		CX3CR1$^+$	Induction of TH17 response	Mathers, A.R. 2009
		TLR1$^+$			Induction of Th22 response	Fujita, H. 2009
		TLR2$^+$				
		TLR3$^+$				
		TLR6$^+$				
		TLR7$^+$				
		SIRP1a$^+$				
SKIN CD1A	CD1a$^+$	DEC205$^+$	CD11c$^+$	CCR2$^-$	Upon CD40L stimulation, they produce IL-8 and IL-15.	Kletchevsy, E. 2008
	CD1c$^+$	CD206$^+$	CD11b$^+$	CCR5$^+$	Efficient crosspresenting capacity.	Kletchevsy, E. 2008
		CD208$^+$		CCR6$^-$	They stimulate effitiently naïve CD4 and CD8 T cells. They induce preferentially a Th2 reponse. Their phenotype is intermediate between LCs and CD14$^+$ dermal DC.	Kletchevsy, E. 2008
		CD209$^-$		CCR7$^+$		
		CLEC9a$^-$		CXCR4$^+$		
		TLR1$^+$				
		TLR2$^+$				
		TLR3$^+$				
		TLR6$^+$				
		TLR7$^+$				
		SIRP1a$^+$				
SKIN CD14	CD1a$^-$	DEC205$^+$	CD11c$^+$	CCR2$^-$	Upon CD40L stimulation, they produce IL-1β, IL-6, IL-8, IL-10, IL-12, TGF-β, TNFα and GM-CSF.	Kletchevsy, E. 2008
	CD1c$^+$	CD206$^+$	CD11b$^+$	CCR7^{lo}	They prime CD4 T cells to induce isotype switch on naïve B cells and Igs secretion.	Kletchevsy, E. 2008
		CD209$^+$		CX3CR1$^+$	They do not stimulate efficiently naïve CD4 and CD8 T cells	Kletchevsy, E. 2008
		CLEC9a$^-$			Poor crosspresenting capacity.	Kletchevsy, E. 2008
		TLR1$^+$				
		TLR2$^+$				
		TLR3$^+$				
		TLR6$^+$				
		TLR7$^+$				
		SIRP1a$^+$				
SKIN BDCA3	CD1a^{lo}	CLEC9A$^+$	CD11c^{lo}	XCR1$^+$	Efficient crosspresenting capacity.	Haniffa, M. 2012
	CD1c$^+$	TLR3$^+$				
INFLAMMATORY DC	CD1a$^+$	CD206$^+$	CD11c$^+$		They produce IL-1, IL-6, TNFα, IL-12, IL-23.	Segura, E. 2013
	CD1c$^+$	FcεR1$^+$	CD11b$^+$		They can prime Th1 and Th2 responses in atopic dermatitis (IDECS) and Th1 and Th17 responses in psoriasis.	Nakano, K.L. 2009; Hammad, H. 2010
		SIRP1a$^+$			In sinovial and ascitis fluids from reumathoid arthritis and cancer patiens they induce Th17 responses.	Segura, E. 2013

Table 1-1 : Dendritic cell subset phenotypes at steady state.

Transcriptomic profiles have given rise to complete phenotypes of the human DC subsets. In this table we present the major characteristic CD1, PPRs, adhesion molecules and chemokine receptors of each subset. The black color means protein expression, red color means RNA expression. (PRR, pattern recognition receptors; SLO, secondary lymphoid organs).

1.4.5 DIFFERENT SUBSETS SUGGEST DIFFERENT FUNCTIONS

As the study of different subsets of DCs in human blood and tissues samples evolved, several attempts to link the phenotypic differences to different functions and T cell profile induction have been made.

In mice, functional specializations have been attributed to the different DC subsets. For example CD8α^+ and CD103$^+$ subsets are specialized in the activation of CD8$^+$ T cells [120]. These two subsets are also enabled with the capacity to cross-present antigens. In the case of CD4$^+$ T cell priming, the different mice subsets CD8α^+, CD8α^-, CD103$^+$ and LCs show different behaviors depending on the signal triggering the DC activation [120]. Nevertheless it has been shown that adoptive transfer of antigen-pulsed CD8α^+ versus CD8α^- DCs differentially induces Th2 versus Th1 responses [121, 122]. Moreover, it has been shown that targeted CD8α^+ and CD8α^- DCs induce CD8$^+$T and CD4$^+$T cell responses respectively [123].

In humans, it is clear that PDCs are more involved than DCs in antiviral responses. Moreover, already in 1999, Rissoan et al. established, for the first time, a direct link between different sup-populations of DCs (DC1 and DC2) and different T helper cell profiles (Th1 and Th2) [124]. Nevertheless the DC subsets have overlapping functions concerning cross-presentation, tolerance induction and Th1, Th2, Treg, and Th17 primings. The functional differences between human DC subsets are less clear than in murine model. A summary of the overlapping functions of human DC subsets is shown in Table 1-1.

In the case of skin DCs, there is evidence that functional differences between LCs and dermal CD14$^+$ cells exist. For example, Kletchevsky et al, compared functionally human skin subsets [25]. They found that CD14$^+$ dermal DCs stimulated with CD40 secrete IL-1α, IL-6, IL-8, IL-10, IL-12 GM-CSF and TGF-β, whereas LCs stimulated with CD40 only secrete IL-15 and small amounts of IL-8. Even if LCs and CD14$^+$ DCs were both able to induce naive B cell production of IgM, CD14$^+$ and not LCs were able to induce isotype switching to IgG and IgA. On the other hand LCs stimulated better naïve CD4$^+$T cell proliferation than CD14$^+$ cells, and primed a Th2 cell response. They were also found to be more efficient in the induction of antigen specific CD8$^+$Tcells and cross-presentation. Moreover, it was later shown by the same authors that LCs stimulated a better cytotoxic response through the secretion of IL-15 while IL-10 and TGF-β secreted by dermal CD14$^+$ inhibited this response [125]. These studies suggest that dermal CD14$^+$ cells preferentially activate B cells while LCs preferentially prime a Th2 cell response.

In tolerance induction, LCs and dermal cells were also found to behave differently. LCs were shown to induce a higher proliferation of autologous memory Treg cells than the dermal DCs [126]. Concerning Th17 differentiation controversial results were found. Mathers et al showed that LCs had a superior capacity than dermal DCs in the generation of Th17 cells [127], yet, Fujita et al found no Th17 induction by LCs but the induction of IL-22 secreting T cells [128]. In general several functions have been attributed to LCs [127-129]. Controversial results are often attributed to different protocols of isolation of the skin DCs.

In the case of blood BDCA-1^{+} and BDCA-3^{+} subsets, the cross-presenting capacities have been extensively evaluated giving rise to controversial results. First, the comparison between human blood BDCA-1^{+} and BDCA-3^{+} subsets let to the conclusion that after activation with a TLR3 ligand, poly-IC, BDCA3^{+} cells were specialized in antigen cross-presentation [41, 90, 91, 130]. Secondly, tonsillar BDCA3^{+} cells were also found to be more efficient at cross-presenting death associated antigens than the BDCA-1^{+} counterpart. These results led to the conclusion that BDCA-3^{+} cells as the murine CD8α^{+} cells were specialized in cross-presentation. As non activated DCs are have a poor cross-presentation capacity [94], these results were obtained activating DC subsets with TLR3 ligands that preferentially stimulate BDCA-3^{+} cells. Therefore, Segura et al, used tonsillar BDCA-1^{+}and BDCA-3^{+} subsets (which are *per se* more activated than the blood counterparts) and showed that both cell subsets are equally able to cross-present soluble antigens in the absence of additional activation stimuli [94]. This result was further confirmed by two other studies showing that these subsets have the same cross-presenting capacities but different TLR stimulation requirements [131, 132].

These studies infer that human DC subsets overlap in their functions, and that the functional specialization of DC subsets can be in part attributed to their differential capacities to sense single stimuli. Uncoupling differential activation of DC subsets induced by the signals of the microenvironment (e.g. TLR activation requirements) from their functional specializations remains a big challenge. Another factor to take into account is the isolation procedure. Different protocols of DC isolation result often in controversies as it is the case of Th17 induction by LCs. DC functional differences are mainly evaluated in the context of the T cell responses. However differential DC subset secretion of cytokines and chemokines may mediate different innate immune responses.

To study the functional differences between human DCs cell subsets stimulatory signals that activate the DC subsets to the same extent must be used. One of these stimulatory signals could be the cytokine TSLP. To address functional differences between blood BDCA-1^{+} and BDCA-3^{+} DCs, I used TSLP as a model of inflammatory tissue factors. Therefore the following chapters of my introduction will address our current knowledge on human TSLP biology, and its role in the immune system through the activation of DCs.

1.5 THYMIC STROMAL LYMPHOPOIETIN BIOLOGY IN HUMANS

TSLP is a cytokine secreted by epithelial cells and keratinocytes at the barrier surfaces like the skin and the mucosa. It is detected in atopic dermatitis lesional skin and not in healthy skin or non-lesional skin; this highlights its important role in allergic disorders [133]. In humans the main responders to this cytokine are the DCs [134]. TSLP primed DCs (TSLP-DCs) induce Th2 cells and are closely linked to the initiation of the allergic immune responses [133]. Nevertheless a homeostatic role has been attributed to TSLP -DCs in the thymus and the periphery [135, 136]. Although mice studies have greatly helped us to understand TSLP role in the immune system, TSLP biology in humans differs in comparison to the mouse model.

The purpose of this chapter is to review the knowledge gathered until now about human TSLP and its implications in health and disease. I will present first TSLP and TSLP receptor characteristics followed by TSLP effects on DCs and its role in allergic disorders and immune tolerance. At the end I will present in depth two main studies addressing TSLP –treated PDC and DC functions in immune tolerance and TSLP-treated LC implication in allergy.

1.5.1 TSLP AND TSLP RECEPTOR

TSLP was first identified in the supernatants of a murine thymic stromal cell line. It was described as a factor supporting B cell growth and thymocyte survival [137]. Later on, this factor was cloned in mice and humans and defined as a member of the hematopoietic cytokines family [134, 138, 139]. The homology between the human and mouse protein was found to be poor (43% of the amino acid sequence) [134]. In humans, TSLP messenger RNA was identified in skin keratinocytes, lung fibroblasts, bronchial epithelial cells, mammary epithelial cells, smooth muscle cells and activated mast cells [133]. By inmmunohistological techniques, TSLP has been found in the crypts of the tonsillar epithelium, the Hassals corpuscles in the thymic stroma and the apical layers of lesional skin in atopic dermatitis [133, 135].

The TSLP receptor was cloned in mice and humans as a heterodimeric receptor constituted by the TSLPR chain and the IL-7Rα chain [140, 141]. It was found that TSLP binds to its receptor with high affinity only if the two chains are expressed. Moreover, the IL-7Rα chain is needed to trigger an intracellular signal [141]. In the case of TSLPR the homology between mice and humans was also found to be poor (39% aminoacid sequence).

The TSLP receptor complex has a restricted expression. Both chains of the receptor are expressed mainly by dendritic cells [134]. It has been reported that CD4T cells can also respond to TSLP in vitro [142]. Although this has been well established in mice, in humans CD4T cells do not seem to co-express both chains of the receptor, or do it very poorly considering the levels reached by DCs [134].

TSLP signaling pathway implicates the phosphorilation of STAT3 and STAT 5 [143]. These factors are activated by several other cytokines. In the case of human DCs, TSLP activates the JAK-STAT pathway by inducing the phosphorilation of janus activating kinases 1 and 2. It was shown that it also induces the phosphorilation of STAT 1, 4 and 6, AKT, and the MAPKs ERK and JNK. Finally it triggers the nuclear translocation of the NF-κB members, p50, p52 and RelB [143]. However the study of TSLP receptor signaling on human primary DCs is very difficult due to the scarcity of these cells and the detailed signaling pathway is still unknown. A recent study by Pandey et al on a murine pro-B cell line (Ba/F3) transfected with the human TSLPR complex implicates additional molecules in the signaling pathway of TSLP [144]. This last study suggest that different members of the Src and Tec kinases families (Btk, Lyn and Tec), and the protein phosphatases Ptpn6 (Shp-1) and Ptpn11 (Shp2) participate in the protein complex activated downstream TSLP signaling.

1.5.2   TSLP EFFECTS ON HUMAN DENDRITIC CELL FUNCTION

TSLP strongly activates DCs in vitro. It triggers the up regulation of MHC class I molecules and of costimulatory molecules CD80, CD83, CD86 and CD40 [133]. It also enhances DC survival in culture. TSLP-DCs, as opposed to LPS, CD40L or IL-7 treated DCs do not secrete IL-12, IL-6 or IL-1 α/β, cytokines described as Th1 polarizing signals. Instead, they were shown to produce large amounts of the chemokines CCL17 (TARC) and CCL22 (MDC), IL-8 and eotaxin-2 known to recruit Th2 cells, neutrophils and eosinophils respectively [133]. Moreover, TSLP-DCs induce a potent proliferation of allogenic naïve CD4 T cells in vitro and the primed T cells produce high levels of IL-4, IL-5 and IL-13 compared to DCs stimulated with LPS, CD40L or IL7 [133]. These T cell cytokines are characteristic of the Th2 profile. Nevertheless, this Th2 profile is unconventional as CD4 T cells primed by TSLP-DCs do not secrete IL-10 but considerable levels of TNF-α. Therefore, as opposed to a conventional Th2 profile it has been named "inflammatory Th2 profile" [133]. In the context of allergic inflammation, IL-10 is recognized as an anti-inflammatory cytokine whereas TNF-α is one of the most potent pro-inflammatory cytokines involved [145, 146]. Thus the inflammatory Th2 cells primed by TSLP-DCs have a critical role in the development of uncontrolled allergic inflammation.

It has been shown that TSLP-DCs capacity to induce the inflammatory Th2 profile is mediated by the up-regulation of the surface molecule OX40L [147] (Figure 1-8). Indeed, the use of a neutralizing antibody against OX40L changed the T cell profile induced by TSLP-DCs to a profile characterized by the absence of Th2 cytokines and TNF-α and the secretion of IL-10. The current model proposes that the OX40L expression by human TSLP-DCs in the absence of IL-12 secretion, induces the secretion of the Th2 cytokines and TNF-α, whereas, the presence of IL-12 induces a Th1 profile and the subsequent production of IL-10 [143]. The IL-12 production is dependent on the activation of STAT4 and interferon regulatory factor 8 which are not induced by TSLP. In contrast, OX40L promoter has NF-κB binding

sites, and it is known now, that is the p50 unit that mediates its transcription upon TSLP binding [143](Figure 1-8).

In conclusion, TSLP generates an environment for Th2 response development, first, by inducing Th2-attracting chemokines, and second, by inducing Th2 cells through the up-regulation of OX40L in the absence of IL-12.
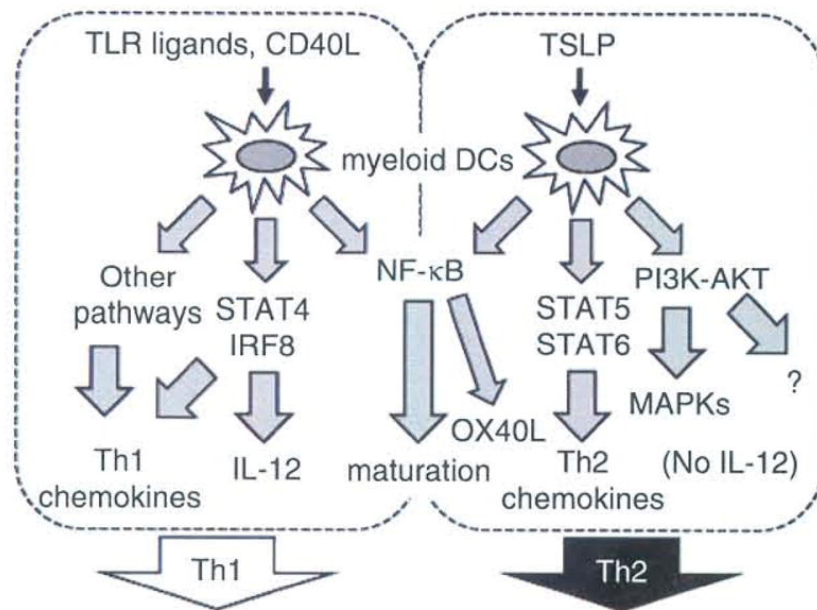
Figure 1-8 : TSLP induces a Th2 profile. Adapted from Ito, T. et al 2012.

TLR ligands and CD40L induce the activation of STAT4 and IRF8 leading to the secretion of IL-12 and the priming of a Th1 response. By contrast TSLP does not induce STAT4 and IRF8 activation. It induces OX40L in an Nf-κB dependent way; in the absence of IL-12, OX40L triggers a Th2 response. Through STAT5 and 6 activation, TSLP triggers the secretion of CCL17 and CCL22 chemokines, characterizing further the Th2 response.

1.5.3   TSLP AND ALLERGIC DISORDERS

The different allergic states are characterized by an exaggerated immune response against a harmless antigen. The type of T cell response linked to allergy is the previously mentioned Th2 response.

TSLP has been linked for a long time to different allergic disorders. First, because it was found to be present in the skin lesions of patients suffering from atopic dermatitis and second because it induces an inflammatory Th2 response [133]. Moreover, the human TSLP gene is found close by the Th2 cytokine gene cluster locus [134].

TSLP production has been reported not only in atopic dermatitis, but also in other allergic disorders such as atopic asthma [148], allergic rhinitis [149] and atopic keratoconjuntivitis [150].

In the case of atopic dermatitis, elevated serum TSLP levels were reported in children [151] although it has not been possible to detect TSLP in adult serum. In the case of atopic asthma, TSLP has been reported in the broncoalveolar fluids of the patients, correlated with the severity of the disease [148], but it is not known if the levels in serum are elevated. Allergic rhinitis is often linked to asthma. It has been reported that TSLP is produced in these patients in the airway mucosa [149]. Finally in atopic keratoconjuntivitis, TSLP is produced by the epithelial cells of the cornea [150].

In the case of all these allergic disorders, TSLP-DCs first help in the recruitment of Th2 cells through the secretion of CCL17 and CCL22. The chemokines IL-8 and eotaxin-2 attract also neutrophils and eosinophils to the site of inflammation. TSLP also activates mast cells to produce Th2 cytokines in the presence of IL-1β and TNF-α [152]. These initial steps already trigger an innate phase of allergic inflammation. Then, once in the secondary lymphoid organs TSLP-DCs prime naïve $CD4^+$ and $CD8^+$ T cells towards inflammatory Th2 cells that will be further recruited to the inflammatory site [133, 153] (Figure 1-9).

The regulatory factors that trigger TSLP production are slowly being elucidated. Today we know that TSLP promoter has NF-kB binding sites and that its expression is NF-kB-dependent. Indeed, TNF-α and IL-1β can induce TSLP production by human airway epithelial cell lines in an NF-κB dependent way [154]. This effect can be promoted also by the Th2 cytokines IL-4 and IL-13 that synergize with TNF-α and IL-1α to induce the TSLP secretion [155]. Moreover, 9is –retinoic acid blocks the binding of NF-κB to human TSLP promoter and therefore the induction of TSLP by IL1-β on human epithelial cells [156]. *Staphylococcus Aureus* membrane has been shown to induce TSLP production by human keratinocytes in a TLR-2/6 dependent way [157]. However the mechanism of this induction and the implication of NF-kB pathway in this process are unknown.

In mice, it has been shown that the in skin keratinocytes TSLP production is regulated by the vitamin D receptor and the retinoic X receptor complex. This complex represses the production of TSLP. It was shown that vitamin D treatment, leads to vitamin D receptor binding and separation from retinoic X receptor therefore blocking the transcription repression function of the complex, triggering TSLP production and the development of an atopic dermatitis phenotype [158]. In line with these findings, in humans, the topical administration of Vitamin D3 analogues induces TSLP production in human psoriatic skin lesions [159].

These results would imply that Vitamin D treatment or oral supplementation could increase the risk of developing TSLP-related allergic disorders. However the different clinical studies linking Vitamin D3 treatment and serum levels to the development of allergy have given controversial results [160]. In many cases researchers have found that the serum levels of Vitamin D are inversely correlated to asthma and atopic dermatitis and its severity. Other studies have shown that high doses of Vitamin D might, on the contrary, contribute to the

development of atopic diseases [160]. Moreover Vitamin D has been shown to induce the production of the antimicrobial peptide LL-37 that has been shown to inhibit TSLP production by poly-IC treated keratinocytes [161]. These studies show that Vitamin D may be implicated in the development of allergy at different levels, and that further larger prospective and controlled trials are required to conclude on the benefits and disadvantages of Vitamin D treatment in the context of TSLP-linked allergic disorders.

Besides LL-37, the Th17 cytokines IL-17A and IL-17F have been also shown to inhibit TSLP production by human skin explants; furthermore, Th17 polarizing cytokines inhibit the Th2 response induced by TSLP primed-DCs [162] suggesting that there might be several different factors that inhibit TSLP production.

Even if the initial regulation factors leading to TSLP secretion by keratinocytes and epithelial cells are not fully understood, the link between TSLP and allergic disorders is clear enough today to justify the development of two blocking antibodies against TSLP that are currently been tested by two pharmaceutical societies (MERCK and AMGEN) in phase I trials.
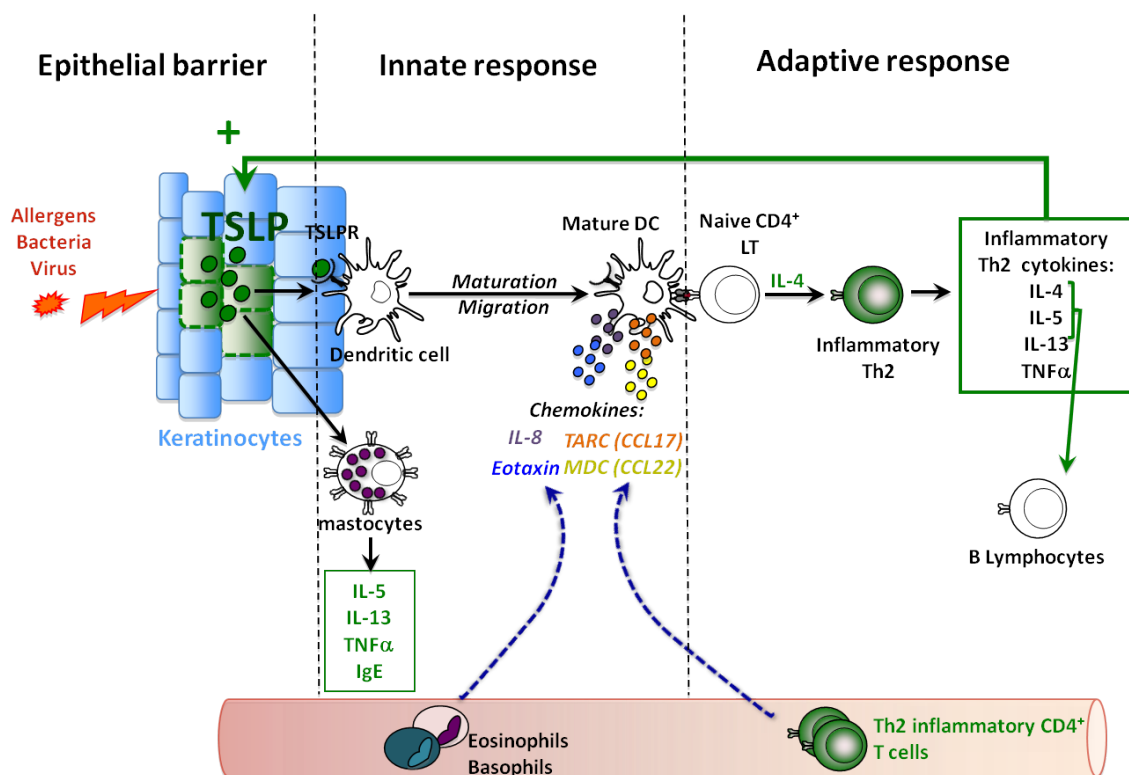
Figure 1-9: TSLP role in allergic disorders. (Adapted from Delost, M. unpublished)

Allergen and antigen activated keratinocytes secrete TSLP. Mast cells are activated by the allergen and the TSLP and secrete proinflammatory Th2 cytokines. Upon TSLP activation DCs secrete chemoattractant chemokines that help in the recruitment of eosinophils, basophils and Th2 inflammatory CD4T cells. TSLP-stimulated DCs mature and migrate to the secondary lymphoid organs to prime an inflammatory Th2 response. The inflammatory cytokines IL-4, and TNF-α induce further TSLP secretion by the skin keratinocytes. The Th2 cytokines are implicated in the activation of B cell and the secretion of IgE.

1.5.4 TSLP AND IMMUNE HOMEOSTASIS

It has been suggested that TSLP also has an important role in the maintenance of the immune homeostasis.

TSLP is found in the Hassall corpuscles in the human thymic medulla. These structures are constituted by thymic epithelial cells, and it has been suggested that it is the place where dead thymocytes are removed and developing thymocytes mature [135]. Moreover, human thymic DCs can be activated by TSLP. It has been suggested that such TSLP activated DCs in the thymic medulla have an essential role in the selection of self-reacting thymocytes and the development of T regulatory cells [135]. Indeed isolated human thymic DCs form prolonged conjugates with autologous CD4 T cells, secrete IL-2 and bind CD28, all features required for T regulatory cells generation [135]. Moreover TSLP-DCs in contrast to IL-7, CD40L, or poly-IC activated DCs induce the expansion of human single positive thymocytes and their differentiation to T regulatory cells characterized by the expression of the transcription factor forkhead box 3 (FoxP3)[135].

In the periphery, under physiological conditions, TSLP is found in the epithelial crypts in the human tonsils in close link to activated CD208$^+$ (DC-LAMP) activated DCs [136] . TSLP-DCs specifically induce the expansion of autologous naïve CD4T cells in the absence of other antigens. The resulting T cells have a central memory T cell phenotype (CD45RO$^+$CCR7$^+$CD27$^+$CD62L$^+$) and the potential to be further differentiated to Th1 or Th2 cells. This suggests that TSLP plays an important role in the maintenance of peripheral T cell homeostatic expansion [136].

This hypothesis is further supported by several studies in mice showing that TSLP can promote the differentiation of FoxP3$^+$ T regulatory cells in the periphery and the thymus [163, 164]. Finally in mice, it has also been shown that TSLP is important to maintain gut homeostasis [165, 166].

1.5.5 TSLP AND DENDRITIC CELL SUBSETS

Most of the information about TSLP effects on DCs comes from studies on total blood DCs. I have already discussed that the DC population is heterogeneous. The different DC subsets could have specific roles in the development of the TSLP-linked allergic response or the TSLP induced immune homeostasis. Nevertheless there are no studies assessing particularly the differential effects of TSLP in DC subsets. There are only two studies that address, independently and not comparatively, TSLP effects on different types of DCs. First a study by Hanabuchi et al on human thymic PDCs [167] , second a study by Ebner et al on human LCs [168]. These studies will be described in the following chapters.

1.5.5.1 TSLP-STIMULATED PLASMACYTOID DENDRITIC CELLS

Shino Hanabuchi and colleagues, showed that human blood PDCs expressed constitutively IL-7Rα and upon stimulation with TLR-7 and TLR-9 ligands (R848 and CpG-B), they expressed TSLPR chain as well. Other stimuli as IL-3 and CD40L, CpG-C, Herpes simplex virus, or influenza A also induced the TSLPR chain up-regulation, highlighting that activated PDCs can express the complete TSLP receptor complex. They showed that upon TSLP stimulation, these cells further up-regulated costimulatory molecules and secreted CCL17 and CCL22. Although, consistent with their nature they still produced large amounts of IFN-α. They assessed the function of TSLP treated PDCs (TSLP-PDCs) in vitro and showed that they induced the expansion and differentiation of thymocytes into $FoxP3^+$ T regulatory cells. Moreover, besides the results obtained after culture, they showed that thymic PDCs expressed TSLP receptor complex at the steady state and co-localized with T regulatory cells in the human thymic medulla. These results position TSLP-PDCs as important players in the development of central immune tolerance.

Interestingly, in this article they compared the T regulatory cells generated by TSLP-DCs and the TSLP-PDCs, and showed that the first ones preferentially induced $IL-10^{lo}$ TGF-β^{hi} T regulatory cells, whereas the later induced an opposed phenotype, $IL-10^{hi}$ TGF-β^{lo} [167]. These two different types of T regulatory cells had been already identified in the human thymus and the periphery [169]. Although TSLP-DCs and TSLP-PDCs could contribute differentially to their generation, the aim of this publication was not to compare differential effects of TSLP on DCs and PDCs. The stimulation of PDCs by TSLP required a previous TSLPR induction by different TLR ligands that were not systematically applied to DCs. Therefore there is no evidence that the differential induction of Tregs by TSLP-DCs and TSLP-PDCs relies on differential effects of TSLP in these populations. The fact that PDCs get further activated by TSLP treatment and secrete CCL17 and CCL22 together with the capacity of both, TSLP-PDCs and TSLP-DCs to induce Tregs cells shows that TSLP function is conserved in DCs and PDCs and highlights more similarities than differences in TSLP effects on these populations.

1.5.5.2 TSLP- STIMULATED LANGERHANS CELLS

Susanne Ebner and colleagues studied TSLP effects on human skin LCs. The aim of their study was to validate previous TSLP effects observed on blood DCs [133] in primary LCs.

They used two different protocols to isolate the human skin LCs. One protocol of epidermis digestion followed by $CD1a^+$ selection, gave rise to "freshly-isolated LCs". These cells were further treated with or without TSLP or GM-CSF. In the second protocol LCs were allowed to emigrate from cultured human skin epidermal explants for three days in the presence or absence of TSLP. This resulted in "migratory LCs" [168].

In this study, they showed that after TSLP stimulation, freshly-isolated LCs had an increased survival at 48h in comparison with GM-CSF stimulated LCs or unstimulated ones. Upon TSLP treatment, freshly-isolated LCs cells up-regulated the costimulatory molecules CD86 and CD83. They already expressed CD40 and CD80 before TSLP stimulation and no further up-regulation was observed upon TSLP.

The "migratory LCs" had a fully activated phenotype even in the absence of TSLP; they strongly expressed CD86, CD83, CCR7, and CD40. Nevertheless CD80 was the only co-stimulatory molecule still further up-regulated by TSLP treatment in agreement with the pervious results on TSLP-DCs [133].

In allogeneic mixed leukocyte reaction experiments, they did not see significative differences in T cell proliferation between migratory LCs in the presence or absence of TSLP. The freshly-isolated LCs stimulated with TSLP for 48 hours, had a higher immunostimulatory capacity than GM-CSF stimulated LCs or unstimulated ones on the same experiments. The different behavior of migratory LCs and freshly-isolated LCs in this experiment is certainly due to the fact that emigrated LCs have since the beginning, an activated phenotype and the differences between TSLP-treated or untreated LCs become less clear.

The migratory LCs in the presence or absence of TSLP were further evaluated for their capacity to produce CCL17 and IL-12. Migratory LCs, un-stimulated, or stimulated with either TSLP or CD40L secreted CCL17. Stimulation with TSLP and CD40L resulted in a higher level of CCL17 and in any of the cases they found production of IL-12. In co-culture experiments with naïve CD4 T cells, they found that TSLP-treated migratory LCs induced a Th2 polarization that was higher than in the absence of TSLP.

Finally in this study they see that emigrated LCs in the presence of TSLP are more abundant. They suggested that TSLP induced the migration of LCs from the skin, in accordance to what had been proposed before by Soumelis et al, [133]. Yet, the authors conclusions are based on indirect observations, in particular, they did not compare TSLP treated and untreated LCs in migration experiments. In their experiments, the higher counts of LCs emigrating from the skin in the presence of TSLP can be related to TSLP effects on LC survival.

The results from Ebner et al. show that TSLP-treated primary LCs behave in a similar way than TSLP-DCs. Nevertheless the authors did not compare in their experiments TSLP-LCs and TSLP-DCs.

Although in these two studies, Hanabuchi, et al. and Ebner et al., addressed TSLP effects in PDCs and LCs they do not allow us to conclude on the differential effects of TSLP on human DC subsets. Furthermore no evidence allows us to conclude on TSLP induction of DC migration. These were the subjects that I decided to address specifically during my PhD thesis, using a combination of specific and large-scale approaches.

2   OBJECTIVES

In this introduction, I summarized the essential role that DCs play in the organization and the response of the immune system; from the early studies that resulted in their identification to their ontogeny and the recent description of different subtypes in several sites of the human body. I also reviewed the studies suggesting that the different DC subsets have different functions. Nevertheless I pointed out that functional specialization of DC subsets in humans is not as clear-cut as in the mouse system and that we need to look further for specific different functions of human DC subsets the immune system.

Owing to its strong capacity to activate DCs, TSLP is directly linked to DC biology. I summed up our current knowledge about human TSLP biology and reviewed the mechanisms implicated in TSLP-DCs induction of Th2 responses. Nevertheless we don't know if and how TSLP instructs the DCs to migrate to the lymph nodes to meet the naïve T cells.

DC subsets might differentially participate in the development of TSLP-linked allergic disorders or in the maintenance of the immune homeostasis. Still we do not know if different DC subsets can respond to TSLP and if they respond in the same way.

In this context, I decided to focus my PhD work on:

1- The differential effects of TSLP on different subtypes of DCs.

2- The induction of DC migration by TSLP.

3- The mechanisms implicated in TSLP-DC migration.

The study of the differential effects of TSLP on DC subsets led me to the observation that TSLP induced a particular skin-homing pattern of chemokine receptors on blood BDCA-1$^+$ DCs. These findings led me to explore if TSLP was implicated in the recruitment of skin-DC precursors or the generation of skin-DCs under inflammatory conditions. I found that TSLP in combination with TGF-β induced the differentiation of blood BDCA-1$^+$ cells into LCs. This work will be presented as a submitted manuscript, in the first section of the results chapter.

I joined an ongoing project, in the team of V. Soumelis, that addressed whether TSLP could trigger human DC migration or not. By directly assessing the migratory capacity of TSLP treated DCs in comparison to other activating stimuli; we showed definitive evidence of the induction of migration of DCs by TSLP. These results will be presented as a published article, in the second section of the results chapter.

As a further step, I decided to study which were the molecular mechanisms implicated in TSLP-induced DC migration. I explored the involvement of chemokines and their receptors in this process. These results will be presented as a manuscript in preparation in the third and last part of the results chapter.

MATERIALS AND METHODS

DENDRITIC CELL ISOLATION

Dendritic cell isolation from human blood

Buffy coats were obtained from healthy adult blood donors at the Saint Louis hospital site of the "Etablissement Français du Sang". PBMC's were isolated by Ficoll density gradient centrifugation (Ficoll-Paque; GE Healthcare). Total DC fraction was enriched using the Pan-DC Enrichment kit (EasySep; Stem cell). Total DCs, (Lineage$^-$ CD11c$^+$ CD4$^+$) and DC subsets, (Lineage$^-$ CD11c$^+$ CD4$^+$ BDCA-1$^+$ or Lineage$^-$ CD11c$^+$ CD4$^+$BDCA-3$^+$) were purified to 99% by FACS sorting (ARIA II BD).

Dendritic cell isolation from human tonsils

Tonsils from healthy patients undergoing tonsillectomy were obtained from the "Hôpital Necker" (Paris, France) in accordance with hospital ethical guidelines. Samples were cut into small fragments, digested with 0.8 mg/ml Collagenase IV (Worthington) in the presence of 25 ug/ml DNase (Roche) for 15 min at 37°C in CO_2 –independent medium (Gibco). After incubation the supernatant was recovered and the digestion was repeated 2 or 3 times. The remaining tissue was filtered on a 40-µm cell strainer (BD) and washed in PBS. Light density cells from this suspension were isolated by Ficoll density gradient centrifugation (Ficoll-Paque; GE Healthcare). DCs were enriched by depletion of cells expressing CD3, CD15, CD19, CD56, CD14 and CD235a using antibody-coated magnetic beads and magnetic columns according to the manufacturer's instructions (Miltenyi Biotec). Tonsillar DCs subsets, (Lineage$^-$ CD11c$^+$ CD4$^+$ BDCA-1$^+$ or Lineage$^-$ CD11c$^+$ CD4$^+$BDCA-3$^+$) were purified to 99% by FACS sorting (ARIA II BD).

FLOW CYTOMETRY

Nonspecific binding and cell adhesion were blocked using PBS supplemented with 1% human serum (BioWest) and EDTA 2mM (Gibco). Cells were stained for 15 minutes at 4 degrees with different combinations of specific antibodies or their isotype-matched control antibodies. DAPI was always added before acquisition in a LSRII or Fortessa (BD) analysers. Data were analyzed with FlowJo software (Tree Star). The list of the antibodies used during this study is presented in the following table.

Antibody	Fluorochrome	Company		Antibody	Fluorochrome	Company
Annexin	FITC	R & D		anti-CD3	FITC	BD
anti-BDCA-1	PE	BioLegend		anti-CD34	PE	BD
anti-BDCA-1	PerCP eFluor 710	eBioscience		anti-CD4	PECY5	Immunotech
anti-BDCA-3	APC	Miltenyi		anti-CD4	APC	Miltenyi
anti-BDCA-3	PE	Miltenyi		anti-CD4	VIOB	Miltenyi
anti-BDCA-3	Vioblue	Miltenyi		anti-CD4	VioGreen	Miltenyi
anti-CCR1	AF647	BioLegend		anti-CD40	FITC	BD
anti-CCR2	AF647	BioLegend		anti-CD45	APCCY7	BD
anti-CCR4	PECY7	BD		anti-CD64	FITC	BD
anti-CCR5	AF647	BioLegend		anti-CD80	FITC	BD
anti-CCR6	APC	BD		anti-CD80	AF700	ExBIO
anti-CCR7	FITC	BD		anti-CD83	FITC	BD
anti-CD11b	PECY7	BioLegend		anti-CD83	PERCP/CY5.5	BioLegend
anti-CD11c	APC	BD		anti-CD83	FITC	BD
anti-CD11c	PE	BD		anti-CD86	FITC	BD
anti-CD11c	PECY5	BD		anti-CX3CR1	BIO	eBioscience
anti-CD11c	PECY7	BioLegend		anti-CXCR1	APC	BD
anti-IL7Rα	FITC	eBioscience		anti-CXCR2	FITC	BioLegend
anti-IL7Rα	PE	eBioscience		anti-CXCR3	APC	BD
anti-CD14	FITC	BD		anti-CXCR4	PECY7	BioLegend
anti-CD14	QDOT605	Invitrogen		anti-E-cadherine	APC	R & D
anti-CD16	FITC	BD		anti-EpCAM	PerCP/Cy5.5	BioLegend
anti-CD19	FITC	Miltenyi		anti-FcεPRI	PE	eBioscience
anti-CD1a	FITC	BD		anti-HLA-DR	AF700	BioLegend
anti-CD1a	PECYY5	BD		anti-HLA-DR	APC eFluor 780	eBioscience
anti-CD206	APC	BioLegend		anti-TSLPR	APC	Biolegend
anti-Langerin	PE	Immunotech		anti-TSLPR	PE	eBioscience
anti-Langerin	FITC	Miltenyi		Streptavidin	PECY7	eBioscience
anti-CD209	BIO	Miltenyi				

Table 3-1 : List of the antibodies used during this study.

CELL CULTURE

DC subsets from blood and tonsils were seeded at 1×10^6/ml in flat-bottom 96-well plates in RPMI containing 10% FCS, 1% pyruvate, 1% HEPES, and 1% penicillin-streptomycin (Gibco). Cells were cultured for different times in the absence (untreated) or presence of 50 ng/mL TSLP (R&D Systems).When indicated, other treatments were used. When stated in the text, 200 ng/mL PTX (Calbiochem), 2.5 ng/mL TNF-α (R&D Systems), 1 μg/mL lipopolysaccharide (LPS; Sigma-Aldrich), 100 ng/mL GM-CSF (Miltenyi) or 10ng/ml TGF-β (Prepotech) were added to the culture medium. Cell death after culture was assessed using DAPI and AnnexinV (Miltenyi Biotec) double staining by FACS.

CD34-DERIVED LANGERHANS CELL GENERATION

Blood CD34$^+$ cells were isolated from PBMCs by positive selection using anti-CD34-coated magnetic beads and magnetic columns according to manufacturer's instructions (Miltenyi). CD34$^+$ cells were cultured for 9–10 days in Yssel medium supplemented with 10% fetal calf

serum (FCS), penicillin/streptomycin and 50 ng/ml GM-CSF (Miltenyi), 100 ng/ml Flt3-ligand (R&D Systems), and 10 ng/ml TNF-α (R&D Systems). Culture media and cytokines were refreshed on day 5 of culture and 10ng/ml TGF-β (Prepotech) was added for the last 4 days of culture. DC subsets were isolated by cell sorting on a FACSAria instrument after staining for CD1a, CD207 and CD14.

BLOCKING TSLP EXPERIMENTS

For some experiments TSLP-treated or untreated DC culture conditioned media were used. TSLP blocking antibody or its correspondent isotype control (100 ug/mL; R&D Systems) were added to the conditioned media for one hour at 37°C before usage. A second set of DCs were cultured for 24 hours in these TSLP-blocked or unblocked conditioned media.

SUPERNATANT ANALYSIS

Total DCs and DC subsets supernatants were collected after 20 to 24 hours of culture in RPMI medium (Gibco), containing 10% FCS, 1% pyruvate, 1% HEPES, and 1% penicillin-streptomycin with or without TSLP and were kept at -80°c until assayed. Global chemokine production was assessed for 3 independent donors, using a 48 human chemokine protein array (Raybiotech) following the protocol of the manufacturer. Specific measurements for human CCL17 and CCL22 were done by ELISA (R&D Systems). CCL3, CCL4, CCL5, CXCL8, CXCL10 and CX_3CL1 were measured by Cytometric Bead Array Flex Set (BD Bioscience). MMP12 was measured by Luminex analysis technology (Millipore).

MORPHOLOGICAL ANALYSIS

Immunofluorescence

To determine the cytoskeleton architecture, DCs were cultured on poly-lysine–coated coverslips for 24 hours and examined by epifluorescence microscopy. Cells were fixed in 4% paraformaldehyde in PBS for 15 minutes at room temperature, permeabilized by 0.05% Saponin in PBS 0.2% BSA for 10 minutes at room temperature. For localization of filamentous actin, cells were incubated with Cy3-phalloidin (Invitrogen) for 45 minutes. Localization of α-tubulin was achieved by incubation for 1 hour with a rat anti–human α-tubulin antibody (Serotec) followed by incubation for 30 minutes with Alexa-488 goat anti–rat (Invitrogen). Coverslips were mounted in Fluoromount (Sigma). Fluorescence images were obtained by an epifluorescence microscope (Leica) fitted with appropriate filter sets.

Polarization was assessed after ImageJ picture analysis, by calculating the ratio between the two main perpendicular axes for each cell.

Electron-microscopy

Freshly sorted blood BDCA-1^{+} dendritic cells were cultured with 50ng/ml of TSLP (R&D Systems) and 10ng/ml TGF-β (Prepotech) for three days in RPMI containing 10% FCS, 1% pyruvate, 1% HEPES, and 1% penicillin-streptomycin (Gibco). After three days, cells were stained for CD1a and Langerin. Sorted CD1a^{+}Langerin^{+} cells were seeded in Alcian Blue-Coated coverslips (Sigma) for 1 hour. Cells were fixed in 2 % glutaraldehyde in 0.1 M phosphate buffer, pH 7.4 for 1h, postfixed for 1h with 2% buffered osmium tetroxide, dehydrated in a graded series of ethanol solution, and then embedded in epoxy resin. Images were acquired with a digital camera Keen View (SIS) mounted on a Tecnai 12 transmission electron microscope (FEI Company) operated at 80kV.

MIGRATION EXPERIMENTS

The transwell system was used to test cell migration. This system is constituted by an upper and a lower compartment separated by a filter that allows the passage of small cells. Cells that are seeded in the upper compartments and that have migrated can be recovered in the lower compartment and can be counted.

Collagen type I (5 μg/mL rat tail collagen type I; BD Bioscience) coated transwells (Costar, 3-μm pores) were placed in 96-well plates filled with 200 μL of RPMI containing 10% FCS, 1% pyruvate, 1% HEPES, and 1% penicillin-streptomycin (Gibco) medium. Overnight treated DCs (1×10^6/mL) with and without TSLP and PTX were re-suspended in 50 μL of culture medium, added to the upper chamber of the transwells, and incubated at 37°C for 6 hours. SDF-1 (100 ng/mL; Prepotech) was added to the lower chamber as a positive control to induce DC migration where mentioned. After 6 hours, living cells (DAPI negative) in the upper and the lower chambers of the transwell were counted by FACS using counting beads (Polybead; Biovalley). Results were expressed as percentage of total counted viable DCs.

CD4 T HELPER DIFFERENTIATION

CD4 naïve T cells (CD4^{+}CD45RA^{+}CD25^{-}CD45RO^{-}) were isolated from blood buffy coats after Ficoll density gradient centrifugation (Ficoll-Paque GE Healthcare), enrichment (CD4 T cell Isolation kit; Miltenyi Biotec) and further FACS purification; Purity was higher than 98%. Naïve CD4 T cells were cultured with allogeneic DCs or DC subsets at 5:1 ratio in XVIVO 15 medium (Lonza). After 6 days of co-culture, T cells were washed, counted, re-seeded at 1×10^6/mL in flat-bottom 96-well plates and re-stimulated for 24 hours with anti-CD3/CD28 microbeads (Dynal). To obtain typical Th0, Th1, Th2 and Th17 profiles, naïve T cells were stimulated with polarizing cytokines for 6 days before re-stimulation, as previously reported [170]. Th0 profile was obtained in the absence of polarizing cytokines, Th1 was obtained using 10 ng/ml of IL-12 (R&D), Th2 was obtained using 25 ng/ml of IL-4 (R&D)

and Th17 was obtained using 10 ng/ml of IL-1β (R&D), 20 ng/ml of IL-6 (R&D), 100 ng/ml IL-23 (R&D) and 1 ng/ml of TGF-β (Prepotech).

Cell culture supernatants were collected and cytokine measurement was performed by Cytometric Bead Array Flex Set (BD Biosciences) and multiplex bead assay (Millipore, Milliplex MAP Human TH17 Magnetic Bead Panel) on a Bio-Plex-200 reader (Biorad).

GENE EXPRESSION PROFILING

Total RNA was extracted from primary human blood dendritic cells, directly after sorting or after 6 hours culture with and without TSLP (50 ng/mL; R&D Systems) or 2.5 ng/mL TNF-α (R&D Systems), using the Rneasy micro kit (Qiagen). Samples were then double amplified and labeled according to the protocol recommended by Affymetrix for hybridization to Human Genome U133 Plus 2.0 arrays. Microarray data were normalized using the GC-RMA algorithm and expression levels were centered, reduced and log-normalized on base 2. Probes with no annotation were removed from analysis. Genes with small profile ranges (in the low 50% of the global distribution) were filtered out using the Matlab function generangefilter. Differential analysis was done with a t-test (function mattes). A gene was declared as differentially expressed when exhibiting a p-value of less than 5% and an absolute fold-change of at least 2.

STATISTICAL ANALYSIS

The statistical analysis was performed using Prism (GraphPad Software). Comparisons between different conditions were performed using the Wilcoxon paired test. Statistical significance was retained for p values below 0.05. The principal component analysis (PCA) of T cell profiles was performed using the FactoMineR package [171] of the R software (version 2.15.0). The two first components of the PCA resume about 80% of the total inertia. The barycenters were computed from the set of observations in each condition and projected into the PCA plot. In addition, 95% confidence ellipses were drawn around the barycenters.

QUANTITATIVE PCR

Total RNA was extracted from DC subsets after 24 hours culture with and without TSLP (50 ng/mL; R&D Systems) using the Rneasy micro kit (Qiagen). To synthesize cDNA I used a mix containing random hexamers, oligo (dT) 15 (Promega) and the reverse transcriptase Superscript II (Invitrogen). Transcripts were quantified by real-time quantitative PCR on a Light Cycler 480 II (Roche) using TaqMan Gene Expression Assays (Applied Biosystems) and QPCR mix (Nalgene). We used the flowing probes from Applied Biosystems. The following probes were used B2M (Hs99999907_m1); GAPDH (Hs99999905_m1); HPRT1 (HS 99999909_m1); RPL34 (Hs00241560_m1); CCL3 (HS 00234142_m1); CCL4

(Hs99999148_m1); CCL17 (HS 00171074_m1) and CCL22 (Hs01574247_m1). All the Cts were normalized to the housekeeping gene B2M (beta 2 microglobulin).

RESULTS

4.1   PUBLICATION 1

Manuscript submitted.

Human blood BDCA1 dendritic cells differentiate into bona fide Langerhans cells with Thymic Stromal Lymphopoietin and TGF-β.

Carolina Martinez-Cingolani, Maximilien Grandclaudon, Mabel Jouve, Raphaël Zollinger, Vassili Soumelis.

It has been shown that in vitro human monocytes and CD34^{+} bone marrow precursors stimulated with different combinations of cytokines, can give rise to DCs and LCs [23, 38]. This suggests that in humans, as in mice, DCs and LCs can be generated by such precursors under inflammatory conditions. The observation that TSLP triggered a skin-phenotype on blood DCs encouraged us to study the implication of this inflammatory cytokine on skin-DC generation.

We started this study first analyzing the expression of skin-related molecules on transcriptomic data of TSLP-DCs. We found TSLP-DCs strongly up-regulated CD1a, a molecule characterizing dermal DCs and LCs. Furthermore, TSLP-DCs up-regulated CD207 (Langerin) and CCR6 which are related specifically to human epidermal LCs.

As the human blood DC compartment is constituted by two different subsets, BDCA-1^{+} and BDCA-3^{+} cells, we decided to check which of these subsets was contributing to the observed phenotype. We found that only the BDCA-1^{+} cells were able to up-regulate the CD1a molecule upon TSLP treatment. However we could not detect CD207 protein expression. In previous works, an essential role in LC generation had been accorded to TGF-β [35]. Accordingly, when we stimulated BDCA-1^{+} DCs with a combination of TGF-β and TSLP we obtained a population of cells co-expressing CD1a and CD207. We further checked if this population could also be generated from tonsillar BDCA-1^{+} DCs finding that only blood BDCA-1^{+}DCs could differentiate into CD1a^{+}CD207^{+} cells. By electron-microscopy we detected Birbeck granules in the CD1a^{+}CD207^{+} cells, defining them as LCs. Therefore we could conclude that TSLP and TGF-β induced the differentiation of blood BDCA-1^{+} DCs into LCs (TSLP-LCs).

Further characterization showed that TSLP-LCs were activated and had a skin-homing chemokine receptor phenotype. At the functional level, we assessed the capacity of TSLP-LCs to induce naïve T cell activation and polarization. We found that similarly to TSLP-DCs

and to primary LCs, TSLP-LCs induced aTh2 differentiation. However TSLP-LCs induced IL-9 and the secretion of TNF-α and IL-6 by T helper cells.

Overall our results show first that human blood BDCA-1^{+} DCs have a progenitor capacity. Secondly they provide evidence of functional differences in DC subsets from blood and tonsils. Finally they introduce a novel role of TSLP in the ontogeny of LCs under inflammatory conditions. This work opens new perspectives in the study of inflammatory cytokines differential effects on DC subsets.

57

Human blood BDCA1 dendritic cells differentiate into *bona fide* Langerhans cells with Thymic Stromal Lymphopoietin and TGF-β

Carolina Martinez-Cingolani [1,2,3], Maximilien Grandclaudon [1,2,3], Marine Jeanmougin[1,2,3], Mabel Jouve [1,2,3], Raphaël Zollinger [1,2,3], Vassili Soumelis [1,2,3]

AFFILIATIONS

1 Institut Curie, Department of Immunology, Paris, F-75248 France

2 Institut National de la Santé et de la Recherche Médicale U932, Paris, F-75248 France

3 Institut Curie, Research Section, Paris, F-75248 France

CORRESPONDENCE SHOULD BE ADRESSED TO:

Vassili Soumelis, 26 rue d'Ulm, Paris, F-75248 France. Tel.+33 (0) 44 32 42 27. Fax.+33 1 53 10 40 25. vassili.soumelis@curie.net

Carolina Martinez-Cingolani, 26 rue d'Ulm, Paris, F-75248 France. Tel.+33 (0) 1 56 24 57 05. Fax.+33 1 53 10 40 25. carolina.martinez@curie.fr

Abstract

The ontogeny of human Langerhans cells (LCs) under inflammatory conditions remains poorly characterized, in particular the nature of LC precursors and the factors that may drive LC differentiation. Here we report that Thymic Stromal Lymphopoietin (TSLP), a keratinocyte-derived cytokine involved in skin inflammation, cooperates with transforming growth factor (TGF)-β for the generation of LCs. We show that primary human blood BDCA-1^+, but not BDCA3$^+$ dendritic cells (DCs), stimulated with TSLP and TGF-β harbor a typical CD1a$^+$Langerin$^+$ skin LC phenotype. Electron microscopy established the presence of Birbeck granules, an intra-cellular organelle specific to LCs. LC differentiation was not observed from tonsil BDCA1$^+$ and BDCA3$^+$ subsets. TSLP-LCs had a mature phenotype with high surface levels of CD80, CD86, and CD40. They induced a potent CD4$^+$ T helper cell expansion, and differentiation into Th2 cells with increased production of TNF-α and IL-6, as compared to CD34-derived LCs. Our findings establish a novel LC differentiation pathway from BDCA1$^+$ blood DCs relevant to skin inflammatory conditions. Therapeutic targeting of TSLP may interfere with skin LC repopulation from circulating precursors.

Introduction

Langerhans cells (LCs) of the epidermis are the main antigen presenting cells in the skin, and play a major role in maintaining homeostasis [1, 2], inducing a protective immune response to invading pathogens [3], but also promoting and sustaining pathogenic chronic skin inflammation [4, 5]. Given the importance of skin as a natural interface with the environment, it is critical to maintain a pool of epidermal LCs in a regulated manner at steady state, and also allow for the recruitment and/or de novo differentiation of LCs during inflammation. In the mouse, it was shown that LCs homeostasis at steady state could be achieved through the differentiation of local proliferating precursors [6]. During inflammation, circulating monocytes were the main source of newly differentiated LCs [7], in a process depending on M-CSF [8, 9] and TGF-β [10, 11].

In the human, LC ontogeny, as well as the link between LCs and other dendritic cell (DC) subsets has remained controversial. Human LCs were shown to be of hematopoietic origin [12, 13]. In vitro studies have shown that CD1a$^+$ LC-like cells could be differentiated from CD34$^+$ hematopoietic progenitors [14]. Monocytes were also described as a possible source of LCs when cultured with GM-CSF, IL-4 and TGF-β [15]. After transplantation, LCs of donor origin have been observed in the skin of the host for up to 10 years [16], suggesting the presence of a local precursor that remains to be identified. However, the pathways leading to LC differentiation during inflammation are still poorly defined, both in terms of differentiation factors, and of possible LC precursor cells. In particular, it is not known whether blood CD1a-negative DCs may serve as LC precursors and acquire a bona fide LC phenotype. The recent identification of the BDCA1$^+$ and BDCA3$^+$ subsets of human DCs [17] raises additional questions on their ability to further differentiate into another DC subset.

Thymic Stromal Lymphopoietin (TSLP) is a keratinocyte-derived cytokine playing a critical role in skin inflammation, in particular atopic dermatitis [18], and psoriasis (Volpe, unpublished), by strongly activating blood DCs [19]. Through a systematic transcriptomic analysis of TSLP-activated DCs, we unexpectedly identified markers that have been associated with a skin-homing potential as well as with a LC phenotype. Addition of TGF-β synergized with TSLP leading to the differentiation of *bona fide* Birbeck granule-positive LCs.

Results and discussion

TSLP induces a skin-like transcriptional signature in human blood DCs

In order to get a detailed insight into molecular changes induced by TSLP in human blood DCs, we performed a transcriptomic analysis of TSLP-activated blood DCs, as compared to freshly purified, Medium-, and TNF-activated DCs after 6 hours of culture (Figure 1). Affymetrix U133 plus 2.0 chips were used for transcriptomic analysis of 5 independent donors (data will be available on GEO). Among TSLP differentially-regulated genes, we identified molecules associated with skin homing (CCR6), LC phenotype (CD1a, CD207 (Langerin), and LC function (MMP12, CCL17), as determined by a literature-based survey (Figure 1A). CD205 was also described on LCs [20] and up-regulated by TSLP (Figure 1A). Conversely, genes not expressed in LCs were also not found among TSLP-induced genes, for example CD209 (DC-Sign) and CD14 (Figure 1A). Overall, this revealed a LC-like signature suggesting that TSLP may be involved in LC differentiation of blood DCs.

TSLP and TGF-β synergize for the differentiation of Langerhans cells from blood BDCA1^{+} DCs

Langerhans cells are usually defined by their co-expression of CD1a and CD207. First, we used flow cytometry to assess the expression of CD1a and CD207 on TSLP-activated blood DCs after sorting of the BDCA1^{+} and BDCA3^{+} subsets. We found a strong and consistent induction of CD1a by TSLP in the BDCA1^{+} subset, matching our microarray data, but not in BDCA3^{+} DCs (data not shown). However, CD207 was induced inconsistently and at low levels (Median 6.2%; Range 2.1 to 33.5 %) (Figure 2A). Because of the importance of TFG-β in skin homeostasis, and its established role in the differentiation of LCs [11], we hypothesized that it may potentiate the effects of TSLP. Although TGF-β alone induced significant amounts of CD207 after 24 hours on BDCA1^{+} DCs, it did not promote CD1a

expression, which indicates a partial LC phenotype (Figure 2A). Importantly, combination of TSLP and TGF-β resulted in a synergistic effect on BDCA1$^+$ DCs with differentiation of a large proportion (25.6±2.2%) of CD1a$^+$CD207$^+$ cells (Figure 2A), a phenotype typical of LCs. However, BDCA3$^+$ DCs remained refractory to LC differentiation even with the TSLP+TGF-β combination (Figure 2A).

A standard method to induce human LC differentiation is from CD34$^+$ hematopoietic progenitors in the presence of Flt3-ligand, TNF-α, GM-CSF and TGF-β [2, 21]. LC differentiation was effective in 85% of normal blood donor buffy coats (11 of 13), with an average 4.1±0.8% CD1a$^+$CD207$^+$ LCs (Figure 2A), as compared to a 71% differentiation efficiency (32 of 45), with 25.6±2.2% CD1a$^+$CD207$^+$ LCs when using TSLP and TGF-β on BDCA1$^+$ DCs. These results show that TSLP and TGF-β induce an effective LC differentiation from blood BDCA1$^+$ DCs. In our hands, BDCA1$^+$ DCs were found to be more potent LC precursors as compared to CD34 progenitors.

Our data show that human blood BDCA1$^+$ DCs retain a potential to differentiate into another DC subset, suggesting that this subset is not terminally differentiated. In order to address the differentiation potential of secondary lymphoid tissue DCs, we repeated these experiments using BDCA1$^+$ and BDCA3$^+$ subsets purified from human tonsils. Neither of these subsets was able to differentiate into LCs with TSLP and TGF-β (Figure 2A), suggesting that lymphoid tissue environment may induce a block in their differentiation potential.

Since tonsil DCs, as well as blood BDCA3$^+$ DCs, did not differentiate into LCs in response to TSLP, we questioned whether they were able to respond to TSLP. By flow cytometry, BDCA1$^+$ and BDCA3$^+$ subsets from both blood and tonsil expressed the two chains of the TSLP receptor complex, IL-7R-alpha and TSLPR (Figure 2B). Accordingly, all subsets responded to TSLP activation, as assessed by surface CD80 expression (Figure 2B).

TSLP-induced Langerhans cells express Birbeck granules

Although CD1a and CD207 are typical of a LC phenotype, Birbeck granules are the most specific and distinctive feature of human LCs [22]. We assessed by electron microscopy the presence of Birbeck granules on the CD1a^{+}CD207^{+} population differentiated from blood BDCA-1^{+} DCs after 1 to 3 days of stimulation with TSLP and TGF-β (Figure 3). On the sorted CD1a^{+}CD207^{+} cells, at day 1, we could not observe any structure reminiscent of the double-membrane rod-shaped cytoplasmic organelles typical of Birbeck granules, even with a combination of TSLP and TGF-β (data not shown), although we could not exclude a low number of these structures that could have been missed by careful examination. Nevertheless, typical Birbeck granules appeared by day 3 in the sorted DCs cytoplasm (Figure 3), suggesting a minimum amount of time required for organelle formation. The CD1a and CD207 single positive, as well as double negative cells, were consistently negative for Birbeck granules (data not shown).

TSLP-induced Langerhans cells bear a mature phenotype and skin-homing receptors

In order determine   the phenotype of TSLP-induced LCs (TSLP-LCs), we assessed the expression of surface markers characteristic of DC lineage, maturation state, and homing receptors. TSLP-LCs expressed higher levels of CD1a and CD207 as compared to blood BDCA-1^{+} DCs treated with optimal doses of either TSLP or TGF-β alone, confirming the synergistic effect of these cytokines on LC generation (Figure 4A). We found low levels of FcεRI expression as previously reported in skin-isolated LCs [20], and CD206 (Mannose Receptor 1) previously reported to be expressed by DCs and macrophages from human inflammatory fluids [23]. Other markers of inflammatory DCs such as CD14 and CD11b were absent in TSLP-LCs (Figure 4A). In comparison to TSLP-induced LCs, CD34^{+}-derived LCs expressed   CD11b and higher levels of CD206 (Supplemental Figures 1 and 2).

It has been shown that TSLP strongly activates total human blood DCs inducing the expression of HLA-DR, CD80, CD86 and CD40 [18]. Accordingly, TSLP-LCs expressed high levels of HLA-DR and CD80 (Figure 4B). Nevertheless they expressed significantly lower amounts of CD86 and CD40 as compared to TSLP-treated BDCA-1^{+} DCs, consistent with a down-regulation of these markers by TGF-β. TSLP-derived LCs were found to express lower levels of CD83, CD86 and CD40 in comparison to CD34^{+} derived LCs but higher levels of HLA-DR and CD80 (Supplemental Figures 1 and 2).

It has been suggested that under inflammatory conditions, LC precursors reach the dermis through the expression of the chemokine receptor CCR2. In a second step, they up-regulate CCR6 that allows them to reach the epidermis [6], where E-cadherin mediates their binding to keratinocytes [24]. Activated LCs down-regulate E-cadherin and reach the lymph nodes through the sequential involvement of CXCR4 [25] and CCR7 [26]. We found that TSLP-LCs expressed lower levels of CCR2, as compared to medium, TGF-β or TSLP-treated BDCA-1^{+} DCs, but higher levels of CCR6 (Figure 4C). Neither E-cadherin nor the epithelial cell adhesion molecule Epcam, characterizing LCs were found to be expressed in any of the conditions. TSLP-LCs expressed lower levels of CCR7 and CXCR4, compared to untreated and TGF-β-treated BDCA-1^{+} cells (Figure 4C). These results suggest that under inflammatory conditions, CCR2 and CCR6 may act in a coordinated manner to induce the sequential recruitment of TSLP-LC to the dermis and then epidermis. CD34^{+}-derived LCs expressed CCR2, CCR7, E-cadherin and higher levels of CCR6 than TSLP-LCs (Supplemental Figures 1 and 2). Therefore CD34^{+}-derived LCs have a mixed skin and lymph node homing phenotype.

Induction of T-helper (Th) differentiation by TSLP-induced BDCA1-derived LCs

A major function of LCs is to induce naïve CD4^{+} T cell activation and differentiation into Th effectors. TSLP-LCs induced a 2-3 fold expansion of naïve CD4^{+} T cells after 6 days of co-culture, which was slightly higher than CD34-LCs (Figure 5A).

Primary and CD34-derived skin LCs were shown to induce Th2 differentiation [2]. In our study, TSLP-LCs also preferentially induced CD4^{+} Th cells to produce IL-4, IL-5, and IL-13, at levels similar or higher to/than CD34-derived LCs (Figure 5B). This indicates that our system recapitulates important features of primary LCs [2]. However, consistent with LCs generated under inflammatory conditions, TSLP-LCs induced Th cells producing higher levels of TNF-α and IL-6, as compared to CD34-LCs (Figure 5B), which may be closer to steady-state LCs. Interestingly, we found that TSLP-LCs, similar to TSLP-DCs that did not differentiate into LCs, induced high levels of IL-9 production by Th cells, which were not observed with CD34-derived LCs (Figure 5B). IL-9 production by CD4^{+} T cells has been attributed to a subset of Th2 cells that develops into Th9 cells under TGF-β influence [27] and has been associated to TSLP-linked allergic disorders [28]. Our results suggest that TSLP may trigger intrinsic TGF-β production by BDCA-1^{+} DCs which supports previous reports of autocrine TGF-β signal requirement for LC generation [10].

In order to get a global integrated view of Th cytokine profiles generated with different DCs, we used principal component analysis, a multivariate approach which reduces the dimensionality of the data by extracting the smallest number of components that account for most of the variation in our data. . It appeared that CD34-LC-induced Th profile was closer to Medium-DC and TGF-β-DC (Figure 5C), all three DC being potentially more relevant to steady-state conditions. TSLP-LCs were more similar to TSLP-DCs than to TGF-β-DCs (Figure 5C), suggesting a dominance of the inflammatory environment as represented by

TSLP. Importantly, TSLP-LCs were distinct from CD34-LCs at the global Th cytokine profile level, confirming that these two subsets have different functional features, and may be involved in different types of physiopathological conditions.

In conclusion we provide definitive evidence that blood BDCA-1^{+} DCs differentiate into LCs in the presence of TSLP and TGF-β. This defines a novel LC differentiation pathway in the human. TSLP-LCs had characteristic features of primary epidermal LCs, including expression of CD1a and CD207, presence of cytoplasmic Birbeck granules, and priming for Th2 differentiation. However, they also had distinctive functional features, including induction of IL-9, as well as inflammatory cytokines TNF-α and IL-6, in Th cells. Although monocytes can differentiate into LCs with GM-CSF, IL-4, and TGF-β [15], the relevance of this cytokine combination to physiopathology has remained elusive. Our study provides a direct link between the skin inflammatory microenvironment, and LC differentiation, bringing new insight into LC generation from blood precursors during inflammation. Future studies may determine whether other inflammatory mediators may also harbor an LC differentiation capacity. Dissecting DC subset diversity at steady-state and inflammation may facilitate the therapeutic manipulation of the immune response, and its tailoring to specific types of inflammation.

Material and methods

Samples and cell isolation

Buffy coats were obtained from healthy adult blood donors at the Saint Louis hospital site of the Etablissement Français du Sang. Peripheral blood mononuclear cells (PBMCs) were isolated by Ficoll density gradient centrifugation (Ficoll-Paque; GE Healthcare). Total DC fraction was enriched using Pan-DC Enrichment kit according to the manufacturer's instructions (EasySep; Stem cell). Total DCs, (Lineage$^-$ CD11c$^+$ CD4$^+$) and DC subsets, (Lineage$^-$ CD11c$^+$ CD4$^+$ BDCA-1$^+$ or Lineage$^-$ CD11c$^+$ CD4$^+$BDCA-3$^+$) were purified to 99% by FACS sorting (ARIA II BD). Blood CD34$^+$ cells were isolated from PBMCs by positive selection using anti-CD34-coated magnetic beads and magnetic columns according to manufacturer's instructions (Miltenyi). Tonsils from healthy patients undergoing tonsillectomy were obtained from Hôpital Necker (Paris, France) following the hospital ethical guidelines. Tonsils were cut into small fragments and digested with 0.8 mg/ml Collagenase IV (Worthington) and 25 ug/ml DNase (Roche) for 15 min at 37°C in C02 – independent medium (Gibco). After incubation the supernatant was recovered and the digestion was repeated 2 or 3 times. The remaining tissue was filtered on a 40-µm cell strainer (BD) and washed in PBS. Following Ficoll density gradient centrifugation, DC fraction was by magnetic depletion of cells expressing CD3, CD15, CD19, CD56, CD14 and CD235a according to the manufacturer's instructions (Miltenyi Biotec). Tonsillar DC subsets, (Lineage$^-$ CD11c$^+$ CD4$^+$ BDCA-1$^+$ or Lineage$^-$ CD11c$^+$ CD4$^+$BDCA-3$^+$) were purified to 99% by FACS sorting (ARIA II BD).

Flow Cytometry

Cells were stained with FITC anti-CD3 (BD), FITC anti-CD14(BD) or Qdot605 anti-CD14(Invitrogen), FITC anti-CD16 (BD), FITC anti-CD19 (Miltenyi), PECy5 anti-CD11c

(BD), APC or VioGreen anti-CD4 (Miltenyi), APC eFluor 780 anti-HLA-DR (eBioscience), PerCP eFluor 710 anti-BDCA1 (eBioscience), APC, PE or VioBlue anti-BDCA3 (Miltenyi), PE anti-CD207/Langerin (Immunotech) or FITC anti-CD207/Langerin (Miltenyi), PECy5 or FITC anti-CD1a (BD), FITC anti-IL7Rα (eBioscience), APC anti-TSLPR (BioLegend), FITC anti-CD80 (BD) or AlexaFluor 700 anti-CD80 (ExBio), FITC anti-CD83, (BD), FITC anti-CD86 (BD), FITC anti-CD40 (BD), PECy5 anti-CD206 (BioLegend), PECy7 anti-CD11b (Biolegend), AlexaFluor 647 anti-CCR2 (BioLegend), APC anti-CCR6 (BD), FITC anti-CCR7 (BD), PECy7 anti-CXCR4 (BioLegend), PE anti-FcεRI (eBioscience), FITC anti-CD64 (BD), APC anti-ECadherin (R&D), PECy7 anti-EPCAM (BioLegend) and biotinilated anti-CD209 (Miltenyi) followed by PECy7 streptavidin (eBioscience) staining.

Nonspecific binding and cell adhesion were blocked using PBS supplemented with 1% human serum (BioWest) and EDTA 2mM (Gibco). Cells were stained for 15 minutes at 4 degrees with different combinations of specific antibodies or their isotype-matched control antibodies. DAPI (Sigma-Aldrich) was added before acquisition in a LSRII or Fortessa (BD) analysers. Data were analyzed with FlowJo software (Tree Star).

Cell culture

Myeloid DC subsets from human blood and tonsils were seeded at 1×10^6/mL in flat-bottom 96-well plates cultured in RPMI containing 10% heat inactivated fetal calf serum (FCS/BioWest), 1% pyruvate (Gibco), 1% HEPES (Gibco), and 1% penicilin-streptomycin (Gibco). Cells were cultured for the indicated time in the absence or presence of 50 ng/mL TSLP (R&D Systems) and 10 ng/mL of TGF-β (Prepotech). The CD1a$^+$ Langerin$^+$ Langerhans cells were sorted on a FACSAria instrument.

Peripheral blood CD34$^+$ cells were cultured for 9–10 days in Yssel medium supplemented with 10% heat inactivated FCS, penicillin/streptomycin 50 ng/ml GM-CSF (Miltenyi), 100

ng/ml Flt3-ligand (R&D Systems), and 10 ng/ml TNF-α (R&D Systems). Culture media and cytokines were refreshed on day 5 of culture and 10 ng/mL of TGF-β was added for the last 4 days of culture. $CD14^+CD1a^-$, $CD14^-CD1a^+Langerin^-$, and $CD14^-CD1a^+Langerin^+$ cells were isolated by cell sorting on a FACSAria instrument.

Electron microscopy

After 1 and 3 days of culture with TSLP and TGF-β, the BDCA-1^+ DCs differentiated into $CD1a^+$ Langerin$^+$ Langerhans cells were sorted and seeded in Acian Blue-Coated coverslips (Sigma) for 1 hour. Cells were fixed in 2 % glutaraldehyde in 0.1 M phosphate buffer, pH 7.4 for 1h, postfixed for 1h with 2% buffered osmium tetroxide, dehydrated in a graded series of ethanol solution, and then embedded in epoxy resin. Images were acquired with a digital camera Keen View (SIS) mounted on a Tecnai 12 transmission electron microscope (FEI Company) operated at 80kV.

CD4 T helper cell differentiation

Naïve CD4 T cells ($CD4^+CD45RA^+CD25^-CD45RO^-$) were isolated from blood buffy coats after Ficoll density gradient centrifugation (Ficoll-Paque GE Healthcare), enrichment (CD4 T cell Isolation kit; Miltenyi Biotec) and further FACS sorting purification; Purity was higher than 98%. Naïve CD4 T cells were cultured with allogeneic BDCA-1^+ or CD34$^+$-derived antigen presenting cells at a 5:1 ratio in XVIVO 15 medium (Lonza). After 6 days of co-culture, T cells were counted, re-seeded at 1×10^6/mL in flat-bottom 96-well plates and re-stimulated for 24 hours with anti-CD3/CD28 microbeads (Dynal). Cell culture supernatants were collected and cytokine measurement was performed by multiplex bead assay (Millipore, Milliplex MAP Human TH17 Magnetic Bead Panel) on a Bio-Plex-200 reader (Biorad).

Gene expression profiling

Total RNA was extracted from DCs, directly after sorting (Ex-vivo) or after 6 hours culture with and without TSLP (50 ng/mL; R&D Systems) and TNF-α (2.5 ng/mL; R&D Systems), using the RNeasy kit (Qiagen). Samples were then double amplified and labeled according to the protocol recommended by Affymetrix for hybridization to Human Genome U133 Plus 2.0 arrays. The microarray data are available in the (Gene Expression Omnibus) GEO database. Data were normalized using the GC-RMA algorithm and expression levels were centered, and reduced. Probes with no annotation were removed from analysis. Genes with small profile ranges (in the low 50% of the global distribution) were filtered out using the Matlab function generangefilter.

Statistical analysis

Wilcoxon paired test and paired Student's t test were performed using Prism (GraphPad Software) at a significance level of 5%. The principal component analysis (PCA) of T cell profiles was performed using the FactoMineR package [29] of the R software (version 2.15.0). The two first components of the PCA resume about 80% of the total inertia. The barycenters were computed from the set of observations in each condition and projected into the PCA plot. In addition, 95% confidence ellipses were drawn around the barycenters.

Acknowledgements

References

1. Seneschal, J., et al., *Human epidermal Langerhans cells maintain immune homeostasis in skin by activating skin resident regulatory T cells.* Immunity, 2012. **36**(5): p. 873-84.
2. Klechevsky, E., et al., *Functional specializations of human epidermal Langerhans cells and CD14+ dermal dendritic cells.* Immunity, 2008. **29**(3): p. 497-510.
3. Moll, H., et al., *Langerhans cells transport Leishmania major from the infected skin to the draining lymph node for presentation to antigen-specific T cells.* Eur J Immunol, 1993. **23**(7): p. 1595-601.
4. Geissmann, F., et al., *Accumulation of immature Langerhans cells in human lymph nodes draining chronically inflamed skin.* J Exp Med, 2002. **196**(4): p. 417-30.
5. Ashworth, J. and R.M. Mackie, *A quantitative analysis of the Langerhans cell in chronic plaque psoriasis.* Clin Exp Dermatol, 1986. **11**(6): p. 594-9.
6. Merad, M., et al., *Langerhans cells renew in the skin throughout life under steady-state conditions.* Nat Immunol, 2002. **3**(12): p. 1135-41.
7. Ginhoux, F., et al., *Langerhans cells arise from monocytes in vivo.* Nat Immunol, 2006. **7**(3): p. 265-73.
8. Wang, Y., et al., *IL-34 is a tissue-restricted ligand of CSF1R required for the development of Langerhans cells and microglia.* Nat Immunol, 2012. **13**(8): p. 753-60.
9. Greter, M., et al., *Stroma-derived interleukin-34 controls the development and maintenance of langerhans cells and the maintenance of microglia.* Immunity, 2012. **37**(6): p. 1050-60.
10. Kaplan, D.H., et al., *Autocrine/paracrine TGFbeta1 is required for the development of epidermal Langerhans cells.* J Exp Med, 2007. **204**(11): p. 2545-52.
11. Borkowski, T.A., et al., *A role for endogenous transforming growth factor beta 1 in Langerhans cell biology: the skin of transforming growth factor beta 1 null mice is devoid of epidermal Langerhans cells.* J Exp Med, 1996. **184**(6): p. 2417-22.
12. Katz, S.I., K. Tamaki, and D.H. Sachs, *Epidermal Langerhans cells are derived from cells originating in bone marrow.* Nature, 1979. **282**(5736): p. 324-6.
13. Volc-Platzer, B., et al., *Cytogenetic identification of allogeneic epidermal Langerhans cells in a bone-marrow-graft recipient.* N Engl J Med, 1984. **310**(17): p. 1123-4.
14. Caux, C., et al., *GM-CSF and TNF-alpha cooperate in the generation of dendritic Langerhans cells.* Nature, 1992. **360**(6401): p. 258-61.
15. Geissmann, F., et al., *Transforming growth factor beta1, in the presence of granulocyte/macrophage colony-stimulating factor and interleukin 4, induces differentiation of human peripheral blood monocytes into dendritic Langerhans cells.* J Exp Med, 1998. **187**(6): p. 961-6.
16. Kanitakis, J., et al., *Self-renewal capacity of human epidermal Langerhans cells: observations made on a composite tissue allograft.* Exp Dermatol, 2011. **20**(2): p. 145-6.
17. Dzionek, A., et al., *BDCA-2, BDCA-3, and BDCA-4: three markers for distinct subsets of dendritic cells in human peripheral blood.* J Immunol, 2000. **165**(11): p. 6037-46.
18. Soumelis, V., et al., *Human epithelial cells trigger dendritic cell mediated allergic inflammation by producing TSLP.* Nat Immunol, 2002. **3**(7): p. 673-80.
19. Reche, P.A., et al., *Human thymic stromal lymphopoietin preferentially stimulates myeloid cells.* J Immunol, 2001. **167**(1): p. 336-43.
20. Santegoets, S.J., et al., *Transcriptional profiling of human skin-resident Langerhans cells and CD1a+ dermal dendritic cells: differential activation states suggest distinct functions.* J Leukoc Biol, 2008. **84**(1): p. 143-51.
21. Strobl, H., et al., *flt3 ligand in cooperation with transforming growth factor-beta1 potentiates in vitro development of Langerhans-type dendritic cells and allows single-cell dendritic cell cluster formation under serum-free conditions.* Blood, 1997. **90**(4): p. 1425-34.

22. Birbeck, M.S., *An electron microscopy study of basal melanocytes and high level clear cells (Langerhans cells) in vitiligo.* J Invest Dermatol, 1961. **37**: p. 51-64.

23. Segura, E., et al., *Human inflammatory dendritic cells induce Th17 cell differentiation.* Immunity, 2013. **38**(2): p. 336-48.

24. Tang, A., et al., *Adhesion of epidermal Langerhans cells to keratinocytes mediated by E-cadherin.* Nature, 1993. **361**(6407): p. 82-5.

25. Ouwehand, K., et al., *CXCL12 is essential for migration of activated Langerhans cells from epidermis to dermis.* Eur J Immunol, 2008. **38**(11): p. 3050-9.

26. Villablanca, E.J. and J.R. Mora, *A two-step model for Langerhans cell migration to skin-draining LN.* Eur J Immunol, 2008. **38**(11): p. 2975-80.

27. Veldhoen, M., et al., *Transforming growth factor-beta 'reprograms' the differentiation of T helper 2 cells and promotes an interleukin 9-producing subset.* Nat Immunol, 2008. **9**(12): p. 1341-6.

28. Yao, W., et al., *Interleukin-9 is required for allergic airway inflammation mediated by the cytokine TSLP.* Immunity, 2013. **38**(2): p. 360-72.

29. R, H.F., JOSSE J., LE S., MAZET J., *FactoMineR : Factor Analysis and Data Mining. .* 2012.

30. Nestle, F.O., et al., *Characterization of dermal dendritic cells obtained from normal human skin reveals phenotypic and functionally distinctive subsets.* J Immunol, 1993. **151**(11): p. 6535-45.

31. Rust, R., et al., *Gene expression analysis of dendritic/Langerhans cells and Langerhans cell histiocytosis.* J Pathol, 2006. **209**(4): p. 474-83.

32. Lundberg, K., *Transcriptional profiling of human dendritic cell populations and models-unique profiles of in vitro dendritic cells and implications on functionality and applicability.* PLoS One, 2013. **8**(1): p. e52875.

Figure legends

Figure 1: Gene profile of TSLP-treated blood DCs and skin DCs

(A) [a]Gene transcripts expression on purified blood DCs directly after sorting (Ex-vivo) or after a 6 hour treatment with medium alone or supplemented with TSLP or TNF-α. Genome wide expression was determined by Affymetrix chips Human Genome U133 Plus 2.0 microarray analysis. [b]Expression described in the literature by Santegoets [20], Nestle [30], Rust [31]and Lundberg [32]. Langerhans cells (LC); Dermal Dendritic Cells (DDC); Not determined (nd). Signal intensity levels: -, $\leq$200; +, 200-500; ++, 500-5000; +++, $\geq$ 5000.

(B) Data represent signal intensity levels for the correspondent gene transcripts under the different conditions (Ex-vivo n=5, medium and TNF-α n=3, TSLP n=4).

Figure 2: TSLP and TGF-β induce the differentiation of blood BDCA-1^{+} DCs into LCs

(A) Upper panel: Representative flow cytometry density dot plots of CD207 and CD1a expression by human blood and tonsillar BDCA-1^{+} and BDCA-3^{+} DCs after 24h treatment with and without TSLP and TGF-β. Blood CD34^{+}-derived LCs after treatment with Flt3-L, TNF-α, GM-CSF and TGF-β (Cocktail) are shown as a positive control of the staining. Quadrants were adjusted to the matching correspondent isotype controls. Numbers represent the percentage of viable cells. Lower panel: Quantification of the percentage of viable cells differentiated into CD1a^{+}CD207^{+} LCs, CD207+ and CD1a^{+} cells for all the conditions. Each dot represents an independent experiment. *p* $\leq$0.05**p* $\leq$ 0.005 ***p* $\leq$ 0.0005, Wilcoxon non-parametric paired test was used. Bars represent medians.

(B) Left panel: Representative Flow cytometry density plots of TSLP receptor and IL-7 receptor α chains by human blood and tonsillar BDCA-1^{+} and BDCA-3^{+} DCs. Quadrants were adjusted to the matching correspondent isotype controls. Numbers represent the

percentage of viable cells. Below, percentage of viable cells expressing both chains of TSLP receptor. Right panel: Representative histograms of CD80 expression by human blood and tonsillar BDCA-1^{+} and BDCA-3^{+} DCs after 24h culture with and without TSLP. Plain histograms represent the matching correspondent isotype controls and numbers represent specific median fluorescence intensities (MFIs). Below, quantification of MFIs for CD80 for 4 independent donors.

Figure 3: Birbeck granules on blood BDCA-1^{+} DCs treated with TSLP and TGF-β

After 3 days of culture with TSLP and TGF-β blood BDCA-1+ derived LCs were sorted according to the expression of CD1a and CD207. Electronmicroscopy pictures show the presence of LC characteristic Birbeck granules in the cytoplasm (arrows). The Birbeck granules shown in the lower pictures correspond to different independent cells.

Figure 4: TSLP- LCs expression of myeloid, maturation markers and skin-homing receptors.

Representative histograms of the expression of myeloid lineage molecules (A), activation markers (B) and skin-homing receptors (C) by human blood BDCA-1^{+} after 24h culture with or without TSLP or TGF-β. Data on BDCA-1^{+} DCs treated with both TSLP and TGF-β correspond to the CD1a^{+} CD207^{+} cells. Plain histograms represent the matching correspondent isotype controls and numbers represent specific median fluorescence intensities (MFIs). *n= 4 to 11*

Figure 5: TSLP-LCs induce a Th2 profile on naive CD4^{+} T cells.

BDCA-1^{+} DCs subsets were stimulated with or without TSLP and TGF-β for 24h. CD34^{+} cells were stimulated with Flt3-L, TNF-α, GM-CSF and TGF-β (Cocktail). CD34^{+}- derived LCs and BDCA-1^{+} -derived LCs were sorted according to CD1a and CD207 expression and

cultured with allogeneic naive CD4$^+$T cells for 6 d before T cell restimulation. Symbols represent cells purified from the same donor.

(**A**) T cell expansion was assessed by calculating the ratio of the number of T cells at the end of the culture divided by the number of T cells plated at the start of the culture. **p ≤ 0. Paired T test was used. Bars represent medians.

(**B**) Data represent cytokine concentration at the end of the culture measured by multiplex bead array. *p ≤0.05**p ≤ 0.005 Paired T test was used. Bars represent medians.

(**C**) Principal Component Analysis (PCA) analysis showing the resemblance of the naïve T cell profiles (secretion of 13 cytokines) induced under the different conditions. Components 1 and 2 were selected as the axes explaining most of the data variance. The crosses represent individual donors (n=4). The squares represent the barycenters. Confidence ellipses at 95% are depicted in each condition.

Supplemental figure legends

Supplemental Figure 1: CD34- LCs expression of myeloid, maturation markers and skin-homing receptors.

Representative histograms of the expression of myeloid lineage molecules (A), activation markers (B) and skin-homing receptors (C) by human CD34- derived LCs. Cocktail: Flt3-L, TNF-α, GM-CSF and TGF-β. Plain histograms represent the matching correspondent isotype controls and numbers represent specific median fluorescence intensities (MFIs). *n= 5*

Supplemental Figure 2: TSLP-LC and CD34- LCs expression of myeloid, maturation markers and skin-homing receptors.

Quantification of MFIs for myeloid lineage molecules (A), activation markers (B) and skin-homing receptors (C) by human TSLP-LCs and CD34- derived LCs. Each dot represents one donor. Bars represent medians. *p* ≤0.05**p* ≤ 0.005 ***p* ≤ 0.001 Wilcoxon paired test was used.

Figure 1

A

TCELL TYPE	mRNA expression profile				[b]Literature based		
	[a]BLOOD TOTAL DC				DDC	LC	Reference
TREATMENT	EX VIVO	Medium	TNF	TSLP	-	-	-
CD1A	+	-	-	++	++	+++	Santegoets, S. 2008
CD14	-	-	-	-	Expressed	-	Nestle, O. 1993
Langerin (CD207)	-	-	-	++	-	+++	Santegoets, S. 2008
CD205	++	+	++	++	+	++	Santegoets, S. 2008
MRC1 /// MRC1L1	++	++	-	+++	++	-	Santegoets, S. 2008
CD209	-	-	-	-	+	-	Santegoets, S. 2008
CDH1	++	++	++	++	++	+++	Santegoets, S. 2008
MMP12	-	-	-	++	nd	Expressed	Rust, R. 2006
CCL22	++	+++	+++	+++	nd	Expressed	Rust, R. 2006
CCL17	-	-	-	+	nd	Expressed	Rust, R. 2006
CCR2	-	-	-	-	-	-	Lundberg, K. 2013
CCR6	-	-	-	+	-	+	Santegoets, S. 2008
CCR7	+	+++	+++	+++	+++	-	Santegoets, S. 2008
CXCR4	+++	++	++	++	+++	++	Santegoets, S. 2008

B
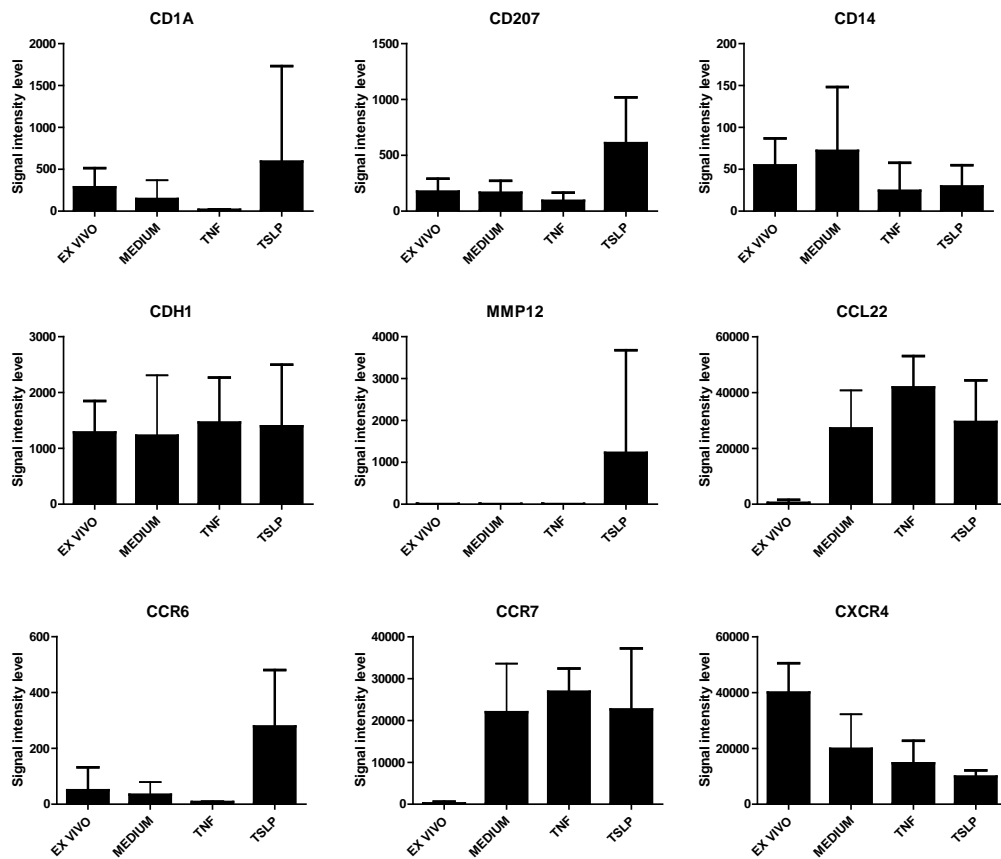
Figure 2
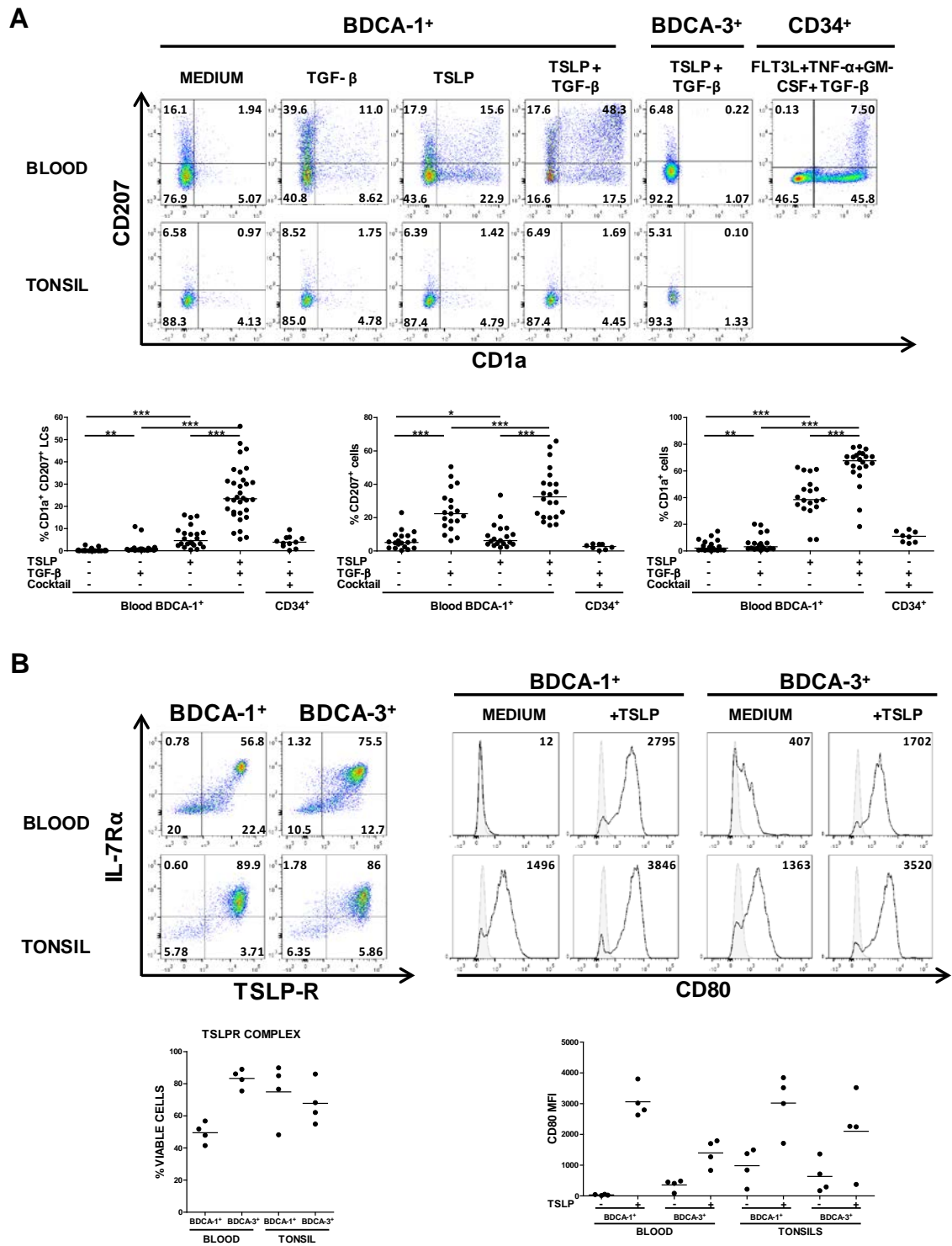
Figure 3
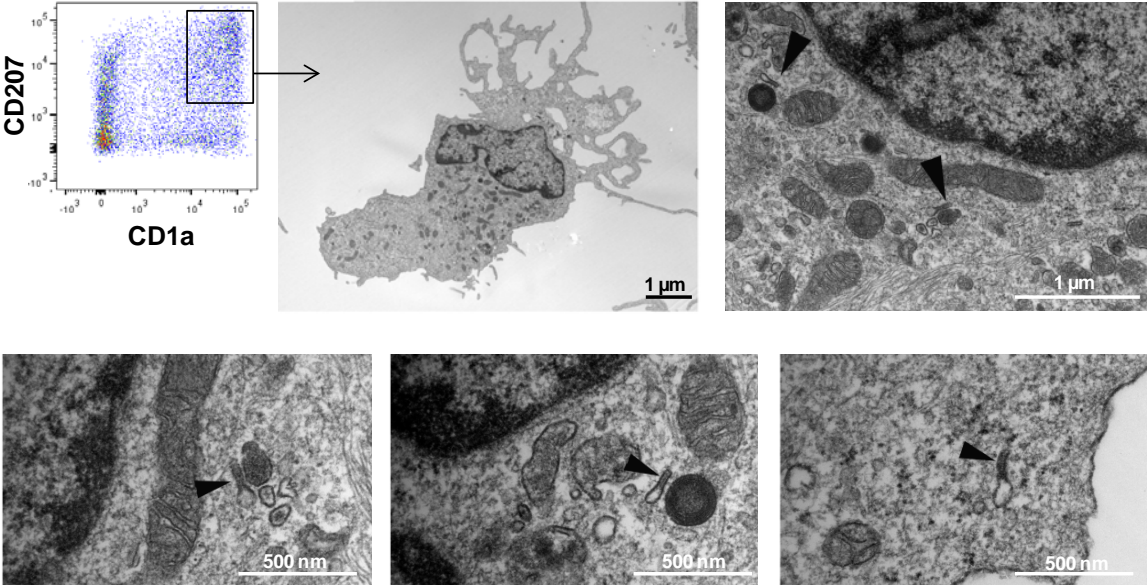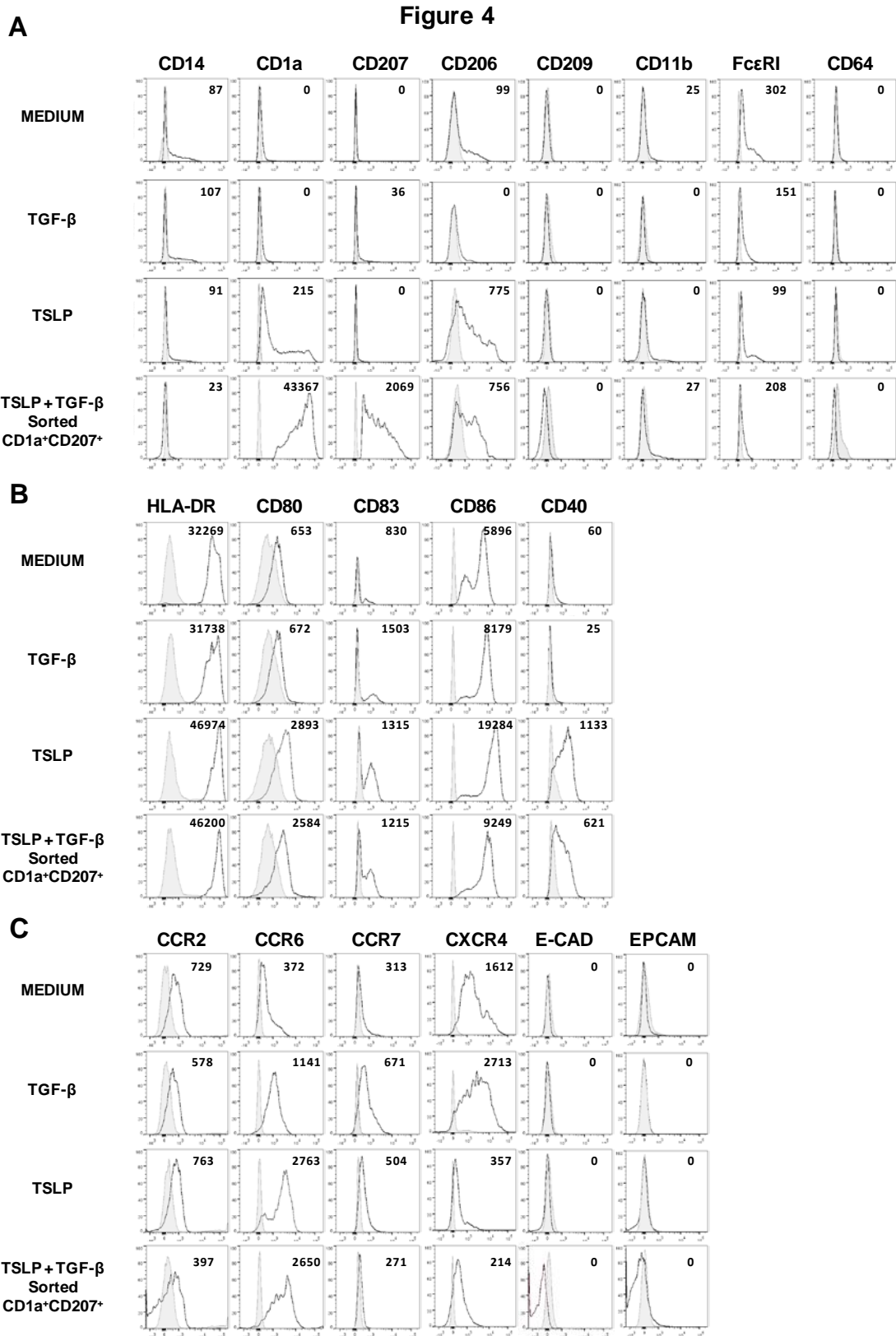
Figure 4

Figure 5

Supplemental Figure 1
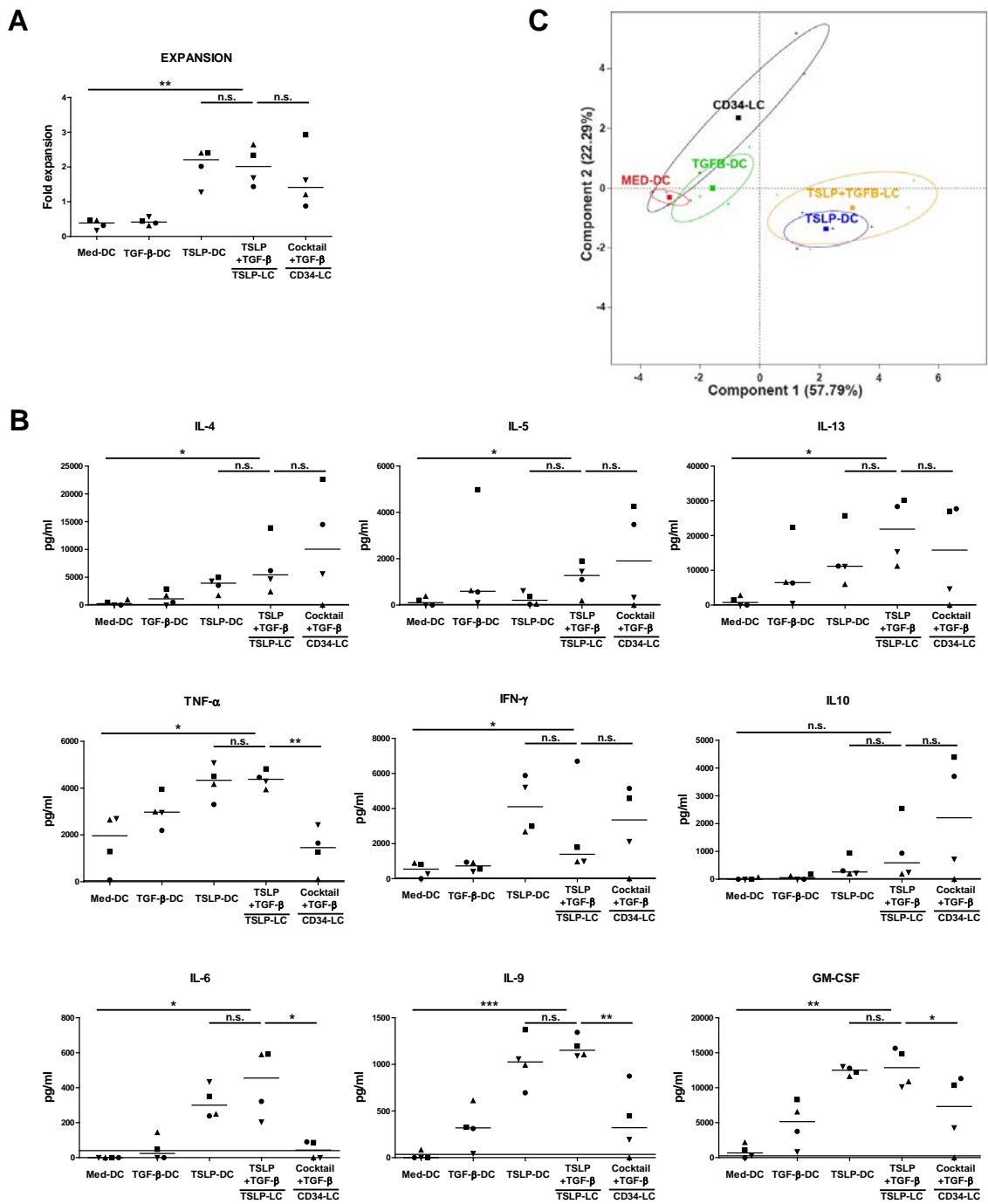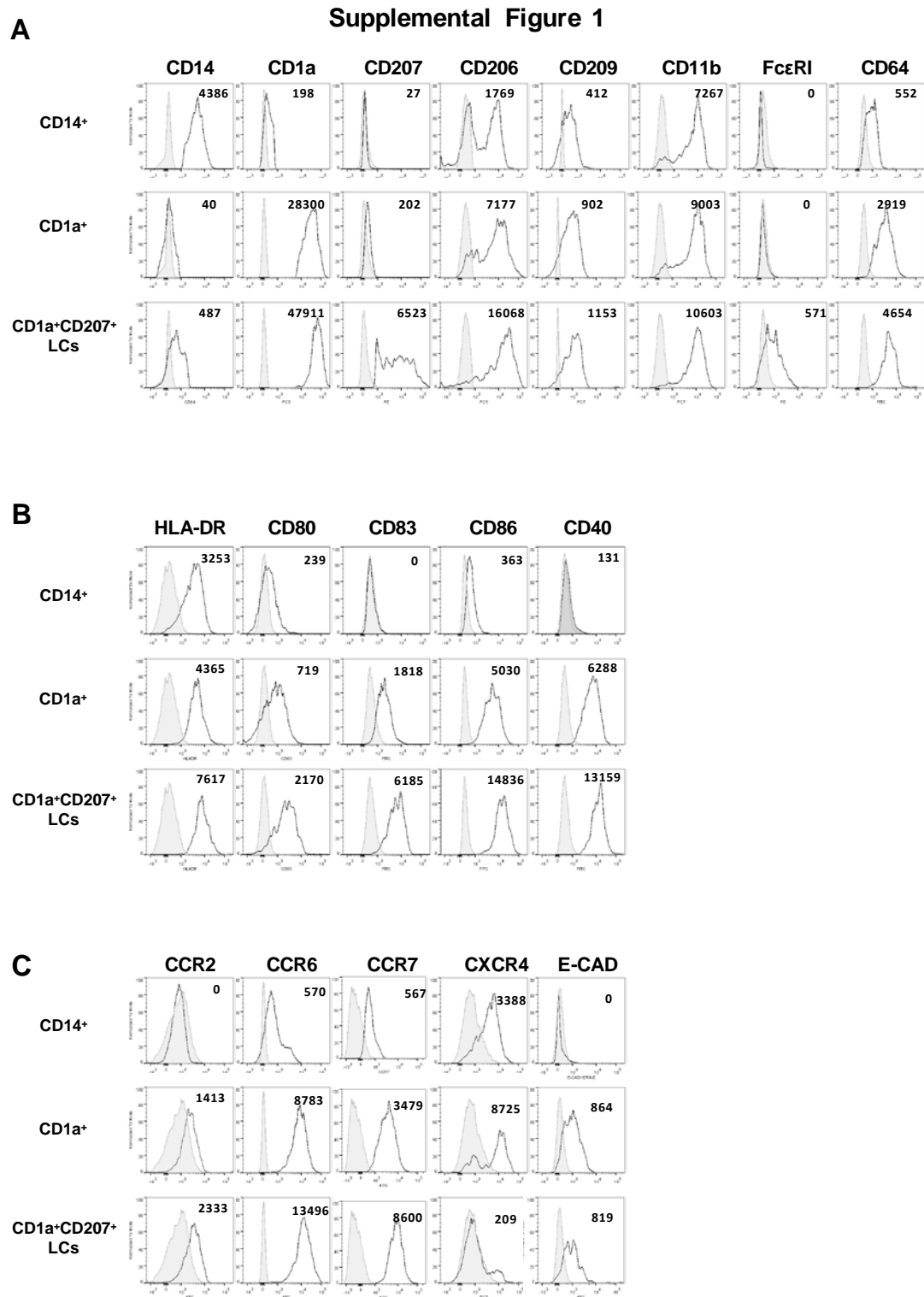
Supplemental Figure 2
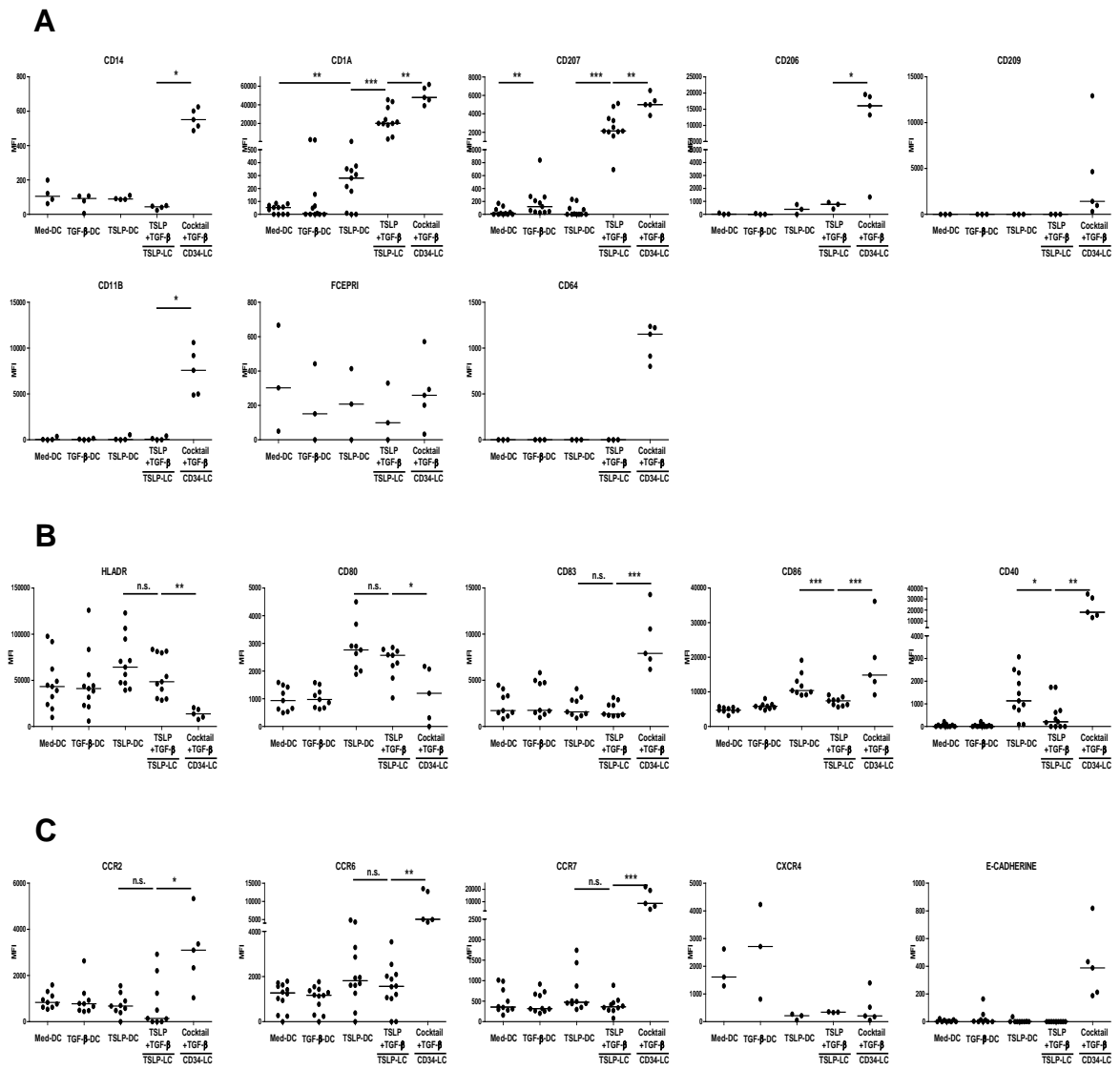
4.2 PUBLICATION 2

The human cytokine TSLP triggers a cell-autonomous dendritic cell migration in confined environments.

Maria-Isabel Fernandez, Mélina L. Heuzé, Carolina Martinez-Cingolani, Elisabetta Volpe, Marie-Hélène Donnadieu, Matthieu Piel, Bernhard Homey, Ana-Maria Lennon-Duménil and Vassili Soumelis.

The concept that TSLP may induce DC migration emerged from an initial observation by Soumelis et al. They noticed that in atopic dermatitis lesional skin, the strong expression of TSLP was associated with the absence of Langerin^{+} cells in the epidermis and the appearance of activated DCs and Langerin^{+} cells in the dermis [133] . In the study presented here, we directly assessed the capacity of TSLP to trigger DC migration.

To this end we assessed the effects of TSLP on in vitro migration of human blood primary DCs using collagen I coated and uncoated transwells (see Materials and methods). This system allowed us to show that TSLP induced chemokinesis of primary human DCs. This was not the case for the other activating stimuli applied to DCs such as LPS, Influenza virus (Flu), TNF-α and GM-CSF.

By immunofluorescence staining of TSLP-treated DCs (TSLP-DCs) we showed that TSLP, as opposed to other stimuli, induced a polarization of the actin and microtubule cytoskeleton in DCs. Myosin-II, an essential molecule for leukocyte migration, was found to be present in the uropod and in the nuclear edge of the cells suggesting contractibility of this area. Using microfabricated channels that enabled us to assess three-dimensional cell migration under confinement, we found that TSLP-induced migration was myosin-II-dependent. This system was designed to mimic the tight intercellular areas constituted by epithelial cells that DCs need to confront to emigrate from the tissue.

TSLP activates DCs and can trigger the secretion of at least two chemokines (CCL17 and CCL22) [133]. Since chemokines are known to regulate cell migration [61, 62], I particularly assessed whether TSLP itself was required to trigger DC-migration or whether there was a role for TSLP-induced molecules acting in an autocrine manner. To test this, I collected the supernatants of TSLP-DCs after a 24 hour culture. These supernatants contained TSLP and the factors secreted by the DCs after TSLP treatment (Supplemental Figure 2). To assess specifically the effects of the secreted factors, I blocked direct TSLP effects using an anti-TSLP neutralizing antibody. DCs treated for 24 hours with this blocked supernatants were assessed for their capacity to migrate in collagen I-coated transwells. A percentage of migration was calculated taking into account the cell count in the lower chamber divided by

the total cell count (low and upper chambers). As DCs constitutively express CXCR4 and migrate towards its ligand SDF-1 (CXCL12) [181, 182], I used it in the lower chamber of the transwells as a chemoattractant and a positive control of the intrinsic capacity of the cells to migrate. CD80 surface expression was evaluated in the different conditions as a marker of TSLP-induced maturation of DCs.

TSLP-DC culture supernatants induced DC migration to the same levels (41.4 ± 9 %) than recombinant human TSLP (42.3 ± 5 %). Interestingly, when TSLP effect was neutralized in TSLP-DC culture supernatants, DC migration was inhibited to the levels of spontaneous migration (18.7 ± 4 % and 20.3 ± 4 % respectively).TSLP-DC unblocked supernatants induced CD80 expression and when TSLP was neutralized CD80 expression was inhibited. These results showed that TSLP-induced secreted molecules were not sufficient to recapitulate neither the migration effect nor the maturation effect induced by TSLP on DCs.

Overall our data showed that TSLP triggered DC migration through the polarization of DCs and the activation of the molecular motor myosin-II. This was important to link TSLP stimulation of DCs in peripheral organs like the skin, to the ability of TSLP-DCs to activate naïve T cells in the lymph nodes.

We showed that TSLP was required to induce DC maturation and migration suggesting direct effects of TSLP on these processes. As a further step I wanted to determine which were the molecular mechanisms implicated in TSLP-induced migration. This is the subject of a second work that is still in preparation.

The human cytokine TSLP triggers a cell-autonomous dendritic cell migration in confined environments

*Maria-Isabel Fernandez,[1-3] *Mélina L. Heuzé,[1,3,4] Carolina Martinez-Cingolani,[1-3] Elisabetta Volpe,[1-3] Marie-Helene Donnadieu,[1-3] Matthieu Piel,[3-5] Bernhard Homey,[6] Ana-Maria Lennon-Duménil,[1,3,4] and Vassili Soumelis[1-4]

[1]Inserm U932, Paris, France; [2]Department of Immunology, Institut Curie, Paris, France; [3]CBT507 IGR-Curie (Inserm Center of Clinical Investigation), Paris, France; [4]Research Section, Institut Curie, Paris, France; [5]Centre National de la Recherche Scientifique, Unité Mixte de Recherche 144, Paris, France; and [6]Department of Dermatology, Heinrich Heine University, Düsseldorf, Germany

Dendritic cells (DCs) need to migrate in the interstitial environment of peripheral tissues to reach secondary lymphoid organs and initiate a suitable immune response. Whether and how inflamed tissues instruct DCs to emigrate is not fully understood. In this study, we report the unexpected finding that the epithelial-derived cytokine TSLP triggers chemokinesis of resting primary human DCs in a cell-autonomous manner. TSLP induced the polarization of both microtubule and actin cytoskeletons and promoted DC 3-dimensional migration in transwell as well as in microfabricated channels that mimic the confined environment of peripheral tissues. TSLP-induced migration relied on the actin-based motor myosin II and was inhibited by blebbistatin. Accordingly, TSLP triggered the redistribution of phosphorylated myosin II regulatory light chain to the actin cortex, indicating that TSLP induces DC migration by promoting actomyosin contractility. Thus, TSLP produced by epithelial cells in inflamed tissue has a critical function in licensing DCs for cell-autonomous migration. This indicates that cytokines can directly trigger cell migration, which has important implications in immune physiopathology and vaccine design. (*Blood*. 2011;118(14): 3862-3869)

Introduction

Competence of dendritic cells (DCs) to induce the differentiation of naive T cells into effector T cells relies on their ability to migrate from the peripheral sites of inflammation to the secondary lymphoid organs where T-cell priming takes place.[1,2] During this process, DCs must emigrate out of peripheral tissue and move through a variety of narrow spaces, such as tight intercellular junctions in epithelia, basal membrane, extracellular matrix, and endothelia. This motility is in part orchestrated by chemokine gradients, such as CCL19 or CCL21, which dictate the directionality of the movement toward lymphoid organs where these chemokines are abundantly expressed.[3] Whether endogenous signals produced by injured tissue at the inflammatory site can instruct DCs to migrate is currently unknown.

Cytokines are proteins that act through specific surface receptors to modulate critical cellular functions, such as cell proliferation, differentiation, and survival.[4] They are important components of the inflammatory microenvironment. Their precise function in inducing or modulating cell migration has not been elucidated. Thymic stromal lymphopoietin (TSLP) is an epithelial cell-derived cytokine that strongly activates DCs and initiates a Th2 type of CD4 T-cell response.[5] It plays a critical role in allergic diseases and, in particular, atopic dermatitis where it is highly produced by keratinocytes in human lesions[6] and mouse models.[7,8] Thus, TSLP mediates a cross-talk between inflamed epithelia and the innate immune response.[5]

Previous studies from our group and others suggested that TSLP may be associated with Langerhans cell migration in situ[6] and ex vivo.[9] In this study, we demonstrate that TSLP is sufficient to induce the polarization, and 3-dimensional and confined migration of human DC in vitro, through the actin-based motor protein, myosin II. This constitutes a novel property of cytokines in triggering a cell-autonomous DC migration in interstitial spaces.

Methods

Blood DC purification and culture

CD11c^{+} DCs were purified to 99% by FACS sorting from buffy coats of healthy adult volunteer blood donors (Crozatier Blood Bank) as previously described.[6] Freshly sorted CD11c^{+} DCs were cultured in RPMI containing 10% FCS, 1% pyruvate, 1% HEPES, and 1% penicilin-streptomycin. Cells were seeded at 1×10^6/mL in flat-bottom 96-well plates in the absence (untreated cells) or presence of 50 ng/mL TSLP (R&D Systems), 2.5 ng/mL TNF (R&D Systems), 20 µg/mL influenza virus (H1N1, A/PR/8/34 strain; Charles River Laboratories), 1 µg/mL lipopolysaccharide (LPS; Sigma-Aldrich), or 100 ng/mL GM-CSF (BruCells).

Immunofluorescence

To determine the cytoskeleton architecture, DCs were cultured on poly-lysine–coated coverslips for 24 hours and examined by epifluorescence microscopy. Cells were fixed in 4% paraformaldehyde in PBS for 20 minutes at room temperature, permeabilized by 1% Triton X-100 in PBS for 5 minutes, and blocked with 1% BSA in PBS for 20 minutes at room temperature. For localization of filamentous actin, cells were incubated with Cy3-phalloidin (Invitrogen) for 30 minutes. Counting of the number of polarized DCs from 5 different donors assessed polarization index.

Polarization was expressed as proportion polarized cells respect to total number of cells. Localization of α-tubulin was achieved by incubation for 1 hour with a rat anti–human α-tubulin antibody (Serotec). Myosin II was detected by a rabbit anti–human myosin II heavy chain antibody (BTI) followed by incubation for 30 minutes with Alexa-488 goat anti–rabbit (Invitrogen). Coverslips were mounted in ProLong Gold antifade reagent (Invitrogen). Fluorescence images were obtained by an epifluorescence microscope (Leica) fitted with appropriate filter sets. For phospho-myosin II light chain and actin staining, cells were permeabilized in 0.2% BSA, 0.05% saponin for 10 minutes, and antibodies were diluted in the same solution. Phospho-myosin II light chain was detected with a rabbit anti–phospho-myosin light chain 2 (pMLC2; Rockland) followed by incubation with Alexa-488 goat anti–rabbit antibody. For quantification of pMLC2 association to actin, images were acquired on an epifluorescence Nikon microscope (Eclipse 90i Upright) with a 100× objective. After deconvolution, colocalization was quantified on each plane by the colocalization analysis program of Metamorph and represented as the percentage of pMLC2 area colocalized with actin area. For each cell analyzed, the result is expressed as a mean of all the planes.

Transwell DC migration

Uncoated or collagen type I (5 μg/mL rat tail collagen type I; BD Biosciences) coated transwells (Costar, 3-μm pores) were placed in 96-well plates filled with 200 μL of DC culture medium. Overnight treated DCs (1×10^6/mL) with TSLP, TNF, LPS, influenza virus, or GM-CSF were resuspended in 50 μL of this solution, added to the upper chamber of the transwells, and incubated at 37°C for 6 hours. CCL20 (500 ng/mL; R&D Systems) was added to the lower chamber as a positive control to induce DC migration where mentioned. After 6 hours, cells in the upper and the lower chambers of the transwell were counted. Results were expressed as percentage of total DCs.

DC migration in microchannels

The microfluidic device was fabricated in polydimethylsiloxane (PDMS).[10] The PDMS piece, with embedded microchannels and holes for the inlet and outlet ports, and a glass Iwaki chamber (Milian) were activated in a plasma cleaner (PDC-32G Harrick) and bonded to each other. The chambers were left under strong vacuum for 5 minutes in the plasma cleaner, and plasma was turned on to render the top surface of the PDMS and the inlet and outlet holes hydrophilic. Fibronectin solution at 50 μg/mL was placed on top of the inlet and outlet ports. The solution spontaneously invaded the channels, and all air bubbles were resorbed into the PDMS because of the previous vacuum treatment. Fibronectin was incubated for 1 hour at room temperature, then washed with PBS, and then replaced by cell culture medium. The cells were concentrated, and micropipette tips containing the cells were inserted in the inlet port. Cells fell inside the port, bound to the bottom coverslip, and started migrating. They entered the channels spontaneously, without any mechanical or chemical stimulation.

Phase-contrast images at various positions in the chambers were recorded with time lapses of 1-2 minutes during 6-10 hours, using an automated microscope (Nikon Eciplse TE1000-E, and Olympus X71, with a Marzhauser motorized stage and an HQ2 Roper camera) equipped with an environmental chamber for temperature, humidity, and CO_2 (Life Imaging Services). Cells remained alive and motile during the entire period of recording.

Kymograph extraction and instantaneous velocity analysis

Without any intervention from the user, a program written in C++, taking as input an image sequence, provides as output a set of kymographs corresponding to each channel by automatically performing motion compensation, background subtraction, channel detection, and kymograph computation. A number of parameters are accessible when the program is started. Each resulting kymograph is an image that contains, in each horizontal line, the gray values found along a given channel at a given time point. The consecutive time points form the consecutive lines of the image, with time zero at the top. This allowed us to reduce large datasets into a smaller set of

images. Specifically, 1 image per channel was obtained, which contains all the necessary information for cell movement analysis. The space dimension perpendicular to the channel length that contains no information was suppressed. The program first performed image cleaning: indeed, at 10× magnification, with phase-contrast microscopy, 4-μm-wide channel displays a strong contrast, and cells in the channels are hardly visible on original images. Moreover, because of fast movements of the stage to get enough positions recorded at a high temporal rate, image sequences displayed slight jiggling because of repositioning errors. Subpixel phase correlation[11] and robust multiresolution estimation of translation motion model were used for registration. Then background subtraction was done before the computation of the kymograph. The background was estimated by taking the average intensity along the image sequence. To produce kymographs, first, channels were detected using the Hough transform. An average width for the lines was defined as the half the distance between 2 channels (this parameter can be varied). Intensities of the kymographs were then defined as the maximum intensity inside the bound of the line encountered perpendicularly to it.

Kymographs were then analyzed using homemade routines in MATLAB. Cell signature was identified in each line, and the cells' center of mass and boundaries were found. Statistics and graphs were extracted from the data using MATLAB.

Blebbistatin treatment of DCs

To study the role of myosin II in the morphology of TSLP-DCs, cells were incubated for 12 hours in TSLP with or without 50μM blebbistatin on poly-lysine–coated slides to permit the polarization of cells. To analyze the importance of myosin II in DCs migration, untreated or pretreated DCs for 24 hours were incubated during the migration time with 50μM blebbistatin in collagen-coated transwells. For the migration analysis in microchannels, cells were pretreated with 50μM blebbistatin and then concentrated and inserted in the microchannels.

Statistical analysis

Statistical analysis of the differences between experimental groups was performed using a nonparametric ANOVA (Mann-Whitney test). Differences were considered statistically significant when P was $< .05$. Results were expressed as mean ± SD.

Results

TSLP directly induces chemokinesis of primary human DCs

To address the role of TSLP in DC migration, we analyzed its impact on in vitro migration of nonactivated and activated primary human DCs using uncoated semipermeable filters (Transwells). We observed that ∼ 7% of untreated DCs showed a spontaneous baseline migration (Figure 1A). Two TLR ligands, LPS and influenza virus (flu), which strongly activate DCs, did not induce DC migration (Figure 1A). This equally applied to GM-CSF, a cytokine produced by epithelial cells and leukocytes during inflammation. On the contrary, TSLP-treated DCs (TSLP-DCs) became highly efficient for migration in the absence of exogenous chemokines, with up to 30% migrating cells, equivalent to a CCL20-driven chemotaxis (Figure 1A). Thus, TSLP was able to induce 2-dimensional migration of human DCs ex vivo.

Next, we analyzed the ability of TSLP-DCs to migrate through the 3-dimensional space of collagen type I–coated filter. TSLP-DCs became highly efficient for migration (Figure 1B) contrary to TNF-DCs, which migrated comparably to untreated DCs. LPS, flu, and GM-CSF did not induce human DC migration (Figure 1B), similar to uncoated transwells (Figure 1A). TSLP-induced DC migration was detectable as soon as 3 hours after TSLP exposure (supplemental Figure 1A, available on the *Blood* Web site; see the
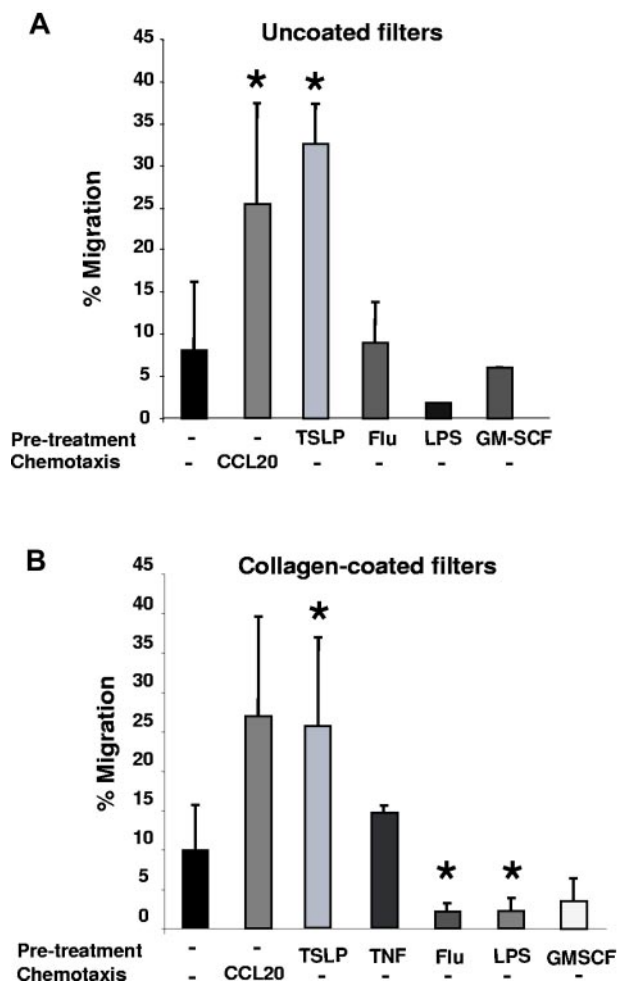
Figure 1. TSLP induces chemokinesis of resting DCs in a cell-autonomous manner. (A) Purified blood DCs were precultured in medium (untreated), TSLP, influenza virus (Flu), LPS, or GM-CSF. After 24 hours, cells were washed, counted, and seeded in equal numbers in the upper chamber of an uncoated transwell system in the absence of chemotactic factors. After 6 hours, DCs migrating into the lower chamber were harvested and counted. Data are represented as percentage of input DCs. In the positive control, CCL20 was used in the lower chamber during migration as a chemotactic factor. Data are mean ± SD; n = 7. *P < .05 vs untreated. (B) Primary blood DCs were precultured in medium, TSLP, TNF, influenza virus (Flu), LPS, or GM-CSF. After 24 hours, cells were washed, counted, and seeded in equal numbers in the upper chamber of a collagen-coated transwell system in the absence of chemotactic factors. After 6 hours, DC migration was quantified. Data are represented as percentage of input DCs. In the positive control, CCL20 was added in the lower well. Data are mean ± SD; n = 5. *P < .05 vs untreated.

Supplemental Materials link at the top of the online article), in accordance with the up-regulation of TSLP receptor expression by human DCs in culture (data not shown). TSLP-DC migration was dose-dependent and could be activated at TSLP concentrations > 1 ng/mL TSLP (supplemental Figure 1B). To discriminate between chemokinesis and chemotaxis, we added TSLP to the lower chamber of the transwell. This did not affect the migration of untreated DCs, excluding chemotactic properties of TSLP (data not shown).

The fact that TSLP could induce DC migration independently of exogenous factors indicated a cell-autonomous mechanism. However, this does not exclude a role for TSLP-induced molecules acting in an autocrine manner. To address whether TSLP itself was required or whether TSLP-induced secreted factors could recapitulate the increase in DC migration, we performed experiments using TSLP-DC supernatants in the presence and absence of an anti-TSLP blocking monoclonal antibody (mAb; supplemental Figure 2).

First, we assessed CD80 expression as a marker of DC activation. TSLP induced a strong up-regulation of CD80, which was inhibited by anti-TSLP mAb (supplemental Figure 2A). TSLP-DC supernatants, which contained both TSLP and TSLP-induced secreted molecules, had a similar effect on CD80 expression compared with TSLP alone. This effect was almost completely blocked by anti-TSLP mAb, indicating that TSLP-induced secreted molecules were not sufficient to recapitulate the maturation effect of TSLP (supplemental Figure 2A). In a parallel set of experiments, we assessed DC migration in transwell under similar conditions as for CD80 expression (supplemental Figure 2B). TSLP and TSLP-DC supernatant both increased DC migration, and their effect was inhibited by anti-TSLP blocking mAb (supplemental Figure 2B). This showed that TSLP was required for the induction of a cell-autonomous DC migration and that TSLP-induced secreted molecules could not recapitulate this effect.

TSLP induces a marked polarization of the cytoskeleton of DCs

The cell-autonomous TSLP-induced DC motility suggested that cell-intrinsic mechanisms might be involved. Because cell polarization is an essential feature for cell locomotion, we questioned whether TSLP could induce the polarization of human DCs. To address this hypothesis, we performed a detailed analysis of TSLP-DC morphology. Untreated human DCs cultured on poly-lysine-coated coverslips appeared mostly round, with actin filaments enriched at the cell cortex as well as in podosomes, which are actin-rich adhesion structures that form close contacts with the substrate and are most likely involved in cell motility[12,13] (Figure 2A). A similar morphology was observed in DCs activated by influenza virus (Figure 2A). LPS induced the formation of multiple dendritic expansions and the dissolution of podosomes, as previously described[14] (Figure 2A). Remarkably, TSLP treatment increased the fraction of polarized cells from 12% (spontaneous polarization) to 43% (P < .05; Figure 2A-B). In these cells, the nucleus was located at one cell pole, whereas the other was formed by a long and thin uropod. Podosomes were dissoluted in many cells, but when present they clustered predominantly in the perinuclear area where actin filaments were enriched (Figure 2A). As observed for the actin cytoskeleton, the microtubule network was also reorganized in TSLP-treated DCs, with the microtubule-organizing center localized behind the nucleus at the level of the uropod, as previously described in polarized T cells (Figure 2C). Microtubule-organizing center polarization was not observed in untreated or LPS-treated DCs (Figure 2C; supplemental Figure 1C). Interestingly, spontaneous DC polarization was significantly inhibited by TLR ligands, such as flu and LPS (Figure 2B). In conclusion, TSLP induced an important reorganization of the cell cytoskeleton, leading to the polarization of human DCs, which may license DCs for migration.

TSLP induces myosin II-dependent DC motility

It was recently shown that the actin-based motor protein myosin II is essential for the 3-dimensional movement of mouse leukocytes.[15] Thus, we addressed its role in TSLP-induced human DC motility. Myosin II consists of 2 heavy chains whose N-terminus contains a globular head that includes the actin- and adenosine triphosphate (ATP)-binding sites, and of 2 regulatory light chains (MLCs), whose phosphorylation status controls the activity of the protein motor. When phosphorylated, MLC binds to myosin II heavy chain and triggers ATP hydrolysis followed by head displacement toward the plus-end of actin filaments, resulting in actomyosin contraction.

Figure 2. TSLP induces polarization of the DC cytoskeleton. (A) DCs on poly-lysine–coated coverslips were cultured in medium (untreated), influenza virus (Flu), LPS, or TSLP. Cells were stained for actin (red) and DAPI (blue) and observed under a fluorescence microscopy. Podosomes appeared as round actin-stained formations. Actin skeleton was reorganized in a polarized manner in TSLP-DCs. Data are from one representative of 5 independent experiments. (B) After 24 hours of culture, DCs with a polarized actin skeleton were quantified. Results are represented as percentage of total DCs. Data are mean ± SD; n = 5. *$P < .05$ vs untreated. $^+P < .05$ vs TSLP. (C) After 24 hours of culture, DCs were stained with an anti–α-tubulin mAb (green) and DAPI (blue). TSLP-DCs showed a reorganization of the microtubules. Data are from 1 representative of 5 independent experiments.
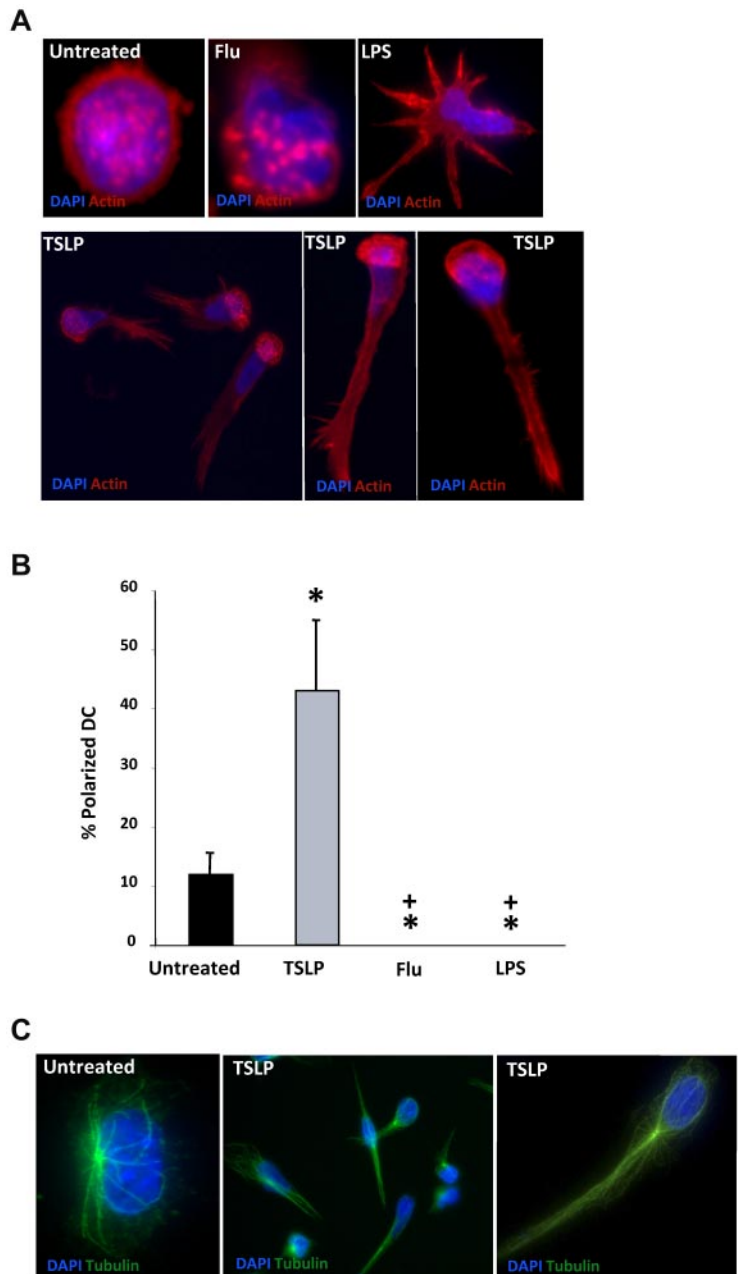
In TSLP-DCs, myosin II heavy chain showed a cortical distribution and was found to be preferentially associated with actin filaments in the cell uropod (Figure 3A), as was described for mouse leukocytes.[15,16] Moreover, myosin II accumulated also in the nuclear edge of DCs (Figure 3A), suggesting contractibility of this area. Importantly, TSLP-induced myosin II redistribution was also observed for activated phospho-MLCs in TSLP-DCs (Figure 3B). Quantification after 3-dimensional reconstruction showed an increase in the colocalization of phospho-MLC and actin after TSLP treatment (Figure 3C), suggesting an increased actomyosin contractility.

To directly address the role of myosin II in TSLP-induced DC polarization, we inhibited myosin II-ATPase activity using its specific inhibitor blebbistatin.[17] Inhibition of myosin II prevented TSLP-induced DC polarization (Figure 4A). Blebbistatin-treated DCs displayed an elongated cellular shape with multidirectional extensions.[18] Last, we questioned whether loss of cytoskeleton

polarization affected the migration of DCs. Blebbistatin treatment decreased the TSLP-DC migration through collagen-coated semipermeable filter (from 30% to 11%; $P < .01$; Figure 4B). Migration of TSLP-DCs was inhibited by doses as low as 20μM blebbistatin (supplemental Figure 3). We conclude that myosin II activity is essential for both polarization and migration of human DCs induced by TSLP.

TSLP promotes DC migration in the confined environment of microfabricated channels

In vivo, DCs migrate in confined spaces, and recent evidence shows that the geometry of tissues directly impacts the requirements and mechanisms involved in cell movement.[15] To assess whether TSLP may impact human DC migration in tissues, we used micro-fabricated channels that mimic the constrained interstitial space of peripheral tissues.[19] Live cell imaging of DC migration
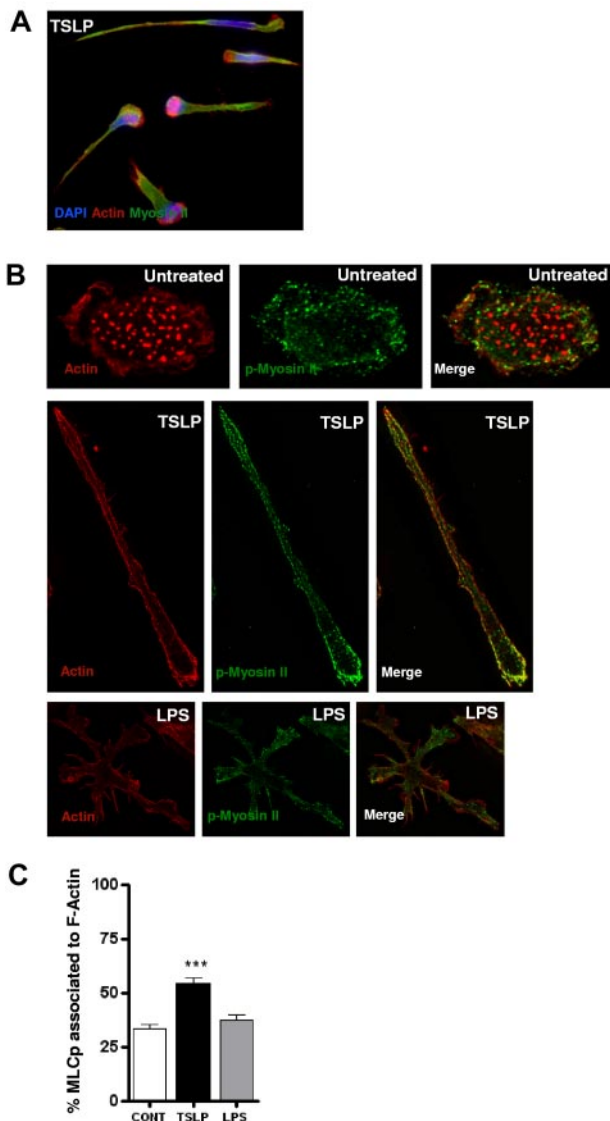
Figure 3. TSLP induces redistribution and colocalization of actin and phospho-myosin II light chain. (A) After 24 hours of culture, TSLP-DCs were stained for myosin II (green), actin (red), and DAPI (blue). TSLP-DCs acquired a polarized morphology, and actin and myosin filaments largely colocalized. Data are from 1 representative of 3 independent experiments. (B) DCs on poly-lysine–coated coverslips were cultured in medium, TSLP, or LPS for 20 hours. Cells were stained for F-actin (red) and pMLC9 (green). Images were acquired as z-series, deconvoluted, and reconstructed as a maximum-intensity projection of all the planes. (C) Quantification of the mean percentage of pMLC area colocalized with F-actin area. For each cell, the percentage is a mean of all the planes. Data are mean ± SEM of 2 independent experiments; n = 20. ***$P < .005$.

revealed that TSLP-DCs were more efficient in reaching the border and entering the 4-μm-wide channels than untreated cells (Figure 5A; supplemental Videos 1-2). This effect of TSLP resulted in increased numbers of DCs traveling along microchannels at a given time after TSLP pretreatment (Figure 5A). For each migration experiment, sequential pictures of cells migrating along microchannels were visualized as kymographs, which were used to analyze persistence and calculate instantaneous velocities (Figure 5B). Once inside the channels, TSLP-DCs were more persistent and displayed a more regular and continuous movement compared with untreated DCs (changes of direction in movement inside channels: 10% of TSLP-DCs vs 32% of untreated-DCs; Figure 5B-C). No significant migration was observed when treating

DCs with flu (supplemental Video 3). We found no significant difference between the median instantaneous speed of TSLP-DCs and untreated DCs, both reaching ~ 11 μm/min in both conditions (5D). Similar results were obtained for maximal DC velocities (Figure 5D). We conclude that TSLP promotes the motility of DCs in confined environments but did not modify their velocity.

To assess whether the increased ability of TSLP-DCs to enter microchannels results, at least in part, from TSLP-induced polarization, we analyzed whether TSLP-induced human DC motility was compromised when inhibiting myosin II activity. Blebbistatin treatment of TSLP-DCs reduced by 50% their ability to enter microchannels (Figure 6A). Similar results were obtained using ML7/Y27632, a combination of 2 MLC phosphorylation inhibitors (Figure 6A), confirming the specificity of the inhibitory process to myosin II. 4,6-Diamidino-2-phenylindole (DAPI)/annexin V staining showed no significant change in DC viability when either myosin II inhibitors were added to TSLP, indicating that the inhibition of DC migration was not the result of an increased cell death (supplemental Figure 4). The velocity of TSLP-treated DCs was also decreased on myosin II inhibition, confirming the involvement of actomyosin contraction in DC migration in confined environments. In addition, blebbistatin modified the velocity distribution of TSLP-treated DCs: whereas 70% of TSLP-DCs exhibited velocities > 10 μm/min, only 32% of blebbistatin-treated TSLP-DCs did so (Figure 6B). We conclude that myosin II activity is required for TSLP-treated DCs to initiate a polarized movement and maintain high speed during motion along microchannels. Altogether, our results revealed that TSLP has the unexpected capacity to induce DC polarization in a myosin II-dependent manner, thereby licensing DCs to migrate in confined spaces.

Discussion

DC migration is a complex process that involves multiple cell-intrinsic and extrinsic factors.[2,20] Chemokines are important players that orchestrate migration and mostly act through chemoattraction, guiding the responding cell toward its target tissue destination.[3,21] The contribution of local inflammation in peripheral tissue is generally viewed as permitting and/or facilitating the action of chemokines in several ways: (1) danger signals can induce DC maturation and the up-regulation of chemokine receptors[1,2]; (2) inflammatory mediators, such as leukotrienes, can potentiate the effect of certain chemokines[22]; and (3) edema and vasodilation have a facilitating effect by promoting the nonspecific influx but also emigration of various immune cell types. In our study, we provide new evidence for an active role of the inflamed tissue in instructing DCs to migrate through the production of the cytokine TSLP.

It is commonly accepted that DC activation and migration are coupled, essentially through the induction of CCR7,[1] which would guide DCs toward secondary lymphoid organs through a CCL21 gradient.[3] Accordingly, DC-activating cytokines, such as GM-CSF and TNF, promoted Langerhans cell emigration in skin explants.[23-25] Our data challenge this view in many aspects. First, we did not observe any effect of GM-CSF and TNF in triggering a cell-autonomous DC migration. This suggests that cofactors provided by the tissue environment in the skin explants may be required. Alternatively, these cytokines may act indirectly on other skin cell types, which would support subsequent DC migration. Second, TLR ligands (LPS and flu) did not induce DC migration, although they promote strong DC maturation. This is in keeping

Figure 4. Myosin II is required for TSLP-induced polarization and motility. (A) After 24 hours of culture in the absence or presence of blebbistatin (50μM), TSLP-DCs were stained for myosin II (green), actin (red), and DAPI (blue). Blebbistatin inhibited TSLP-induced cytoskeleton rearrangements with a loss of cell polarization. Data are from 1 representative of 3 independent experiments. (B) DCs were cultured as described in Figure 1A, in the absence or presence of blebbistatin. An increased migration (6 hours) was observed after TSLP pretreatment, which was significantly decreased in the presence of blebbistatin (50μM). Each dot represents cell counts of individual experiments and bars represent the mean. *$P < .05$.
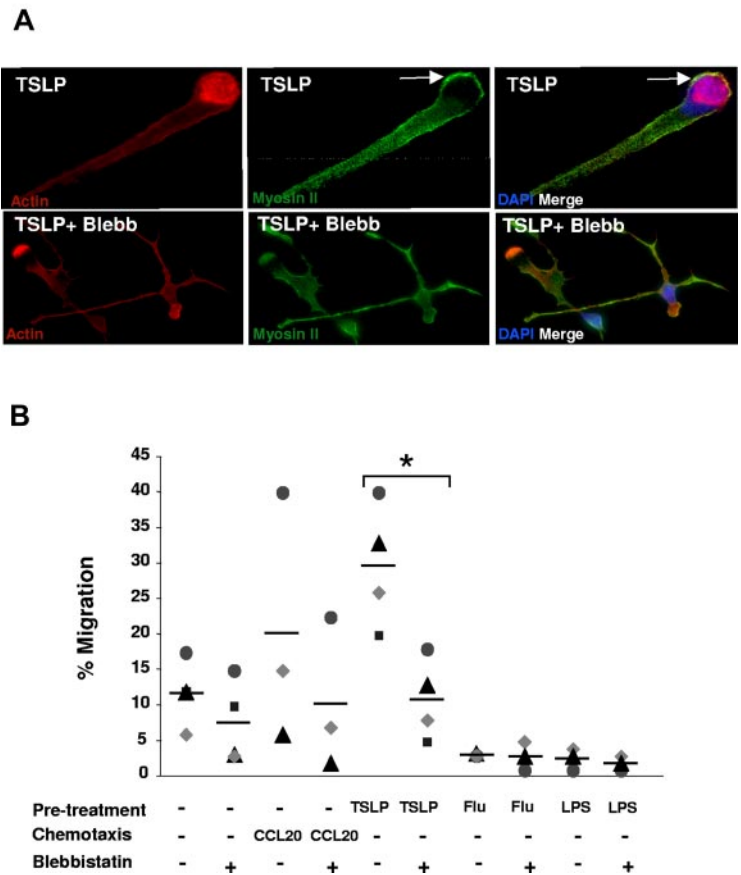
with another study showing that early LPS activation inhibited mouse DC migration,[26] which may favor an efficient antigen uptake and processing at the site of inflammation.[19] Thus, some DC-activating factors induce maturation without migration, whereas TSLP efficiently couples both functional responses. This suggests that the interplay between TLR ligands and proinflammatory cytokines at the inflammatory site may be important to coordinate maturation and migration in DCs.

To demonstrate the ability of TSLP to induce a 3-dimensional migration, we used microfabricated channels that enable cell confinement during motion and thus mimic the microenvironment encountered by DCs in the constrained interstitial spaces of peripheral tissues and lymphoid organs.[19] Microchannels impose a directional migration to DCs, which facilitates the automatic extraction from important cell numbers of accurate measurable parameters, which cannot be achieved in systems, such as 3-dimensional artificial collagen matrices.[19] We could demonstrate that, although TSLP did not increase the cell velocity compared with untreated DCs, it triggered the entry and subsequent migration of DCs inside the microchannels. This may reflect the first steps in the emigration of DCs out of the epithelium that necessitates the passage through constricted intercellular areas, the basal membrane, and the fibrotic connective tissue of the dermis.

The finding that epithelial-derived TSLP can instruct DCs to migrate reveals inflamed tissue as an important player in the complex regulation of DC migration. It will be important to identify other tissue-derived factors that may share with TSLP the ability to induce cell-autonomous chemokinesis and confined migration of DCs. The chemokinetic properties of TSLP open

numerous perspectives for our understanding and pharmacologic manipulation of DC migration in settings, such as vaccination.

Acknowledgments

Authorship

Contribution: M.-I.F. designed and performed research and drafted the manuscript; M.L.H. helped with experiment design, performed

Correspondence: Maria-Isabel Fernandez, Inserm U932, Paris, F-75248, France; e-mail: isabel.fernandez.hsj@ssss.gouv.qc.ca; and Vassili Soumelis, Inserm U932, Paris, F-75248, France; e-mail: vassili.soumelis@curie.net.
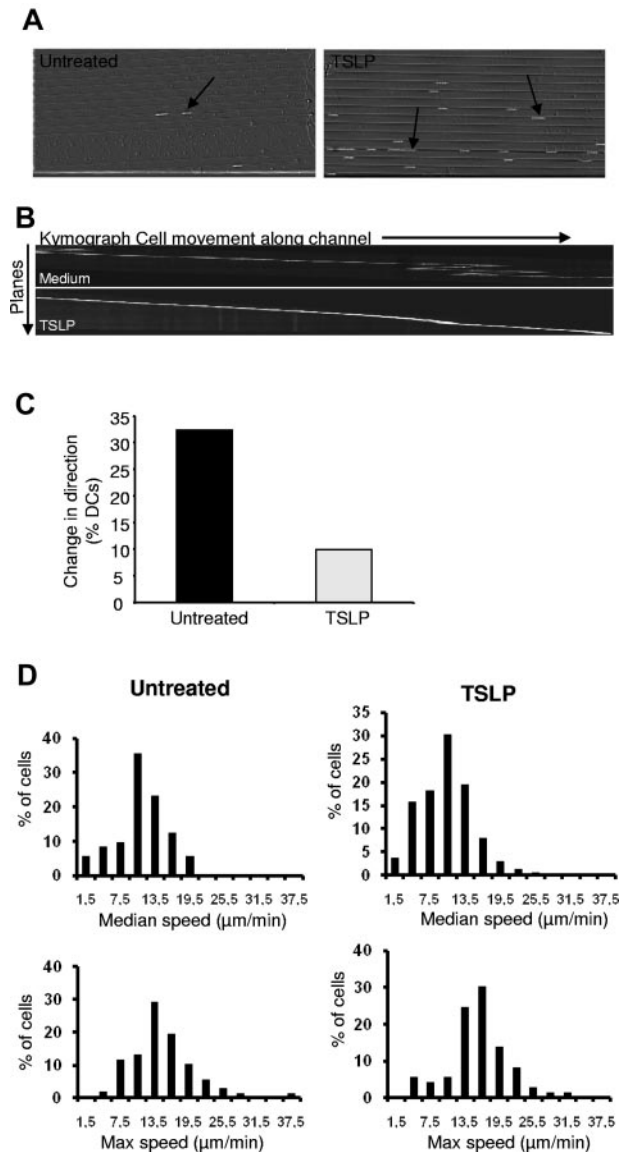
Figure 5. TSLP promotes DC migration in the confined environment of microchannels. (A) After 20 hours of culture in medium or TSLP, DCs were added in the starting chamber of the microchannel system. They were allowed to spontaneously enter the fibronectin-coated 4-μm-wide channels, and phase-contrast images were recorded. The number of cells entering the channels dramatically increased after TSLP activation of DCs (arrow indicates an individual cell inside a microchannel). (B) Representative kymograph of an untreated DC and a TSLP-DC generated by sequential pictures of a DC within a microchannel. We can see the untreated DC changing direction several times during the recording. Raw phase-contrast images were processed to analyze cell movement as described in "Kymograph extraction and instantaneous velocity." (C) After 20 hours of culture, DCs were allowed to spontaneously enter the fibronectin-coated 4-μm-wide channels, and phase-contrast images were recorded. Changes of direction through the channels were quantified for individual cells. TSLP-DCs exhibited a more straight movement. Only 10% of TSLP-DCs show changes in direction inside the microchannels. (D) Kymographs obtained in panel C were processed and analyzed to extract instantaneous speed of individual cells. The distributions of median and maximal speed of DCs precultured in control medium (left panels) or with TSLP (right panels) are not significantly different ($P > .05$). Data are from one representative of 3 independent experiments.

Figure 6. Myosin II-ATPase activity is essential for DC confined migration. (A) After a pretreatment of 20 hours with TSLP in the absence or presence of blebbistatin (50μM) or a mix of ML7/Y27632 (10μM/10μM), DCs were loaded in the entry chamber of the channels. The number of DCs entering the channels during a 12-hour time-lapse movie was quantified. TSLP induced a 4-fold increase in the capacity of DCs to enter microchannels compared with control. Blebbistatin and ML7Y27632 significantly inhibited TSLP-induced migration. Data are mean ± SD; n = 3. **$P < .01$. ***$P < .005$. (B) After 20 hours of culture in the absence or presence of blebbistatin (50μM), DCs were loaded in the entry chamber and allowed to spontaneously enter in the channels. Phase-contrast images were recorded. Kymographs were processed and analyzed to extract instantaneous speed of individual cells. Distribution of the median speed of DCs precultured in TSLP in the absence or presence of blebbistatin is significantly different ($P < .05$). Data are from 1 representative of 2 independent experiments.

experiments, and analyzed migration data; C.M.-C., E.V., and M.-H.D. performed experiments; M.P. designed migration device and analyzed data; A.-M.L.-D. and B.H. gave conceptual advice and helped with experiment design; and V.S. supervised research and wrote the manuscript.

References

1. Banchereau J, Briere F, Caux C, et al. Immunobiology of dendritic cells. *Annu Rev Immunol.* 2000; 18:767-811.

2. Randolph GJ, Angeli V, Swartz MA. Dendritic-cell trafficking to lymph nodes through lymphatic vessels. *Nat Rev Immunol.* 2005;5(8):617-628.

3. Rossi D, Zlotnik A. The biology of chemokines and their receptors. *Annu Rev Immunol.* 2000;18: 217-242.

4. Ozaki K, Leonard WJ. Cytokine and cytokine receptor pleiotropy and redundancy. *J Biol Chem.* 2002;277(33):29355-29358.

5. Liu YJ, Soumelis V, Watanabe N, et al. TSLP: an epithelial cell cytokine that regulates T cell differentiation by conditioning dendritic cell maturation. *Annu Rev Immunol.* 2007;25:193-219.

6. Soumelis V, Reche P, Kanzler H, et al. Human epithelial cells trigger dendritic cell mediated allergic inflammation by producing TSLP. *Nat Immunol.* 2002;3(7):673-680.

7. Li M, Messaddeq N, Teletin M, Pasquali JL, Metzger D, Chambon P. Retinoid X receptor ablation in adult mouse keratinocytes generates an atopic dermatitis triggered by thymic stromal lymphopoietin. *Proc Natl Acad Sci U S A.* 2005; 102(41):14795-14800.

8. Yoo J, Omori M, Gyarmati D, et al. Spontaneous atopic dermatitis in mice expressing an inducible thymic stromal lymphopoietin transgene specifically in the skin. *J Exp Med.* 2005;202(4):541-549.

9. Ebner S, Nguyen V, Forstner M, et al. Thymic stromal lymphopoietin converts human epidermal Langerhans cells into antigen-presenting cells that induce proallergic T cells. *J Allergy Clin Immunol.* 2007;119(4):982-990.

10. McDonald JC, Metallo SJ, Whitesides GM. Fabrication of a configurable, single-use microfluidic device. *Anal Chem.* 2001;73(23):5645-5650.

11. Foroosh H, Zerubia J, Berthod M. Extension of phase correlation to subpixel registration. *IEEE Trans Image Process.* 2002;11(3):188-200.

12. van Helden S, Krooshoop D, Broers K, Raymakers R, Figdor C, van Leeuwen F. A critical role for prostaglandin E2 in podosome dissolution and induction of high-speed migration during dendritic cell maturation. *J Immunol.* 2006;177(3): 1567-1574.

13. Svensson HG, West MA, Mollahan P, Prescott AR, Zaru R, Watts C. A role for ARF6 in dendritic cell podosome formation and migration. *Eur J Immunol.* 2008;38(3):818-828.

14. West MA, Prescott AR, Eskelinen EL, Ridley AJ, Watts C. Rac is required for constitutive macropinocytosis by dendritic cells but does not control its downregulation. *Curr Biol.* 2000;10(14):839-848.

15. Lämmermann T, Bader B, Monkley S, et al. Rapid leukocyte migration by integrin-independent flowing and squeezing. *Nature.* 2008;453(7191):51-55.

16. Friedl P, Weigelin B. Interstitial leukocyte migration and immune function. *Nat Immunol.* 2008; 9(9):960-969.

17. Straight A, Cheung A, Limouze J, et al. Dissecting temporal and spatial control of cytokinesis with a myosin II Inhibitor. *Science.* 2003;299(5613): 1743-1747.

18. Morin NA, Oakes PW, Hyun YM, et al. Nonmuscle myosin heavy chain IIA mediates integrin LFA-1 de-adhesion during T lymphocyte migration. *J Exp Med.* 2008;205(1):195-205.

19. Faure-Andre G, Vargas P, Yuseff MI, et al. Regulation of dendritic cell migration by CD74, the MHC class II-associated invariant chain. *Science.* 2008;322(5908):1705-1710.

20. Yoneyama H, Matsuno K, Matsushimaa K. Migration of dendritic cells. *Int J Hematol.* 2005;81(3): 204-207.

21. Sallusto F, Lanzavecchia A. Understanding dendritic cell and T-lymphocyte traffic through the analysis of chemokine receptor expression. *Immunol Rev.* 2000;177:134-140.

22. Robbiani DF, Finch RA, Jager D, Muller WA, Sartorelli AC, Randolph GJ. The leukotriene C(4) transporter MRP1 regulates CCL19 (MIP-3beta, ELC)-dependent mobilization of dendritic cells to lymph nodes. *Cell.* 2000;103(5):757-768.

23. Cumberbatch M, Dearman RJ, Kimber I. Langerhans cells require signals from both tumour necrosis factor-alpha and interleukin-1 beta for migration. *Immunology.* 1997;92(3):388-395.

24. Rupec R, Magerstaedt R, Schirren CG, Sander E, Bieber T. Granulocyte/macrophage-colony-stimulating factor induces the migration of human epidermal Langerhans cells in vitro. *Exp Dermatol.* 1996;5(2):115-119.

25. Matthews K, Bailey SL, Gossner AG, Watkins C, Dalziel RG, Hopkins J. Gene gun-delivered pGM-CSF adjuvant induces enhanced emigration of two dendritic cell subsets from the skin. *Scand J Immunol.* 2007;65(3):221-229.

26. Zaru R, Mollahan P, Watts C. 3-Phosphoinositide-dependent kinase 1 deficiency perturbs TLR signaling events and actin cytoskeleton dynamics in dendritic cells. *J Biol Chem.* 2008;283(2):929-939.

Kymograph extraction and instantaneous velocities analysis

Without any intervention from the user, a program written in C++, taking as input an image sequence provides as output a set of kymographs corresponding to each channel by automatically performing motion compensation, background subtraction, channels detection and kymographs computation. A number of parameters are accessible when the program is started. Each resulting kymograph is an image which contains, in each horizontal line, the grey values found along a given channel at a given time point. The consecutive time points form the consecutive lines of the image, with time zero at the top. This allowed us to reduce large data sets into a smaller set of images. Specifically, one image per channel was obtained, which contains all the necessary information for cell movement analysis. The space dimension perpendicular to the channels length that contains no information was suppressed. The program first performed image cleaning: indeed, at 10× magnification, with phase contrast microscopy, 4 µm wide channel display a strong contrast and cells in the channels are hardly visible on original images. Moreover, due to fast movements of the stage in order to get enough positions recorded at a high temporal rate, image sequences displayed slight giggling, due to re-positioning errors. Sub pixel phase correlation (26) and robust multi-resolution estimation of translation motion model was used for registration. Then background subtraction was done before the computation of the kymograph. The background was estimated by taking the average intensity along the image sequence. To produce kymographs, first, channels were detected using the Hough transform. An average width for the lines was defined as the half of the distance between two channels (this parameter can be varied). Intensities of the kymographs were then defined as the maximum intensity inside the bound of the line encountered perpendicularly to it.

Kymographs were then analysed using homemade routines in Matlab. Cell signature was identified in each line and the cells center of mass and boundaries were found. Statistics and graphs were extracted from the data using Matlab.
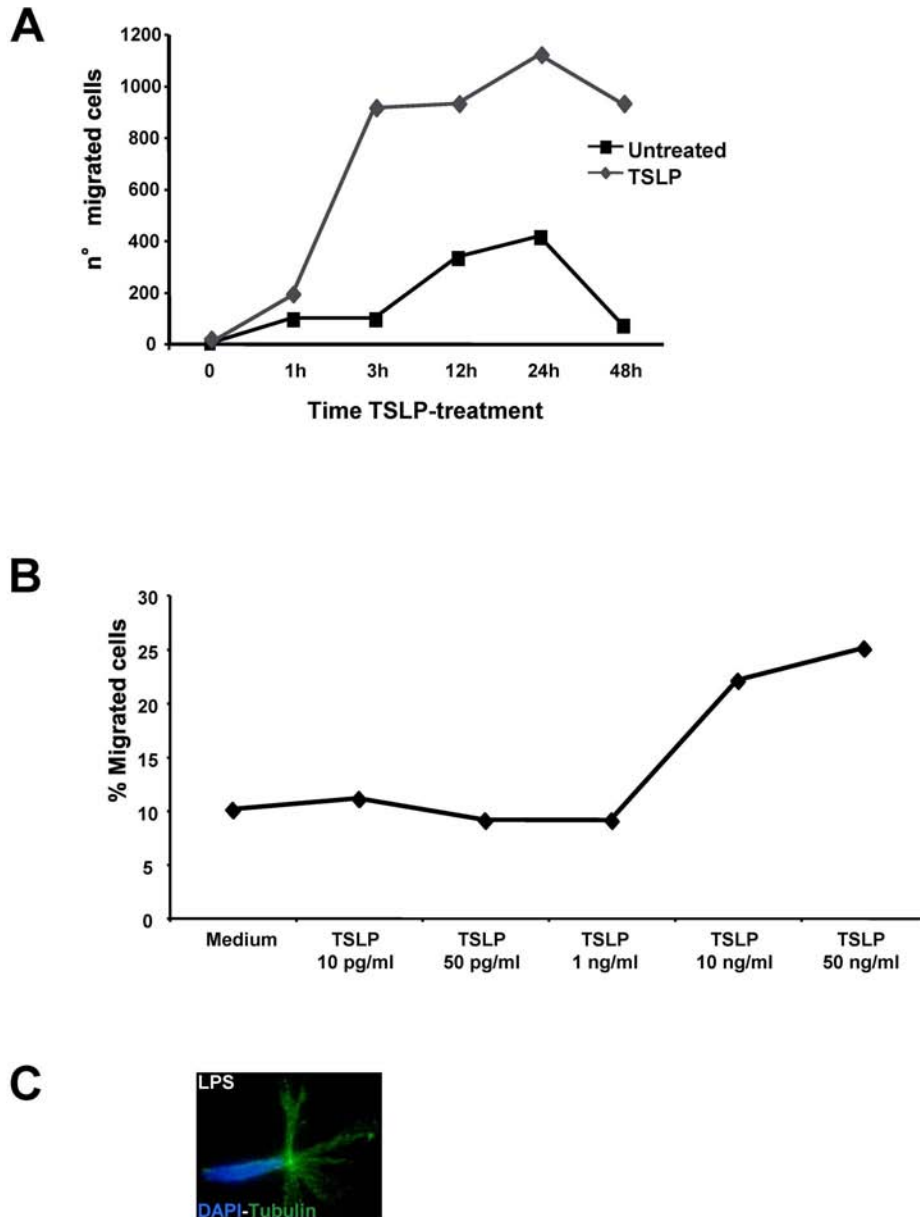
Figure S1. Kinetics and dose-response of TSLP-induced DC migration
(A) DCs were cultured with different TSLP concentrations for different duration from 1 to 48h and seeded in equal numbers in the upper well of collagen-coated transwells. TSLP-DC migration was observed starting at 3h of pre-activation, and up to 48h. Data are represented as number of migrated cells from one representative of two independent experiments. (B) DCs were cultured with different TSLP concentrations for 24h and seeded in equal numbers in the upper well of collagen-coated transwells. TSLP-DC migration can be activated at TSLP concentrations higher than 1 ng/ml. Data are represented as % of input from one representative of two independent experiments. (C) LPS-activated DCs show a non polarized morphology as assessed after tubulin staining (green).
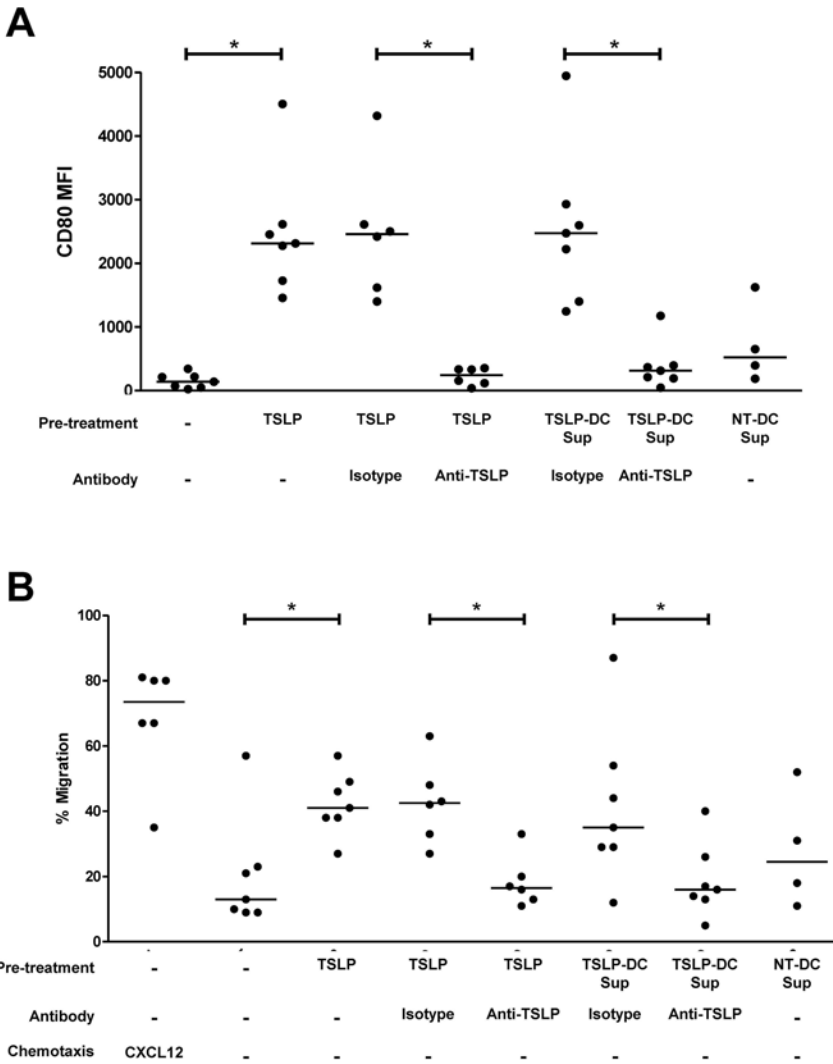
Figure S2. TSLP effect on DC activation and migration is not dependent on TSLP-DC secreted factors

(A) DC isolated from a first donor were cultured in medium with or without TSLP (50ng/ml) for 20 hours. Cell culture supernatants were stored at 80°C until we isolated DC from a second donor. TSLP-DC culture supernatants were incubated with Anti-TSLP antibody or its correspondent isotype for 2 hours at 37°C. DC from the second donor were incubated for 20 hours with different treatments: medium with or without TSLP (50ng/ml), the previously TSLP-DC supernatant with Anti-TSLP or isotype and untreated-DC supernatant. DC activation was determined by flow cytometry based on CD80 expression. (B) DC migration was evaluated using collagen-coated transwells in the absence of chemotactic factors. Cells were seeded in equal numbers in the upper chamber and after 6h, DC present in the lower and upper chambers were harvested and counted by FACS using beads. Data are represented as % of total cell counts. In the positive control, CXCL12 was used in the lower chamber during migration as a chemotactic factor. Each dot corresponds to a different donor of DC and a different cell culture supernatant. *($p<0.05$ Wilcoxon test)
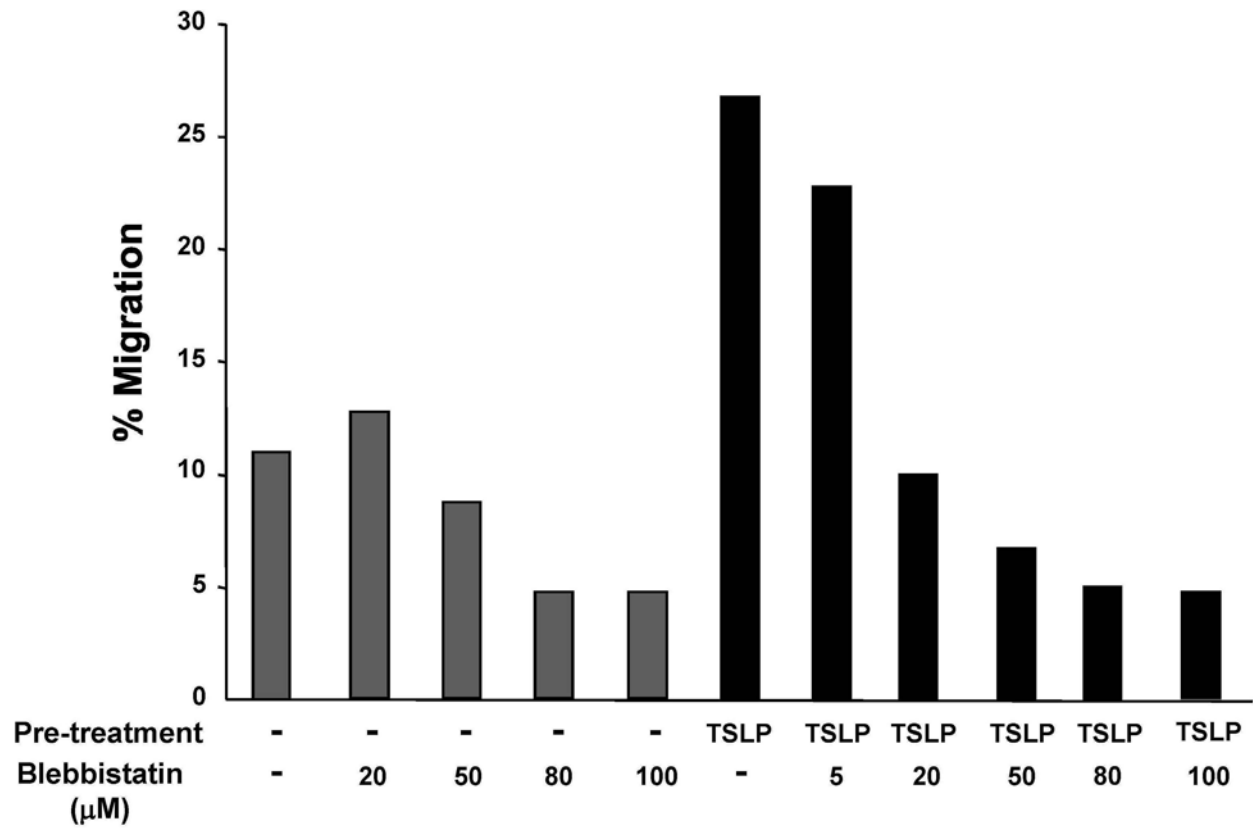
Figure S3. Blebbistatin inhibits TSLP-induced DC migration in a dose-dependent manner
DC migration was assayed in collagen I-coated transwells in the absence or presence of increasing concentrations of blebbistatin, a specific myosin II inhibitor.
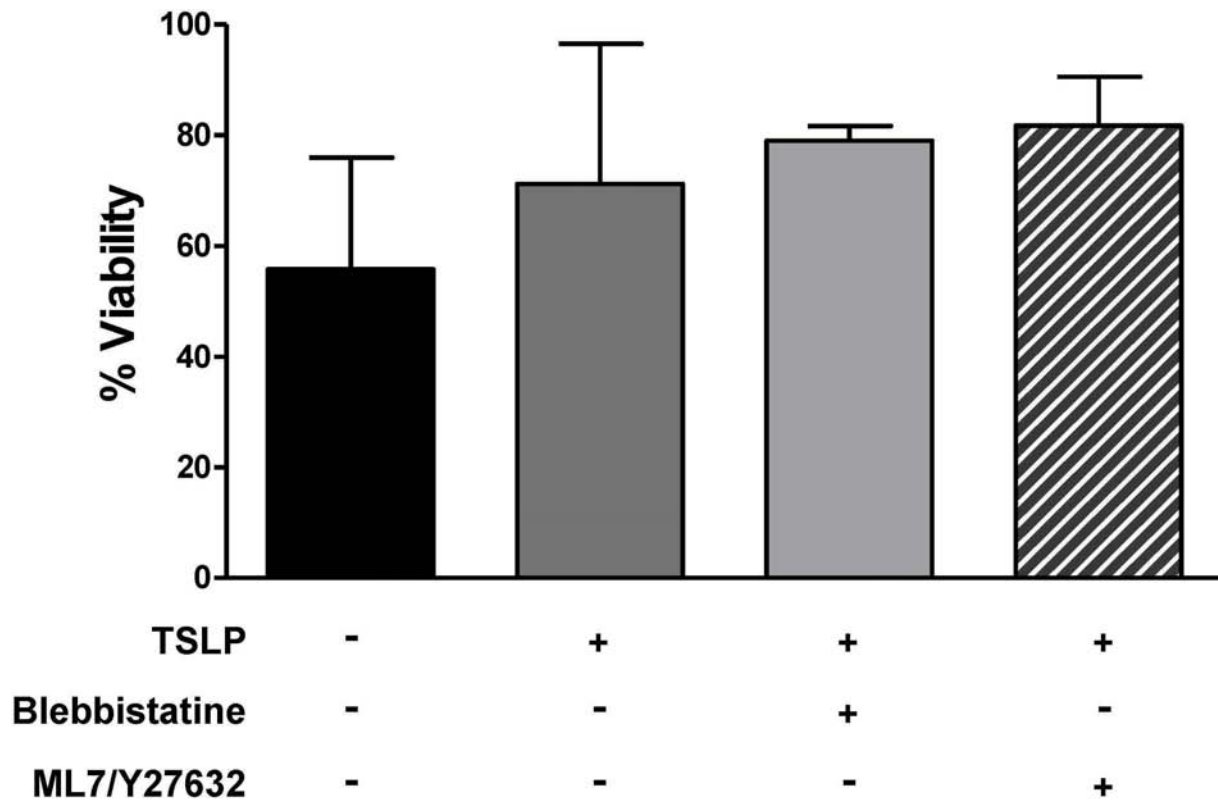
Figure S4. Effect of Myosin II inhibitors on TSLP-DC viability
DCs were cultured in medium with or without TSLP (50ng/ml) in the presence or absence of blebbistatin (50 µM) or ML7 and Y27632 inhibitors (10 µM) for 20 hours. Cell viability was determined by flow cytometry using Annexin V and DAPI staining. Data shown are representative of 3 experiments.

4.3 PUBLICATION 3

Manuscript in preparation.

Molecular mechanisms implicated in TSLP induction of dendritic cell migration.

Carolina Martinez-Cingolani, Raphael Zollinger and Vassili Soumelis.

Mature DCs need to migrate from the periphery to the secondary lymphoid organs to activate the immune adaptive response [54]. They follow chemokine gradients that guide them through the interstitial spaces of the tissue to the lymph vessels and the lymph nodes [183]. The microenvironment signals that activate DCs often regulate their expression of chemokine receptors enabling them to sense these gradients. In this process a major role has been attributed to the lymph node chemokines CCL19 and CCL21 and their receptor CCR7 [62]. Indeed, inflammatory stimuli trigger DC up-regulation of CCR7 to a point that this receptor is often used as a marker of the activated state of DCs. We showed in the preceding chapter that TSLP triggered DC migration. This process was found to be independent of the chemokine secretion induced by TSLP on DCs. However we did not study whether TSLP could induce chemokine receptor regulation on DCs. Therefore we could not completely exclude the possibility that TSLP induced the expression of a chemokine receptor that indirectly mediated TSLP-induced migration.

In this study, I assessed in a systematic way the implication of chemokine receptors on TSLP-induced migration. My results led to the conclusion that a G protein coupled receptor (GPCR) such as the chemokine receptors was indeed, implicated in TSLP-induced migration although we were not able to identify it. The blood DC compartment is constituted by two subsets. A mayor subset characterized by the cell surface expression of the marker BDCA-1 and a minor subset characterized by the expression of the marker BDCA-3. In the field of human DC biology, these two subsets have been exhaustively evaluated for their differential functions in the immune system. I decided to test whether TSLP induced a differential migration on blood DC subsets finding differences relevant to their function.

TSLP-induced DC migration is partially dependent on a G protein coupled receptor

Chemokine receptors are members of the GPCR superfamily. They are characterized by the presence of a small G inhibitory protein α (Giα) that is involved in the intracellular signaling triggered by chemokine ligands. The pertussis toxin (PTX) has the capacity to bind irreversibly to the Giα and inhibit the intracellular signaling pathway upon chemokine receptor binding [182].

To test if a chemokine receptor was implicated in TSLP-DC induced migration, I cultured primary human blood DCs with and without TSLP in the presence or absence of PTX. After a 24 hours culture, I assessed cell migration using collagen I-coated transwells. Cells were allowed to migrate for 6h and the percentage of migration was calculated as the percentage of cells in the lower chamber related to the total cell count. The inhibition of SDF-1 chemoattraction by PTX pretreatment was used as a control of the inhibiting capacity of PTX in my experiments. As previously shown, I found that TSLP enhanced DC chemokinesis. The percentage of migrating cells after treatment was 44 ± 5 % as compared to the spontaneaous migration of the untreated cells, 27 ± 4 % (Figure 4-1). Pretreatment with PTX inhibited TSLP-induced migration on DCs by 1.7 fold (28 ± 5 %), to the same levels as the spontaneous migration (Figure 4-1).
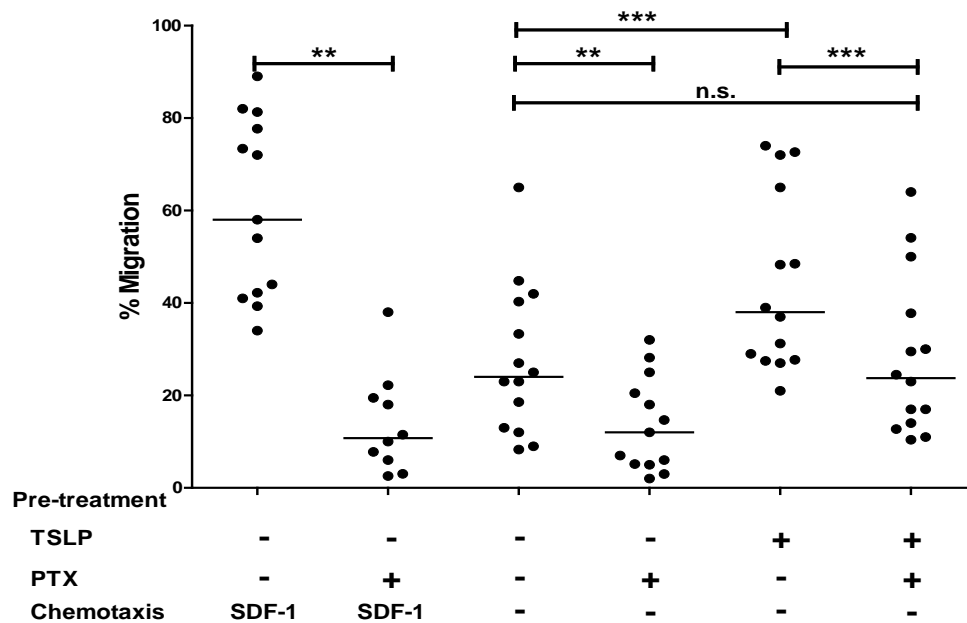
Figure 4-1: TSLP-induced DC migration is PTX – sensitive.

Percentage of migrating cells relative to total cell count. As a positive control SDF-1 was used in the lower compartment as a chemotactic factor. *$p \leq 0.05$**$p \leq 0.005$ ***$p \leq 0.0005$, Wilcoxon non-parametric paired test was used. Bars represent medians.

As PTX is a toxin, I checked if the inhibition of TSLP-induced migration by PTX was due to a decreased DC viability. I found that TSLP increased DC survival by 2.2 fold. PTX did not affect either untreated or TSLP-treated DC survival (Figure 4-2A). I also tested if PTX could affect TSLP receptor expression by DCs and therefore their capacity to respond to TSLP. Nevertheless there was no difference in the surface expression of neither of the two chains of TSLP receptor complex after treatment with PTX (Figure 4-2B). Moreover, CD80 expression, up-regulated by TSLP, was not affected by PTX treatment suggesting that TSLP receptor was functional in all the cases and that PTX did not affect TSLP-DC maturation (Figure 4-2C). Therefore I could conclude that the PTX inhibition of TSLP-induced DC migration was not due to a decreased survival or to a down-regulation of TSLP receptor complex by DCs.
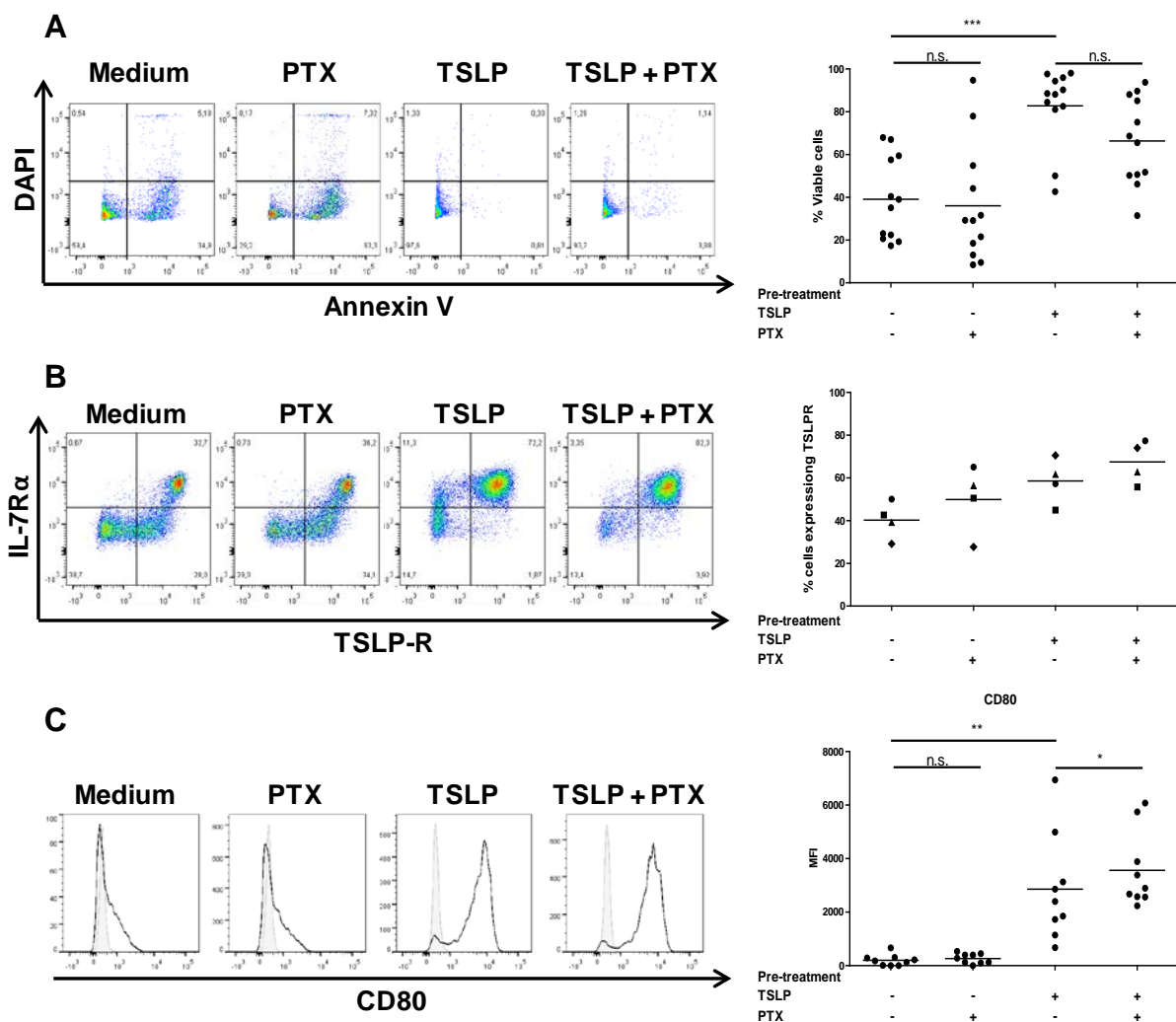
Figure 4-2: PTX does not affect DCs viability, TSLP receptor expression and function.

(A) Left: Representative flow cytometry density plots of DCs treated with and without TSLP and with and without PTX for 24 hours and stained for Annexin V and DAPI viability stainings. Right: percentage of Annexin V and DAPI double negative viable cells in the different conditions. Each dot corresponds to an independent experiment. Bars represent means. ***$p \leq 0.0005$ (Wilcoxon non-parametric paired test).

(B) Left: Representative flow cytometry density plots of DCs treated with and without TSLP and with and without PTX for 24 hours and stained for IL7-Rα and TSLPR chains of TSLP receptor complex. Right: percentage of double positive cells (IL7-Rα and TSLPR chains) expressing TSLPR complex for four independent donors. Symbols represent cells purified from the same donor. Bars represent means.

(C) Left: Representative flow cytometry histograms of DCs treated with and without TSLP and with and without PTX for 24 hours and stained for CD80 expression Filled histograms represent matching isotypic controls. Right: Specific median intense fluorescence (MFI) for CD80 staining. Each dot corresponds to an independent experiment. Bars represent means. **$p \leq 0.005$ (Wilcoxon non-parametric paired test).

PTX was found to inhibit also the spontaneous migration of untreated DCs (Figure 4-1). Moreover, the treatment with PTX of the TSLP-DCs did not inhibit migration to the lowest values of the PTX single-treated cells (Figure 4-1). Therefore PTX could inhibit the spontaneous, TSLP-independent migration of DCs or inhibit TSLP-dependent migration by blocking a GPCR chemokine receptor. Previously we had shown that TSLP-induced DC migration was linked to a cytoskeleton polarization of TSLP-DCs [184] therefore I decided to test to which extent a GPCR could be involved in TSLP-induced polarization of DCs.

TSLP- induced polarization is dependent on GPCR

To check if a GPCR could be involved in TSLP induced polarization of DCs, I treated DCs with and without TSLP and PTX for 24 hours and stained the actin and microtubule cytoskeleton to evaluate cell polarization by immunofluorescence (Figure 4-3A). I analyzed cell morphology by calculating a ratio between the two main axes of the cells' shape; a ratio close to 1 corresponds to a round-shaped cell, whereas a ratio different from 1 implies an elongated shape (Figure 4-3A). The obtained results confirmed that TSLP-induced a clear polarization of DCs with the appearance of a large uropod, the nucleus displacement to the rear of the cell and the MTOC formed next to the nucleus. The axes ratio of TSLP-treated cells in comparison to control was significantly higher (2.4 ± 0.06 versus 1.5 ± 0.02) (Figure 4-3B). In accordance to the results obtained in the previous migration experiments I found that when PTX was added to the TSLP-DC cultures, the number of polarized cells decreased significantly (Figure 4-3B). In my previous experiments of migration I had observed that PTX could also inhibit the spontaneous migration of DCs (Figure 4-1). Nevertheless PTX did not have an effect in the number of spontaneously polarized cells in the untreated control condition.
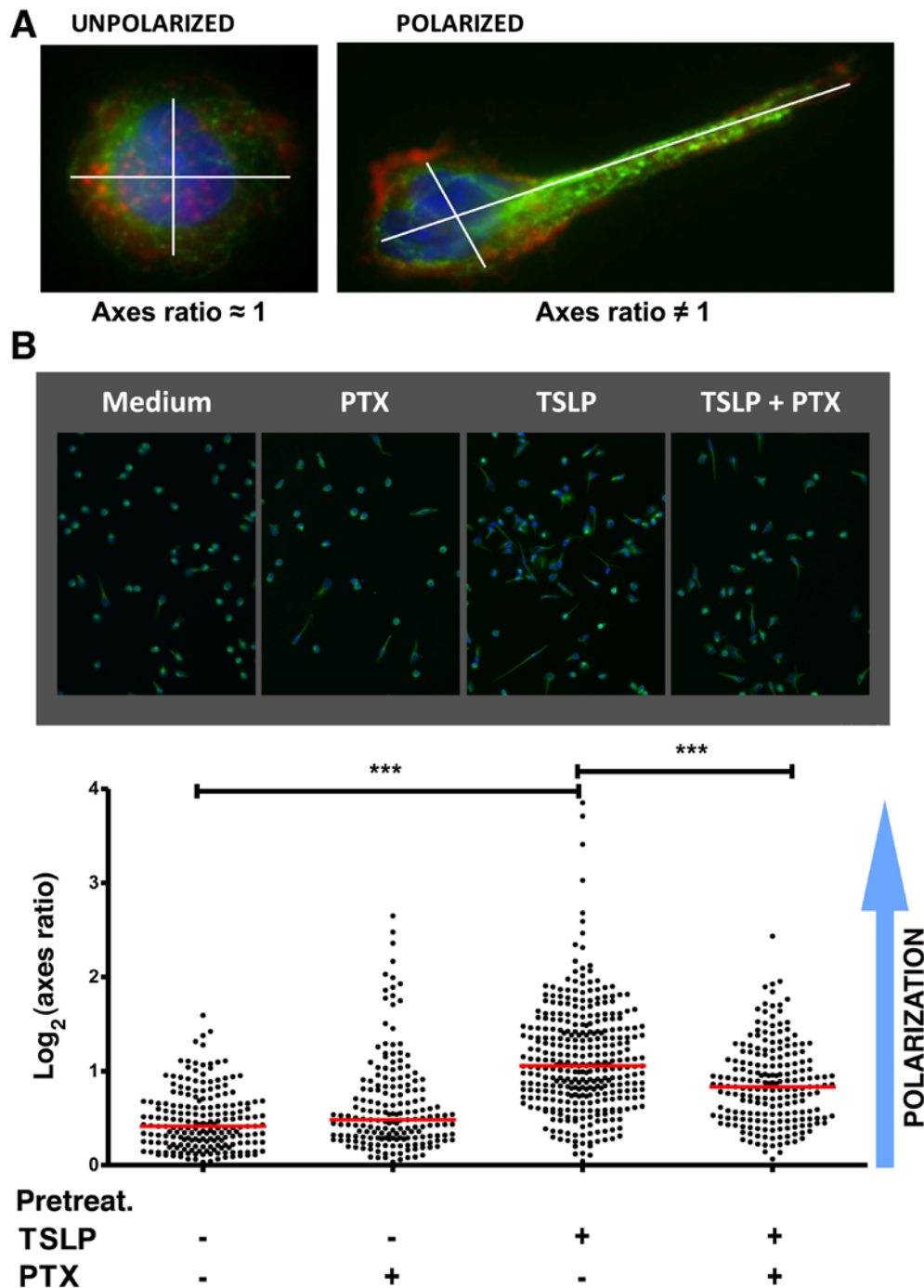
Figure 4-3 : TSLP-induced DC polarization is dependent on a G protein-coupled receptor.

(A) Pictures showing the immunofluorescence staining of an example of an unpolarized cell in the medium condition and a polarized cell after TSLP treatment. Cells were stained for actin (red), DAPI (blue) and tubulin (green). The two main axes of the cell are depicted illustrating the way the axes ratio was calculated for each cell.

(B) Upper panel: Representative pictures of three independent experiments. DAPI nucleus staining is shown in blue and tubulin in green. Lower panel: Quantification of the axes ratio in the different conditions. Results are represented as the log2 of the axes ratio. ***$p \leq 0.0001$ calculated using a one way ANOVA test and Dunn's post-test. Bars represent medians.

These results showed that PTX treatment inhibited TSLP-dependent polarization of DCs. Moreover they suggested that PTX inhibited the TSLP-dependent migration of DCs and not only the background spontaneous migration. We could conclude that a PTX–sensitive GPCR, induced by TSLP treatment on DCs, was implicated in TSLP-DC polarization and thus likely also in TSLP-DC migration. As chemokine receptors (PTX–sensitive GPCRs) are largely implicated in leukocyte migration [185], I decided to check whether TSLP induced the expression of a chemokine receptor that could explain the induction of chemokinesis on DCs.

The analysis of the chemokine receptors and ligands expressed by TSLP-DCs does not highlights the implication of chemokine loops on TSLP-induced migration

To see if TSLP induced the up-regulation of chemokine receptors on DCs, I screened a gene expression profile database of primary blood DCs treated or not with TSLP. This database had previously been developed in our team. I checked the chemokine gene expression of primary blood DCs fresh (ex-vivo), untreated or stimulated either with TSLP or TNF-α for six hours (Table 4-1). I found that TSLP-DCs expressed CCR1, CCR2, CCR5, CCR6, CCR7, CXCR1, CXCR2, CXCR3, CXCR4, CXCR7 and CX3CR1 at the mRNA level. Whereas the majority of chemokine receptor expression levels were equivalent in the medium and TSLP conditions, CXCR4 and CX3CR1 seemed to be down-regulated and CCR6 and CXCR7 seemed to be up-regulated by TSLP-DCs and not TNF-α treated DCs (Table 4-1). Statistical analysis showed statistically significant differential gene expression only for CCR6 receptor expression (p value lower than 0.05 and 2 fold change). These results showed that TSLP could indeed modify the chemokine receptor expression by DCs.

RECEPTOR	LIGANDS											Blood myeloid DCs			
												Ex-vivo	Medium	TSLP	TNF-α
CC SUBFAMILY															
CCR1	CCL3	CCL7	CCL5	CCL14	CCL16	CCL23	CCL15	CCL4				+	++	++	+
CCR2	CCL2	CCL12	CCL13	CCL7	CCL8	CCL4						++	++	++	-
CCR3	CCL13	CCL7	CCL5	CCL15	CCL8	CCL11	CCL24	CCL26	CCL28			-	-	-	-
CCR4	CCL17	CCL22	CCL2	CCL3	CCL5							-	-	-	-
CCR5	CCL4	CCL3	CCL5	CCL8								+++	++++	++++	+++
CCR6	CCL20											-	-	++	-
CCR7	CCL19	CCL21										++	+++++	+++++	+++++
CCR8	CCL1											-	-	-	-
CCR9	CCL25											-	-	-	-
CCR10	CCL28	CCL27										-	-	-	-
CXC SUBFAMILY															
IL8RA/CXCR1	CXCL6	IL8/CXCL8										+	+	+	+
IL8RB/CXCR2	CXCL1	CXCL2	CXCL3	CXCL5	CXCL7	CXCL6	IL8/CXCL8					+	+	+	+
CXCR3	CXCL9	CXCL10	CXCL11	CXCL4								+	+	++	++
CXCR4	CXCL12											+++++	+++++	++++	+++++
CXCR5	CXCL13											-	-	-	-
CXCR6	CXCL16											-	-	-	-
CXCR7	CXCL12	CXCL11										+	+	++	+
C SUBFAMILY															
XCR1	XCL1	XCL2										-	-	-	-
CX3C SUBFAMILY															
CX3CR1	CX3CL1											+++	+++	++	+++
SEQUESTRATING															
D6	CCL2	CCL3	CCL4	CCL5	CCL7	CCL8	CCL12	CCL13	CCL14	CCL17	CCL22	-	-	-	-
DARC	CCL2	CCL5	CCL11	CCL13	CCL14	CXCL1	CXCL2	CXCL3	CXCL7	CXCL8		-	-	-	-
CCR11	CCL19	CCL21	CCL25	CXCL13								-	++	-	+

Table 4-1 : Differential chemokine receptor gene expression of chemokine receptors by TSLP-DCs.

Chemokine receptor transcripts expression on purified blood DCs directly after sorting (Ex-vivo) or after a 6 hour treatment with medium alone or supplemented with TSLP or TNF-α. Genome wide expression was determined by Affymetrix chips Human Genome U133 Plus 2.0 microarray analysis. Signal intensity levels: -, ≤50; +, 50-100; ++, 100-1000; +++, 1000-5000; ++++, 5000-10000; +++++, ≥ 10000.

Gene expression data were confirmed by the analysis of protein expression for chemokine receptors by flow cytometry on DCs treated overnight with or without TSLP (Figure 4-4). In line with the mRNA expression, CCR6 was found to be up-regulated and CXCR4 and CX3CR1 down-regulated significantly after TSLP stimulation. Nevertheless CXCR3 was not found to be up-regulated whereas CCR7 seemed to have a higher surface expression after TSLP treatment (Figure 4-4). All the chemokine receptors expressed by TSLP-DCs at the mRNA were analyzed except CXCR7 which is a silent receptor at the signaling level [186]. These results showed that TSLP significantly induced the expression of the chemokine receptors CCR6 and CCR7. Therefore these chemokine receptors could be involved in TSLP-induced DC migration if their correspondent ligands were found to be available in the cell culture media.
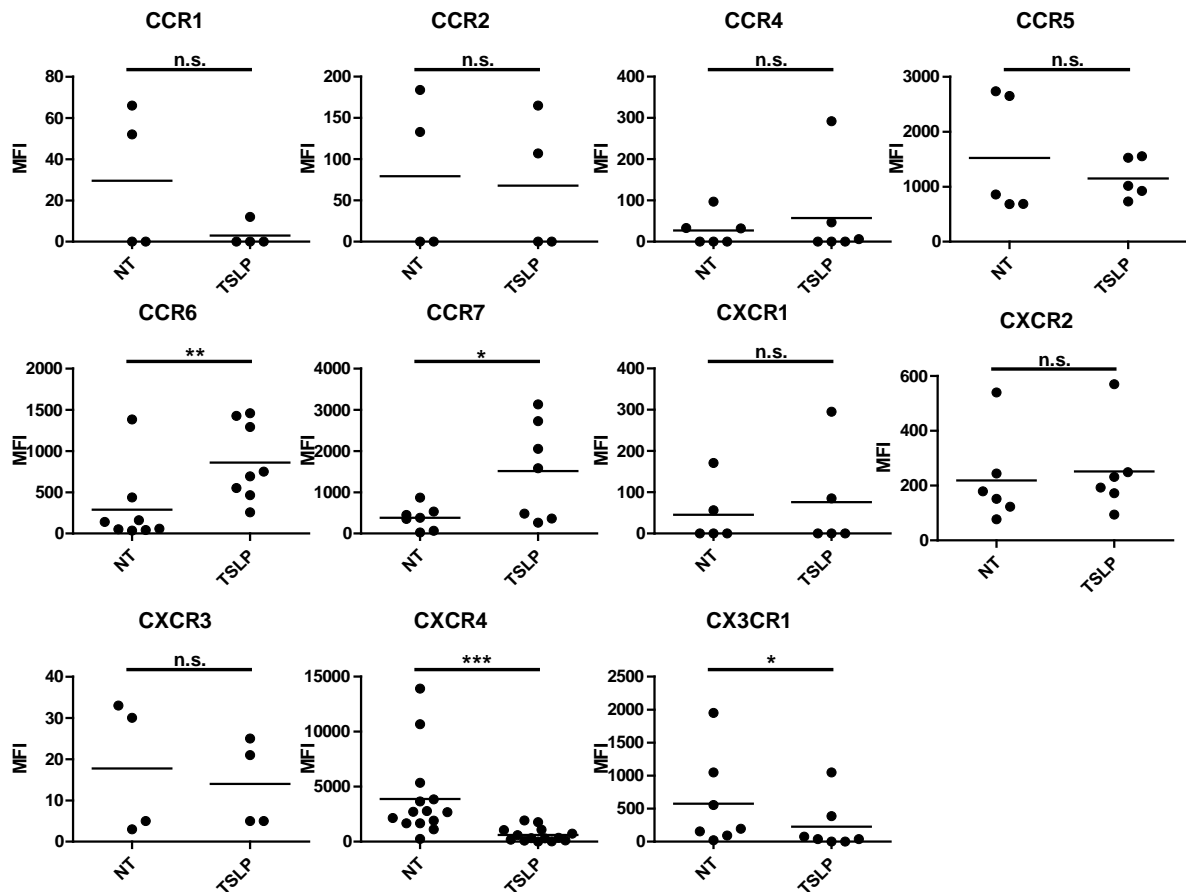
Figure 4-4 : Differential chemokine receptor surface protein expression of chemokine receptors by TSLP-DCs.

Data represent the surface expression of chemokine receptors on 24 hour TSLP treated and untreated DCs as determined by flow cytometry. Data represent specific mean fluorescence intensity. *$p \leq 0.05$**$p \leq 0.005$, Wilcoxon non-parametric paired test was used. Bars represent means.

In parallel to the chemokine receptor expression analysis, I tested which were the possible chemokine ligands available in the culture media during migration. First I tested if they were supplied by the serum added to the medium. DCs treated with and without TSLP for 24 hours were washed, starved for one hour in serum-free media or not starved and seeded in equal numbers in the upper chamber of the transwell system in the absence of chemotactic factors. RPMI medium supplemented with or without serum was used during migration. I found that DCs migrated overall less in serum-free medium than in serum-supplied medium. Nevertheless TSLP still induced a higher DC migration compared to medium-DCs in serum-free culture medium (3.6 fold increase). These results suggested that serum could not be the source of the ligand (Figure 4-5).
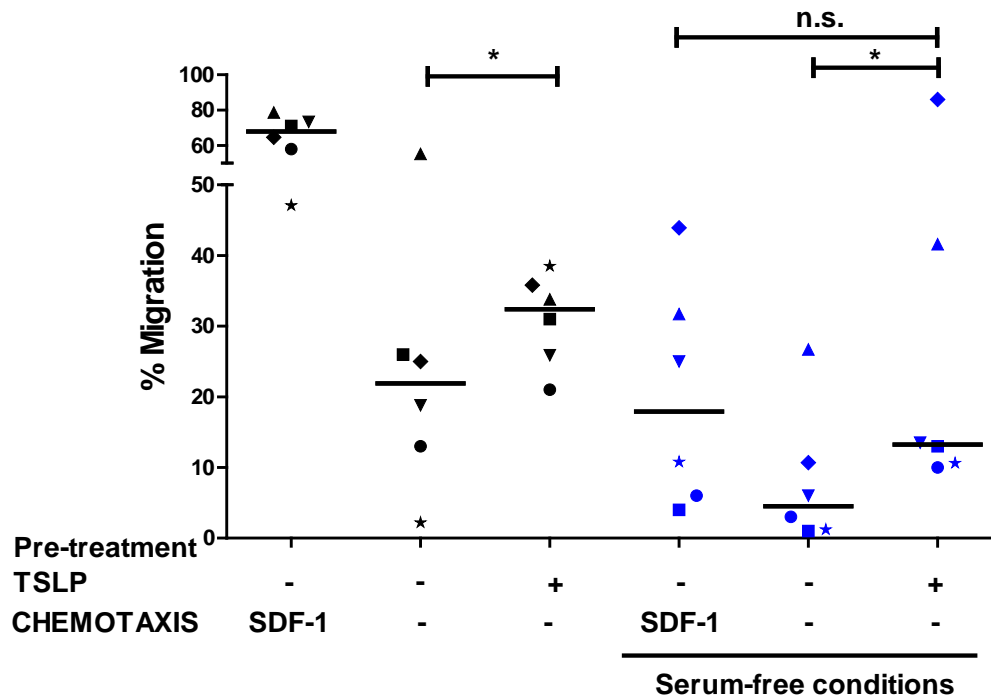
Figure 4-5: TSLP induces DC migration in serum-free conditions.

Percentage of migrating cells relative to total cell count. As a positive control SDF-1 was used in the lower compartment as a chemotactic factor. Black dots represent migration in serum-supplemented medium, blue dots represent migration in serum-free conditions. Symbols represent cells from the same donor. *$p \leq 0.05$, Wilcoxon non-parametric paired test was used. Bars represent medians.

I analyzed, using a chemiluminiscence-based protein array, a total of 38 chemokine ligands in the untreated and TSLP-DCs culture media (Figure 4-6). As expected, I found that the chemokines CCL17 and CCL22 were differentially secreted by TSLP-DCs. Surprisingly, CCL3 and CCL4 were also found to be differentially induced by TSLP (Figure 4-6). Nevertheless TSLP-DCs did not express differentially their correspondent receptors (CCR4 for CCL17 and CCL22 and CCR1, CCR2 and CCR5 for CCL3 and CCL4) (Figure 4-4). Moreover, I did not find either the presence of CCR6 ligand CCL20 or the CCR7 ligands CCL19 and CCL21 (Figure 4-6).
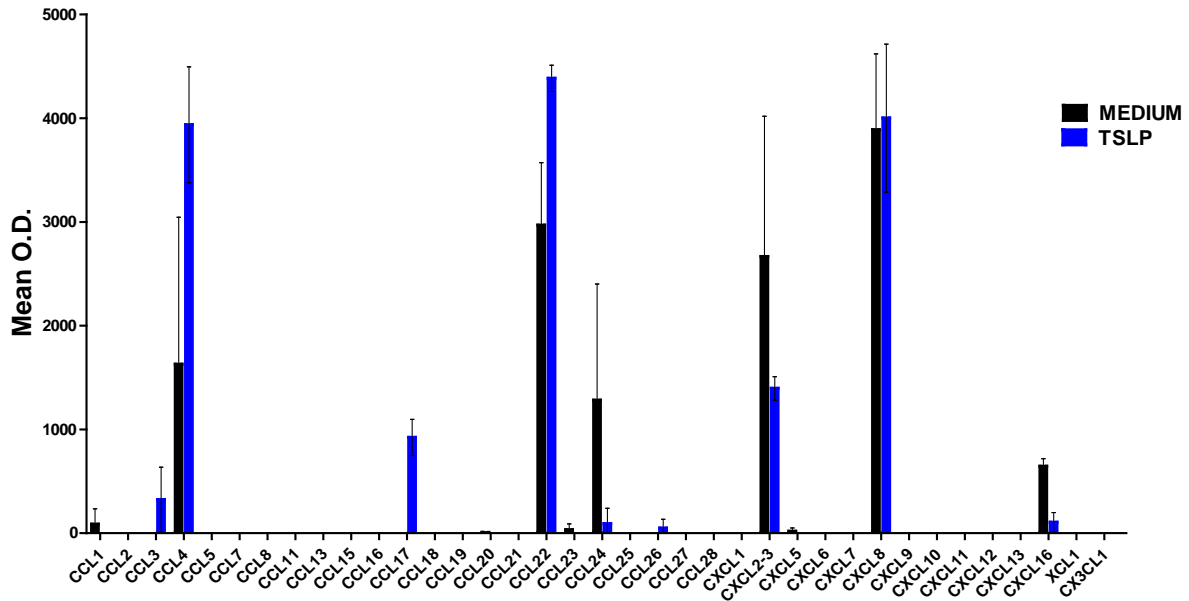
Figure 4-6 : TSLP-DC chemokine secretion.

Data represent the mean optical densities obtained for 38 different chemokines evaluated in the 24 hours culture supernatants of medium and TSLP-treated DCs. The analysis was done using a chemiluminiscence protein array. Fresh media with and without TSLP were used as background controls. *n=3.*

The analysis of TSLP-induced chemokine receptors and chemokine ligands did not reveal a known chemokine receptor-ligand match. These results did not provide enough evidence to implicate the tested chemokine-chemokine receptors in TSLP-induced migration. I evaluated the GPCR-chemokine receptors that are the most well known and the ones recognized for their capacity to affect general leukocyte migration [182]. Nevertheless, on one hand, chemokines have been shown to regulate the activity of chemokine receptors different from their cognate correspondent receptor [187]. On the other hand, the intracellular pathways of chemokine receptors have been shown to be activated by molecules different from their cognate chemokine ligand [188, 189]. Finally there are other protein and lipid molecules that can affect leukocyte migration through a GPCR. These different possibilities explaining the involvement of a GPCR in TSLP-induced DC migration and polarization will be analyzed in the discussion of this manuscript.

In these experiments using total DCs, I had not been taking into account that blood DC compartment is constituted by two subsets the BDCA-1$^+$ and the BDCA-3$^+$ DCs. In my previous experiments I had been evaluating mainly the effects of TSLP on BDCA-1$^+$ DCs as BDCA-3$^+$ DCs represent a small percentage of total DCs (less than 10%). As blood DC subsets may respond differently to TSLP, I decided to test if TSLP induced migration in both of these subsets.

TSLP-induced migration is restricted to BDCA-1$^+$ blood DC subset

To see if TSLP differentially induced the migration of blood DC subsets, I cultured primary human blood DCs with and without TSLP and assessed again a 6 hours migration using collagen I-coated transwells. The fractions in the upper and lower compartments of the transwells were recovered, and viable cells were counted. These fractions were also stained with anti-human BDCA-1 and BDCA-3 antibodies to evaluate by flow cytometry the differential migration of the blood subsets. I used SDF-1 in the lower chamber of the transwells as a positive control of the ability of the cells to migrate (Figure 4-7A). Both cell types migrated towards SDF-1 chemokine, suggesting that they both have the intrinsic capacity to migrate. Nevertheless BDCA-3$^+$ cells were found to stay in the upper compartment, and seemed to be less migratory than BDCA-1$^+$ after TSLP treatment (Figure 4-7A).

To assess specifically TSLP induction of migration in both subsets, I isolated BDCA-1$^+$ and BDCA-3$^+$ blood cells by cell sorting. The cells were cultured independently for 24 hours with and without TSLP. As in the previous experiments, I tested migration for 6 hours (Figure 4-7B). My results confirmed that both subsets had the capacity to migrate towards SDF-1. Nevertheless, BDCA-3$^+$ cells migrated 1.4 fold less than BDCA-1$^+$ cells towards SDF-1 and 6.9 fold less than BDCA-1$^+$ cells in the medium condition (Figure 4-7B). As previously shown for total DCs, TSLP induced significantly the migration of BDCA-1$^+$ cells (42.05 $\pm$ 6.9%) in comparison to the untreated cells (24 $\pm$ 3.1%). Interestingly, TSLP did not induce BDCA-3$^+$ cell migration at all (3.5 $\pm$ 1% in the medium condition and 1.1 $\pm$ 0.4% in TSLP condition) (Figure 4-7B).
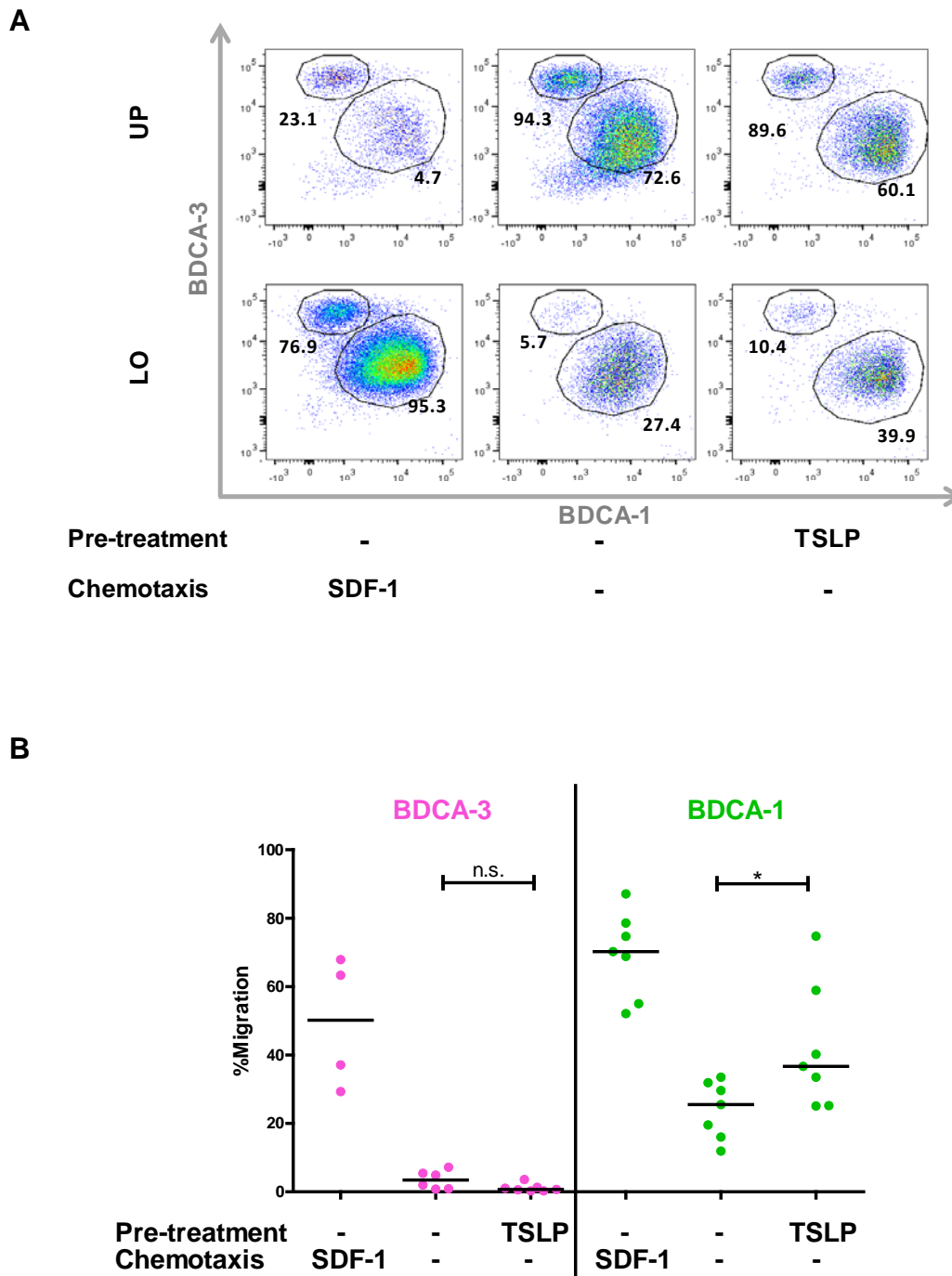
Figure 4-7: TSLP induces migration only on BDCA-1$^+$ subset of blood dendritic cells.

(A) Flow cytometry density plots showing BDCA-1 and BDCA-3 stainings of total DCs present on the upper and lower cellular fractions of the transwell system after a 6 hour migration. Numbers represent the percentage of viable cells from each subset. Data are representative of three independent experiments.

(B) Percentage of migrating cells relative to total cell count. BDCA-1 and BDCA-3 cell migration was assessed independently. As a positive control SDF-1 was used in the lower compartment as a chemotactic factor. *$p \leq 0.05$, Wilcoxon non-parametric paired test was used. Bars represent means.

These data showed that TSLP induced migration only on BDCA-1$^+$ subset. As this differential behavior could be due to differences in the expression TSLP receptor by the subsets I checked the expression of both of its chains (TSLPR and IL-7Rα) on blood BDCA-1$^+$ and BDCA-3$^+$ DCs. I also analyzed TSLP capacity to activate these cells as a proof of TSLP receptor function.

TSLP receptor complex was found to be expressed equally by BDCA-1$^+$ and BDCA-3$^+$ DCs (Figure 4-8A). Moreover I found that after 24 hour culture with TSLP, BDCA-1$^+$ and BDCA-3$^+$ DCs acquired both a mature phenotype. TSLP was able to induce CD80, CD86 and CD40 in both subsets as compared to the medium condition (Figure 4-8B). CD83 was not found to be up-regulated by TSLP in the BDCA-1$^+$ subset and BDCA-3$^+$ cells expressed CD83 already at high levels in the medium condition and did not further up-regulated this marker in the presence of TSLP. Overall these data showed that TSLP was able to activate BDCA-1$^+$ and BDCA-3$^+$ DCs in a similar way demonstrating that TSLP receptor is equivalently functional on both subsets. I also evaluated BDCA-1$^+$ and BDCA-3$^+$ cell survival upon TSLP treatment. No differences in cell viability between TSLP-BDCA-1$^+$ and TSLP-BDCA-3$^+$ DCs were found (Figure 4-8C).

These results show that TSLP differential induction of migration on blood BDCA-1$^+$ and BDCA-3$^+$ subsets is neither due to a difference in TSLP receptor expression and function nor to a difference in DC subsets viability. This suggests that the differential migration induced by TSLP on blood DC subsets may be due to the activation of different signaling pathways in these cells.
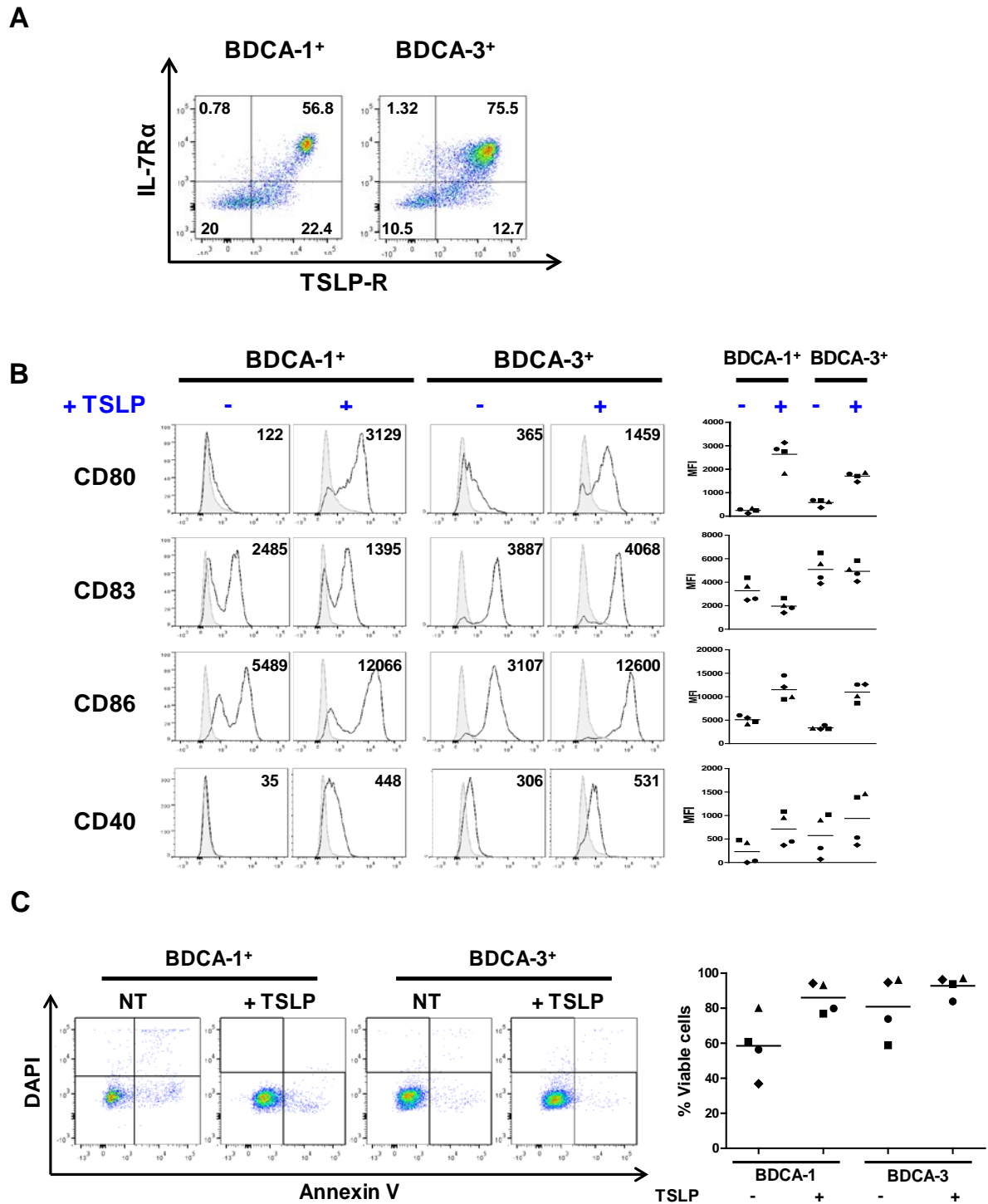
Figure 4-8: Blood DC subsets express a functional TSLP receptor

(A) Representative Flow cytometry density plots of TSLP receptor and IL-7 receptor α chains by human blood BDCA-1^{+} and BDCA-3^{+} DCs. Quadrants were adjusted to the matching correspondent isotype controls. Numbers represent the percentage of viable cells. *n=4*.

(B) Left: Histograms representing the surface expression of the activation markers by TSLP-treated BDCA-1^{+} and BDCA-3^{+} cells, plain histograms represent the matching correspondent isotype control. A representative donor is shown. Numbers represent specific median fluorescence intensity.

Right: Median fluorescence intensity for 4 independent experiments is shown for each marker. Symbols represent cells from the same donor. The bars represent means.

(C) Left: density plots representing the staining of DAPI and Annexin V on TSLP-treated BDCA-1$^+$ and BDCA-3$^+$ cells. A representative donor is shown. Right: percentage of DAPI-Annexin V- viable cells in the different conditions. Each dot corresponds to an independent donor. Symbols represent cells from the same donor. The bars represent means.

Altogether our results suggested that TSLP used a GPCR to induce DC migration and polarization, although our screening of known chemokine receptors was not enough to determine its identity. The differential migration triggered by TSLP on blood DC subsets together with the equal capacity of these sub-populations to respond to TSLP suggest functional differences and specific TSLP-signaling pathways in blood BDCA-1$^+$ and BDCA-3$^+$ DCs. To identify these different signaling pathways we are currently generating transcriptomic profiles of TSLP treated blood BDCA-1$^+$ and BDCA-3$^+$ DCs. Importantly the differential response to TSLP may stand for a differential implication of blood DC subsets in TSLP-linked inflammation.

DISCUSSION

DC migration is a complex process that requires the coordinated contribution of different types of secreted, extracellular and intracellular molecules [183]. This step is essential for the initiation of an efficient immune response. We had previously shown that TSLP, a proinflammatory cytokine that activates DCs, induces DC migration through the cell cytoskeleton re-organization and the activation of actin-motor myosin II [184]. In the present study, I showed that TSLP- DC migration and polarization are affected by PTX treatment and therefore are dependent on a GPCR. As chemokine receptors are PTX-sensitive GPCRs and are tightly linked to DC migration [53], I systematically studied the gene and protein expression of chemokine receptors and ligands regulated by TSLP on DCs. TSLP induced the up-regulation of CCR6 and CCR7 and the down regulation of CXCR4 and CX3CR1. Moreover TSLP not only induced CCL17 and CCL22 as previously reported [133], but also CCL3 and CCL4. Although my results reveal a TSLP regulation of chemokine and chemokine receptors on DCs we could not find enough evidence linking this to TSLP-induced migration. There are several other possibilities that may explain the involvement of a GPCR in TSLP-induced DC migration.

1- Besides the interaction with their cognate correspondent receptors, chemokines have been shown to cooperate with each other to trigger cell migration [190, 191]. An example of this cooperation is the synergy between CXCR3 and CXCR4 ligands in PDCs. Indeed CXCR3 ligands have been shown to be implicated in the migratory response of PDCs towards SDF-1, a CXCR4 ligand, without affecting the expression of CXCR4 itself [190, 191]. Moreover, it has been reported that CCL17 is required for murine cutaneous DC random and directed migration independently of the expression of CCL17 receptor, CCR4 [187]. Indeed, Stutte et al. showed that, in a murine model of atopic dermatitis, CCL17 deficient LCs failed to emigrate from the skin. In vitro, CCL17 deficient DCs had an impaired migration toward CCR7 ligands and also a reduced random migration (haptokinesis). This was not linked to an altered chemokine receptor expression but rather to a reduction in intracellular $Ca2^+$ release. As CCL17 affected migration independently of CCR4 expression the authors suggested the existence of a different extra CCL17/CCL22 receptor.

Therefore, even if we could not find a specific matching couple implicated in TSLP-DC migration we cannot rule out the possibility that TSLP-induced chemokines, such as CCL17, act through a different known or unknown receptor that is up-regulated by TSLP. To assess this possibility, the independent use of specific neutralizing antibodies against TSLP-induced chemokines (CCL17, CCL22, CCL4 and CCL3) and chemokine receptors (CCR6 and CCR7) should highlight their contribution in TSLP-DC migration.

2-Besides chemokines, inflammatory lipid mediators have been shown to regulate indirectly or directly, DC migration. The Prostaglandin E2 and the cysteinyl leucotrienes have been shown to regulate DC migration towards CCR7 ligands without affecting CCR7 expression [192] [193]. Nevertheless the mechanisms that trigger the activation of CCR7 receptor by these bio-active lipids are not known. Lipid mediators such as sphingosine-1 phosphate and

lysophosphatidic acid trigger mature DC migration upon binding to their own specific GPCRs [71, 194]. Therefore, these bioactive lipids and their correspondent receptors need to be assessed for their implication in TSLP-DC induced migration.

3- Finally, it has been shown that GPCRs can be activated in the absence of their cognate ligand by the ligands of tyrosine kinase receptors (RTKs). This effect is known as GPCR-RTK "transactivation" or "GPCR jacking" and can lead to the induction of cell migration [188]. An example of a ligand-independent mechanism of GPCR jacking is the case of the insulin-like growth factor -1 (IGF-1) -mediated migration in metastatic human breast cancer cell lines. Upon IGF-1 binding, IGF-1R co-precipitates with CXCR4 and the G protein subunits, Giα2 and Gβ, suggesting the activation of an intracellular proteic complex that results in cell migration [195]. Interestingly GPCR-RTK crosstalk was first highlighted by the fact that PTX altered the RTK signaling without affecting its expression. The specificity of this mechanism to RTKs remains unexplored. Little is known about the intracellular events downstream TSLPR signaling and some of our preliminary data show that PTX affects TSLP induced molecules at the transcriptional level (data not shown). Therefore we cannot exclude the possibility of a cross-communication between GPCRs and TSLPR. Nevertheless using our primary DC culture system, it is very challenging to prove this hypothesis, as experiments such as the immunoprecipitation of TSLPR would require very large amounts of protein.

Our experiments using isolated BDCA-1^{+} and BDCA-3^{+} blood DC subsets show that although untreated blood BDCA-3^{+} were more mature than BDCA-1^{+} cells, as previously reported [132], both subsets had the same capacity to respond to TSLP. However, TSLP induced migration was restricted to BDCA-1^{+} blood subset. This result reveals that TSLP has differential effects on blood DC subsets. The differences between TSLP-BDCA-1^{+} and TSLP-BDCA-3^{+} DCs can be used as a tool to determine whether TSLP-induced migration is linked to a differential chemokine receptor/ligand or bioactive lipid regulation.

Importantly, the differential migration of TSLP-DC subsets suggests that BDCA[+]3 DCs may need additional stimulation to migrate towards the lymphoid organs and may reach the lymph nodes in a delayed way in comparison to BDCA-1^{+} DCs. Additional experiments including activated innate actors such as mast cells, eosinophils and basophils can be designed to mimic the allergic inflammatory microenvironment and assess TSLP-treated BDCA-3^{+} cell migration. The differential response of blood DC subsets to TSLP opens new perspectives on the roles played by DC sup-populations in TSLP linked inflammation.

GENERAL DISCUSSION AND PERSPECTIVES

What we define as the inflammatory microenvironment is a network of multiple cell types of the innate and adaptive immune systems. They communicate with each other through direct interactions and through the secretion of a wide variety and combinations of cytokines and soluble mediators. Dendritic cells have the unique capacity to sense these signals from the environment and to induce the activation and differentiation of naïve T cells. The generated T cell response must be suited to the type of inflammation. This is ensured by DCs at two levels. First DCs are functionally plastic. This means that their behavior is subdued to the integrated signals. Secondly, the DC population is diverse. Indeed, different DC subsets have different functional specializations. I will discuss here the main results I obtained concerning their different functional specializations. In my study TSLP represents a model for an inflammatory signal that is provided by the microenvironment, and human blood DC subsets were evaluated for their differential capacity to respond to this signal. The purpose of this discussion is to highlight the relevance of my work, its limitations and its perspectives.

5.1   Human blood DC subsets as DC precursors.

In mice, blood DC subsets are defined as pre-DCs owing to their capacity to give rise to the tissue-resident DCs [21]. In humans, the equivalents of pre-DCs have not been found yet. It has been suggested that sub-populations of DCs from blood give rise to their correspondent subsets in the tissues [41], but a direct demonstration was lacking. Our results show that TSLP + TGF-β induce the differentiation of blood BDCA-1$^+$ DCs into LCs, and indicate that blood BDCA-1$^+$ still have a precursor capacity. Several questions arise from these results. The first one is whether other inflammatory factors may also induce blood BDCA-1$^+$ DC differentiation into LCs. In vitro experiments show that human blood CD34$^+$ precursors stimulated with GM-CSF, TNF-α, FlT3L and TGF-β [23, 36], as well as blood monocytes stimulated with IL-4, GM-CSF, and TGF-β [38] can give rise to LCs. The effect of these cocktails of cytokines on the precursor capacity of blood BDCA-1$^+$ remains to be explored.

Another question concerns the specificity of BDCA-1$^+$ blood DCs to give rise to LCs. In our study we showed that blood BDCA-3$^+$ DCs and tonsillar DC subsets did not differentiate into LCs upon TSLP + TGF-β treatment. Whether these subsets still have a precursor capacity is not clear. Lymph nodes and tonsillar BDCA-1$^+$ and BDCA-3$^+$ subsets do not cycle as opposed to their blood counterparts [99] suggesting that in the tissues, DC subsets become more terminally differentiated. This could explain their reduced precursor capacity; however, blood BDCA-1$^+$ and BDCA-3$^+$ DCs cycle to the same extent [99]. BDCA-3$^+$ DCs may also have precursor capacities but may need a different stimulation to give rise to other populations.

In our study we show that TSLP is required to induce CD1a up-regulation by blood BDCA-1$^+$ DCs, and that CD207 expression depends on further stimulation with TGF-β. Together these stimuli gave rise to the differentiation into LCs of only a fraction of BDCA-1$^+$ cells. Whether the other fractions correspond to BDCA-1$^+$ cells that differentiated into dermal DC

populations is not known. Indeed, it is possible that BDCA-1^{+} DCs give rise to DC populations other than LCs. This possibility and the required stimuli still need to be explored.

5.2 Relevance of TSLP + TGFβ -derived LCs to human pathology

The fact that TSLP acts in coordination with TGF-β to induce blood BDCA-1^{+} DC differentiation into LCs can be relevant to human physiopathology in two ways. First BDCA-1^{+} DC –derived LCs may have a relevance to TSLP-linked pathologies and secondly, TSLP could be relevant to LCs-related pathologies.

Relevance of LCs to TSLP-linked pathologies

TSLP is linked to atopic dermatitis, atopic asthma and other allergic disorders [133, 148, 149]. LCs have been shown to play an essential role in the initiation of the allergic inflammation in atopic dermatitis. First, in atopic dermatitis lesions, epidermal LCs, up-regulate IgE-binding FcεRI receptor, which enhances the presentation of IgE-bound allergens [196, 197]. Moreover, LCs have been shown to preferentially induce the Th2 profile that characterizes the allergic response [25]. Finally TSLP-DCs have been shown to secrete Th2-attracting chemokines (CCL17 and CCL22) and induce a strong Th2 response [133]; the same behavior is obtained by human primary LCs treated with TSLP [168].

Although the role of LCs in atopic rhinitis and asthma is less known, these disorders together with atopic dermatitis constitute a classical triad that often occurs in the same patients [198]. Whether epidermal LCs represent a common physiopathological mechanism remains to be explored.

TSLP and TGF-β are present in the allergic microenvironment [133, 199, 200]. Therefore they could induce the differentiation of recruited blood BDCA-1^{+} DCs into LCs, which can be relevant for the maintenance of the allergic state. Although an immunoregulatory role has been attributed to TGF-β in atopic dermatitis patients [201], the presence of TNF-α may counteract this role [200]. Indeed, we found that TGF-β could be responsible for the down-regulation of CD86 and CD40 in TSLP + TGF-β -derived LCs, and not in CD34^{+}-derived LCs; these last have been stimulated with a TNF- α (present in the differentiation cocktail). This suggests that TNF-α may inhibit the TGF-β immune modulation. Moreover, in our experiments TGF-β did not affect the Th2 profile induced by TSLP + TGF-β -derived LCs, suggesting that TGF-β does not interfere with their possible active role in the generation of the allergic response.

There is a single article in which TSLP implication on LCs development in atopic dermatitis has been addressed [202]. Indeed, Chorro L. et al, used a murine model in which vitamin D3 treatment induced TSLP production and atopic dermatitis features in the mice skin. They shown that vitamin D –treated mice have more LCs per skin mm3 than ethanol-treated

controls. They attribute this increase to a burst in local LC proliferation in situ and showed that there was little contribution from bone marrow- derived progenitors. However they did not test the possible contribution of blood-derived precursors to this phenotype. The proliferation of LCs was dependent on Vitamin D treatment. However they found that there was no difference in LC proliferation between wild-type and TSLP knockout mice treated with vitamin D. These results suggest that in this model of atopic dermatitis, TSLP is not involved in the local proliferation of LCs. However a diminished number of LCs by mm3 in TSLP knockout mice in comparison to wild-type after vitamin D suggest that TSLP might still contribute to the increased number of LCs seen in the atopic dermatitis epidermis. However the authors did not comment on this and further experiment will be required to test TSLP implications in atopic dermatitis LCs numbers.

TSLP is also present in psoriatic lesions (Volpe et al, unpublished results). The role of LCs in this disease remains controversial. Different studies have found diminished, increased, or equal numbers of LCs in the psoriatic lesions [174, 203, 204]. However Volpe et al showed that skin DCs stimulated with TSLP + CD40L secrete IL-23 and induce Th17 cells, pointing to a significant role of skin DCs in psoriasis (Volpe et al unpublished results). Therefore the differentiation of blood BDCA-1^{+} DCs into LCs upon TSLP + TGF-β stimulation may be relevant to the pathophysiology of psoriasis.

Relevance of TSLP to LC-linked pathologies

Dermatopathic lymphadenitis is a disease in which a skin inflammatory lesion leads to an enlargement of one draining lymph node. The lymph node is enriched in LCs [205]. Geissman et al. characterized these LCs [173] and showed that they had mainly an immature phenotype (they did not express CD83 or CD86). In vitro experiments using monocyte-derived DCs showed that despite further stimulation with TNF-α or bacterial products, monocyte-derived LCs did not show a mature phenotype. However, these cells could efficiently migrate towards CCR7 ligands. We proposed that TGF-β could be responsible for the down-regulation of CD86 and CD40 in TSLP + TGF-β -derived LCs, and that further stimulation with inflammatory cytokines such as TNF–α may induce a full activation profile. Further experiments specifically testing this hypothesis could solve the controversy. Although Geissman's study suggests that LCs in the lymph nodes of dermatopathic lymphadenitis patients represent LCs migrating from the epidermis, it does not define the precursors or the function of these cells. The presence of TSLP in the lesions giving rise to this disease could highlight a potential role of blood BDCA-1^{+} DC -derived LCs in this pathology.

The most important pathology in humans that implicates LCs, is Langerhans cell histiocytosis (LCH). This pathology is characterized by the accumulation of LC-like cells in the bone, skin and other tissues [206]. It has features of a neoplastic but also immune/inflammatory disorder [207]. The origin of LCH cells remains controversial. These cells were found to express similar gene expression levels than primary LCs. Nevertheless, large scale analysis of transcriptomic profiles, clustered primary LCs and LCH cells in independent groups [208]. This suggested that LCH cells may not derive from primary LCs, but rather from a common precursor. The wide distribution of the lesions, points towards blood monocytes and CD34^{+}

precursors as ideal candidates. However it has also been proposed that LCH cells derive from epidermal LCs undergoing transcriptional re-programming [207]. These controversies have not been solved yet.

It has been determined that several cytokines relevant to LC generation (GM-CSF, Flt3L, M-CSF) are present in the serum of LCH patients [209]; however TSLP has never been evaluated in these patients. TSLP + TGF-β -derived LCs did not express E-cadherin, but high levels of CCR6, as it has been reported for LCH cells [210, 211]. Our results suggest blood BDCA-1$^+$ DCs as a new possible precursor of LCH cells. A comparison between LCH cells, primary epidermal LCs, CD34$^+$ and monocyte -derived LCs as well as TSLP + TGF-β blood BDCA-1$^+$ -derived LCs might contribute to define the cellular source of LCH cells.

Finally to reconcile the fact that different blood precursors have been associated to LC generation in inflammatory conditions, I would like to cite the work of Sere et al. [212]. They showed, that in the murine model, LCs were generated at least in two waves. The first wave implicated monocyte-generation of short-term LCs whereas the second implicated CD34$^+$ -generation of long-term LCs. Although this has not been evidenced in humans, it implies that the precursor imprints special characteristics on the generation of LCs and their life-time. Blood BDCA-1$^+$ DC -derived LCs could represent a more direct and immediate source of LCs in inflammatory conditions.

5.3 Differential migration of TSLP blood BDCA-1$^+$ and BDCA-3$^+$ DCs

We provided in our study direct evidence of TSLP-induced DC migration. However TSLP did not affect the directionality of this migration. Rather than chemotaxis, the effects of TSLP on DC migration were more related to chemokinesis (random migration) than to directed migration. In my attempt to find an involvement of chemokine receptors on TSLP-induced migration, I could not find a chemokine candidate explaining this process. However, I found that a GPCR was implicated in TSLP-induced DC migration. These results were already discussed. However the TSLP differential induction of migration on blood DC subsets raises several questions.

The first question concerns the fact that blood BDCA-3$^+$ DCs do not migrate upon TSLP treatment. We propose that BDCA-3$^+$ DCs may need additional signals to be able to reach the lymph nodes. The nature of these stimuli remains to be determined. However if additional factors from the inflammatory milieu are required, it may be possible that BDCA-3$^+$ DCs reach the lymph nodes in a delayed way. This "two-step process" has already been proposed by Gilliet et al [153]. Indeed they show that in order to induce effective cytotoxic cells, TSLP-DCs need further stimulation with CD40L. In appendix 1, I show that blood BDCA-3$^+$ DCs stimulated by TSLP, do not secrete chemokines (CCL17, CCL22, CCL3, CCL4) as opposed to TSLP-treated blood BDCA-1$^+$ DCs. These data support the idea that blood BDCA-3$^+$ and BDCA-1$^+$ DCs respond differentially to TSLP. Even if we could not find significant differences in the T cell profile induced by these subsets (appendix 1), the differential

chemokine secretion suggests that blood subsets have different functions in the innate phase of the inflammatory response and in the recruitment of other cell types. Moreover, it provides an additional possible link between chemokine secretion and migration.

DCs need to reach the lymph nodes and stimulate naïve T cells. The fact that TSLP induced DC migration provided a missing link between TSLP activation of DCs in the periphery and the induction of a Th2 profile. However, we did not provide evidence for the directionality of this migration. In the case of total DCs, we found the up-regulation of both CCR7 and CCR6, and down-regulation of CXCR4. While CCR7 is linked to lymph node homing [53], CCR6 is defined as a skin homing molecule [66]. Down-regulation of CXCR4 characterizes the homing in both directions. This suggested that TSLP -stimulated blood DCs had the capacity to migrate to the lymph nodes and to the periphery. However, TSLP + TGF-β -derived LCs expressed a skin homing phenotype, suggesting that they participate in the replenishment of LCs in the epidermis under inflammatory conditions. Soumelis et al. had observed that the presence of TSLP in atopic dermatitis lesions was associated with the depletion of Langerhans cells in the epidermis, and their enrichment in the dermis, suggesting an emigration away from the epidermis [133]. However the presence of higher numbers of LCs in the dermis can also reflect the process of differentiation of newly recruited blood BDCA-1$^+$ cells into LCs.

The abilities of TSLP to induce migration towards the lymph nodes and towards the skin are not necessarily exclusive. While TSLP might trigger the homing to the lymph nodes in some resident cells, such as fully mature LCs and DCs, it may trigger the recruitment to the epidermis in more immature cells, like blood circulating BDCA-1$^+$ DCs entering the dermis.

Therefore DC subsets responding actively to TSLP might be differentially directed to different sites. A systematic assessment of chemokine receptor expression on TSLP –treated DC subsets should clarify this hypothesis.

The last point I would like to discuss is the fact that activation, migration and function of different DC subsets can be uncoupled. We previously discussed the uncoupling of activation and migration, when we showed that other activating stimuli different from TSLP did not trigger DC migration (Publication 2). As blood BDCA- 3$^+$ cells get fully activated by TSLP but do not migrate, the activation of DC subsets by TSLP might also be uncoupled from migration. To experimentally determine if the activation induced by a particular ligand on DC subsets is uncoupled from its specific function is a challenging task. In the case of blood DC subsets, differences in cross-presentation have been attributed to different stimulation requirements [94]. We showed that blood DC subsets get equally activated by TSLP but still behave in a different way upon TSLP treatment. This shows that DC subset function can be uncoupled from the activation induced by TSLP.

Finally our study showed that even if TSLP promotes an equal activation of different blood and tonsillar DC subsets, there is a differential response to this inflammatory cytokine. TSLP stimulation revealed precursor capacities of blood BDCA-1$^+$ DCs, their migration and chemokine secretion and did not induce these properties on blood BDCA-3$^+$ cells or tonsillar

DC subsets. However TSLP imprinted the induction of a Th2 inflammatory profile on blood BDCA-1$^+$ and BDCA-3$^+$ subsets and on TSLP + TGF-β -derived LCs. Further analysis of TSLP signaling pathways and gene expression profiles on several blood, tonsillar and skin - DC subsets may reveal other functional differences of TSLP-treated DC subsets and their differential implication in the inflammatory response.

REFERENCES

1. Langerhans, P., *Ueber die Nerven der menschlichen Haut.* Virchows Arch Pathol Anat, 1868. **44**: p. 325-337.
2. Jolles, S., *Paul Langerhans.* J Clin Pathol, 2002. **55**(4): p. 243.
3. Steinman, R.M. and Z.A. Cohn, *Identification of a novel cell type in peripheral lymphoid organs of mice. I. Morphology, quantitation, tissue distribution.* J Exp Med, 1973. **137**(5): p. 1142-62.
4. Steinman, R.M., et al., *Dendritic cells are the principal stimulators of the primary mixed leukocyte reaction in mice.* J Exp Med, 1983. **157**(2): p. 613-27.
5. Birbeck, M.S., *An electron microscopy study of basal melanocytes and high level clear cells (Langerhans cells) in vitiligo.* J Invest Dermatol, 1961. **37**: p. 51-64.
6. Reams, W.M., Jr. and S.P. Tompkins, *A developmental study of murine epidermal Langerhans cells.* Dev Biol, 1973. **31**(1): p. 114-23.
7. Basset, F., C. Nezelof, and J. Turiaf, *[Presence in electron microscopy of odd filamentous structures in pulmonary and osseous lesions of histiocytosis X. Current status of the question].* Bull Mem Soc Med Hop Paris, 1966. **117**(5): p. 413-26.
8. Katz, S.I., K. Tamaki, and D.H. Sachs, *Epidermal Langerhans cells are derived from cells originating in bone marrow.* Nature, 1979. **282**(5736): p. 324-6.
9. Volc-Platzer, B., et al., *Cytogenetic identification of allogeneic epidermal Langerhans cells in a bone-marrow-graft recipient.* N Engl J Med, 1984. **310**(17): p. 1123-4.
10. Schuler, G. and R.M. Steinman, *Murine epidermal Langerhans cells mature into potent immunostimulatory dendritic cells in vitro.* J Exp Med, 1985. **161**(3): p. 526-46.
11. Steinman, R.M., *The dendritic cell system and its role in immunogenicity.* Annu Rev Immunol, 1991. **9**: p. 271-96.
12. Auffray, C., Y. Emre, and F. Geissmann, *Homeostasis of dendritic cell pool in lymphoid organs.* Nat Immunol, 2008. **9**(6): p. 584-6.
13. Merad, M. and M.G. Manz, *Dendritic cell homeostasis.* Blood, 2009. **113**(15): p. 3418-27.
14. Kondo, M., et al., *Biology of hematopoietic stem cells and progenitors: implications for clinical application.* Annu Rev Immunol, 2003. **21**: p. 759-806.
15. Manz, M.G., et al., *Dendritic cell potentials of early lymphoid and myeloid progenitors.* Blood, 2001. **97**(11): p. 3333-41.
16. Chicha, L., D. Jarrossay, and M.G. Manz, *Clonal type I interferon-producing and dendritic cell precursors are contained in both human lymphoid and myeloid progenitor populations.* J Exp Med, 2004. **200**(11): p. 1519-24.
17. D'Amico, A. and L. Wu, *The early progenitors of mouse dendritic cells and plasmacytoid predendritic cells are within the bone marrow hemopoietic precursors expressing Flt3.* J Exp Med, 2003. **198**(2): p. 293-303.
18. Karsunky, H., et al., *Flt3 ligand regulates dendritic cell development from Flt3+ lymphoid and myeloid-committed progenitors to Flt3+ dendritic cells in vivo.* J Exp Med, 2003. **198**(2): p. 305-13.
19. Maraskovsky, E., et al., *In vivo generation of human dendritic cell subsets by Flt3 ligand.* Blood, 2000. **96**(3): p. 878-84.
20. Pulendran, B., et al., *Flt3-ligand and granulocyte colony-stimulating factor mobilize distinct human dendritic cell subsets in vivo.* J Immunol, 2000. **165**(1): p. 566-72.
21. Geissmann, F., et al., *Development of monocytes, macrophages, and dendritic cells.* Science, 2010. **327**(5966): p. 656-61.
22. Doulatov, S., et al., *Revised map of the human progenitor hierarchy shows the origin of macrophages and dendritic cells in early lymphoid development.* Nat Immunol. **11**(7): p. 585-93.
23. Caux, C., et al., *GM-CSF and TNF-alpha cooperate in the generation of dendritic Langerhans cells.* Nature, 1992. **360**(6401): p. 258-61.
24. Sallusto, F. and A. Lanzavecchia, *Efficient presentation of soluble antigen by cultured human dendritic cells is maintained by granulocyte/macrophage colony-stimulating factor plus*

interleukin 4 and downregulated by tumor necrosis factor alpha. J Exp Med, 1994. **179**(4): p. 1109-18.

25. Klechevsky, E., et al., *Functional specializations of human epidermal Langerhans cells and CD14+ dermal dendritic cells.* Immunity, 2008. **29**(3): p. 497-510.

26. Strunk, D., et al., *Generation of human dendritic cells/Langerhans cells from circulating CD34+ hematopoietic progenitor cells.* Blood, 1996. **87**(4): p. 1292-302.

27. Merad, M., et al., *Langerhans cells renew in the skin throughout life under steady-state conditions.* Nat Immunol, 2002. **3**(12): p. 1135-41.

28. Merad, M., F. Ginhoux, and M. Collin, *Origin, homeostasis and function of Langerhans cells and other langerin-expressing dendritic cells.* Nat Rev Immunol, 2008. **8**(12): p. 935-47.

29. Czernielewski, J., P. Vaigot, and M. Prunieras, *Epidermal Langerhans cells--a cycling cell population.* J Invest Dermatol, 1985. **84**(5): p. 424-6.

30. Czernielewski, J.M. and M. Demarchez, *Further evidence for the self-reproducing capacity of Langerhans cells in human skin.* J Invest Dermatol, 1987. **88**(1): p. 17-20.

31. Krueger, G.G., R.A. Daynes, and M. Emam, *Biology of Langerhans cells: selective migration of Langerhans cells into allogeneic and xenogeneic grafts on nude mice.* Proc Natl Acad Sci U S A, 1983. **80**(6): p. 1650-4.

32. Kanitakis, J., P. Petruzzo, and J.M. Dubernard, *Turnover of epidermal Langerhans' cells.* N Engl J Med, 2004. **351**(25): p. 2661-2.

33. Kanitakis, J., et al., *Self-renewal capacity of human epidermal Langerhans cells: observations made on a composite tissue allograft.* Exp Dermatol, 2011. **20**(2): p. 145-6.

34. Guilliam, A., *The human hair follicle: a reservoir of CD40+ B7-deficient Langerhans cells that repopulate epidermis after UVB exposure.* J Invest Dermatol, 1998. **110**: p. 422-427.

35. Borkowski, T.A., et al., *A role for endogenous transforming growth factor beta 1 in Langerhans cell biology: the skin of transforming growth factor beta 1 null mice is devoid of epidermal Langerhans cells.* J Exp Med, 1996. **184**(6): p. 2417-22.

36. Strobl, H., et al., *TGF-beta 1 dependent generation of LAG+ dendritic cells from CD34+ progenitors in serum-free medium.* Adv Exp Med Biol, 1997. **417**: p. 161-5.

37. Strobl, H., et al., *flt3 ligand in cooperation with transforming growth factor-beta1 potentiates in vitro development of Langerhans-type dendritic cells and allows single-cell dendritic cell cluster formation under serum-free conditions.* Blood, 1997. **90**(4): p. 1425-34.

38. Geissmann, F., et al., *Transforming growth factor beta1, in the presence of granulocyte/macrophage colony-stimulating factor and interleukin 4, induces differentiation of human peripheral blood monocytes into dendritic Langerhans cells.* J Exp Med, 1998. **187**(6): p. 961-6.

39. Ginhoux, F., et al., *Langerhans cells arise from monocytes in vivo.* Nat Immunol, 2006. **7**(3): p. 265-73.

40. Ito, T., et al., *A CD1a+/CD11c+ subset of human blood dendritic cells is a direct precursor of Langerhans cells.* J Immunol, 1999. **163**(3): p. 1409-19.

41. Haniffa, M., et al., *Human tissues contain CD141hi cross-presenting dendritic cells with functional homology to mouse CD103+ nonlymphoid dendritic cells.* Immunity, 2012. **37**(1): p. 60-73.

42. Harman, A.N., et al., *Identification of lineage relationships and novel markers of blood and skin human dendritic cells.* J Immunol, 2012. **190**(1): p. 66-79.

43. Filion, L.G., et al., *Detection of surface and cytoplasmic CD4 on blood monocytes from normal and HIV-1 infected individuals.* J Immunol Methods, 1990. **135**(1-2): p. 59-69.

44. Hambleton, S., et al., *IRF8 mutations and human dendritic-cell immunodeficiency.* N Engl J Med. **365**(2): p. 127-38.

45. Collin, M., et al., *Human dendritic cell deficiency: the missing ID?* Nat Rev Immunol. **11**(9): p. 575-83.

46.   Bigley, V. and M. Collin, *Dendritic cell, monocyte, B and NK lymphoid deficiency defines the lost lineages of a new GATA-2 dependent myelodysplastic syndrome.* Haematologica, 2011. **96**(8): p. 1081-3.

47.   Cisse, B., et al., *Transcription factor E2-2 is an essential and specific regulator of plasmacytoid dendritic cell development.* Cell, 2008. **135**(1): p. 37-48.

48.   Bigley, V., et al., *The human syndrome of dendritic cell, monocyte, B and NK lymphoid deficiency.* J Exp Med, 2011. **208**(2): p. 227-34.

49.   Hambleton, S., et al., *IRF8 mutations and human dendritic-cell immunodeficiency.* N Engl J Med, 2011. **365**(2): p. 127-38.

50.   Meredith, M.M., et al., *Expression of the zinc finger transcription factor zDC (Zbtb46, Btbd4) defines the classical dendritic cell lineage.* J Exp Med, 2012. **209**(6): p. 1153-65.

51.   Satpathy, A.T., et al., *Zbtb46 expression distinguishes classical dendritic cells and their committed progenitors from other immune lineages.* J Exp Med, 2012. **209**(6): p. 1135-52.

52.   Palm, N.W. and R. Medzhitov, *Pattern recognition receptors and control of adaptive immunity.* Immunol Rev, 2009. **227**(1): p. 221-33.

53.   Sallusto, F., et al., *Rapid and coordinated switch in chemokine receptor expression during dendritic cell maturation.* Eur J Immunol, 1998. **28**(9): p. 2760-9.

54.   Banchereau, J., et al., *Immunobiology of dendritic cells.* Annu Rev Immunol, 2000. **18**: p. 767-811.

55.   Joffre, O.P., et al., *Cross-presentation by dendritic cells.* Nat Rev Immunol, 2012. **12**(8): p. 557-69.

56.   Finkelman, F.D., et al., *Dendritic cells can present antigen in vivo in a tolerogenic or immunogenic fashion.* J Immunol, 1996. **157**(4): p. 1406-14.

57.   Jego, G., et al., *Dendritic cells control B cell growth and differentiation.* Curr Dir Autoimmun, 2005. **8**: p. 124-39.

58.   Sixt, M., et al., *The conduit system transports soluble antigens from the afferent lymph to resident dendritic cells in the T cell area of the lymph node.* Immunity, 2005. **22**(1): p. 19-29.

59.   Tang, A., et al., *Adhesion of epidermal Langerhans cells to keratinocytes mediated by E-cadherin.* Nature, 1993. **361**(6407): p. 82-5.

60.   Sozzani, S., et al., *Migration of dendritic cells in response to formyl peptides, C5a, and a distinct set of chemokines.* J Immunol, 1995. **155**(7): p. 3292-5.

61.   Sozzani, S., et al., *Receptor expression and responsiveness of human dendritic cells to a defined set of CC and CXC chemokines.* J Immunol, 1997. **159**(4): p. 1993-2000.

62.   Sozzani, S., et al., *Differential regulation of chemokine receptors during dendritic cell maturation: a model for their trafficking properties.* J Immunol, 1998. **161**(3): p. 1083-6.

63.   Ohl, L., et al., *CCR7 governs skin dendritic cell migration under inflammatory and steady-state conditions.* Immunity, 2004. **21**(2): p. 279-88.

64.   Villablanca, E.J. and J.R. Mora, *A two-step model for Langerhans cell migration to skin-draining LN.* Eur J Immunol, 2008. **38**(11): p. 2975-80.

65.   Ouwehand, K., et al., *CXCL12 is essential for migration of activated Langerhans cells from epidermis to dermis.* Eur J Immunol, 2008. **38**(11): p. 3050-9.

66.   Dieu, M.C., et al., *Selective recruitment of immature and mature dendritic cells by distinct chemokines expressed in different anatomic sites.* J Exp Med, 1998. **188**(2): p. 373-86.

67.   Britschgi, M.R., S. Favre, and S.A. Luther, *CCL21 is sufficient to mediate DC migration, maturation and function in the absence of CCL19.* Eur J Immunol, 2010. **40**(5): p. 1266-71.

68.   Weber, M., et al., *Interstitial dendritic cell guidance by haptotactic chemokine gradients.* Science, 2013. **339**(6117): p. 328-32.

69.   Stoitzner, P., et al., *A close-up view of migrating Langerhans cells in the skin.* J Invest Dermatol, 2002. **118**(1): p. 117-25.

70.   Schumann, K., et al., *Immobilized chemokine fields and soluble chemokine gradients cooperatively shape migration patterns of dendritic cells.* Immunity, 2010. **32**(5): p. 703-13.

71. Czeloth, N., et al., *Sphingosine-1-phosphate mediates migration of mature dendritic cells.* J Immunol, 2005. **175**(5): p. 2960-7.
72. Ratzinger, G., et al., *Matrix metalloproteinases 9 and 2 are necessary for the migration of Langerhans cells and dermal dendritic cells from human and murine skin.* J Immunol, 2002. **168**(9): p. 4361-71.
73. Van Lint, P. and C. Libert, *Chemokine and cytokine processing by matrix metalloproteinases and its effect on leukocyte migration and inflammation.* J Leukoc Biol, 2007. **82**(6): p. 1375-81.
74. Johnson, L.A., et al., *An inflammation-induced mechanism for leukocyte transmigration across lymphatic vessel endothelium.* J Exp Med, 2006. **203**(12): p. 2763-77.
75. Lammermann, T., et al., *Rapid leukocyte migration by integrin-independent flowing and squeezing.* Nature, 2008. **453**(7191): p. 51-5.
76. Merad, M., et al., *Depletion of host Langerhans cells before transplantation of donor alloreactive T cells prevents skin graft-versus-host disease.* Nat Med, 2004. **10**(5): p. 510-7.
77. Grouard, G., et al., *The enigmatic plasmacytoid T cells develop into dendritic cells with interleukin (IL)-3 and CD40-ligand.* J Exp Med, 1997. **185**(6): p. 1101-11.
78. Santegoets, S.J., et al., *Transcriptional profiling of human skin-resident Langerhans cells and CD1a+ dermal dendritic cells: differential activation states suggest distinct functions.* J Leukoc Biol, 2008. **84**(1): p. 143-51.
79. Robbins, S.H., et al., *Novel insights into the relationships between dendritic cell subsets in human and mouse revealed by genome-wide expression profiling.* Genome Biol, 2008. **9**(1): p. R17.
80. Lindstedt, M., K. Lundberg, and C.A. Borrebaeck, *Gene family clustering identifies functionally associated subsets of human in vivo blood and tonsillar dendritic cells.* J Immunol, 2005. **175**(8): p. 4839-46.
81. Lundberg, K., *Transcriptional profiling of human dendritic cell populations and models-unique profiles of in vitro dendritic cells and implications on functionality and applicability.* PLoS One, 2013. **8**(1): p. e52875.
82. van de Ven, R., et al., *Characterization of four conventional dendritic cell subsets in human skin-draining lymph nodes in relation to T-cell activation.* Blood, 2011. **118**(9): p. 2502-10.
83. Collin, M., N. McGovern, and M. Haniffa, *Human dendritic cell subsets.* Immunology, 2013.
84. Thomas, R., L.S. Davis, and P.E. Lipsky, *Isolation and characterization of human peripheral blood dendritic cells.* J Immunol, 1993. **150**(3): p. 821-34.
85. Dzionek, A., et al., *BDCA-2, BDCA-3, and BDCA-4: three markers for distinct subsets of dendritic cells in human peripheral blood.* J Immunol, 2000. **165**(11): p. 6037-46.
86. MacDonald, K.P., et al., *Characterization of human blood dendritic cell subsets.* Blood, 2002. **100**(13): p. 4512-20.
87. Perussia, B., V. Fanning, and G. Trinchieri, *A leukocyte subset bearing HLA-DR antigens is responsible for in vitro alpha interferon production in response to viruses.* Nat Immun Cell Growth Regul, 1985. **4**(3): p. 120-37.
88. Siegal, F.P., et al., *The nature of the principal type 1 interferon-producing cells in human blood.* Science, 1999. **284**(5421): p. 1835-7.
89. Lande, R., et al., *Plasmacytoid dendritic cells sense self-DNA coupled with antimicrobial peptide.* Nature, 2007. **449**(7162): p. 564-9.
90. Crozat, K., et al., *The XC chemokine receptor 1 is a conserved selective marker of mammalian cells homologous to mouse CD8alpha+ dendritic cells.* J Exp Med, 2010. **207**(6): p. 1283-92.
91. Jongbloed, S.L., et al., *Human CD141+ (BDCA-3)+ dendritic cells (DCs) represent a unique myeloid DC subset that cross-presents necrotic cell antigens.* J Exp Med, 2010. **207**(6): p. 1247-60.
92. Lauterbach, H., et al., *Mouse CD8alpha+ DCs and human BDCA3+ DCs are major producers of IFN-lambda in response to poly IC.* J Exp Med, 2010. **207**(12): p. 2703-17.

93. Poulin, L.F., et al., *Characterization of human DNGR-1+ BDCA3+ leukocytes as putative equivalents of mouse CD8alpha+ dendritic cells.* J Exp Med, 2010. **207**(6): p. 1261-71.

94. Segura, E., M. Durand, and S. Amigorena, *Similar antigen cross-presentation capacity and phagocytic functions in all freshly isolated human lymphoid organ-resident dendritic cells.* J Exp Med, 2013. **210**(5): p. 1035-47.

95. Mittag, D., et al., *Human dendritic cell subsets from spleen and blood are similar in phenotype and function but modified by donor health status.* J Immunol, 2011. **186**(11): p. 6207-17.

96. Yamazaki, C., et al., *Conservation of a chemokine system, XCR1 and its ligand, XCL1, between human and mice.* Biochem Biophys Res Commun, 2010. **397**(4): p. 756-61.

97. Galibert, L., et al., *Nectin-like protein 2 defines a subset of T-cell zone dendritic cells and is a ligand for class-I-restricted T-cell-associated molecule.* J Biol Chem, 2005. **280**(23): p. 21955-64.

98. Summers, K.L., et al., *Phenotypic characterization of five dendritic cell subsets in human tonsils.* Am J Pathol, 2001. **159**(1): p. 285-95.

99. Segura, E., et al., *Characterization of resident and migratory dendritic cells in human lymph nodes.* J Exp Med, 2012. **209**(4): p. 653-60.

100. McIlroy, D., et al., *Investigation of human spleen dendritic cell phenotype and distribution reveals evidence of in vivo activation in a subset of organ donors.* Blood, 2001. **97**(11): p. 3470-7.

101. Angel, C.E., et al., *Distinctive localization of antigen-presenting cells in human lymph nodes.* Blood, 2009. **113**(6): p. 1257-67.

102. Bendriss-Vermare, N., et al., *Human thymus contains IFN-alpha-producing CD11c(-), myeloid CD11c(+), and mature interdigitating dendritic cells.* J Clin Invest, 2001. **107**(7): p. 835-44.

103. Vandenabeele, S., et al., *Human thymus contains 2 distinct dendritic cell populations.* Blood, 2001. **97**(6): p. 1733-41.

104. Guerder, S., et al., *Differential processing of self-antigens by subsets of thymic stromal cells.* Curr Opin Immunol, 2012. **24**(1): p. 99-104.

105. Hart, D.N. and J.W. Fabre, *Demonstration and characterization of Ia-positive dendritic cells in the interstitial connective tissues of rat heart and other tissues, but not brain.* J Exp Med, 1981. **154**(2): p. 347-61.

106. Nestle, F.O., et al., *Characterization of dermal dendritic cells obtained from normal human skin reveals phenotypic and functionally distinctive subsets.* J Immunol, 1993. **151**(11): p. 6535-45.

107. Ginhoux, F., et al., *Blood-derived dermal langerin+ dendritic cells survey the skin in the steady state.* J Exp Med, 2007. **204**(13): p. 3133-46.

108. Romani, N., et al., *Cultured human Langerhans cells resemble lymphoid dendritic cells in phenotype and function.* J Invest Dermatol, 1989. **93**(5): p. 600-9.

109. Valladeau, J., et al., *Langerin, a novel C-type lectin specific to Langerhans cells, is an endocytic receptor that induces the formation of Birbeck granules.* Immunity, 2000. **12**(1): p. 71-81.

110. Mc Dermott, R., et al., *Birbeck granules are subdomains of endosomal recycling compartment in human epidermal Langerhans cells, which form where Langerin accumulates.* Mol Biol Cell, 2002. **13**(1): p. 317-35.

111. Mommaas, M., et al., *Functional human epidermal Langerhans cells that lack Birbeck granules.* J Invest Dermatol, 1994. **103**(6): p. 807-10.

112. Verdijk, P., et al., *A lack of Birbeck granules in Langerhans cells is associated with a naturally occurring point mutation in the human Langerin gene.* J Invest Dermatol, 2005. **124**(4): p. 714-7.

113. Nfon, C.K., et al., *Langerhans cells in porcine skin.* Vet Immunol Immunopathol, 2008. **126**(3-4): p. 236-47.

114. Romani, N., et al., *Migration of dendritic cells into lymphatics-the Langerhans cell example: routes, regulation, and relevance.* Int Rev Cytol, 2001. **207**: p. 237-70.

115. Haniffa, M., et al., *Differential rates of replacement of human dermal dendritic cells and macrophages during hematopoietic stem cell transplantation.* J Exp Med, 2009. **206**(2): p. 371-85.

116. Segura, E., et al., *Human inflammatory dendritic cells induce Th17 cell differentiation.* Immunity, 2013. **38**(2): p. 336-48.

117. Zaba, L.C., et al., *Psoriasis is characterized by accumulation of immunostimulatory and Th1/Th17 cell-polarizing myeloid dendritic cells.* J Invest Dermatol, 2009. **129**(1): p. 79-88.

118. Wollenberg, A., et al., *Immunomorphological and ultrastructural characterization of Langerhans cells and a novel, inflammatory dendritic epidermal cell (IDEC) population in lesional skin of atopic eczema.* J Invest Dermatol, 1996. **106**(3): p. 446-53.

119. Wollenberg, A., et al., *Expression and function of the mannose receptor CD206 on epidermal dendritic cells in inflammatory skin diseases.* J Invest Dermatol, 2002. **118**(2): p. 327-34.

120. Merad, M., et al., *The dendritic cell lineage: ontogeny and function of dendritic cells and their subsets in the steady state and the inflamed setting.* Annu Rev Immunol, 2013. **31**: p. 563-604.

121. Pulendran, B., et al., *Distinct dendritic cell subsets differentially regulate the class of immune response in vivo.* Proc Natl Acad Sci U S A, 1999. **96**(3): p. 1036-41.

122. Maldonado-Lopez, R., et al., *Role of CD8alpha+ and CD8alpha- dendritic cells in the induction of primary immune responses in vivo.* J Leukoc Biol, 1999. **66**(2): p. 242-6.

123. Dudziak, D., et al., *Differential antigen processing by dendritic cell subsets in vivo.* Science, 2007. **315**(5808): p. 107-11.

124. Rissoan, M.C., et al., *Reciprocal control of T helper cell and dendritic cell differentiation.* Science, 1999. **283**(5405): p. 1183-6.

125. Banchereau, J., et al., *The differential production of cytokines by human Langerhans cells and dermal CD14(+) DCs controls CTL priming.* Blood, 2012. **119**(24): p. 5742-9.

126. Seneschal, J., et al., *Human epidermal Langerhans cells maintain immune homeostasis in skin by activating skin resident regulatory T cells.* Immunity, 2012. **36**(5): p. 873-84.

127. Mathers, A.R., et al., *Differential capability of human cutaneous dendritic cell subsets to initiate Th17 responses.* J Immunol, 2009. **182**(2): p. 921-33.

128. Fujita, H., et al., *Human Langerhans cells induce distinct IL-22-producing CD4+ T cells lacking IL-17 production.* Proc Natl Acad Sci U S A, 2009. **106**(51): p. 21795-800.

129. Furio, L., et al., *Human langerhans cells are more efficient than CD14(-)CD1c(+) dermal dendritic cells at priming naive CD4(+) T cells.* J Invest Dermatol, 2010. **130**(5): p. 1345-54.

130. Bachem, A., et al., *Superior antigen cross-presentation and XCR1 expression define human CD11c+CD141+ cells as homologues of mouse CD8+ dendritic cells.* J Exp Med, 2010. **207**(6): p. 1273-81.

131. Nizzoli, G., et al., *Human CD1c+ dendritic cells secrete high levels of IL-12 and potently prime cytotoxic T cell responses.* Blood, 2013.

132. Cohn, L., et al., *Antigen delivery to early endosomes eliminates the superiority of human blood BDCA3+ dendritic cells at cross presentation.* J Exp Med, 2013. **210**(5): p. 1049-63.

133. Soumelis, V., et al., *Human epithelial cells trigger dendritic cell mediated allergic inflammation by producing TSLP.* Nat Immunol, 2002. **3**(7): p. 673-80.

134. Reche, P.A., et al., *Human thymic stromal lymphopoietin preferentially stimulates myeloid cells.* J Immunol, 2001. **167**(1): p. 336-43.

135. Watanabe, N., et al., *Hassall's corpuscles instruct dendritic cells to induce CD4+CD25+ regulatory T cells in human thymus.* Nature, 2005. **436**(7054): p. 1181-5.

136. Watanabe, N., et al., *Human thymic stromal lymphopoietin promotes dendritic cell-mediated CD4+ T cell homeostatic expansion.* Nat Immunol, 2004. **5**(4): p. 426-34.

137. Friend, S.L., et al., *A thymic stromal cell line supports in vitro development of surface IgM+ B cells and produces a novel growth factor affecting B and T lineage cells.* Exp Hematol, 1994. **22**(3): p. 321-8.

138. Sims, J.E., et al., *Molecular cloning and biological characterization of a novel murine lymphoid growth factor.* J Exp Med, 2000. **192**(5): p. 671-80.

139. Quentmeier, H., et al., *Cloning of human thymic stromal lymphopoietin (TSLP) and signaling mechanisms leading to proliferation.* Leukemia, 2001. **15**(8): p. 1286-92.

140. Park, L.S., et al., *Cloning of the murine thymic stromal lymphopoietin (TSLP) receptor: Formation of a functional heteromeric complex requires interleukin 7 receptor.* J Exp Med, 2000. **192**(5): p. 659-70.

141. Pandey, A., et al., *Cloning of a receptor subunit required for signaling by thymic stromal lymphopoietin.* Nat Immunol, 2000. **1**(1): p. 59-64.

142. Rochman, I., et al., *Cutting edge: direct action of thymic stromal lymphopoietin on activated human CD4+ T cells.* J Immunol, 2007. **178**(11): p. 6720-4.

143. Arima, K., et al., *Distinct signal codes generate dendritic cell functional plasticity.* Sci Signal, 2010. **3**(105): p. ra4.

144. Zhong, J., et al., *TSLP signaling network revealed by SILAC-based phosphoproteomics.* Mol Cell Proteomics. **11**(6): p. M112 017764.

145. Oh, J.W., et al., *CD4 T-helper cells engineered to produce IL-10 prevent allergen-induced airway hyperreactivity and inflammation.* J Allergy Clin Immunol, 2002. **110**(3): p. 460-8.

146. Kips, J.C., *Cytokines in asthma.* Eur Respir J Suppl, 2001. **34**: p. 24s-33s.

147. Ito, T., et al., *TSLP-activated dendritic cells induce an inflammatory T helper type 2 cell response through OX40 ligand.* J Exp Med, 2005. **202**(9): p. 1213-23.

148. Ying, S., et al., *Thymic stromal lymphopoietin expression is increased in asthmatic airways and correlates with expression of Th2-attracting chemokines and disease severity.* J Immunol, 2005. **174**(12): p. 8183-90.

149. Mou, Z., et al., *Overexpression of thymic stromal lymphopoietin in allergic rhinitis.* Acta Otolaryngol, 2009. **129**(3): p. 297-301.

150. Matsuda, A., et al., *Functional role of thymic stromal lymphopoietin in chronic allergic keratoconjunctivitis.* Invest Ophthalmol Vis Sci, 2009. **51**(1): p. 151-5.

151. Lee, E.B., et al., *Increased serum thymic stromal lymphopoietin in children with atopic dermatitis.* Pediatr Allergy Immunol, 2010. **21**(2 Pt 2): p. e457-60.

152. Allakhverdi, Z., et al., *Thymic stromal lymphopoietin is released by human epithelial cells in response to microbes, trauma, or inflammation and potently activates mast cells.* J Exp Med, 2007. **204**(2): p. 253-8.

153. Gilliet, M., et al., *Human dendritic cells activated by TSLP and CD40L induce proallergic cytotoxic T cells.* J Exp Med, 2003. **197**(8): p. 1059-63.

154. Lee, H.C. and S.F. Ziegler, *Inducible expression of the proallergic cytokine thymic stromal lymphopoietin in airway epithelial cells is controlled by NFkappaB.* Proc Natl Acad Sci U S A, 2007. **104**(3): p. 914-9.

155. Bogiatzi, S.I., et al., *Cutting Edge: Proinflammatory and Th2 cytokines synergize to induce thymic stromal lymphopoietin production by human skin keratinocytes.* J Immunol, 2007. **178**(6): p. 3373-7.

156. Lee, H.C., et al., *Cutting edge: Inhibition of NF-kappaB-mediated TSLP expression by retinoid X receptor.* J Immunol, 2008. **181**(8): p. 5189-93.

157. Vu, A.T., et al., *Staphylococcus aureus membrane and diacylated lipopeptide induce thymic stromal lymphopoietin in keratinocytes through the Toll-like receptor 2-Toll-like receptor 6 pathway.* J Allergy Clin Immunol, 2010. **126**(5): p. 985-93, 993 e1-3.

158. Li, M., et al., *Topical vitamin D3 and low-calcemic analogs induce thymic stromal lymphopoietin in mouse keratinocytes and trigger an atopic dermatitis.* Proc Natl Acad Sci U S A, 2006. **103**(31): p. 11736-41.

159. Sato-Deguchi, E., et al., *Topical vitamin D(3) analogues induce thymic stromal lymphopoietin and cathelicidin in psoriatic skin lesions.* Br J Dermatol, 2012. **167**(1): p. 77-84.

160. Roider, E., T. Ruzicka, and J. Schauber, *Vitamin d, the cutaneous barrier, antimicrobial peptides and allergies: is there a link?* Allergy Asthma Immunol Res, 2013. **5**(3): p. 119-28.

161. Chen, X., et al., *Human antimicrobial peptide LL-37 modulates proinflammatory responses induced by cytokine milieus and double-stranded RNA in human keratinocytes.* Biochem Biophys Res Commun, 2013. **433**(4): p. 532-7.

162. Bogiatzi, S.I., et al., *Multiple-checkpoint inhibition of thymic stromal lymphopoietin-induced TH2 response by TH17-related cytokines.* J Allergy Clin Immunol, 2012. **130**(1): p. 233-40 e5.

163. Besin, G., et al., *Thymic stromal lymphopoietin and thymic stromal lymphopoietin-conditioned dendritic cells induce regulatory T-cell differentiation and protection of NOD mice against diabetes.* Diabetes, 2008. **57**(8): p. 2107-17.

164. Lee, J.Y., et al., *Murine thymic stromal lymphopoietin promotes the differentiation of regulatory T cells from thymic CD4(+)CD8(-)CD25(-) naive cells in a dendritic cell-independent manner.* Immunol Cell Biol, 2008. **86**(2): p. 206-13.

165. Taylor, B.C., et al., *TSLP regulates intestinal immunity and inflammation in mouse models of helminth infection and colitis.* J Exp Med, 2009. **206**(3): p. 655-67.

166. Zeuthen, L.H., L.N. Fink, and H. Frokiaer, *Epithelial cells prime the immune response to an array of gut-derived commensals towards a tolerogenic phenotype through distinct actions of thymic stromal lymphopoietin and transforming growth factor-beta.* Immunology, 2008. **123**(2): p. 197-208.

167. Hanabuchi, S., et al., *Thymic stromal lymphopoietin-activated plasmacytoid dendritic cells induce the generation of FOXP3+ regulatory T cells in human thymus.* J Immunol, 2010. **184**(6): p. 2999-3007.

168. Ebner, S., et al., *Thymic stromal lymphopoietin converts human epidermal Langerhans cells into antigen-presenting cells that induce proallergic T cells.* J Allergy Clin Immunol, 2007. **119**(4): p. 982-90.

169. Ito, T., et al., *Two functional subsets of FOXP3+ regulatory T cells in human thymus and periphery.* Immunity, 2008. **28**(6): p. 870-80.

170. Volpe, E., et al., *A critical function for transforming growth factor-beta, interleukin 23 and proinflammatory cytokines in driving and modulating human T(H)-17 responses.* Nat Immunol, 2008. **9**(6): p. 650-7.

171. R, H.F., JOSSE J., LE S., MAZET J., *FactoMineR : Factor Analysis and Data Mining. .* 2012.

172. Moll, H., et al., *Langerhans cells transport Leishmania major from the infected skin to the draining lymph node for presentation to antigen-specific T cells.* Eur J Immunol, 1993. **23**(7): p. 1595-601.

173. Geissmann, F., et al., *Accumulation of immature Langerhans cells in human lymph nodes draining chronically inflamed skin.* J Exp Med, 2002. **196**(4): p. 417-30.

174. Ashworth, J. and R.M. Mackie, *A quantitative analysis of the Langerhans cell in chronic plaque psoriasis.* Clin Exp Dermatol, 1986. **11**(6): p. 594-9.

175. Wang, Y., et al., *IL-34 is a tissue-restricted ligand of CSF1R required for the development of Langerhans cells and microglia.* Nat Immunol, 2012. **13**(8): p. 753-60.

176. Greter, M., et al., *Stroma-derived interleukin-34 controls the development and maintenance of langerhans cells and the maintenance of microglia.* Immunity, 2012. **37**(6): p. 1050-60.

177. Kaplan, D.H., et al., *Autocrine/paracrine TGFbeta1 is required for the development of epidermal Langerhans cells.* J Exp Med, 2007. **204**(11): p. 2545-52.

178. Veldhoen, M., et al., *Transforming growth factor-beta 'reprograms' the differentiation of T helper 2 cells and promotes an interleukin 9-producing subset.* Nat Immunol, 2008. **9**(12): p. 1341-6.

179. Yao, W., et al., *Interleukin-9 is required for allergic airway inflammation mediated by the cytokine TSLP.* Immunity, 2013. **38**(2): p. 360-72.

180. Rust, R., et al., *Gene expression analysis of dendritic/Langerhans cells and Langerhans cell histiocytosis.* J Pathol, 2006. **209**(4): p. 474-83.

181. Delgado, E., et al., *Mature dendritic cells respond to SDF-1, but not to several beta-chemokines.* Immunobiology, 1998. **198**(5): p. 490-500.

182. Zlotnik, A. and O. Yoshie, *The chemokine superfamily revisited.* Immunity, 2012. **36**(5): p. 705-16.

183. Randolph, G.J., V. Angeli, and M.A. Swartz, *Dendritic-cell trafficking to lymph nodes through lymphatic vessels.* Nat Rev Immunol, 2005. **5**(8): p. 617-28.

184. Fernandez, M.I., et al., *The human cytokine TSLP triggers a cell-autonomous dendritic cell migration in confined environments.* Blood, 2011. **118**(14): p. 3862-9.

185. Sixt, M., *Interstitial locomotion of leukocytes.* Immunol Lett, 2011. **138**(1): p. 32-4.

186. Thelen, M. and S. Thelen, *CXCR7, CXCR4 and CXCL12: an eccentric trio?* J Neuroimmunol, 2008. **198**(1-2): p. 9-13.

187. Stutte, S., et al., *Requirement of CCL17 for CCR7- and CXCR4-dependent migration of cutaneous dendritic cells.* Proc Natl Acad Sci U S A, 2010. **107**(19): p. 8736-41.

188. Delcourt, N., J. Bockaert, and P. Marin, *GPCR-jacking: from a new route in RTK signalling to a new concept in GPCR activation.* Trends Pharmacol Sci, 2007. **28**(12): p. 602-7.

189. Pyne, N.J. and S. Pyne, *Receptor tyrosine kinase-G-protein-coupled receptor signalling platforms: out of the shadow?* Trends Pharmacol Sci, 2011. **32**(8): p. 443-50.

190. Vanbervliet, B., et al., *The inducible CXCR3 ligands control plasmacytoid dendritic cell responsiveness to the constitutive chemokine stromal cell-derived factor 1 (SDF-1)/CXCL12.* J Exp Med, 2003. **198**(5): p. 823-30.

191. Krug, A., et al., *IFN-producing cells respond to CXCR3 ligands in the presence of CXCL12 and secrete inflammatory chemokines upon activation.* J Immunol, 2002. **169**(11): p. 6079-83.

192. Scandella, E., et al., *Prostaglandin E2 is a key factor for CCR7 surface expression and migration of monocyte-derived dendritic cells.* Blood, 2002. **100**(4): p. 1354-61.

193. Robbiani, D.F., et al., *The leukotriene C(4) transporter MRP1 regulates CCL19 (MIP-3beta, ELC)-dependent mobilization of dendritic cells to lymph nodes.* Cell, 2000. **103**(5): p. 757-68.

194. Chan, L.C., et al., *LPA3 receptor mediates chemotaxis of immature murine dendritic cells to unsaturated lysophosphatidic acid (LPA).* J Leukoc Biol, 2007. **82**(5): p. 1193-200.

195. Akekawatchai, C., et al., *Transactivation of CXCR4 by the insulin-like growth factor-1 receptor (IGF-1R) in human MDA-MB-231 breast cancer epithelial cells.* J Biol Chem, 2005. **280**(48): p. 39701-8.

196. Bieber, T., et al., *Fc [correction of Ec] epsilon RI expressing dendritic cells: the missing link in the pathophysiology of atopic dermatitis?* J Dermatol, 2000. **27**(11): p. 698-9.

197. Novak, N., S. Kraft, and T. Bieber, *Unraveling the mission of FcepsilonRI on antigen-presenting cells.* J Allergy Clin Immunol, 2003. **111**(1): p. 38-44.

198. Spergel, J.M. and A.S. Paller, *Atopic dermatitis and the atopic march.* J Allergy Clin Immunol, 2003. **112**(6 Suppl): p. S118-27.

199. Verhagen, J., et al., *Absence of T-regulatory cell expression and function in atopic dermatitis skin.* J Allergy Clin Immunol, 2006. **117**(1): p. 176-83.

200. Homey, B., et al., *Cytokines and chemokines orchestrate atopic skin inflammation.* J Allergy Clin Immunol, 2006. **118**(1): p. 178-89.

201. Samochocki, Z., et al., *T-regulatory cells in severe atopic dermatitis: alterations related to cytokines and other lymphocyte subpopulations.* Arch Dermatol Res. **304**(10): p. 795-801.

202. Chorro, L., et al., *Langerhans cell (LC) proliferation mediates neonatal development, homeostasis, and inflammation-associated expansion of the epidermal LC network.* J Exp Med, 2009. **206**(13): p. 3089-100.

203. Bieber, T. and O. Braun-Falco, *Distribution of CD1a-positive cells in psoriatic skin during the evolution of the lesions.* Acta Derm Venereol, 1989. **69**(2): p. 175-8.

204. Cumberbatch, M., et al., *Impaired Langerhans cell migration in psoriasis.* J Exp Med, 2006. **203**(4): p. 953-60.

205. Shamoto, M., et al., *Do epidermal Langerhans cells, migrating from skin lesions, induce the paracortical hyperplasia of dermatopathic lymphadenopathy?* Pathol Int, 1996. **46**(5): p. 348-54.

206. Soc., W.G.h., *Histiocytosis lesions in children.* Lancet, 1987. **1**: p. 208-209.

207. Badalian-Very, G., et al., *Pathogenesis of Langerhans cell histiocytosis.* Annu Rev Pathol, 2013. **8**: p. 1-20.

208. Allen, C.E., et al., *Cell-specific gene expression in Langerhans cell histiocytosis lesions reveals a distinct profile compared with epidermal Langerhans cells.* J Immunol, 2010. **184**(8): p. 4557-67.

209. Rolland, A., et al., *Increased blood myeloid dendritic cells and dendritic cell-poietins in Langerhans cell histiocytosis.* J Immunol, 2005. **174**(5): p. 3067-71.

210. Geissmann, F., et al., *Lack of expression of E-cadherin is associated with dissemination of Langerhans' cell histiocytosis and poor outcome.* J Pathol, 1997. **181**(3): p. 301-4.

211. Geissmann, F., et al., *Differentiation of Langerhans cells in Langerhans cell histiocytosis.* Blood, 2001. **97**(5): p. 1241-8.

212. Sere, K., et al., *Two distinct types of Langerhans cells populate the skin during steady state and inflammation.* Immunity, 2012. **37**(5): p. 905-16.

213. Kitajima, M. and S.F. Ziegler, *Cutting edge: identification of the thymic stromal lymphopoietin-responsive dendritic cell subset critical for initiation of type 2 contact hypersensitivity.* J Immunol, 2013. **191**(10): p. 4903-7.

214. Luster, A.D., R. Alon, and U.H. von Andrian, *Immune cell migration in inflammation: present and future therapeutic targets.* Nat Immunol, 2005. **6**(12): p. 1182-90.

215. Homey, B. and A. Zlotnik, *Chemokines in allergy.* Curr Opin Immunol, 1999. **11**(6): p. 626-34.

APPENDIX

7.1 APPENDIX 1

Other effects of TSLP on blood dendritic cell subsets

TSLP induces a differential chemokine secretion on DC subsets

I evaluated TSLP capacity to induce the gene expression and the secretion of CCL3, CCL4, CCL17 and CCL22 chemokines. I found that TSLP was able to induce the gene expression of these chemokines only in the BDCA-1$^+$ subset (Figure 7-1). BDCA-3$^+$ cells were not found to express TSLP-induced chemokine genes. Moreover, CCL3 and CCL4 were detectable at the protein level only in TSLP-treated BDCA-1$^+$ cells and not in medium-treated BDCA-1$^+$ cells or BDCA-3$^+$ cells. CCL17 and CCL22 were found to be secreted at high levels by TSLP-treated BDCA-1$^+$ cells. In some cases we could detect CCL17 and CCL22 secretion by TSLP-treated BDCA-3$^+$ cells, but in most of the cases the levels for these cytokines were below the limits of the assay detection. Therefore we could conclude that TSLP-induced CCL3, CCL4, CCL17 and CCL22 chemokine secretion is restricted to BDCA-1$^+$ blood DC subset.
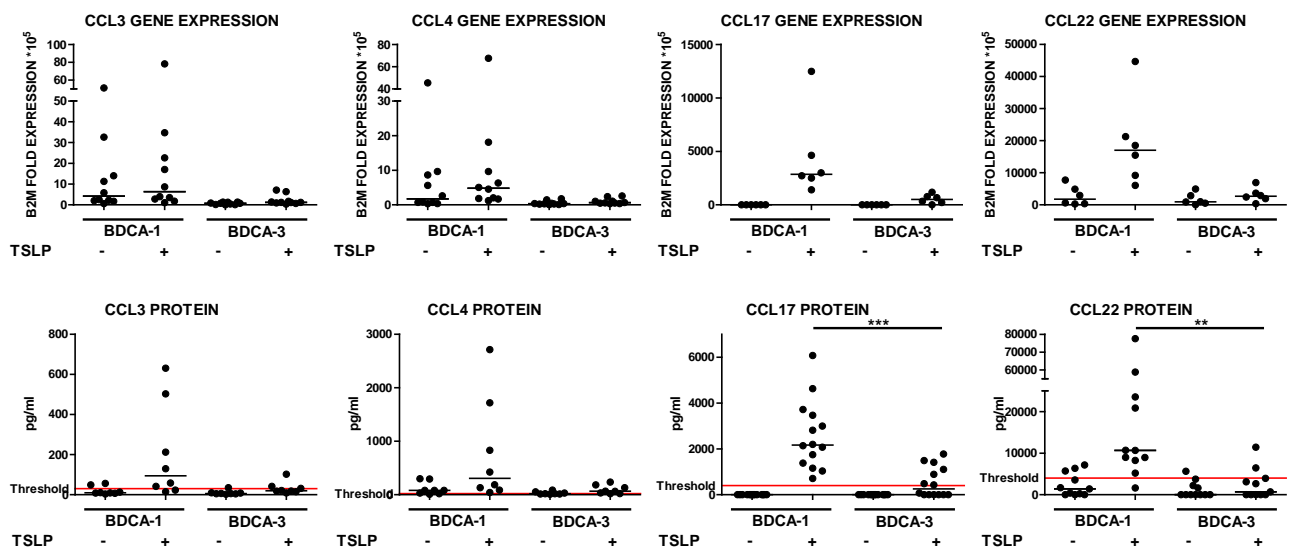
Figure 7-1: TSLP-induced chemokine secretion is restricted to BDCA-1$^+$ DC subset.

Upper panels: Chemokine gene expression on 24h-treated BDCA-1$^+$ and BDCA-3$^+$ DCs. Normalized expression is shown as B2M fold expression as determined by real-time qPCR. The bar represents the mean.

Lower panels: Chemokine protein quantification on 24h-treated BDCA-1$^+$ and BDCA-3$^+$ DCs cell culture supernatants. The bar represents the mean and the red line represents the threshold of sensitivity of quantification method. CCL3 and CCL4 were measured by cytometric bead array (CBA) and CCL17 and CCL22 were measured by ELISA. Each dot represents an independent donor **$p \leq$ 0.005 ***$p \leq$ 0.0005, Wilcoxon non-parametric paired test was used.

TSLP induces a Th2 profile in both blood DC subsets

TSLP-treated DCs induce an inflammatory Th2 cytokine profile on naïve CD4$^+$ helper T cells [133]. To evaluate the functional properties of TSLP-treated DC subsets, I purified human naïve T cells (CD4$^+$CD45RA$^+$) from peripheral blood and cultured them with 24hour TSLP-treated BDCA-1$^+$ or BDCA-3$^+$ cells at a 1:5 ratio. After 6 days of co-culture, I recovered washed and counted the T cells, and re-stimulated them for 24hours with anti-CD3 and anti-CD28 beads. In parallel, naïve T cells were unstimulated (Th0), or stimulated with polarizing cytokines before re-stimulation to induce typical TH1, Th2 and Th17 profiles as reported previously [170]. At the end of the culture, I assessed the proliferation of T cells and the presence, in the culture supernatants, of 13 different cytokines characterizing Th1, Th2, and Th17 profiles. I found that both DC subsets, stimulated with TSLP, induced proliferation of allogeneic naïve CD4$^+$ T cells. TSLP-BDCA-1$^+$ cells induced a stronger proliferation of T cells tan BDCA-3$^+$ cells after TSLP treatment (Figure 7-2A). Principal component analysis of the secreted cytokine profiles was used to determine the degree of similarity between the profiles induced by DC subsets on T cells. The T cells co-cultured with TSLP-treated BDCA-1$^+$ and BDCA-3$^+$ DCs were found close together and closer to the Th2 profile than the T cells co-cultured with untreated DCs (Figure 7-2B). The T cells co-cultured with untreated BDCA-1$^+$ and BDCA-3$^+$ DCs were found close together and closer to the Th0 and the Th1 profiles (Figure 7-2 B). TSLP-BDCA-1$^+$ induced naïve CD4$^+$T cells to produce higher amounts of IL-4 ($p < 0.05$), IL-5 (not significant, $p=0.06$), IL-13 ($p < 0.05$,) and TNF-α (not significant) compared to undertreated BDCA-1$^+$ cells (Figure 7-2C). Similarly, TSLP-BDCA-3$^+$ induced naïve CD4$^+$T cells to produce these same cytokines at significant higher levels than the untreated BDCA-3$^+$ counterpart (all $p < 0.05$) (Figure 7-2C).

Consistent with the PCA analysis, TSLP treated BDCA-1$^+$ and BDCA-3$^+$ DCs did not induce a differential secretion of IL-5, IL-13 and TNF-α. Statistical difference was only reached when comparing the IL-4 induced cytokine production ($p=0.03$). INF-γ was not induced by either of the TSLP treated subsets (Figure 7-2C).

A

T CELL EXPANSION

B

C

IL-4

IL-5

IL-13

TNF-α

IFN-γ

IL-10
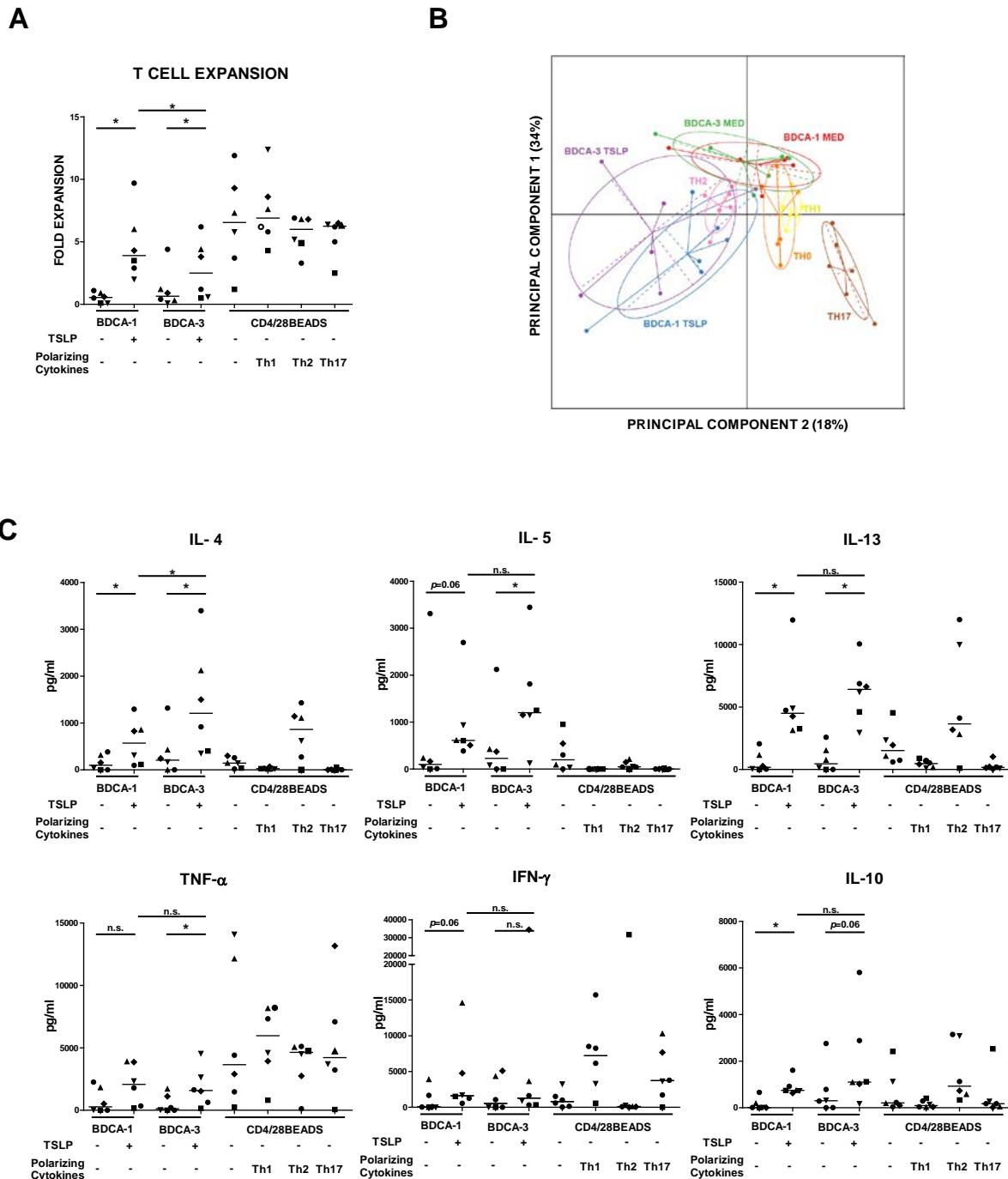
Figure 7-2: Functional properties of TSLP-treated BDCA-1^{+} and BDCA-3^{+} DCs

DC subsets were stimulated with or without TSLP for 24h and cultured with allogeneic naive CD4^{+}T cells for 6 d before T cell restimulation. Cytokine cocktails were used before restimulation to polarize naive T cells into typical Th1, Th2 and TH17 cells. Symbols represent cells purified from the same donor.

(A) T cell expansion was assessed by calculating the ratio of the number of T cells at the end of the culture divided by the number of T cells plated at the start of the culture. $*p \leq 0.05$, Wilcoxon non-parametric paired test was used. Bars represent medians.

(**B**) Resemblance of the naïve T cell profiles induced under the different conditions by Principal analysis Component (PCA). n=6 Principal component 1 and 2 were selected as the axes explaining most of the data variance. The ellipses join the data obtained for each condition.

(**C**) Data represent cytokine concentration at the end of the culture measured by cytometric bead array (CBA). Polarizing Cytokines: Th1, IL-12; Th2, IL-4; Th17, IL-1β, IL-6, TNF-α, TGF-β and IL-23. *p ≤0.05, Wilcoxon non-parametric paired test was used. Bars represent medians.

In this appendix, I show that only the blood BDCA-1$^+$ cells are able to secrete CCL17 and CCL22 after TSLP treatment. Moreover, I had found that TSLP also induced the secretion of CCL3 and CCL4 by total blood DCs. Here I show that the secretion of these two chemokines is also restricted to the BDCA-1$^+$ subset. These data are in accordance with recently published data by Ziegler S. F., et al which show that the murine BDCA-1$^+$ DC counterpart (bone marrow- derived CD11b$^+$ DCs) secrete CCL17 and are able to migrate [213]. However in their study they did not systematically compared TSLP effects on other DC subsets. To study the possible functional differences between TSLP-treated BDCA-1$^+$ and BDCA-3$^+$ DCs I evaluated their capacity to induce naïve CD4$^+$ T cell proliferation and polarization. My results show that both subsets are able to induce naïve CD4$^+$ T cell proliferation. Both subsets triggered the CD4$^+$ T cell polarization towards a Th2 profile. TSLP-BDCA-1$^+$ cells were found to be superior in inducing T cell proliferation and BDCA-3$^+$ cells were found to trigger a higher secretion of IL-4, IL-5 and IL-13 although additional experiments are required to reach statistical significance.

In inflammatory conditions, the chemokines secreted by resident DCs have an important role in the recruitment of other immune cells that help to sustain the inflammatory response [214]. CCL3 and CCL4 are able to recruit T cells, and innate actors such as neutrophils, eosinophils, basophils, NK cells, monocytes and DCs. Moreover CCL17 and CCL22 are known to be able to recruit Th2 cells in the allergic inflammation [215]. The differential secretion of these chemokines by BDCA-1$^+$ and BDCA-3$^+$ DCs after TSLP treatment suggests that these subsets have a differential involvement in the innate phase of the allergic inflammation. In TSLP-linked allergic disorders BDCA-3$^+$ DCs would contribute poorly to the generation of the immune cell infiltration. Nevertheless both subsets prime naïve CD4$^+$ T cells into Th2 cells suggesting that both subsets have an equivalent participation in the acquired phase of the allergic response.

These results are in line with our previous experiments that suggest that the differential response to TSLP by blood DC subsets may be linked to different roles in the induction of the inflammatory response.

7.2   APPENDIX 2

Collaboration

Telomere crisis in kidney epithelial cells promotes the acquisition of a microRNA signature retrieved in aggressive renal cell carcinomas

Luis Jaime Castro-Vega, Karina Jouravleva, Win-Yan Liu, Carolina Martinez, Pierre Gestraud, Philippe Hupé, Nicolas Servant, Benoît Albaud, David Gentien, Sophie Gad, Stéphane Richard, Silvia Bacchetti and Arturo Londoño-Vallejo**.**

Telomere crisis in kidney epithelial cells promotes the acquisition of a microRNA signature retrieved in aggressive renal cell carcinomas

Luis Jaime Castro-Vega[1,2], Karina Jouravleva[1,2], Win-Yan Liu[1,2], Carolina Martinez[3], Pierre Gestraud[4,5], Philippe Hupé[4,5,6], Nicolas Servant[4,5], Benoît Albaud[7], David Gentien[7], Sophie Gad[8], Stéphane Richard[8], Silvia Bacchetti[9] and Arturo Londoño-Vallejo[1,2,*]

[1]UMR3244, Telomeres and Cancer Laboratory, Institut Curie, 26 rue d'Ulm, Paris 75248, France, [2]UPMC University, Paris 06, Paris F-75005, France, [3]INSERM U932, Immunity and Cancer, Institut Curie, 26 rue d'Ulm, Paris 75248, France, [4]INSERM U900, Institut Curie, 26 rue d'Ulm, Paris 75248, France, [5]Mines Paristech, Centre for Computational Biology, 35 rue Saint Honoré, Fontainebleau, Paris 77305, France, [6]CNRS-UMR144, Institut Curie, 26 rue d'Ulm, Paris 75248, France, [7]Department of Translational Research, Institut Curie, 26 rue d'Ulm, Paris 75248, France, [8]INSERM U753, Génétique Oncologique EPHE, Institut de cancérologie Gustave Roussy, 114 rue Edouard Vaillant, Villejuif 94800, France and [9]Department of Experimental Oncology, Istituto Regina Elena, Rome 00158, Italy

*To whom correspondence should be addressed. Tel: +0156 246 611; Fax: +0156 246 674;
Email: Arturo.Londono@curie.fr

Telomere shortening is a major source of chromosome instability (CIN) at early stages during carcinogenesis. However, the mechanisms through which telomere-driven CIN (T-CIN) contributes to the acquisition of tumor phenotypes remain uncharacterized. We discovered that human epithelial kidney cells undergoing T-CIN display massive microRNA (miR) expression changes that are not related to local losses or gains. This widespread miR deregulation encompasses a miR-200-dependent epithelial-to-mesenchymal transition (EMT) that confers to immortalized pre-tumoral cells phenotypic traits of metastatic potential. Remarkably, a miR signature of these cells, comprising a downregulation of miRs with conserved expression in kidney, was retrieved in poorly differentiated aggressive renal cell carcinomas. Our results reveal an unanticipated connection between telomere crisis and the activation of the EMT program that occurs at pre-invasive stages of epithelial cancers, through mechanisms that involve miR deregulation. Thus, this study provides a new rational into how telomere instability contributes to the acquisition of the malignant phenotype.

Introduction

Telomere shortening is frequently detected at early stages of human epithelial cancers (1,2) and likely contributes to chromosome instability (CIN), a hallmark of cancer cells (3,4). Recent studies on the evolution of genome instability in cancer have identified distinctive patterns of CIN that could be explained by a mechanism of breakage-fusion-bridge (BFB) cycles following telomere dysfunction (5). However, the contribution of such rearrangements to tumor progression remains largely uncharacterized. On the other hand, mouse models with short telomeres have demonstrated that telomere-driven CIN (T-CIN) plays a central role in the promotion and progression of epithelial cancers through amplifications and losses of cancer genes (6–10). Moreover, it has been recently shown that a transient period of T-CIN followed by the reactivation of telomerase contributes to the acquisition of the

metastatic phenotype, presumably by the selection of clones carrying mutations in specific loci (11). However, the genetic elements impinged upon by T-CIN in human tumors, particularly from epithelial origin, remain largely undetermined.

MicroRNAs (miRs) are small non-coding RNAs that play a critical role in gene expression regulation through post-transcriptional silencing (12). As miRs participate in key cellular processes that are disrupted in cancer cells, it is not surprising that the altered expression of these molecules has been found in several types of human cancers (13). Interestingly, it has been shown that miR genes are located in cancer-associated genomic regions that are preferentially affected by genome instability events (14). In this study, we have used human epithelial kidney cells (HEK cells), a well-established *in vitro* model of progressive telomere instability, to study the impact of T-CIN in the expression of miRs and the biological consequences that might be relevant for the acquisition of tumor phenotypes.

Materials and methods

Cell culture

HEK cells were maintained under standard culture conditions in a humidified 5% CO_2 atmosphere at 37°C in modified Eagle's culture media without deoxyribonucleases (Invitrogen) and supplemented with 10% fetal bovine serum, essential amino acids and sodium pyruvate. Cell growth was monitored by cell counting and population doublings (PDs) were calculated by using the formula: number of PDs = (log [final count] – log [initial count])/0.301.

Cell transfection

For plasmid transfections, DNA was purified by standard methods using the Maxiprep kit (Qiagen) and 20 µg of plasmids were used to transfect the cells. The following plasmids were used: pSV3 Neo (simian virus 40 [SV40]), pLXSP-hTERT Puro (human telomerase reverse transcriptase [hTERT]), pBabe Puro (rat sarcoma viral oncogene homolog [RAS]) and pRetro-Super (shATM). Medium was changed 6 h after transfections and antibiotic selection was initiated in the following 24–48 h. For HEK cells, 0.5 µg/ml of puromycin and up to 450 µg/ml of G418 were used. Selection is completed in 1 week after which non-transfected controls have died off. Transfections of miRs were carried out using synthetic miR Precursor Molecules (Ambion PremiR) and Lipofectamine 2000 (Invitrogen) as transfection reagent. Cells were transfected with a mixture of pre-miR-200a, pre-miR-200b, pre-miR-141 and pre-miR-200c at a final concentration of 100 nM. An equivalent amount of Precursor Negative Control (Ambion) was used as control. Cells were transfected twice with an interval of 48 h and then analyzed.

Western blot

Cells were harvested at 75% confluence and lysed in RIPA buffer with protease (Roche) and phosphatase (Thermo scientific) inhibitors. Protein quantifications were performed using the Pierce BCA Protein Assay kit (Thermo scientific), and 20–40 µg protein was analyzed either in 3–8% Tris-acetate or in 4–12% Bis-Tris gels. Broad range protein marker (Fermentas) was used as ladder. Transfer was performed for 2 h at 25 V or for 10 min when an iBlot gel transfer system (Invitrogen) was used. Blocking was performed with 5% milk or 5% bovine serum albumin for 1–2 h at room temperature for phosphorylated proteins and primary antibodies were incubated at 4°C overnight. Detection was performed using the ECL plus kit (Amersham) and photos were taken at different exposition times. The following antibodies with their respective specifications were used: mouse monoclonal 419 (LT-SV40; provided by Dr Silvia Bacchetti) dilution 1:1000; mouse monoclonal (ataxia telangiectasia mutated [ATM]) (Abcam; Ref. ab2618) dilution 1:500; mouse monoclonal pATM (Rockland; Ref. 200-301-400) dilution 1:500; rabbit polyclonal CHK2 (Abcam; Ref. ab8108) dilution 1:500; rabbit polyclonal pCHK2 (Cell Signalling; Ref. 2661) dilution 1:500; rabbit polyclonal H2AX (Abcam; Ref. ab11175) dilution 1:500; mouse monoclonal pH2AX (Millipore; Ref. 05-636) dilution 1:500; rabbit polyclonal (telomeric repeat binding factor 2 [TRF2]) (Novus Biologicals; Ref. NB110-57130) dilution 1:500; mouse monoclonal Pan-cytokeratin (Sigma; Ref. C2562) dilution 1:50 000; mouse monoclonal E-cadherin (BD Biosciences; Ref. 610182) dilution 1:5000; rabbit polyclonal transforming growth factor-β1/2/3 (Santa Cruz Biotechnology; Ref. sc-7892)

Abbreviations: BFB, breakage-fusion-bridge; CIN, chromosome instability; DDR, DNA damage responses; ER-SV40, early region of SV40; EMT, epithelial-to-mesenchymal transition; HEK cells, human epithelial kidney cells; hTERT, human telomerase reverse transcriptase; miR, microRNA; RT–qPCR, real-time–quantitative PCR; SSC, standard saline citrate; SV40, simian virus 40; T-CIN, telomere-driven CIN.

dilution 1:200; mouse monoclonal Beta-actin (Santa Cruz Biotechnology; Ref. sc-47778) dilution 1:30 000 and rabbit polyclonal (zinc finger E-box binding homeobox 1 [ZEB1]) (Abcam; Ref. ab64098) dilution 1:500.

Southern blot

DNA extractions were performed by using the method of phenol–chloroform previous digestion with proteinase K. For teloblot, 5–10 µg DNA was digested with 50U HinfI and RsaI enzymes overnight. Then, samples and DNA marker (Low Range PFG marker, Biolabs) were loaded onto an 1% agarose gel in 0.5× Tris–Borate–EDTA buffer. The clamped homogeneous electric field (CHEF) electrophoresis conditions are as follows: initial pulse: 0.1 s; final pulse: 2.5 s; time: 8h and voltage: 200V or 6V/cm^2. Gels were stained with ethidium bromide for 10min and destained with Nanopure water for 20min. DNA was broken with a ultraviolet crosslinker set to 1800×100 KJ (about 1 min). Gels are denatured and transferred in alkaline conditions (0.6M NaCl, 0.4M NaOH) for up to 48h. Fixation and neutralization steps were performed in 0.4 N NaOH for 15 min and in 2× standard saline citrate (SSC), respectively. Prehybridization was carried out overnight at 42°C using 1/50 of Boehringer blocking reagent. The probe (20 pmol) was labeled with γ-adenosine triphosphate and hybridizations were carried out overnight at 42°C. (Sequence 25 bp CCTAACCCTAACCCTAACCCTAACC.) Membranes were washed with 2× SSC, 0.1% sodium dodecyl sulfate at room temperature for 5 min; 0.2× SSC, 0.1% sodium dodecyl sulfate at 37°C for 2min and final wash with 2× SSC. Then, the membranes were exposed for 1–2 days and scanned for analysis.

Immunofluorescence

The day before, 20 000 cells per well were seeded on microscope slides (Thermo scientific). For F-actin staining, cells were washed with phosphate-buffered saline 1× and fixed in 3% formaldehyde and 2% sucrose for 15 min. Next, cells were washed twice and permeabilized for 10 min. Stock solutions of phalloidin–tetramethylrhodamine isothiocyanate (TRITC) (Sigma) conjugates have been made in dimethyl sulfoxide at 0.5 mg/ml and is used at a concentration of 1:400 in phosphate-buffered saline for 40 min at room temperature. Cells were washed several times to remove the conjugate and stained with 0.5 mg/ml 4′,6-diamidino-2-phenylindole.

Migration/invasion assays

Wound healing assays were performed in cells at 75% confluence by scratching with a p200 pipette tip. Images were captured at 0, 6 and 12h. At least 10 images at each time point in two independent experiments were used for analysis and the percentage of invaded area at each time was estimated for quantifications. For matrigel invasion assays, chambers were rinsed with media without serum 4 h before the assay. Then, a coat of matrigel (diluted one-third in media without serum) is applied in the upper side of the chamber and incubated for 1h. A total of 200 000 non-starved cells were seeded for analysis; 10% fetal bovine serum was used as chemoattractant on the bottom side of the chamber. Cells were allowed to traverse the matrigel and filter for a period of 72h after which they were fixed with methanol for 15 min and stained with 0.2% crystal violet in water for 1h. Cells from the upper side of the chamber were removed with cotton swabs. A total of 10 images from two independent experiments were taken for quantifications.

Array-comparative genomic hybridization

To characterize genome instability in HEK cells, human CGH 4×72K Whole-Genome Tiling Arrays (NimbleGen) were used. This platform carries synthetic probes representing loci spaced on average of every 40 Kb. HA1-Early cells were used as normal controls of hybridizations. DNAs for analyses were diluted at 100–200ng/µl and quality was checked by Nanodrop and Qubit (Invitrogen). Labeling reactions (Cy3 normal/Cy5 tumoral) were performed by random priming method using the BioPrime kit (Invitrogen) and 500ng DNA. After precipitation, DNA was quantified again and hybridizations were performed at 42°C overnight in hybridization chambers. After washing steps, slides were scanned using Genepix 400B (Axin scanner). Data were uploaded to the VAMP (Visualization and Analysis of array-CGH, Transcriptome and other molecular profiles) platform at the Curie Institute (12) and CGH data were normalized by using Micro-Array Normalization of array-CGH data (MANOR) (13) and segmented by using Gain and Loss Analysis of DNA (GLAD) (14).

RNA sequencing

Total RNA was purified from immortalized and non-immortalized CIN− and CIN+ HEK cells using miRNEasy (Qiagen). Quality of preparations was checked using Agilent Bioanalyzer 2100 and only RNAs with a RNA integrity number (RIN) > 8.5 were used for subsequent analyses. Small (20–22 nt) RNA libraries were prepared in duplicate with size-purified RNA isolated from two different batches of cells. Approximately, 100 µg of total RNA was submitted to the ImaGif platform (Gif-sur-Yvette, France) for Illumina sequencing. This procedure was performed by fractionating total RNA using polyacrylamide gel electrophoresis to isolate 18–30 nt small RNAs. 3′ and 5′ adapters were ligated to the small RNAs and constructs were amplified following real-time–PCR (RT–PCR) following the conditions specified in the 36 cycles Sequencing Kit v5 (FC1045001, Illumina) protocol. The small RNA library was sequenced using a Solexa/Illumina GA-IIx Genome analyzer. Small RNA sequences were analyzed using the ncPRO-seq pipeline (http://ncproseq.sourceforge.net/) (15). Briefly, reads were mapped to the human genome (hg19) using the Bowtie aligner (16) allowing up to 20 genomic match positions. The genomic positions of mature miRs and miR* were obtained from the miRBase database (17). Aligned reads were then considered to correspond to a mature miR (or miR*) only if the aligned position did not differ from the annotated position of the mature miR (or miR*) by more than 2bp. In order to be able to compare miR expression levels and profiles between libraries, miR read counts were normalized using a two-step procedure. The normalized miRs read counts were then assessed for differential analysis using the R/Bioconductor package DESeq (18) and miRs with an adjusted *P* value (adj *P* < 0.05) were reported as significant.

Expression profiling of mature miRs

Screening for miR expression was performed using the Affymetrix miRNA Galaxy arrays following the manufacturer's protocol. Raw data were uploaded onto the VAMP platform, normalized using standard procedures and analyzed. Differentially expressed miRs between CIN− and CIN+ HEK cells were identified using a *t*-test. For validation, quantitative analysis of mature miRs was performed using the RT–quantitative PCR (RT–qPCR) miRCURY system from (EXIQON). Briefly, 250 ng of DNase-treated RNA was used to prepare complementary DNAs in three independent RT reactions, and qPCR reactions were carried out using miR-specific locked nucleic acid (LNA) primers in a Roche instrument LC480. The expression of hsa-miR-31 was used as endogenous control for normalization and relative quantifications were calculated with the $2^{-\Delta\Delta CT}$ method (19).

Expression profiling of pre-miRs

A total of 178 precursors were analyzed using the MiRmaid miRNA Precursors RT–qPCR primer set (Eurogentec). Universal RT reactions were purified and then amplified using specific pre-miR primers. The qPCR reaction was performed in ABI Prism 7500 thermal cycler (Applied Biosystems). Amplifications with Ct values > 38 and unspecific amplifications (more than two peaks in the melting curve) were considered not reliable for analysis. The geometric mean of three control genes (*5S*, *TBP*, *HBMS*) was used for normalization (20). A second method of normalization was performed using the average of the whole set of miRs present in the same PCR plate (21). Analysis of differentially expressed miR was performed using a two-tail *t*-test. The false discovery rate was controlled using the Benjamini–Hochberg procedure, and a *P* value <0.05 was considered significant. All the analyses were performed using R software with Bioconductor packages and custom functions defined at the Institut Curie Bioinformatics group (http://bioinfo.curie.fr/projects/ema).

Expression profiling of primary miRs

RNA samples were treated with DNase using TURBO-DNA-free (Ambion). The protocol includes a universal RT reaction step using the high-capacity RNA-to-cDNA kit (Applied Biosystems) followed by detection of pri-miRs in qPCR using specific Taqman Pri-miRNA assays (Applied Biosystems). In addition, a Taqman assay for RNU24 was used for normalization. The qPCR reaction was performed in ABI Prism 7500 thermal cycler (Applied Biosystems). Relative quantifications were calculated with the $2^{-\Delta\Delta CT}$ method (19).

Transcriptome analysis

Gene expression profiling was performed using the U133 Plus 2.0 Array platform that contains 47 000 transcripts. Complementary DNA synthesis, fragmentation and hybridization were carried out following an optimized protocol at the Institut Curie Translational Platform. After scanning, data were normalized using GC robust multi-array average (GCRMA) and non-detected probesets were removed (using a threshold of 3.5 in log scale on the maximal value for each probeset), leaving 25 022 probesets for the analysis. Clustering analyses were performed using Pearson's correlation as distance and Ward's linkage. Differentially expressed genes between pre-crisis and post-crisis samples were assessed with *t*-test and false discovery rate was controlled by Benjamini–Hochberg procedure.

Clinical samples

A series of 33 human renal clear cell carcinomas were obtained from the French Kidney Cancer Consortium co-ordinated by S.Richard. This study was approved by the ethical committee of Le Kremlin-Bicêtre University Hospital, France. All patients had provided informed consent before surgery for use of their tumors for further investigation, and samples were frozen immediately in liquid nitrogen. RNAs were extracted using Trizol reagent (Invitrogen)

according to the manufacturer's instructions, and quality and quantity were assessed by Agilent Bioanalyzer 2100. Hybridization was performed by the Genomics Platform of Gustave Roussy Institute (Villejuif, France) using miR 8×16K Agilent Human v3 (G4470C) in one color.

Results

HEK cells model of T-CIN

In this model, primary HEK cells are transfected with the early region of SV40 (ER-SV40), which drives the expression of both large T and small t antigens, to allow them to divide 80–90 times before entering crisis, a period characterized by massive cell death due to rampant CIN (22) (Figure 1A). We have shown previously that T-CIN takes place around population doubling 50 (PD50) and is driven by the shortest telomeres in these cells (23). Using a particular clone (HA1), isolated after introduction of ER-SV40, it is possible to reproducibly recover telomerase positive post-crisis cells with critically short telomeres, whereas other clones (HA2–HA5) never give rise to survivors (22) (Figure 1A–C). On the other hand, the introduction of hTERT in clones HA1 and HA5 before PD50 allows the immortalization of cells without CIN (HA1-early and HA5-early), whereas introduction of hTERT after this point in clone HA5 leads to immortalization of karyotypically abnormal CIN+ cells (HA5-late) as determined by array-comparative genomic hybridization (Figure 1A and Supplementary Figure S1, available at *Carcinogenesis* Online). This system provides a perfect experimental setup to study the impact of T-CIN on gene expression and the derived biological consequences by comparison of CIN+ versus CIN− cells.

### HEK cells with T-CIN exhibit massive miR deregulation

To explore the extent to which T-CIN impacts the gene expression landscape, we chose to monitor miRs, as it has been suggested that genomic regions carrying these genes may be preferentially affected

by genome instability events (24). We performed a comparison of the miR expression profiles between CIN+ and CIN− cells derived from the same HEK-ER-SV40 clone using a next-generation sequencing approach (Supplementary Figure S2A, available at *Carcinogenesis* Online). We found that of about 1008 miRs that are detected in HA5-derived cells, 538 (53.3%) were significantly deregulated (adj $P < 0.05$) in HA5-late versus HA5-early cells (Figure 2A and Supplementary Table S1, available at *Carcinogenesis* Online). A comparison between the 1038 miRs expressed in HA1-derived cells revealed a similar result, with 395 miRs (38.1%) significantly deregulated (adj $P < 0.05$) in post-crisis PC1 versus HA1-early cells (Supplementary Figure S2B and Table S2, available at *Carcinogenesis* Online). In all, 138 miRs presented variations in the same direction (Supplementary Figure S2C, available at *Carcinogenesis* Online), suggesting that a significant proportion of miRs were similarly affected, independently of the genome instability history of both clones. This assumption was confirmed using array hybridization in additional HEK cells, in which around 16% of miRs were deregulated in CIN+ versus CIN− cells ($P < 0.05$) (Supplementary Figure S3A and Table S3, available at *Carcinogenesis* Online). Although array hybridization is less sensitive than massive sequencing, there is a significant correlation between the expression changes detected by both methods (Supplementary Figure S3B, available at *Carcinogenesis* Online). Furthermore, a fraction of the differentially expressed miRs was confirmed by RT–qPCR (Supplementary Figure S3C, available at *Carcinogenesis* Online). Intriguingly, these validated miRs have been found deregulated in human renal cell carcinomas (25,26).

To determine whether the miR deregulation exhibited by cells with T-CIN is restricted to mature strands, we examined the expression of pre-miRs using the same set of RNA samples. A total of 172 pre-miRs were measured by RT–qPCR, from which 102 were expressed across the HEK cells. An unsupervised clustering analysis readily distinguished CIN+ from CIN− cells and, similarly to the sequencing
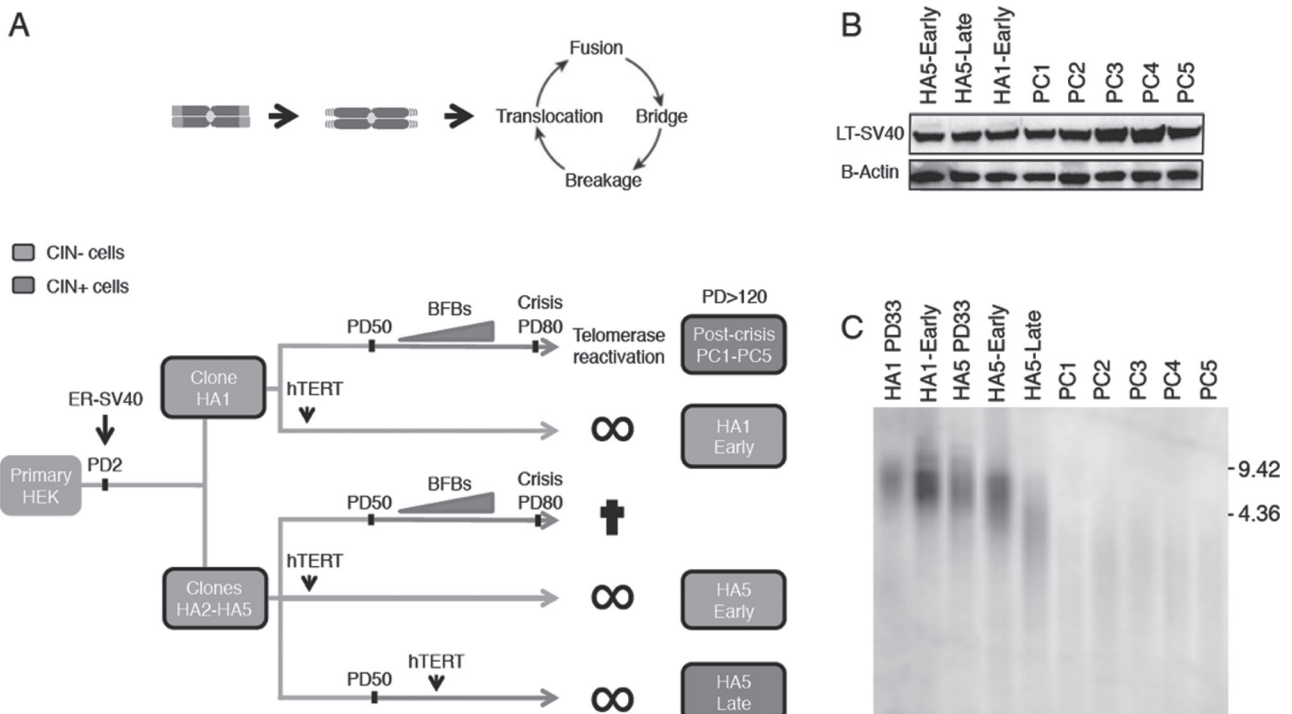
Fig. 1. HEK cell model for analysis of T-CIN. (**A**) Primary HEK cells were transfected with ER-SV40 at early PDs, and clones HA1–HA5 were immediately obtained. CIN due to telomere shortening initiates at PD50 and leads to repeated BFBs. Cells entered crisis after PD80 and clones HA2–HA5 died off, whereas spontaneous reactivation of telomerase in clone HA1 allowed recovering five post-crisis cells (PC1–PC5) in independent experiments. Cells without CIN before PD50 (CIN− cells, in orange) were immortalized through introduction of hTERT in clones HA1 and HA5 and remained karyotypically stable (early cell lines). Exogenous immortalization of cells >PD50 (CIN+ cells, in blue) was also achieved in clone HA5 (HA5-late cells). (**B**) Western blot analysis to examine the expression of LT-SV40 in the panel of HEK cells. (**C**) Southern blot for assessment of telomere length shows shorter telomeres in CIN+ post-crisis HEK cells.
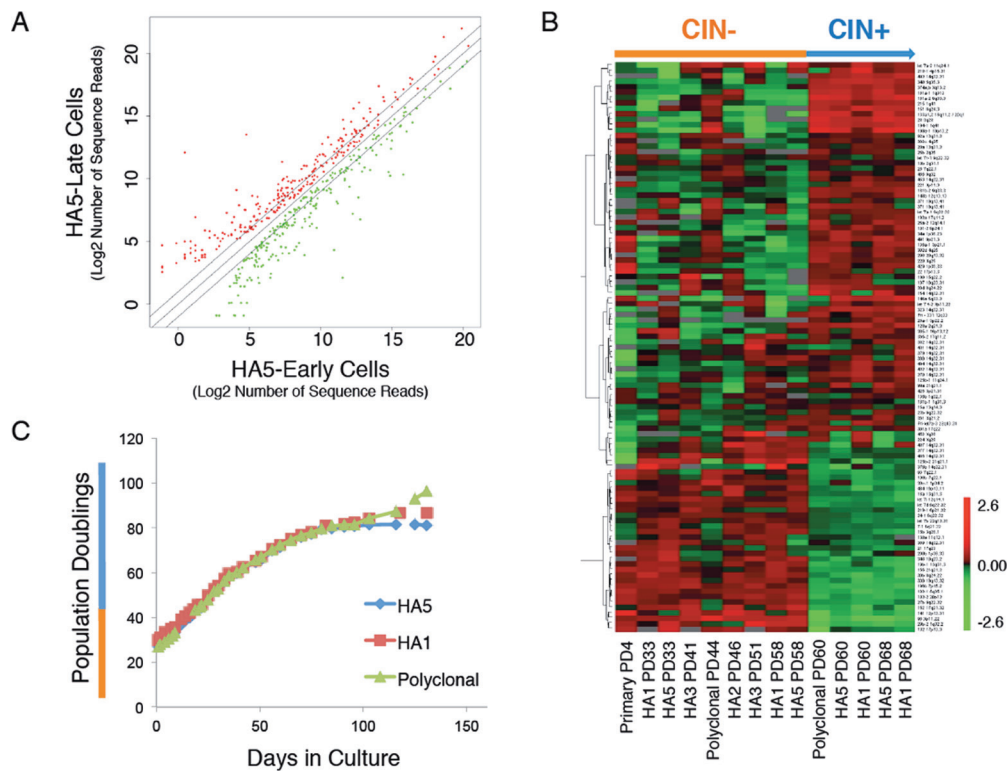
Fig. 2. T-CIN triggers widespread miR deregulation. (**A**) Comparison of miR expression profiles between HA5-late (CIN+) and HA5-early (CIN−) cells using RNA-Seq data. The number of reads (log2) for each miR (*n* = 538) was plotted for both cell lines. Black lines indicate 2-fold changes. Upregulated miRs in HA5-late are shown in red, whereas those that are downregulated are shown in green. (**B**) Pre-miR expression profiles of clones HA1, HA5 and polyclonal populations at equivalent PDs were detected by RT–qPCR. Primary cells, as well as two other clones (HA2 and HA3), were also analyzed at early passages. The normalized expression of each precursor against the mean of three housekeeping genes (ΔCT) was used to generate the heatmap, where red indicates high expression and green indicates low expression. The color bar indicates the magnitude of expression in log2 scale. Clustering was performed only for pre-miRs using Euclidean distance metric. (**C**) Growth curves of clones HA1, HA5 and polyclonal populations undergoing T-CIN.

data for mature strands, this deregulation was significant for half of the pre-miRs analyzed (adj *P* < 0.05) (Supplementary Figure S4A and Table S4, available at *Carcinogenesis* Online). There is also a significant correlation between the expression changes detected for pre-miRs and mature strands (Supplementary Figure S4B, available at *Carcinogenesis* Online). To further test whether this miR deregulation is also reflected at the level of transcription, we measured the expression of some primary strands (pri-miRs) in HA5-late versus HA5-early cells (Supplementary Figure S4C, available at *Carcinogenesis* Online). Most, albeit not all, tested miRs showed a co-deregulation at the levels of both primary and mature strands, suggesting that transcription contributes to miR deregulation in the context of T-CIN.

Collectively, these data indicate a massive deregulation of miR expression associated with T-CIN. Notably, changes in miR expression are completely prevented if telomerase is introduced before, but not after, the initiation of T-CIN (Supplementary Figures S3A and S4A, available at *Carcinogenesis* Online), demonstrating that telomere instability is responsible for the observed miR deregulation. As this miR deregulation could be related to genomic aberrations induced by T-CIN, we closely examined the array-comparative genomic hybridization profiles of immortalized CIN+ HEK cells. Intriguingly, only 12 miR-altered loci in at least three out of six CIN+ cells overlap a significant change in the expression of pre-miRs (Supplementary Figure S4D and Table S5, available at *Carcinogenesis* Online), suggesting that genomic gains and losses had a limited contribution to the miR deregulation in cells that underwent T-CIN.

Ongoing T-CIN triggers transcriptional miR deregulation in the absence of an overt DNA damage response

To determine the time at which T-CIN induces the miR deregulation, we monitored proliferating, non-immortalized HEK cells

before and after the initiation of CIN. We found that changes in the expression of most of the mature miRs examined were similar in clones HA1 and HA5 (Supplementary Figure S5A, available at *Carcinogenesis* Online), with increased deregulation with increasing passages, and a maximum fold change in crisis. When pre-miRs were monitored, a shift in the global expression profile was detected in cells undergoing active T-CIN, a few passages after the initiation of BFBs (Figure 2B and C). This massive deregulation was similar in different clones as well as in polyclonal populations and did not induce changes in cell growth kinetics (Figure 2C). Interestingly, the detected changes affected in a similar way miRs belonging to the same family or to the same genomic cluster suggesting a concerted transcriptional response. In fact, we also detected changes in the expression of pri-miRs, which also tend to accumulate soon after the initiation of CIN (Supplementary Figure S5B, available at *Carcinogenesis* Online), demonstrating that T-CIN directly impacts the expression of miRs at the transcriptional level.

It has been shown that DNA damage responses (DDR) impact miR expression (25). To test whether the miR transcriptional deregulation induced by T-CIN is linked to a DDR due to telomere shortening (26,27), we evaluated the presence of marks for DDR activation by western blot . HEK cells examined after the initiation of T-CIN did not exhibit the classic marks for DDR activation by the time we detected the first changes in pri-miR or pre-miR expression levels (PD55-60) (Supplementary Figure S6A, available at *Carcinogenesis* Online), suggesting that the miR deregulation induced by T-CIN did not require a strong DDR. Supporting this interpretation is the fact that a partial depletion of ATM did not prevent the pre-miR changes exhibited by cells undergoing T-CIN (Supplementary Figure S6B–D, available at *Carcinogenesis* Online).

To determine whether the miR deregulation induced by T-CIN can be also found in situations of telomere dysfunction that are independent of telomere shortening, we evaluated miR expression changes upon depletion of TRF2, an essential component of the telomeric shelterin complex that prevents the recognition of chromosome extremities by the DNA damage machinery (28). As complete loss of TRF2 induces growth arrest (29), we aimed at achieving a partial depletion to allow cells to cycle and to be chronically exposed to telomere dysfunction. Three rounds of transfections with a specific small interfering RNA against TRF2 led to 70% depletion of the protein (Supplementary Figure S7A, available at *Carcinogenesis* Online). This depletion was associated with a 3-fold increase in the percentage of cells with more than two telomere dysfunction-induced foci, as compared with cells transfected with the small interfering RNA control, indicating the presence of DNA damage due to uncapped telomeres (Supplementary Figure S7B and C, available at *Carcinogenesis* Online). Although TRF2 depletion leads to changes in expression of some mature miRs that were also observed in cells undergoing T-CIN (Supplementary Figure S7D, available at *Carcinogenesis* Online), the impact was quite different at the level of pri-miRs, which showed lower expression upon TRF2 depletion (Supplementary Figure S7E, available at *Carcinogenesis* Online), whereas cells reaching crisis pri-miRs tend to be upregulated. This experiment, while supporting the notion that telomere dysfunction influences miR transcription, suggests that different mechanisms of telomere uncapping may have a different biological outcome.

T-CIN leads a miR-200-dependent transdifferentiation

In order to examine the biological consequences of the miR deregulation induced by T-CIN on cell phenotypes, we focused on the miR-200 because members of this family were downregulated in CIN+ cells in most of the comparisons we performed. We confirmed by RT–qPCR that the cluster located on 1p36.33 (miR-200a and miR-200b), which is robustly expressed in primary and CIN− cells, was significantly downregulated in CIN+ cells. Similarly, the miR-200 cluster located on 12p13.31 (miR-141 and miR-200c), which is poorly expressed in primary and CIN− cells, was further downregulated (Figure 3A). The miR-200 family has been directly implicated in the induction of epithelial-to-mesenchymal transition (EMT) (30,31), a physiological phenomenon during organismal development, which is also considered relevant for metastasis (32). This prompted us to examine the phenotypical features of CIN+ HEK cells.

Microscopic evaluation revealed that CIN+ cells have lost the rounded, cobblestone morphology typical of epithelial cells and display a more elongated, spindle-like typical of fibroblasts with a characteristic orientation of actin microfilaments (Figure 3B). In addition, all—but one—CIN+ cells showed modified expression of epithelial markers, E-cadherin and cytokeratins, and enhanced expression of transforming growth factor-β and ZEB1, two well-known EMT inducers (Figure 3C). We also detected a change in the proportion of cells expressing CD24 (epithelial) or CD44 (mesenchymal) surface markers(33), which becomes readily evident in crisis (Figure 3D), as well as enhanced migration and invasion capacities in CIN+ cells (Supplementary Figure S8A–C, available at *Carcinogenesis* Online), suggesting that CIN+ HEK cells underwent transdifferentiation. In keeping with these observations, transcriptome analyses identified 878 genes differentially expressed between CIN+ and CIN− cells that are involved in EMT-related signaling pathways (Supplementary Figures S9A and B and Table S6, available at *Carcinogenesis* Online); indeed several genes downregulated in
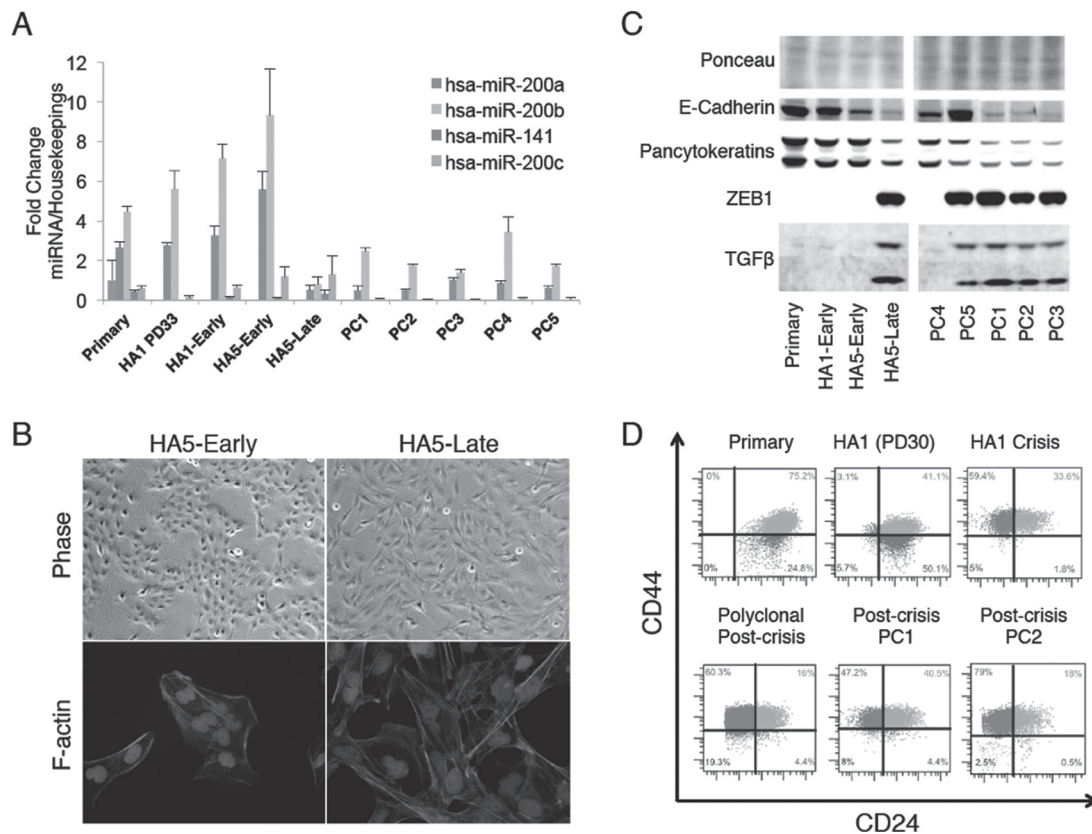
Fig. 3. HEK cells that underwent T-CIN display an EMT-like phenotype. (**A**) Expression levels of the miR-200 family, relative to the mean expression of hsa-Let7 and hsa-miR-365 (housekeeping) as detected by RT–qPCR in CIN− and CIN+ cells. Error bars indicate standard error of the mean from three independent RT reactions. (**B**) Phase contrast microscopy (×40) (upper) and phalloidin–TRITC staining (bottom) in HA5-early and HA5-late cells. (**C**) Expression patterns of E-cadherin, cytokeratins, ZEB1 and transforming growth factor-β in CIN− and CIN+ cells. Ponceau staining is shown as loading control. (**D**) Intensities of surface markers CD44 and CD24 in CIN− and CIN+ cells as detected by flow cytometry.
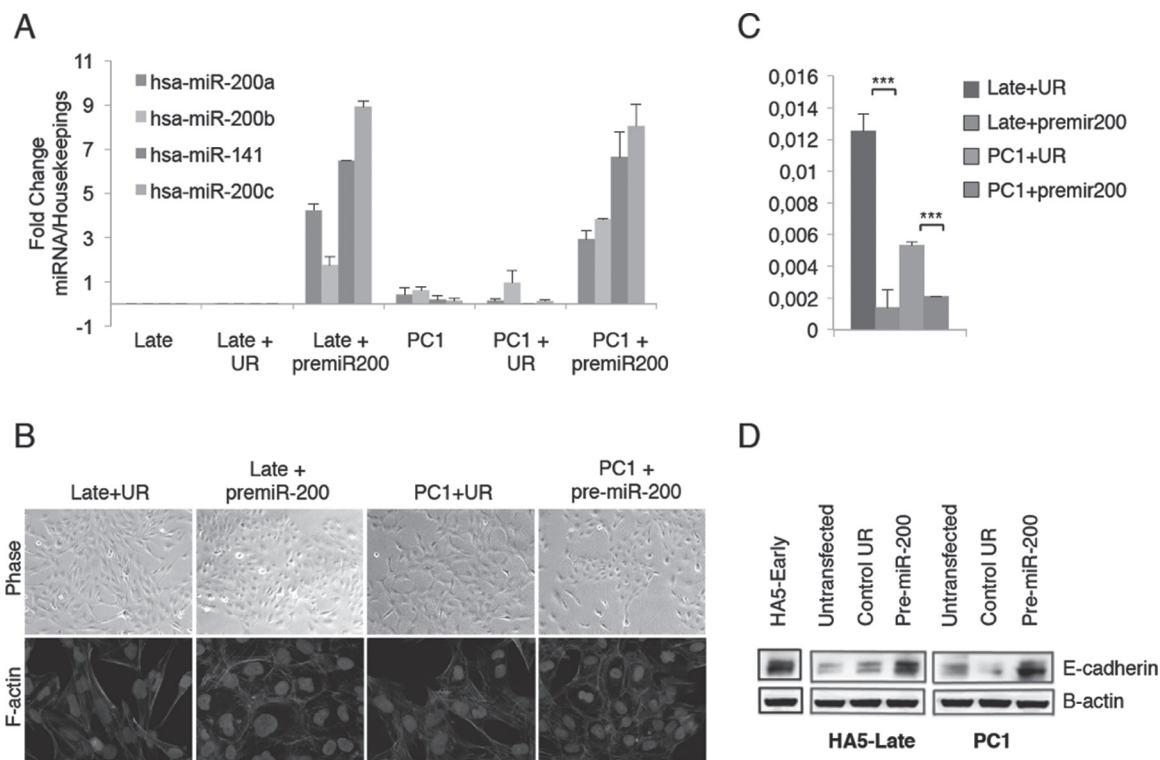
Fig. 4. Re-expression of the miR-200 restores the epithelial phenotype of CIN+ HEK cells. (**A**) Immortalized HEK CIN+ cells (HA5-late and PC1) were transfected twice at 48 h interval either with a mixture of pre-miR-200 or with a scrambled pre-miR preparation used as negative control (UR). The histogram shows the restored expression of mature miR-200, as detected by RT–qPCR. The expression value of each miR was normalized against the mean of hsa-Let7 and hsa-miR-365 used as housekeepings. Error bars indicate standard error of the mean from three independent RT reactions. (**B**) Phase contrast of CIN+ cells transfected with control UR or pre-miR-200 (upper) and phalloidin–TRITC staining (bottom) were used to monitor changes in morphology. (**C**) The expression of ZEB1, a repressor of E-cadherin and well-known target of the miR-200 family, was evaluated by RT–qPCR in CIN+ cells 48 h after the last transfection with control UR or pre-miRs-200. The histogram shows the expression of ZEB1 relative to B2MG used as housekeeping, for each condition. Error bars indicate standard error of the mean from three independent RT reactions; ***$P < 0.001$ (unpaired *t*-test). (**D**) Western blot analysis of E-cadherin 48 h after the last transfection of CIN+ cells with control UR or pre-miRs-200. HA5-early cells (CIN−) are showed as positive control for comparison. B-actin was used as loading control.

CIN+ cells are involved in kidney development (Supplementary Table S7, available at *Carcinogenesis* Online), supporting the notion that T-CIN impinges on the differentiation program of renal epithelial cells. To test whether the downregulation of the miR-200 family in CIN+ HEK cells is responsible for the observed EMT, as described for other epithelial systems (30–32), we transfected these cells with a mixture of pre-miRs representing the miR-200 family (Figure 4). This experiment shows that re-expression of these miRs in CIN+ HEK cells is sufficient to restore the epithelial phenotype (Figure 4).

The miR expression signature of post-crisis HEK cells is displayed by advanced renal cell carcinomas

Several studies have shown a deregulated expression of miRs in renal cell carcinomas when compared with normal tissues (34,35). Some of the miR changes frequently found across published studies include overexpression of members of the miR-17–92 cluster, miR-224 and miR-34a, as well as downregulation of members of the miR-200 family and the miR-143/145 cluster, the latter being associated with early renal cancer relapse (26). Remarkably, all these miRs are deregulated in HEK cells undergoing T-CIN, and this deregulation persists in immortalized CIN+ cells. Because short telomeres are associated with a high incidence of chromosome abnormalities (36) and higher risk of renal cancer (37), we examined the *in vivo* relevance of the miR expression pattern acquired by HEK cells upon T-CIN. To this end, we defined a signature composed of a set of 20 miRs that were significantly downregulated in post-crisis HEK cells and which belong to a core signature of miRs expressed in normal kidney tissues (38). This signature was used to interrogate a set of human renal cell carcinomas (Gad *et al.*, in preparation). Unsupervised clustering

analysis indicated that this miR signature correctly classifies 28 out of 33 renal tumors (Figure 5 and Supplementary Table S8, available at *Carcinogenesis* Online). Outstandingly, advanced renal carcinomas with the highest Fuhrman's nuclear grade and tumor stage are considered poorly differentiated and exhibit, as post-crisis HEK cells, low expression levels of these miRs.

Discussion

This work provides unprecedented evidence indicating that T-CIN in human epithelial cells induces widespread changes in miR expression ultimately leading to a major perturbation in the differentiation program. Interestingly, T-CIN impacts miR expression at the transcriptional level soon after the initiation of BFB cycles in the absence of a strong DDR. Given the reproducibility of miR expression changes in clonal and polyclonal cell populations in which chromosome rearrangements accumulate stochastically, it is very likely that this transcriptional activity is independent of local rearrangements. Alternatively, there is a possibility, although this remains to be shown, that changes in miR expression are linked to pervasive epigenetic changes. Such changes could be related either to the spreading in cis of chromatin changes that reach far away from the point of double-strand breaks or to the activation in trans of chromatin remodeling complexes able to impact the transcription program of the cell.

Remarkably, the miR deregulation induced by T-CIN recapitulated the most common miR expression changes described in renal cancers that have been proposed to be associated with tumor progression. Specifically, we showed that a downregulation of the miR-200 family is directly responsible for the activation of the EMT program in CIN+ cells. Of note, although telomere crisis and EMT have been proposed

Furhman grade ≥3 + Tumor stage ≥3a
Furhman grade <3 + Tumor stage <3a
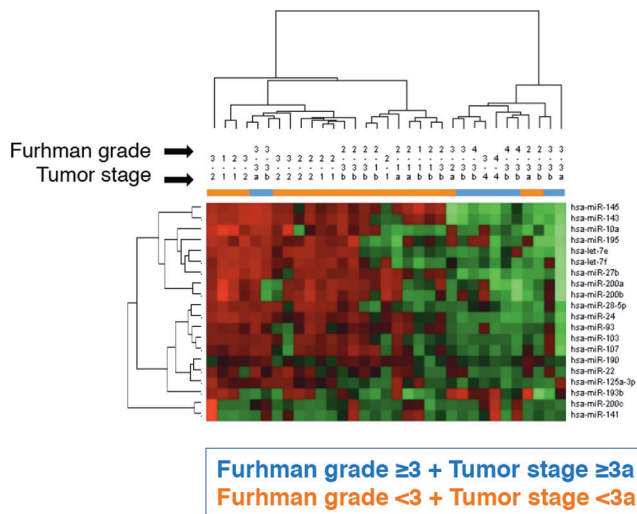
Fig. 5. The miR expression signature of post-crisis HEK cells is retrieved in high-grade, undifferentiated renal cell carcinomas. Two-way clustering analysis of 33 human renal cancers was performed using 20 miRs that were significantly downregulated in CIN+ HEKs and that belong to a core signature of normal kidney tissue. The heatmap was generated using Euclidean distance and Ward's criteria as linkage rule. Red and green indicate high and low expressions, respectively.

to occur at pre-invasive lesions of epithelial cancers (39,40), this is the first time that a connection between these two phenomena is firmly established. Indeed, our results appear to be relevant for the oncogenic process *in vivo* because the miR expression pattern displayed by transdifferentiated post-crisis HEK cells was also retrieved in poorly differentiated, high-grade renal tumors.

The EMT program has been fully documented as being required for the acquisition of metastatic potential (41). Intriguingly, however, post-crisis HEK cells are poorly tumorigenic (data not shown), as opposed to immortalized HEK cells expressing oncogenic RAS (42). Nevertheless, as circulating tumor cells can be detected at early stages during tumorigenesis (40), our data support a model whereby telomere shortening at early stages of human epithelial cancers might promote the acquisition of the malignant phenotype, perhaps with post-crisis cells reflecting an intermediate step in the road to oncogenic transformation. Therefore, we provide a new mechanistic rational to understand the long-standing association among aging, short telomeres and the progression of carcinomas toward the metastatic disease.

Conclusions

This study shows that in the context of telomere instability, there is a vast deregulation in miRs transcription that is not connected with corresponding DNA copy number changes. We demonstrated that HEK cells that have traversed a period of T-CIN both display low expression levels of genes and miRs that are normally expressed in kidney tissue and undergo a miR-200-dependent EMT. Importantly, a miR signature of HEK post-crisis cells was found in high-grade undifferentiated aggressive cancers of the same tissue origin, suggesting that *in vitro* transformation models could help us to understand the mechanisms by which tumor cells adapt their gene programs and acquire aggressive phenotypes.

Supplementary material

Supplementary Tables 1–8 and Figures 1–9 can be found at http://carcin.oxfordjournals.org/

Funding

Acknowledgement

Conflict of Interest Statement: None declared.

References

1. Romanov,S.R. *et al.* (2001) Normal human mammary epithelial cells spontaneously escape senescence and acquire genomic changes. *Nature*, **409**, 633–637.
2. Meeker,A.K. *et al.* (2004) Telomere length abnormalities occur early in the initiation of epithelial carcinogenesis. *Clin. Cancer Res.*, **10**, 3317–3326.
3. DePinho,R.A. (2000) The age of cancer. *Nature*, **408**, 248–254.
4. Lengauer,C. *et al.* (1998) Genetic instabilities in human cancers. *Nature*, **396**, 643–649.
5. Campbell,P.J. *et al.* (2010) The patterns and dynamics of genomic instability in metastatic pancreatic cancer. *Nature*, **467**, 1109–1113.
6. Rudolph,K.L. *et al.* (1999) Longevity, stress response, and cancer in aging telomerase-deficient mice. *Cell*, **96**, 701–712.
7. Rudolph,K.L. *et al.* (2001) Telomere dysfunction and evolution of intestinal carcinoma in mice and humans. *Nat. Genet.*, **28**, 155–159.
8. Artandi,S.E. *et al.* (2000) Telomere dysfunction promotes non-reciprocal translocations and epithelial cancers in mice. *Nature*, **406**, 641–645.
9. Bojovic,B. *et al.* (2011) Telomere dysfunction promotes metastasis in a TERC null mouse model of head and neck cancer. *Mol. Cancer Res.*, **9**, 901–913.
10. O'Hagan,R.C. *et al.* (2002) Telomere dysfunction provokes regional amplification and deletion in cancer genomes. *Cancer Cell*, **2**, 149–155.
11. Ding,Z. *et al.* (2012) Telomerase reactivation following telomere dysfunction yields murine prostate tumors with bone metastases. *Cell*, **148**, 896–907.
12. La Rosa,P. *et al.* (2006) VAMP: visualization and analysis of array-CGH, transcriptome and other molecular profiles. *Bioinformatics*, **22**, 2066–2073.
13. Neuvial,P. *et al.* (2006) Spatial normalization of array-CGH data. *BMC Bioinformatics*, **7**, 264.
14. Hupé,P. *et al.* (2004) Analysis of array CGH data: from signal ratio to gain and loss of DNA regions. *Bioinformatics*, **20**, 3413–3422.
15. Chen,C.J. *et al.* (2012) ncPRO-seq: a tool for annotation and profiling of ncRNAs in sRNA-seq data. *Bioinformatics*, **28**, 3147–3149.
16. Langmead,B. *et al.* (2009) Ultrafast and memory-efficient alignment of short DNA sequences to the human genome. *Genome Biol.*, **10**, R25.
17. Griffiths-Jones,S. *et al.* (2008) miRBase: tools for microRNA genomics. *Nucleic Acids Res.*, **36**, D154–D158.
18. Anders,S. *et al.* (2010) Differential expression analysis for sequence count data. *Genome Biol.*, **11**, R106.
19. Schmittgen,T.D. *et al.* (2008) Analyzing real-time PCR data by the comparative C(T) method. *Nat. Protoc.*, **3**, 1101–1108.
20. Vandesompele,J. *et al.* (2002) Accurate normalization of real-time quantitative RT-PCR data by geometric averaging of multiple internal control genes. *Genome Biol.*, **3**, RESEARCH0034.
21. Mestdagh,P. *et al.* (2009) A novel and universal method for microRNA RT-qPCR data normalization. *Genome Biol.*, **10**, R64.
22. Counter,C.M. *et al.* (1992) Telomere shortening associated with chromosome instability is arrested in immortal cells which express telomerase activity. *EMBO J.*, **11**, 1921–1929.
23. der-Sarkissian,H. *et al.* (2004) The shortest telomeres drive karyotype evolution in transformed cells. *Oncogene*, **23**, 1221–1228.
24. Calin,G.A. *et al.* (2004) Human microRNA genes are frequently located at fragile sites and genomic regions involved in cancers. *Proc. Natl. Acad. Sci. U.S.A.*, **101**, 2999–3004.

25. Zhang,X. *et al.* (2011) The ATM kinase induces microRNA biogenesis in the DNA damage response. *Mol. Cell*, **41**, 371–383.

26. d'Adda di Fagagna,F. *et al.* (2003) A DNA damage checkpoint response in telomere-initiated senescence. *Nature*, **426**, 194–198.

27. Reaper,P.M. *et al.* (2004) Activation of the DNA damage response by telomere attrition: a passage to cellular senescence. *Cell Cycle*, **3**, 543–546.

28. de Lange,T. (2005) Shelterin: the protein complex that shapes and safeguards human telomeres. *Genes Dev*., **19**, 2100–2110.

29. van Steensel,B. *et al.* (1998) TRF2 protects human telomeres from end-to-end fusions. *Cell*, **92**, 401–413.

30. Gregory,P.A. *et al.* (2008) The miR-200 family and miR-205 regulate epithelial to mesenchymal transition by targeting ZEB1 and SIP1. *Nat. Cell Biol*., **10**, 593–601.

31. Park,S.M. *et al.* (2008) The miR-200 family determines the epithelial phenotype of cancer cells by targeting the E-cadherin repressors ZEB1 and ZEB2. *Genes Dev*., **22**, 894–907.

32. Kalluri,R. *et al.* (2009) The basics of epithelial-mesenchymal transition. *J. Clin. Invest*., **119**, 1420–1428.

33. Ivanova,L. *et al.* (2010) Ontogeny of CD24 in the human kidney. *Kidney Int*., **77**, 1123–1131.

34. Redova,M. *et al.* (2011) MicroRNAs and their target gene networks in renal cell carcinoma. *Biochem. Biophys. Res. Commun*., **405**, 153–156.

35. Heinzelmann,J. *et al.* (2011) Specific miRNA signatures are associated with metastasis and poor prognosis in clear cell renal cell carcinoma. *World J. Urol*., **29**, 367–373.

36. Chen,M. *et al.* (2009) Genome-wide profiling of chromosomal alterations in renal cell carcinoma using high-density single nucleotide polymorphism arrays. *Int. J. Cancer*, **125**, 2342–2348.

37. Wentzensen,I.M. *et al.* (2011) The association of telomere length and cancer: a meta-analysis. *Cancer Epidemiol. Biomarkers Prev*., **20**, 1238–1250.

38. Saal,S. *et al.* (2009) MicroRNAs and the kidney: coming of age. *Curr. Opin. Nephrol. Hypertens*., **18**, 317–323.

39. Chin,K. *et al.* (2004) In situ analyses of genome instability in breast cancer. *Nat. Genet*., **36**, 984–988.

40. Hüsemann,Y. *et al.* (2008) Systemic spread is an early step in breast cancer. *Cancer Cell*, **13**, 58–68.

41. Polyak,K. *et al.* (2009) Transitions between epithelial and mesenchymal states: acquisition of malignant and stem cell traits. *Nat. Rev. Cancer*, **9**, 265–273.

42. Hahn,W.C. *et al.* (1999) Creation of human tumour cells with defined genetic elements. *Nature*, **400**, 464–468.

AKNOWLEDGEMENTS